Kate Happee

Master Thesis

Modelling the influence of variability on the sediment dynamics in Canal Emilio Mitre

A study on the effect of climate, deepening and wind scenarios on a navigation channel through the Rio de la Plata estuary

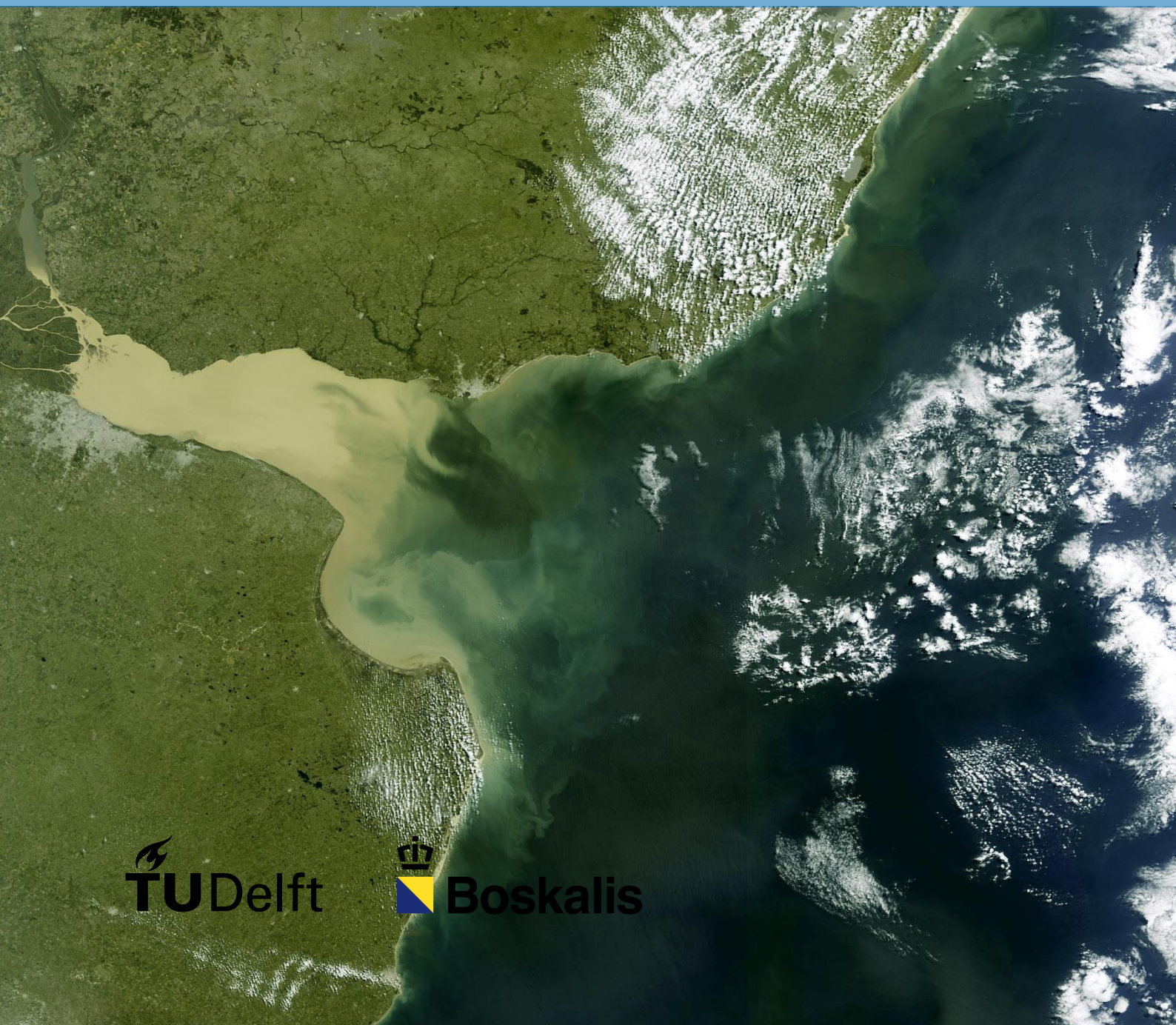

Master Thesis

Modelling the influence of variability on the sediment dynamics in Canal Emilio Mitre

A study on the effect of climate, deepening and wind scenarios on a navigation channel through the Rio de la Plata estuary

By

Kate Happee
4286413

Thesis committee:	Prof. Dr. Ir. S. G. J. Aarninkhof,	TU Delft, Chair
	Dr. Ir. B.C. van Prooijen	TU Delft
	Dr. Ir. C.J. Sloff	TU Delft, Deltares
	Dr. Ir. M.D. Klein	Boskalis

Date 28-10-2019

TU Delft Boskalis

Preface

Before you lies the final effort in obtaining my master's degree in Hydraulic Engineering at Delft University of Technology. This research has been conducted at Hydronamic, the engineering department of Boskalis.

While working on my thesis, it became clear to me that changes in hydrodynamic forcings due to (human-induced) climate change and variability are highly relevant in today's development of the dredging industry. The combination of the scientific element in this research and the challenge posed by the real-world problem of the Emilio Mitre navigation channel in the Rio de la Plata estuary has truly fascinated me over the previous months. The inspiring site-visit to the Universidad de la Republica in Uruguay has made me aware of the complexity of the system and improved my understanding of the system and parties using and investigating it.

I would like to express my gratitude to my supervisors Mark Klein (Boskalis) and Bram van Prooijen (TU Delft) for their truly engaging support and positive energy. I would also like to thank the rest of my graduation committee, Stefan Aarninkhof (TU Delft) and Kees Sloff (Deltares), for their critical reviews and insights. Special thanks to Pablo Santoro (Universidad de la Republica de Uruguay) and the rest of the Uruguayan team for providing me with insight in all the local knowledge and contact with local institutes and for helping me learn (some) Spanish and providing me access to many new scientific sources.

Finally, I would like to thank my friends and family for their guidance and unconditional support!

Kate Happee
Delft, October 2019

Summary

Canal Emilio Mitre is a navigation channel granting access to the second largest inland waterway system of South America. The navigation channel has a continuous need for maintenance dredging (average 4.5 Mm^3 excluding CSD and 5.7 Mm^3 including CSD annually). The dredging effort is shown to be highly dependent on the El Niño phenomena, the strong 2010 El Niño event led to twice as much dredging (200%) and the very strong El Niño event of 2016 resulted in 400% of the annual average effort. These extremes are linked to El Niño and the dredging strategy: during El Niño years CSDs are used to dredge buffer pits in the channel. The goal of this thesis is to assess the dredging effort and its variability, in order to reduce the risks in the foreseen 10-year long dredging contract.

The sedimentation in the navigation channel is forced by the upstream supply of sediment from the Parana de las Palmas river branch, and the magnitude of this input is highly dependent on El Niño. Infill from the flats also leads to sedimentation, the locally generated wind waves are responsible for the (up)stirring of the sediment while the tide moves the sediment-laden water over the trench. A small part of the suspended fine sediment leaves the system at the downstream end.

A numerical model is set-up to address the effect of scenarios on the dredging effort in the navigation channel. The numerical model was validated by comparing the reported dredged volumes in the system to the simulated sedimentation. For the Base Case, the model accurately represents the main trend of sedimentation with a decreasing volume downstream and peaks in the pits. In order to assess the variability of the dredging volumes the Base Case simulation is compared with climate, deepening and wind scenarios:

- Climate scenarios: Based on the IPCC reports two climate scenarios were determined. The climate change scenario consists of an increase of 8.5% of the discharge of the Rio Parana de las Palmas, which results in an increase of 6.2% in the simulated sedimentation in combination with a spatial shift from upstream to between the pits. The 8.5% increase is the projected discharge in 10 years due to a shift in precipitation regime and land use. The climate variability scenario is linked to El Niño, which leads to a 20.7% increase of the discharge. The chance that a strong El Niño will occur is 13% per year. The model simulates an increase of 17.2% of the sedimentation, with a similar spatial shift as the climate change scenario. The upstream supply does not affect pit 2 and the region downstream of pit 2, which matches the documentation of the current contractor.
- Deepening scenarios: The Argentine government is interested in deepening Canal Emilio Mitre by 2 or 4 feet in order to prevent the current queuing due to the tidal window. The numerical model predicts a reduction of the simulated sedimentation in both deepening scenarios of 7.8 and 4.8% respectively due to the attraction of discharge due to the reduced effect of resistance, this leads to higher flow velocities and thus less infill of sediment from the flats. When temporally-varying wind is added, this induces a reverse effect.
- Temporally varying wind scenarios: literature suggests that highly energetic wind events lead to redistribution of the sediment in the estuary, the effect of temporally varying wind on the simulated sedimentation is indeed large, both when looking at the absolute values and the temporal variation of the sedimentation speed in the model results. It is concluded that with temporally varying wind the deepened channel (4 feet) attracts 7.8% more sedimentation than the regular bathymetry and that the sedimentation speed is high during highly energetic events.

This study added to the overall knowledge on the physical system in and around Canal Emilio Mitre, on which only a small number of studies was done before. All in all the current dredging strategy with the upstream pit as a sediment trap and the downstream pit as an alternative disposal location is effective to reduce the risks due to variability. The optimal capacity of the pits is dependent on the strength of the El Niño event, the selected depth of the channel and the mobilisation time of a CSD. This study highlights the importance of taking into account the risks and chances due to climate variability in dredging projects in regions affected by teleconnections with a duration of 10 years.

Resumen (Spanish version)

Canal Emilio Mitre es un canal de navegación que da acceso al segundo más grande sistema de navegación interior de Sud América. El canal de navegación necesita mantenimiento continua de dragado (promedio anual de 4.5 Mm^3 excluyendo CSD y 5.7 Mm^3 incluyendo CSD). La cantidad de dragado depende altamente de los fenómenos de El Niño, el evento de El Niño 2010 llevo dos veces la cantidad de dragado (200%) y el evento de El Niño de 2016 resultó en un 400% del promedio anual. En los anos de El Niño los CSD se utilizan para dragar pozos en el canal. El objetivo de esta tesis es evaluar el dragado y su variabilidad, con el fin de reducir los riesgos en los 10 años que dura el contrato de dragado.

La sedimentación en el canal de navegación es forzada por el suministro de sedimentos desde el Rio Paraná de las Palmas, la descarga depende de El Niño. En segundo lugar el relleno de la tierra también resulta en la sedimentación, los vientos generados localmente son responsables de la agitación de los sedimentos, mientras la marea mueve los sedimentos de la trinchera llevando agua encima. Una pequeña parte de la suspensión del sedimento fino exista el sistema en las rio abajo.

Un modelo numérico es preparado para enfrentar los efectos de los escenarios climáticos del dragado en el canal de navegación. El modelo fue validado mediante una comparación con los volúmenes de dragado reportados en el sistema con la sedimentación simulada, el Base Case del modelo es mostrada para representar la tendencia principal de sedimentación con el fin de disminuir el volumen en las zonas rio abajo e incrementar el volumen en las fosas.

- Escenarios climáticos: Tomando en cuenta los informes del IPCC dos escenarios climáticos se han determinado. El cambio climático consiste en un aumento de 8,5% de la descarga del Río Paraná de las Palmas, que se traduce en un incremento de 6.2% en la simulación de la sedimentación y una translación desde una zona arriba a una zona en medio de los pozos. El 8.5% de aumento es la descarga projectada de 10 años que es debido a un cambio en el régimen de precipitaciones y el uso de la tierra. La variabilidad del clima se enlaza con El Niño, lo que significa un 20.7% de aumento de la descarga. La probabilidad de que El Niño va a ocurrir es de 13% por año. El modelo simula un incremento de 17.2 % de la sedimentación, con un cambio parecido a los escenarios de cambio climático. El suministro en las zonas arriba no afecta a la fosa 2 y la región abajo de la fosa 2, esto coincide con la documentación de la actual contratista.
- Escenarios de profundización: El gobierno Argentino está interesado en la profundización del Canal Emilio Mitre por 2 o 4 pies con el fin de evitar la corriente de cola debido a la marea de mar. El modelo numérico predice una reducción de la simulación de la sedimentación en los dos escenarios de profundización de 7.8 y 4.8% respectivamente, debido a la atracción de la descarga, debido a la disminución del efecto de la resistencia. Esto resulta en mayores velocidades de flujo y por lo tanto menos relleno de sedimentos desde las tierras.
- Vientos temporales: la literatura sugiere que los eventos de vientos energeticos causan redistribución de los sedimentos en el estuario, el efecto de la fluctuacion de los vientos temporales en la simulación de la sedimentación es realmente grande, tanto en los valores absolutos como en los resultados del modelo. Se puede concluir que con la variación de vientos temporales el canal profundizado (4 pies) atrae a un 7,8% más de la sedimentos que la batimetría regular y que la velocidad de sedimentación es alta durante eventos altamente energéticos.

Concluyendo, la estrategia actual de dragado con un pozo en la zona arriba funcionando como una trampa de sedimentos y un pozo en la zona abajo como un lugar alternativo de disposición final es eficaz para reducir el tiempo de navegación de los buques. La capacidad óptima de las piscinas depende de la fuerza de El Niño, la profundidad del canal y el tiempo de movimiento de un CSD. Este estudio releva la importancia de tomar en cuenta los riesgos y las oportunidades debido a la variabilidad del clima en los proyectos de dragado en las regiones afectadas por teleconexiones con una duración de 10 años.

Table of contents

List of symbols and abbreviations

List of symbols:

Symbol	Explanation	Unit
c	Sediment concentration	kg/m^3
c_f	Skin friction coefficient	-
c_s	Scaling parameter	-
D_{50}	Median diameter sediment particle	m
F	Tidal character	-
g	Gravitational acceleration	m/s^2
h	Water depth	m
H_s	Significant wave height	m
i_b	Bed slope	-
M	Erosion parameter	$kg/m^3/s$
n	Gauckler–Manning coefficient	$s/m^{1/3}$
$\tau_{c,d}$	Critical shear stress for deposition	N/m^2
$\tau_{c,e}$	Critical shear stress for erosion	N/m^2
T_m	Typical time scale mixing sediment	s
T_p	Peak period wave	s
T_s	Typical time scale settling sediment	s
v_t	Horizontal eddy viscosity	m^2/s
w_s	Settling velocity	m/s
Δx	Horizontal grid size	m
ρ	Density	kg/m^3

List of abbreviations:

Abbreviation	Explanation
BA	Buenos Aires
CSD	Cutter suction dredger
ENSO	El Niño- Southern Oscillation
IMFIA	Facultad de Ingenieria (Montevideo)
INA	Instituto Nacional del Agua
IPCC	Intergovernmental Panel on Climate Change
KP	Kilometre point
ONI	Oceanic Niño Index
PPT	Parts per thousand
TSHD	Trailing suction hopper dredger

1 Introduction

1.1 Background and relevance

Canal Emilio Mitre is a continuously dredged navigation channel in South America, through the Rio de la Plata estuary (in red in Figure 1). It is one of the main bottlenecks for navigation, granting access to the Parana-Paraguay waterway system (detail in Figure 1). The hinterland of this waterway system consists of Argentina, Uruguay, Brazil, Paraguay and Bolivia, of which the latter two are land-locked. According to the World Bank it has a large economic potential considering the development of the hinterland in combination with the reduction of the emission of greenhouse gasses due to a shift in transport mode (World Bank, 2010).

For the Argentinian part of the waterway system the high interannual variability of the dredging effort poses economic risks for both the users and responsible authorities. Especially Canal Emilio Mitre is heavily influenced by the interannual differences in sedimentation. Furthermore, access from the Rio de la Plata estuary to the Rio Parana for ocean going vessels through Canal Emilo Mitre, is only guaranteed during high tide with the current dredging effort.

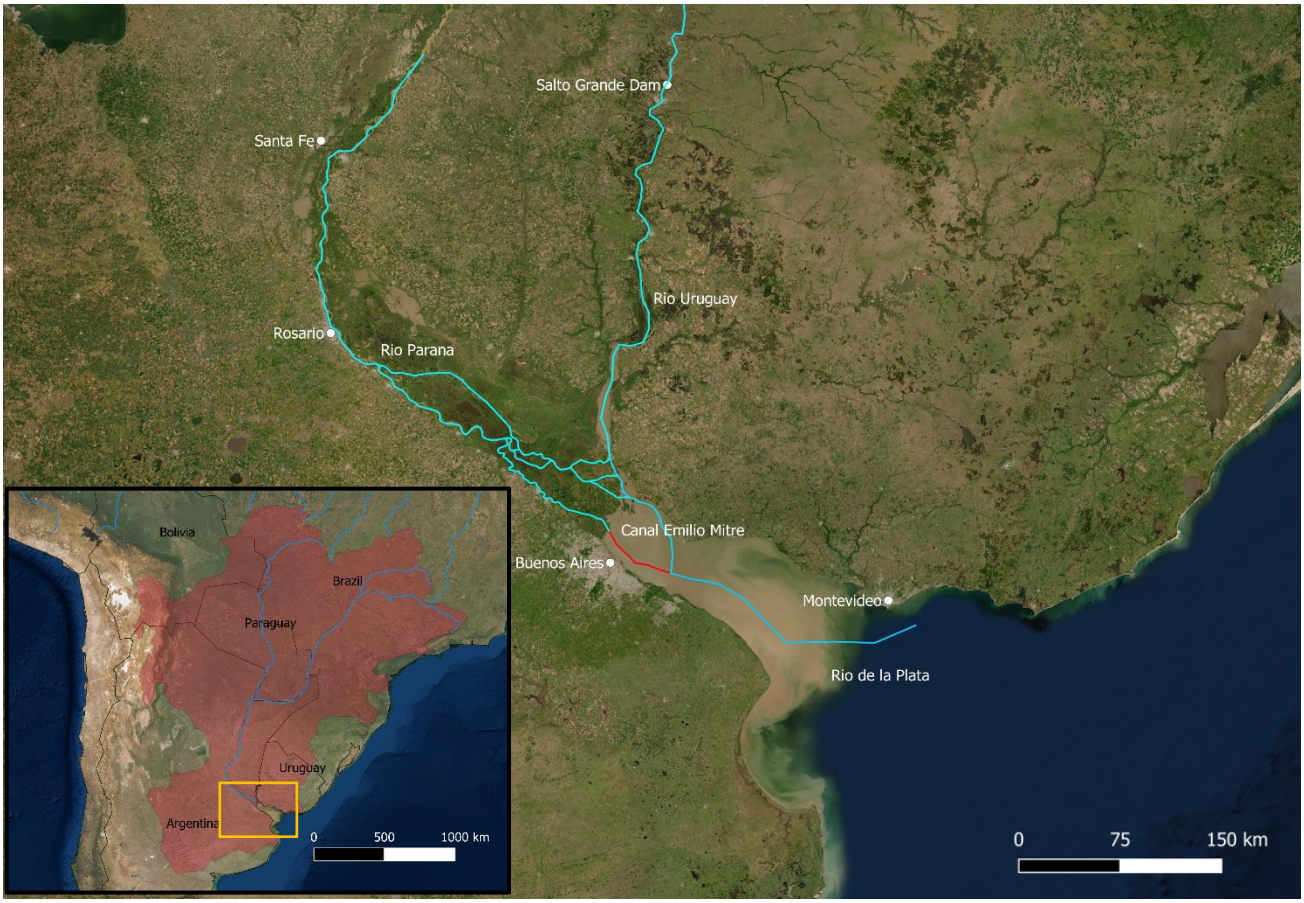

Figure 1 Location Canal Emilio Mitre in the waterway system. Detail: Catchment basin Rio de la Plata with detail

1.2 Problem description

In 2020 the Argentine government will assign a new contractor for the maintenance dredging of the waterway between Santa Fe and the Atlantic Ocean (~600 km) for 10 years. Canal Emilio Mitre is around 45 kilometre of this waterway, it is heavily dredged and the volumes show high variations between years. The interannual variability of the dredging effort leads to risks for the users and responsible authorities. Interruption of the navigability has serious economic consequences, being the main commercial waterway in Argentina and the land-locked countries north of it. Therefore

understanding what the dredging effort in the system is, and what processes it is driven by is essential. Additionally, understanding the effect of variability on the dredging effort is important, since it affects the optimal dredging strategy. Future variability is expected to be linked to both climatic forcers and potential deepening scenarios. The Argentine government considers deepening since currently ocean going vessels can only cross during a tidal window, resulting in queuing. Understanding the effect of variability on the dredging effort in the navigation channel is essential in optimizing the future dredging strategy of the system in order to make the navigability of the waterway system resilient to extremes in forcing in the future. The goal of the thesis is to incorporate this knowledge in recommendations on the future dredging strategy in order to reduce the risks due to variability.

1.3 Research objective and research questions

Research objective: To assess the potential dredging effort and its variability in Canal Emilio Mitre, in order to reduce the risks in the 10-year long dredging contract

Research questions:

1. What is, and what influences, the dredging effort in the navigation channel?
2. What is the variability of this effort, due to climate, deepening and temporally varying wind scenarios?
3. What are possible strategies to reduce the risks due to variability?

1.4 Methodology and structure of the thesis

Figure 2 presents the methodology of the thesis, below the link between this methodology and the structure of the thesis is presented.

Chapters 2, 3 and 4 combine literature study, contact with local scientist and data analysis to address research question one. Chapter 2 presents the conceptual model of the physical forcers which force the sedimentation in the navigation channel. Supply of sediment from upstream and infill from the flats, under the influence of the tide and waves, are identified as the main forcers. Effects of the upstream supply, tide, atmospheric forcing and climate variability (including ENSO) are reviewed and data is gathered for modelling.

In Chapter 3 the sources of climate variability and change are identified, the IPCC reports are used as the basis, again supported by contact with local specialists and data analysis. Analysis of the ONI record shows the chances of the occurrence of El Niño events during the project duration (10 years). This chapter introduces two climate scenarios which are considered to have most effect on the dredging effort, both of them lead to an increase of the supply of sediment from the river.

Chapter 4 completes the answer to research question one. Based on the analysis of the dredging record (2007-2018) the current dredging is around 5 Mm^3 annually. Moreover, it concludes that the interannual variability in the dredging record is correlated with the ONI index, but that also the dredging strategy plays a role here. The chapter presents two possible deepening scenarios (2 feet and 4 feet) following from the interest of the Argentine government.

In order to answer research question two and three, a depth-averaged Delft3D model has been developed. In Chapter 5 the set-up, calibration and validation of the model is presented. It is verified that the physical processes which were identified in Chapter 2 as main forcers, indeed strongly influence the sedimentation volume. The absolute values of the simulated sedimentation is shown to be highly dependent on the wind.

Using the Delft3D model, Chapter 6 shows that both the climate change and climate variability scenario lead to an increase in sedimentation and affect the absolute and spatial simulated sedimentation. Furthermore, the results of the deepening scenarios are presented. Without the effect of temporally varying wind the model predicts a small reduction of the sedimentation volume compared to the Base Case. When adding the effect of temporally varying wind the model shows

more sedimentation for the deepened channel than for the regular bathymetry, this matches the engineering rules. This chapter completes the answer to research question number two.

Chapter 7 answers research question three, concluding that the current dredging strategy is effective in mitigating the risks due to variability. Recommendations are provided on how the gained knowledge can be used to optimize the size of the pits. Based on the gained understanding of the origin and implications of the variability also the waterway is put in a broader perspective. Last but not least, recommendations on how to deal with the risks due to variability in other dredging projects in regions affected by teleconnections are presented. To conclude, Chapter 8 presents the main outcomes of the research.

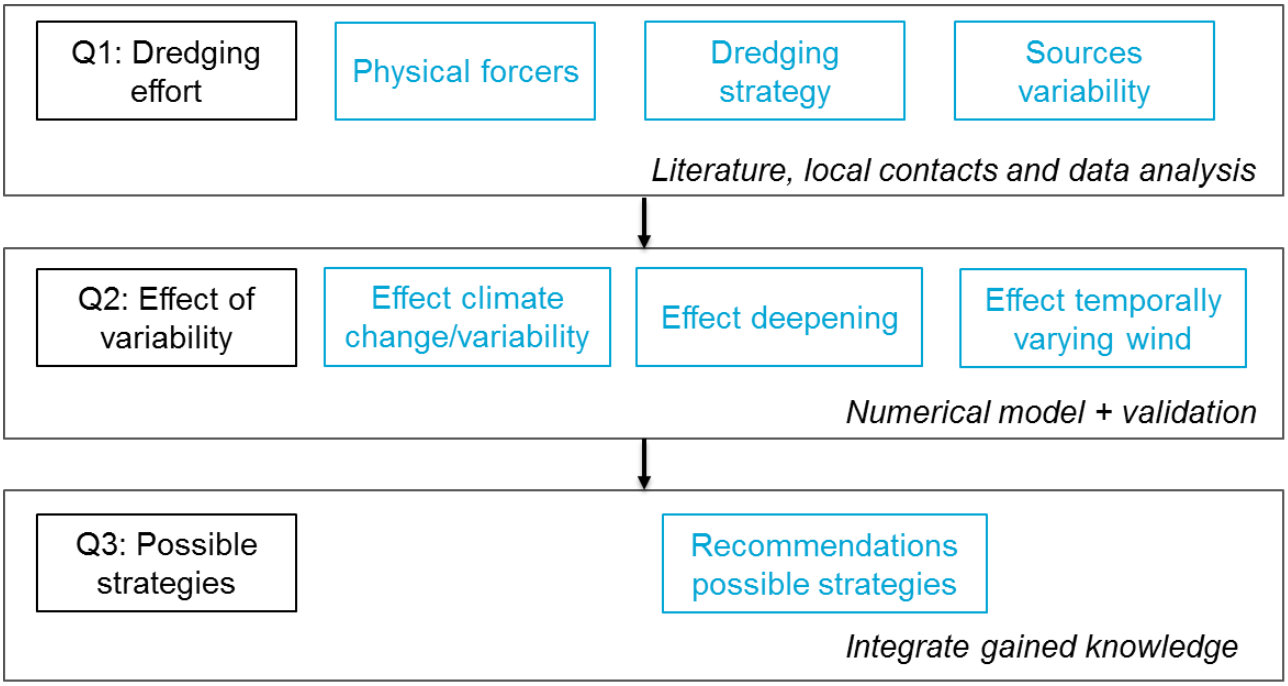

Figure 2 Methodology of the thesis

2 Analysis of physical processes in the system

Understanding the physical processes which force the sedimentation in Canal Emilio Mitre is essential in the assessment of the dredging effort in the system. This chapter addresses the physical processes in the waterway system from large to small scale and from upstream to downstream. Each paragraph ends with a conclusion on how this process affects the sedimentation in the channel of interest. The outcome of the chapter is twofold. Paragraph 2.9 presents a conceptual model capturing which physical processes play a role in which part of the catchment basin. Paragraph 2.10 presents the conceptual model of the forcers of the sedimentation in Canal Emilio Mitre.

2.1 Geographical location and long-term geological processes

The Rio de la Plata estuary is one of the largest estuaries in the world (see Figure 3). It is mainly fed by the Rio Parana and the Rio Uruguay. The catchment basin of this system of rivers has a size of around 3.1 million km^2. On the West it is bounded by the Pampean ridges and the pre-mountain range of the Andes. To the northeast it is bounded by the Brazilian plateaus and on the East by the Serro do Mar mountain range in Brazil. The catchment basin is the second largest in South America, and the fifth in the world, extending over a total of five countries.

The Rio de la Plata estuary is bordered by Argentina in the south and Uruguay in the north. Both capitals (Buenos Aires and Montevideo) are located on the coasts of the estuary. The dimensions of the estuary are impressive, with 280 km in length and 220 km in width at the Atlantic Ocean.

Figure 3 Rio de la Plata catchment basin indicating its main rivers and location Canal Emilio Mitre in red (From Wikipedia: Rio de la Plata)

Considering the long-term geological processes of plate tectonics, the coast of the Atlantic Ocean at the Rio de la Plata is a trailing-edge coast, with its wide continental shelf (extending over 150 kilometres of the coast) and extensive sedimentary features (growing islands within the estuary). The large horizontal extent of the continental shelf facilitates the development of extensive sedimentary features. Trailing-edge coasts are shaped by the interaction of currents, winds and waves. The American trailing edge coasts receive a lot of sediment due to the large drainage basins and the effect that they originate in mountainous areas. Due to the abundance of sediment and the mild climate, these conditions lead to large, meandering river systems which have been carrying sediment across a gentle slope for a long time. This has led to low relief coastal plains and subaqueous features (Bosboom & Stive, 2015). These characteristics are all present at the Rio de la Plata estuary. However in different regions along the coast of the estuary very different coastal features are distinguished. These range from coastal wetlands along the Argentinian side near Punto Indio, to the sand beaches on the Uruguayan side near Montevideo. These differences are caused by the magnitude of the influence of the physical processes at the different parts of the estuary. These physical processes

and their relative importance are addressed in the coming paragraphs. Right now the Parana-delta is fluvial dominated, as a result the bottom is expected to consist mainly of fines, but the presence of coastal ridges in the delta shows that between 5300 and 1700 years ago the area was wave-dominated (Milana & Kröhling, 2015).

2.2 Bathymetry of the Rio de la Plata estuary

The Rio de la Plata estuary has a rather complex bathymetry with natural channels and extensive flats (Prario et al., 2011). In short, the estuary is divided into two parts based on its bathymetry. These areas are split by the Barra del Indio, a quick increase in depth that crosses between Montevideo (Uruguay) and Punta Piedras (Argentina) (see Figure 4).

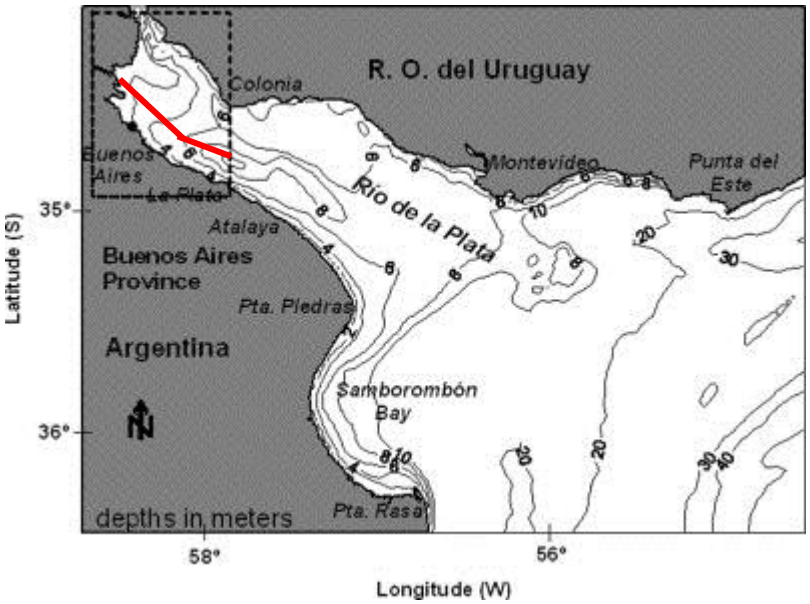

Figure 4 Bathymetry Rio de la Plata estuary, with Canal Emilio Mitre in red (Prario et al. , 2011)

The region north of the Barra del Indio is characterized by shallow banks with water depths between 1 and 4 meters. Channels run between the banks and the coasts, these natural channels have depths of 5-8 m (Simionato et al., 2006). Furthermore, dredged channels connect the Rio Parana and the Rio Uruguay to the deeper parts of the estuary, these are called Canal Emilio Mitre and Canal Martin Garcia respectively and have a depth of approximately 10 meters. Canal Emilio Mitre grants access to the Rio Parana de las Palmas while Canal Martin Garcia grants access to the Rio Uruguay and the Rio Parana Guazu (the other major branch of the Rio Parana). The major depression in the bathymetry of up to 10 meters depth is called the big hole of the Intermediate Channel, the downstream part of Canal Emilio Mitre runs through this deep area.

South of the Barra del Indio the estuary in significantly deeper with depths between 8 up to 30 m. The Samborombon Bay area is between 10 and 20 meters deep. The Alto Maritimo is a bank of around 8 meters deep (56 W, 35.5 S), north of this bank runs the Oriental Channel, this is the deepest natural channel of the estuary with depths of up to 25 m.

The hinterland of the Rio de la Plata is formed by the delta of the Rio Parana with its extensive flood plains, the bathymetry of this area is discussed in paragraph 2.3.

To conclude, Canal Emilio Mitre with a depth of around 10 meters runs through extensive flats with depths between 1 and 4 meter. The channel runs into the natural depths of the big hole of the Intermediate Channel with depths up to 10 m.

2.3 River discharge and its variability

A full overview of the measurement locations of the water level, discharge, wave and wind stations is provided in Appendix 10.1.

The catchment basin of the Rio de la Plata is built up of three sub-basins together supplying 97% of the discharge to the Rio de la Plata. At the confluence of the Parana and the Paraguay rivers, the Paraguay river contributes on average 19% of the discharge (Simionato et al., 2007 and other sources providing the same numbers). The Parana river contributes on average 76% of the discharge to the estuary, the Rio Uruguay is responsible for the rest of the discharge (see Figure 3 for orientation).

Parana river sub-basin

The Parana sub-basin consists of two regions, the upper and lower-Parana. The upper region (located in Brazil) is characterized by quick run-off and supplies about 73% of the freshwater that the Parana supplies to the Rio de la Plata. Roughly the rest of the discharge is supplied by the Paraguay river. In the upper Parana several dams have been built around the 1980s, locations include: Yacyreta, Itaipu, Porto Primavera, Ilha Solteira and Jupia. As a result of the dams the supply of fine sediments to the river has decreased (Brea & Spalletti, 2010) and the extreme low waters do not occur anymore (Barros, 2005).

The confluence of the rivers Paraguay and Parana is located at Corrientes, from there on the lower Parana river extends with a low slope towards the Rio de la Plata. Since the Parana river contributes more to the overall flow of the river, major changes in the discharge of the lower-Parana river are mainly caused by climatic forcings in the drainage basin of the upper Parana river.

Due to low banks and a low surface slope, the lower part of the Parana is susceptible to changes in the water level due to high discharge. Periodic inundations take place on average every 2 or 3 years, linked to ENSO events. The influence of moderate inundations is limited to the ponds and lagoons close to the river while major floods inundate the whole valley which is up to 60 kilometres wide (Depetris, 2007). The Parana Delta consists of a system of branches with a complex confirmation that flow between a group of islands. Due to the increase in width of the river at the delta, sediments are deposited, leading to a continuous delta front progradation of around 70 m/year at some stretches of the delta (Badano et al., 2012). Another important feature of this area is that it is affected by high water levels in the Rio de la Plata as a result of sudestadas (persistent SE winds). Due to the floods in the Rio de la Plata the drainage of the river Parana is blocked leading to serious floods.

Valor característico	*Caudal (m^3/s)*
Mínimo Absoluto	7752
Mínimo Característico (Q95%)	8394
Semipermanente (Q50%)	14410
Máximo Característico (Q5%)	29007
Máximo Absoluto	51230

Figure 5 Characteristic discharges Rio Parana at city of Timbues between 1931 and 2001 (From Jaime and Menendez 2002)

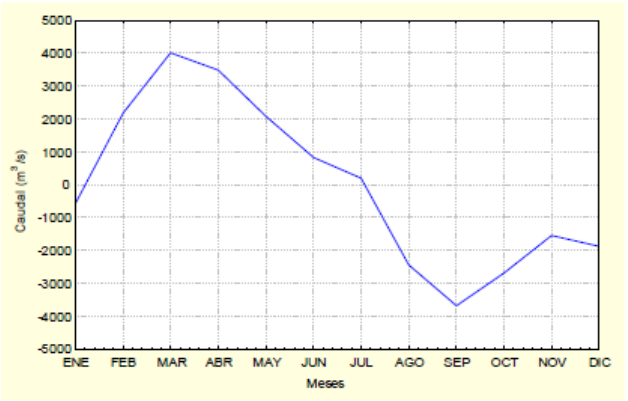

Figure 6 Seasonal component of the annual discharge Parana (1931-2001) (From Jaime and Menendez 2002)

Jaime and Menendez analysed the discharges of the lower-Parana between 1931 and 2001 and came to characteristic values for the discharge at the city of Timbues (close to Rosario) that can be found in Figure 5 (Jaime & Menendez, 2002). The minimum discharge occurs between July and December, the maximum discharge between January-June (see Figure 6). The region downstream of Corrientes (and thus also Timbues) does not receive important runoffs.

Paraguay river sub-basin

The Paraguay River has its source in the west of Brazil, it has a drainage basin area of 1.1 million km^2. The drainage basin is characterized by its very small and uniform slope (below 1.5 cm/km), it is situated in a great plain (Tossini, 1959).

The upper part of the drainage basin has the same behaviour as the Parana basin with rapid runoff. The next part of the drainage basin is the Pantanal, this is the largest wetland on Earth. Due to the fact that 50-60% of the water volume and sediments from the tributaries is stored here, the peaks in

the downstream discharge are largely reduced. Moreover the lag between flood peaks between the north and south of this region is about 4 months (Doyle & Barros, 2011). From the exit of the Pantanal to the outlet of the Paraguay into the Parana, it has low plains, leading to flooding in Argentina and Paraguay.

The Paraguay River has its major discharge in autumn and winter and low water in spring and summer (opposite of Rio Parana). The behaviour is to a large extent influenced by the Pantanal which diminishes the large discharges and length of low waters. Therefore the Rio Paraguay does not show extreme peaks in discharge.

Uruguay river sub-basin

The sub-basin area of the Uruguay river has an area of 365,000 km^2, which is small when compared to the Parana. The forcing of the river is caused by synoptic events. Together with the narrow transverse section this leads to a short delay between precipitation and discharge (order of few days), sometimes leading to flooding (Tossini, 1959).

Anomalies in the discharge of the rivers leading to flooding have been attributed mainly to El Niño events, but also regional forcing of the climate might play a role (Barros et al., 2005).

Jaime and Menendez analysed the discharges of the Uruguay between 1931 and 2001 and came to the characteristic values for the discharge at the city of Concordia (320 km upstream) that can be found in Figure 8 (Jaime et al., 2002). The minimum discharge occurs between January and March, the maximum discharge exists between May and October (see Figure 7).

Valor característico	*Caudal (m^3/s)*
Mínimo Absoluto	382
Mínimo Característico (Q95%)	755
Semipermanente (Q50%)	3613
Máximo Característico (Q5%)	11902
Máximo Absoluto	22347

Figure 8 Characteristic discharges Rio Uruguay at city of Concordia between 1931 and 2001 (From Jaime and Menendez 2002)

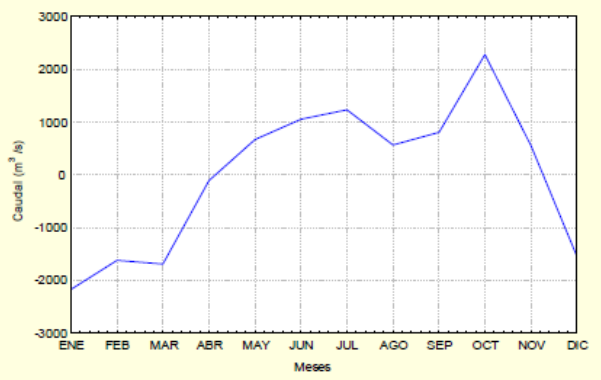

Figure 7 Seasonal component of the annual discharge Uruguay (1931-2001) (From Jaime and Menendez 2002)

Total discharge to Rio de la Plata estuary

Figure 9 shows that the total discharge per month to the Rio de la Plata does not differ too much during the year, an average of about 21,000 m^3/s is found (Berbery & Barros, 2002). A clear seasonal cycle of the total discharge cannot be distinguished since the variation in the runoff of the rivers is moderated and the cycles are partly opposed.

Although Figure 9 suggests that extremes do not play an important role in the Rio de la Plata this is not the case. Large anomalies have occurred in discharge, also leading to flooding. These anomalies are related to El Niño cycles (Barros et al., 2005) which is elaborated on in paragraph 2.8.

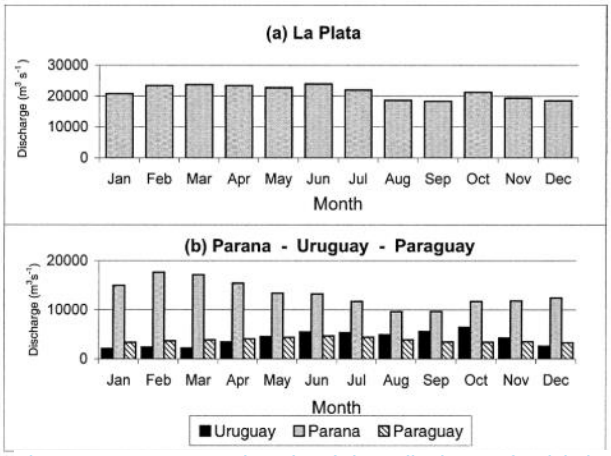

Figure 9 Mean annual cycle of river discharge for (a) the La Plata basin and (b) the three main tributaries: Parana, Paraguay and Uruguay (m^3/s) (From Berbery and Barros 2002)

Corridors of flow

Figure 10 shows the corridors of flow of the different rivers flowing into the estuary, when comparing this figure with the location of Canal Emilio Mitre in Figure 1 it is concluded that the channel of interest is only influenced by the discharge from the Parana de las Palmas river branch. As can be concluded from Figure 11 the sediment load of the different rivers can be very different, therefore from now the analysis is focused on the Rio Parana de las Palmas.

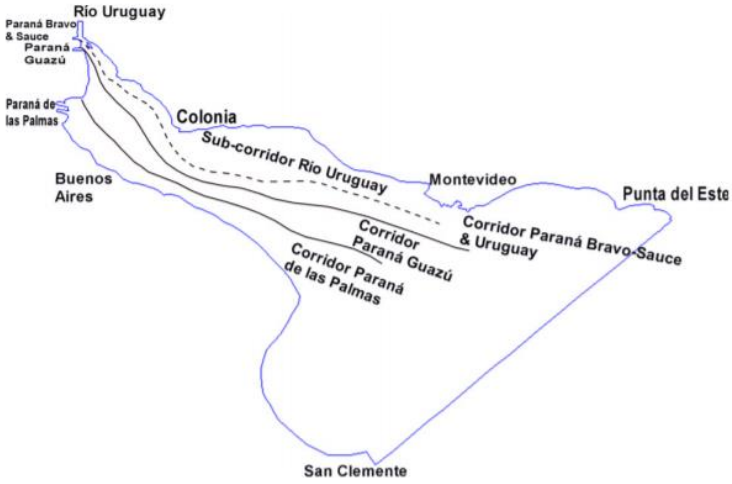

Figure 10 Corridors of flow estuary (Piedra-Cueva & Fossati, 2007)

Figure 11 NASA satellite image January 23, 2003

Analysis discharge data Rio Parana

In order to address the seasonal and interannual trends raw discharge data of the INA (Instituto Nacional de Agua, Argentina) were analysed. The ultimate goal was also to derive a reliable discharge signal for the numerical modelling. Daily discharge data of the Parana river is available at Corrientes, Santa Fe and Timbues (see Figure 12 for location). This discharge data is based on daily water level measurement which have been transferred to discharge data by using a fitted Q,h-curve. The fitted Q,h curve is updated with 2 monthly measurement at these locations (personal contact with Mariano Re (INA, 2019)).

The main conclusions are (see Figure 13 for signals):

- The yearly peak in discharge around January matches the observations by Jaime & Menendez (2002).
- The flood peaks during the El Niño years 2010 and 2016, which lasted longer than other years, are clearly recognised.
- Timbues is the most suitable station to use in the numerical model, although during high discharges the signal needs to be corrected.

Although Corrientes, Santa Fe and Timbues are all located on the main branch of the Parana river the downstream stations show lower discharges during the whole period. From contact with Mariano Re it is found that this is because

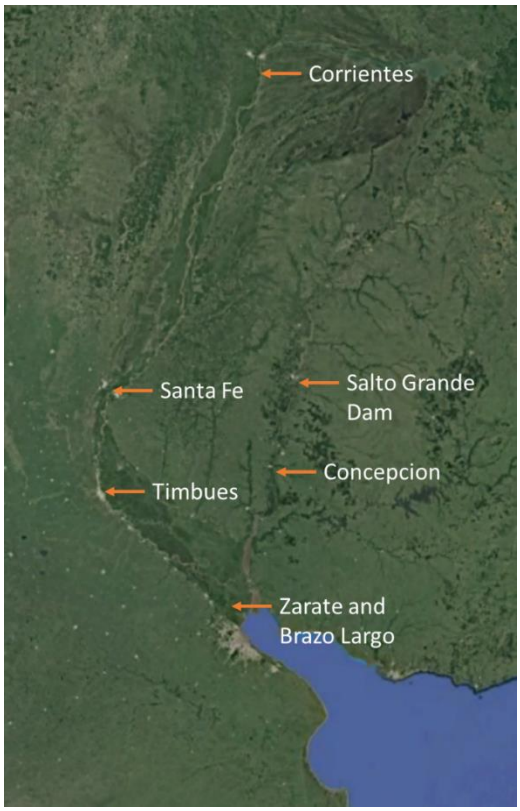

Figure 12 Discharge stations Parana and Uruguay

at Santa Fe only one branch of the river is measured (around 80% of the discharge) and at Timbues significant flood plains exist which also lead to unreliable results if water starts flowing over the plains. In order to assess the effect of high discharges on the interaction with the flood plains an analysis of satellite imagery has been done, the full explanation is presented in Appendix 10.2. This interaction is especially important since it has an effect on the sediment load of the river.

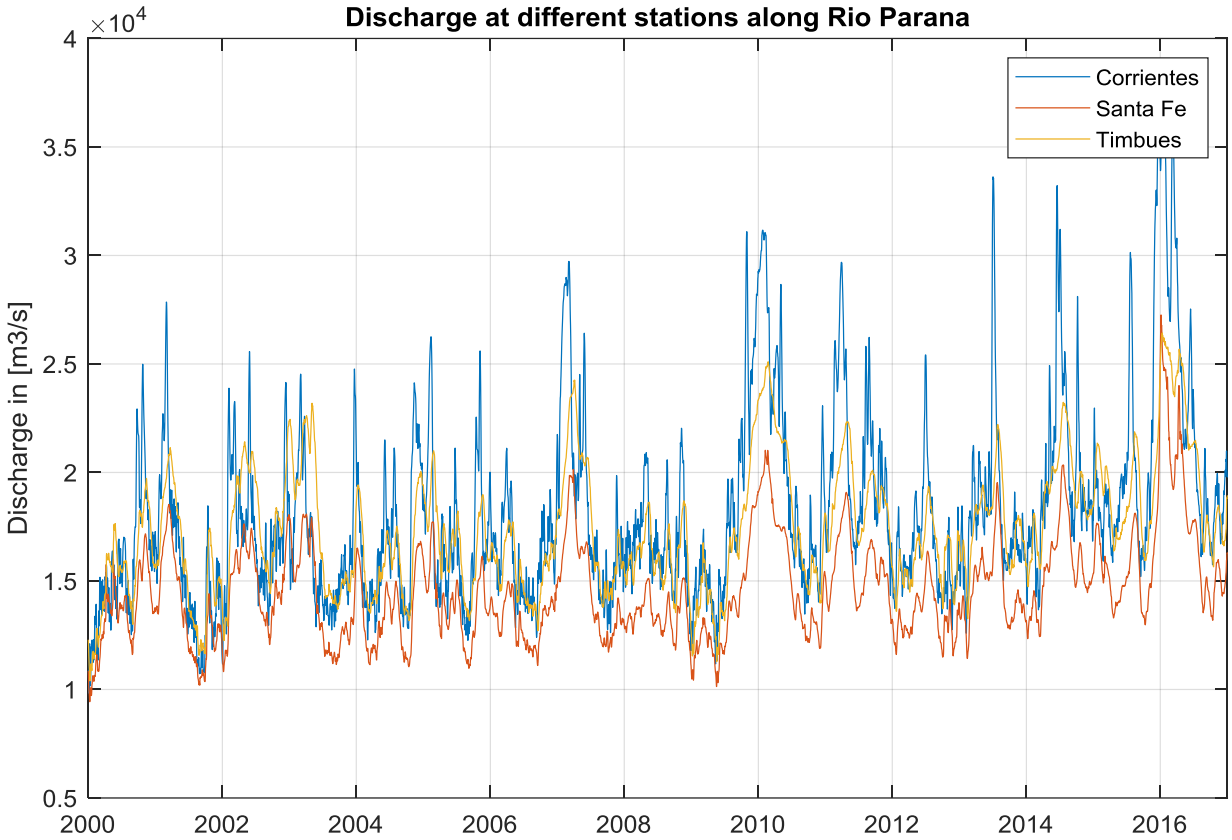

Figure 13 Discharge Parana at various stations (Corrientes most upstream, Timbues most downstream)

The analysis of the satellite imagery shows that during extreme discharges the flood plains around Timbues are flooded. In close contact with local specialists the water levels and discharges have been determined which lead to storage of water on the plains and which levels lead to the plains contributing to the discharge. When the water level in Timbues rises more than 4.4 m above the local zero (corresponds to a discharge of around 25,000 m^3/s) there is storage on the flood plains. In case the water level rises more than 5 m above the local zero (corresponds to a discharge of around 30,000 m^3/s) in Timbues there is a contribution to the discharge. A rough estimate of the flow velocities over the flood plains in this case is around 0.1 m/s. Contact with Mariano Re (INA) and Ismael Piedracueva (IMFIA) has confirmed this situation. Although it is a serious simplification, the modelling of the flood plains is not taken into account as not enough data is available on the flow over the plains and the modelling of the flooding of the plains in the numerical model is not within the scope of this study.

In spite of the limitations of the available discharge data the upstream discharge time-series is considered an important forcer to the sediment dynamics in Canal Emilio Mitre. With the knowledge of the discharge data a representative discharge signal is composed taking into account the following considerations:

- Corrientes: reliable station, no influence of flood plains and total discharge is measured, timing of flood peak does not match the timing of the flood peak in the area of interest due to extensive flood plains between Corrientes and Santa Fe
- Santa Fe: Only discharge through the main branch is measured, shape and timing are reliable but constant underestimation of absolute value of the discharge

- Timbues: Discharge signal is reliable until 25,000 m^3/s (both timing and magnitude), above that value the discharge over the flood plains is not taken into account in the record, this situation only occurs during the flood peak of the El Niño year 2015-2016.

Therefore the representative discharge signal is composed of the discharge at Timbues during discharges below 25,000 m^3/s, when the discharge is above that value the shape of the discharge at Santa Fe is superimposed by multiplying the values of Santa Fe by 1.19 (which is the ratio between Timbues and Santa Fe discharge). The created discharge signal is shown as the purple line in Figure 14. For the other years the discharge signal is similar to the signal at Timbues. An important observation is that the corrected discharge over the whole period is in absolute sense still 4% lower than the discharge at Corrientes, this might be attributed to measurement errors. The signal has not been corrected for this deviation since both the time-series at Corrientes and Timbues are constructed using a Q,h-curve and it is unknown which one of them is imprecise.

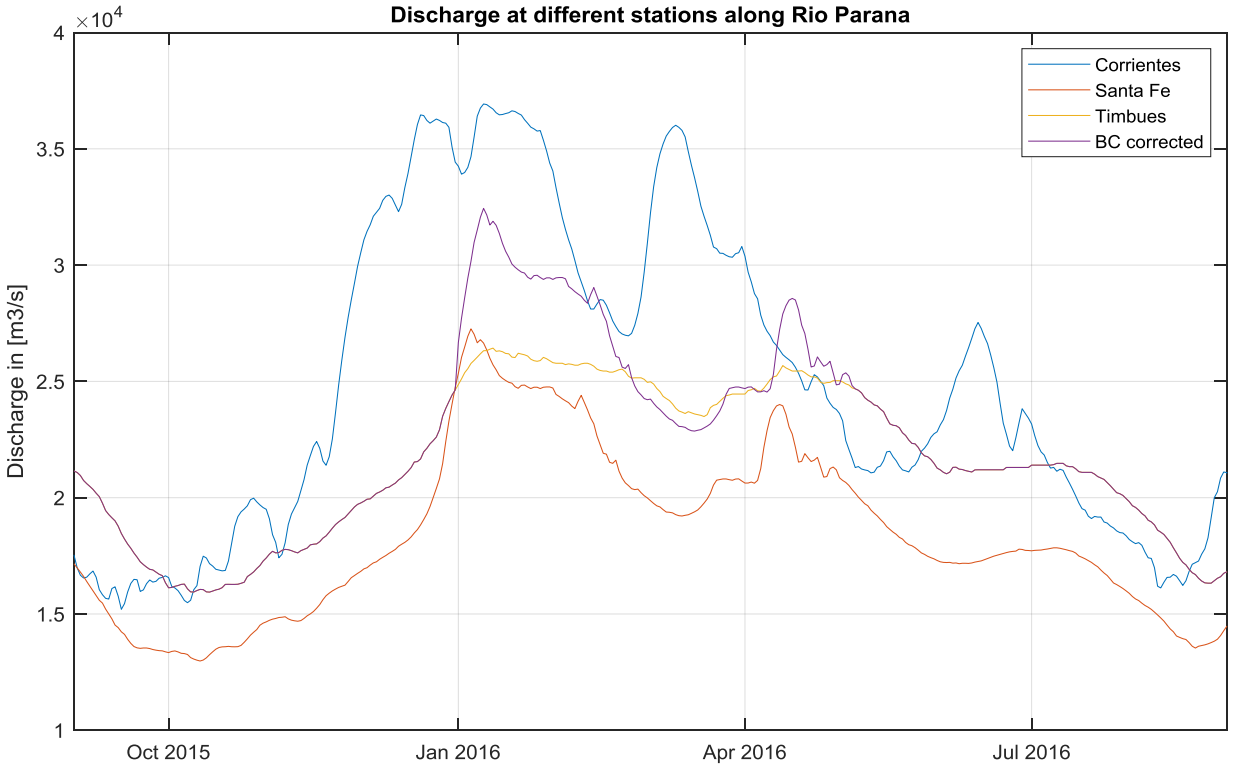

Figure 14 Representative discharge station at upstream boundary condition model for 2015-2016

When working with scenarios interannual variations play an important role. The data analysis showed that between 2010 and 2017, 2009-2010 and 2015-2016 are considered the main El Niño years and that 2013-2014 is considered an average year when assessing the discharge of the Parana. Therefore in the rest of the thesis these years are studied. Furthermore, the choice has been made to look at the years from November until the next November since this takes into account the whole flood peak.

Analysis discharge data Rio Uruguay

For the Uruguay river the upstream boundary condition is chosen at Salto Grande Dam (see Figure 12 for location) which is a reliable source of data as the division of the energy that the dam generates is divided between both neighbouring countries is based on this data (personal contact Nicolás Failache Gallo, Salto Grande Dam). No significant tributaries are found downstream of the dam, except for the Rio Negro river which has an average discharge of around 722 m^3/s (GRDC, 2019). This tributary is disregarded since the discharge of the Uruguay does not seem to be of major importance for to the area around Canal Emilio Mitre considering the flow corridors of the estuary. The Salto Grande dam is located around 150 km north of Concepcion de Uruguay which is the most

northern station that is influenced by the levels of the Rio de la Plata as followed from the literature study, therefore this is conservative choice.

In short Canal Emilio Mitre is mainly influenced by the discharge from the Rio Parana de las Palmas, since it is located completely in the corridor of flow of that branch. The discharge of the Rio Parana de las Palmas (just like the discharge of the Rio Parana) peaks around January. An annual discharge signal has been derived as input for modelling (Figure 14).

2.4 Sediments in the system

Geological origin of area

The floor of the inner estuary is a subaqueous delta that was formed by the sediment discharge from the rivers long ago. Like the typical delta front formation, the regions close to the delta consist of sandy material, while further towards the ocean finer material like silt and clays were deposited (Schuerch et al., 2016). During the Holocene sea level rise the sandy shoals like the Alto Maritimo (paragraph 2.2) were flooded but they still remain as sandy shoals, but now submerged. These sandy features at the bed of the Rio de la Plata estuary are believed to have been formed due to the advancing shoreline. Around 2000 years ago the sea level stabilised and the regions which were previously mostly sandy are now filled in with finer sediments (Urien, 1972). Therefore the upper layer of the delta of the Rio Parana consists of sand and regions of relatively recent deposition also contain finer material.

Sediment characteristics

The sediment characteristics are highly variable, both in space and time, and on the river and on the estuary. This large variation in time and space is explained by the dependence on the flow conditions and sediment transport (personal contact with Ismael Piedracueva and Monica Fossati).

Yearly sediment samples taken from the dredged waterway show that the bed of the Rio Parana consists of sand and some gravel (Argentine Government, 2018). Close to the delta of the Parana de las Palmas the percentage of fines (silt and/or clay) increases, this increase continues in Canal Emilio Mitre to around 90% fines in Canal Intermedio. Further offshore the percentage of fines decreases again due to the influence of the marine sediments to values of around 60 to 70 percent although the values for that section differ a lot between the years.

Moreira & Simionato (2016) and Schuerch, M., Scholten, J., Carretero, S., García-Rodríguez, F., Kumbier, K., Baechtiger & Liebetrau (2016) give information about the sediment characteristics around Emilio Mitre, both conclude that 10% is clay, 80% is silt and 10% is sand. The first paper mentions a D_{50} of around 40 µm.

Sieve curves inside the navigation channel (see Appendix 10.3, also for locations) show that at KP 20 in Mitre around 10% is clay, 80% is silt and 10% is sand (Deursen, 1993). In Canal Accesso the transition between predominantly silt and predominantly clay is located around KP 26. From there on 0% of the sediment is sand, 50% is silt and 50% is clay. This matches the paper by Fossati: from north to south the silt fraction in the suspended and bottom sediment decreases while the clay fraction increases (Fossati et al., 2014). The fine sands are mainly deposited in the Parana discharge zone near the head of the Rio de la Plata, this sediment is responsible for the delta front progradation. From there on downstream fining occurs. The significant amount of fine sediment highlights that the suspended sediment does not react instantaneously to a change in forcing, the silt stays in suspension which is also visible on aerial pictures. No sieve curves are available of the area around KP 41 (transition Rio Parana de las Palmas to Rio de la Plata estuary) therefore it is assumed that the bed material is sandy due to the energetic conditions.

The presence of different sediment types (clay, silt and sand) in Canal Emilio Mitre implies that selective transport takes place, this is the selective movement of different types of sediment at low bed shear stresses. These effects can only be taken into account if the total distribution of bed material is taken into account, which includes the spatial variations both in horizontal and vertical direction.

From all the literature the sediment is expected to have cohesive properties since the clay-dominated fraction is above the minimum of 5-10%. Therefore the density of the bed is not constant in time due to processes like consolidation (van Rijn, 2007). Fine sediments in an estuary often lead to flocculation increasing the setting velocity of the sediment. Flocculation due to salinity is not expected in Canal Emilio Mitre as the salinity front is located more downstream on the estuary. Paragraph 2.7 elaborates on this.

Input of sediment

An extensive study by a group from Argentina and Bolivia (Brea et al., 2010) mentions the Bermejo catchment as the main source of sediment for the Rio Parana. Although it is a minor river with an average discharge of 600 m^3/s it constitutes between 80-85% of the total sediment load to the Parana at Corrientes. The rate of sediment production per unit of area in the Bermejo catchment is one of the highest in the world leading to an average concentration of 10.0 g/L (Amsler & Drago, 2009). 75-90% of the input of sediment from the Rio Parana consists of fines, of which the major part is silt (Sarubbi, A., Pittau, M., & Menendez, 2004). Additional analysis of sediment data confirms that the peaks in sediment load in the Rio Parana are preceded by peaks in discharge at the Rio Bermejo (Appendix 10.3).

The data on the sediment balance of the Parana Delta is limited and the values are highly variable due to varying hydraulic forcings (Depetris, 2007). An overview of the current knowledge is provided by the INA (A Sarubbi, 2007). The total sediment input of the Rio Parana at the mouth is estimated to be 160 million tons, of which only 15 tons is bed load and the rest is suspended. The origin of the suspended sediment is visualised in Figure 15, again also this research states that the Rio Bermejo

Figure 15 Sediment fluxes Parana Delta in million tons per year

is the main source of sediment for the Rio de la Plata estuary. At the mouth of the Rio Parana the 145 million tons annually consists of 30% sand, 60-65% silt and 5-10% clay. According to the INA the sediment concentration of the Parana river at its mouth fluctuates between 230 and 270 mg/L with a mean value of 250 mg/L. Concerning the destination of the sediment the report mentions that all the sand (25 Mton) is deposited directly at the delta and that part of the silt in deposited as well. Furthermore, it mentions that in total in the navigation channels of the Rio de la Plata 23 Mton is deposited per year which consists of fines, mainly silt. This would amount to around 14 Mm^3 of sedimentation per year (density =1650 kg/m^3).

Other researchers give lower values for the sediment input from the Rio Parana. Urien gives an annual value of 80 Mton per year consisting of 75% coarse to medium silts, 15% fine to very fine silt and 10% clay (Urien, 1972). Depetris (2007) states that the mean sediment load at the start of the lower stretch of the Parana river is 80 $*10^9$ kg/year, but that it fluctuates between 40 and $100*10^9$ kg/year.

The suspended sediment concentration in the inner Rio de la Plata estuary ranges between 60 and 100 mg/L with peaks up to 600 mg/L. Vertical transects show almost complete mixture and decreasing values form the Argentine to the Uruguayan coast (Simionato et al., 2011). The suspended sediment consists of silt and clay and has a long settling velocity, resulting in a slow response to changes in hydrodynamics. Downstream the vertical mixing decreases as the influence of the tributaries decreases and influence of waves gets smaller in deeper water. Along the navigation channels the measured concentrations range from 10 to 1000 mg/L with high values in Canal Punto Indio. Important is that also in the outer Rio de la Plata the sediments are still mainly of riverine origin (Simionato et al., 2011).

The bed material around Canal Emilio Mitre is mainly silty, with around 10% sandy and 10% clayey material. The material is all from fluvial origin and is supplied by the Parana de las Palmas which has a concentration of around 250 mg/L. The fine suspended sediment which is supplied by the river comes from the Rio Bermejo which originates in the Andes mountain range.

2.5 Astronomical tide

The Rio de la Plata estuary does not have enough water mass to be affected directly by the tide generating forces. However it is affected by the co-oscillating tidal forces by the global tidal oscillation. The tidal wave from the Atlantic ocean is affected by the local differences in water depth and by the presence of land masses on its way on the continental shelf and in the estuary (Bosboom et al., 2015). The tidal wave is also affected by the Coriolis acceleration. The tidal wave which eventually reaches the Rio de la Plata has to pass the Patagonian shelf first, this region is known for dissipation and tidal resonance (Meccia et al., 2009). During propagation the period of the tidal wave does not change, however the length of the wave does change due to changes in propagation speed. The tidal wave from the Atlantic reaches the continental shelf break from the south (Kelvin wave), due to the bottom topography and the coastline geometry, the propagation is modified so that the incoming tidal wave comes from the southeast (Balay, 1961). The decrease in celerity in shallower water leads to energy bunching and thus higher amplitudes. Due to the extreme shallowness of the estuary the wavelength of the tidal wave becomes even shorter while it propagates. Therefore almost a whole wavelength is present within the estuary (Vieira & Lanfredi, 1996). Due to the fact that the estuary only converges at its last part and it is long, the tide is not amplified towards the inner parts, due to the effect of bottom friction playing an important role (Framiñan M.B., Etala M.P., Acha E.M., Guerrero R.A., Lasta C.A., 1999).

The tidal amplitude varies over the estuary, being higher at the Argentinian side due to higher tides on the continental shelf to the south than north of the estuary (Vieira et al., 1996). The Coriolis deflection to the left on the Southern Hemisphere also contributes to the tidal amplitude variation (the Rossby radius of deformation indicates that the rotation of the Earth is relevant to the fluid).

All in all the tidal signal results in a tidal range of about 1 meter at the Argentinian coast and a tidal range of about 0.40 meter at the Uruguayan side (Schuerch et al., 2016). Considering the magnitude of the tide the area is thus micro-tidal over the whole estuary.

When identifying the tidal character, the importance of diurnal versus the semi-diurnal component is determined by the form factor F (magnitudes from Santamaria-Aguilar, Schuerch, Vafeidis, & Carretero, 2017):

$$F = \frac{K1 + O1}{M2 + S2} = \frac{4 + 12\ cm}{20 + 5.5\ cm} = 0.62$$

The tidal character is thus mixed, mainly semidiurnal since F is between 0.25 and 1.5. Both the magnitude and the tidal character are important when comparing the influence of the tide to the influence of other forcers such as the river discharge. It has to be mentioned that although the tidal range is small, the combination with the large width of the estuary results in a large tidal prism. The tidal currents have a maximum speed of 0.5-0.8 m/s in front of Montevideo (Piedra-Cueva & Fossati, 2007). Measured current velocities in the Rio de la Plata Interior are maximum 0.48 m/s during flood and 0.68 m/s during ebb. The minimum flow velocities are 0.01 and 0.09 during flood and ebb respectively (Vieira et al., 1996).

According to Balay the tidal regime in the area is heavily dominated by the winds and, given a wind direction, it is possible to relate wind speed linearly with the expected variation in water level, with respect to the mean level (Balay, 1961). This is addressed in paragraph 2.6.

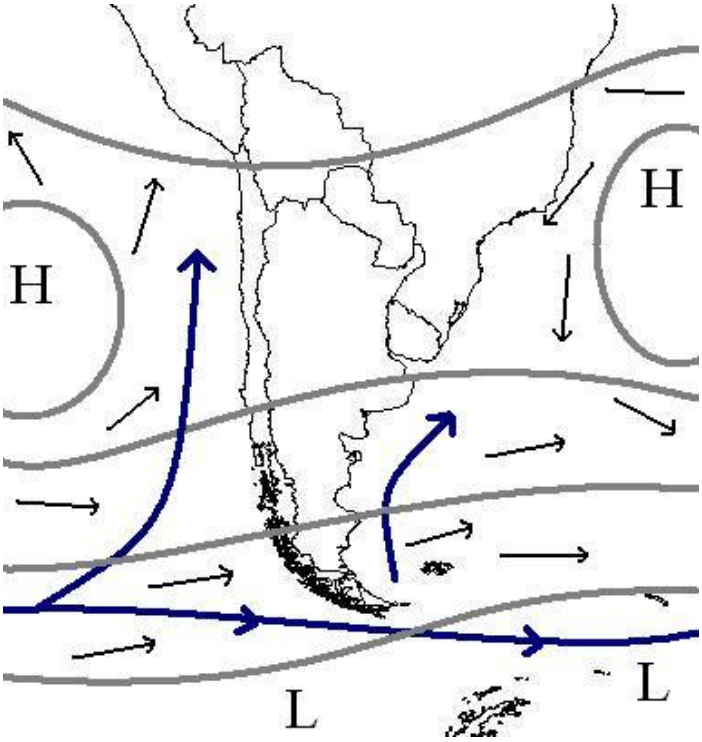

Figure 16 Location of South Pacific high pressure system and South Atlantic high pressure system. (From https://en.wikipedia.org/wiki/South_Pacific_High)

The propagation of the tide also has a significant effect on the levels of the rivers due to the low slope of the hinterland. On the Rio Parana the effect of the tide is recognisable until Villa Constitucion (220 km upstream) if the river discharge is falling, and until San Pedro (140 km) if the river is rising (Balay, 1958). Under unusual circumstances even Rosario is affected (Figure 88 for locations). Additional analysis of the water levels along the river show the same results. Along the Rio Uruguay the tidal wave is usually recognised until Concepcion (200 km), under unusual conditions it can reach up to Concordia (320 km). Extreme circumstances occur when the discharge of the river is low and the water level on the Rio de la Plata is high.

The region is influenced by the micro-tidal regime (mixed, mainly semi-diurnal) which has a range of around 1 m at the Argentinian side and 0.4 m at the Uruguayan side. Due to the low slope of the hinterland the tide protrudes far upstream on both rivers. The maximum current velocities around the region of interest are expected to be around 0.7 m/s.

2.6 Atmospheric forcing

The Rio de la Plata estuary is highly susceptible to wind forcing due to both its shallowness and its decreasing width. The atmospheric forcing results in both locally generated wind waves and storm surge.

The atmospheric general circulation in the Rio de la Plata region is influenced by two large subtropical high pressure zones (anticyclonic). These two high pressure zones are located over the Southern Pacific and the south-western Atlantic (see Figure 16). The atmospheric forcing over the Rio de la Plata catchment basin basically depends on the movement the South Atlantic high pressure system.

Overall the atmospheric forcing over the catchment basin prevails from the northeast, advecting warm and moist air from the South Atlantic high. When during winter (June-August) the high pressure system moves to the north, this increases the frequency of wind from the west, leading to relatively dry air being transported to the Rio de la Plata. During summer (December-February), as the pressure system moves southwards, winds from the east and southeast become more frequent (Barros, V. R., Boninsegna, J. A., Camilloni, I. A., Chidiak, M., Magrín, G. O., Rusticucci, 2015). These winds are called 'sudestadas' and have major effects on storm surge in the estuary.

The predominant wind direction and its magnitude (during the different seasons) can be found in Figure 19, which shows the same pattern as described earlier.

Next to the general circulation, the region of the Rio de la Plata is known as a region of cyclogenesis. The interaction of waves that move from the Pacific subtropical latitudes and the subtropical air masses from the northeast lead to about eight cyclones a year. This phenomena is introduced by anti-cyclonic cells which separate from the Southern Pacific high pressure system to the ENE. These can lead to south-easterly winds with speeds up to 15 m/s (Simionato et al., 2007).

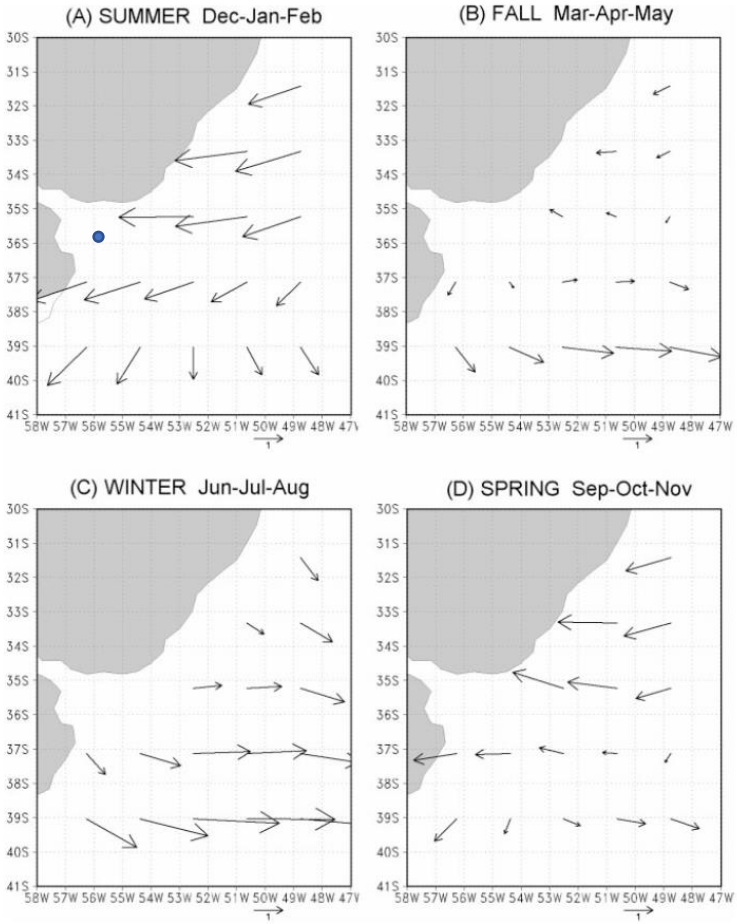

Figure 19 50-year mean vectors of wind velocity for every season (A) summer, (B) autumn, (C) winter, (D) spring. (From Simionato 2003), with location Datawell as blue dot

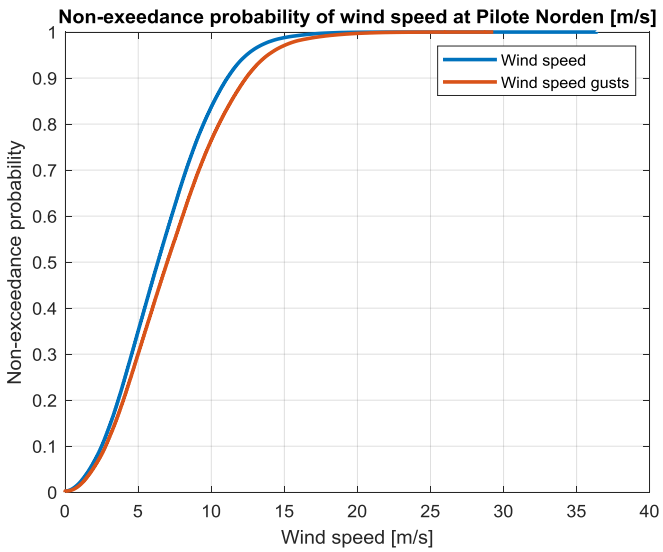

Figure 17 Non-exceedance probability station Pilote Norden 2016 per minute

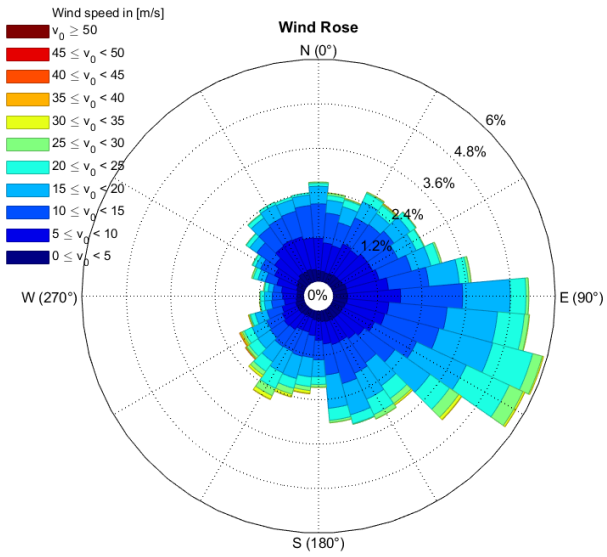

Figure 18 Wind Rose station Pilote Norden 2016 per minute

In addition to the literature study a statistical analysis was done of the wind signal at the Pilote Norden station which is located in the middle of the estuary (see Figure 88) and thus considered representative for Canal Emilio Mitre since it is not affected by the coasts. Wind velocity was recorded every minute in 2016 on a height of 10 meters above the sea surface, resulting in an average speed of 6.62 m/s (Figure 17). Figure 18 shows the directional distribution of the signal averaged over the whole year with the ESE as dominant direction. The analysis per season was also performed and showed similar results as Simionato (2003) with ESE during spring and summer.

As the high velocities are also particularly important for the resuspension of sediments from the bed, an exceedance analysis was done. 90% of the time the average wind speed stays below 11.1 m/s, 95% of the time below 12.4 and 98% of the time below 14.1 m/s (see Figure 17).

Effect of waves

The long-term wave data available is a single 5-year record from the outer area of the estuary (Datawell Waverider located at 35˚40' S and 55˚50' W location in Figure 19 and addition information in Figure 20). Anschutz showed that the wave climate is a combination of swell (period 10-12 seconds) and sea (period 4-6 seconds) waves with predominant heights between 0.5 and 1.5 m (G. Anschütz, 2000). The main directions of propagation from this measurement series are southeast, east and south with a probability of occurrence of respectively 41, 28 and 14%.

When taking into account the orientation of the Rio de la Plata estuary, only swell from the SE propagates to the inner regions. For SE component the distribution of wave heights and periods is given in Figure 20, where a clear sea and swell component can be distinguished.

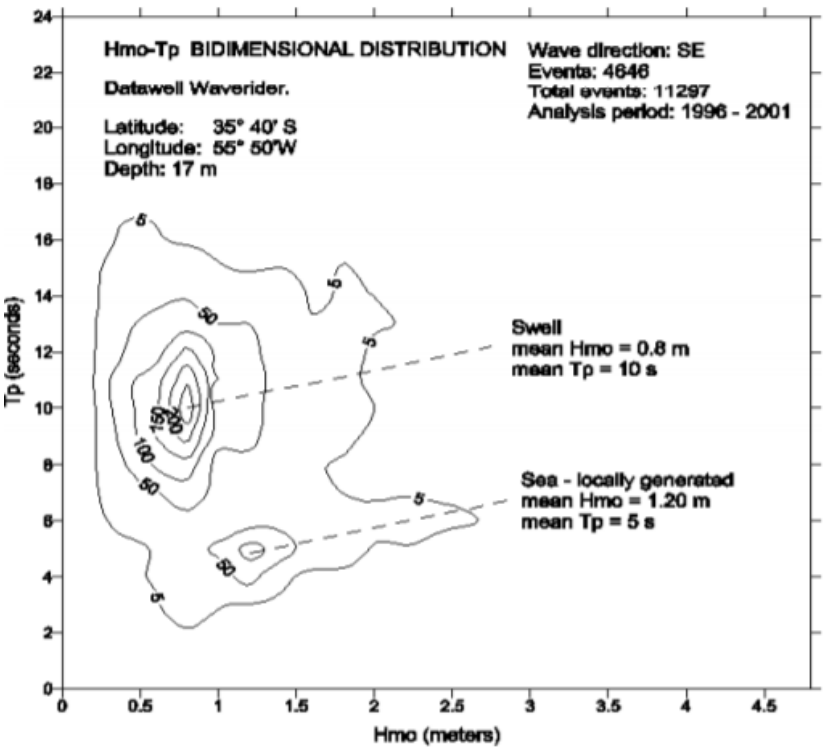

Figure 20 Bidimensional distribution of heights and periods. Mean sea and swell characteristics are indicated (From Barros 2005)

After analysing the wave propagation and transformation from the outer zone towards the inner zone of the Rio de la Plata, Barros (2005) came to the conclusion that the predominant wave climate in the inner zone of the Rio de la Plata is ruled by wind waves which are generated locally. This is because the swell waves refract to the coastline before reaching the inner Rio de la Plata. Therefore for the area around Canal Emilio Mitre only the locally wind generated waves are relevant.

No records exist of wave heights and periods within the inner Rio de la Plata. However Barros (2005) did perform a wave hindcasting analysis to approximate the wave conditions for a location with a depth of 2 meter and the monthly wind statistics from the coast of Buenos Aires City. Fetch-limited conditions have been considered since that is very relevant considering the spatial extent of the estuary (winds from the north do not cause significant waves at Buenos Aires). The data is presented in Figure 21, and shows that especially winds from the east and southeast direction are relevant for Buenos Aires. It has to be taken into account that for the region of interest of this thesis the fetch in southeast direction is longer and that the water depth is different. Still, this figure gives an indication

of the fact that sea waves are below 1.3 m in height and that wind from the SE is most relevant when considering the generation of waves. On both rivers the effect of waves is disregarded due to the short fetch.

Index	Direction	Frequency (%)	Mean wind ms^{-1}	Fetch (Km)	H_{MO} (m)	T_P s (sec.)
1	N	15.8	4.9	36	0.49	3.5
2	NE	11.5	4.6	45	0.50	3.7
3	E	18.4	4.9	125	0.90	5.3
4	SE	12.2	5.8	150	1.22	5.5
5	S	13.7	6.1	2	0.15	1.4
6	SW	7.5	5.5	2	0.13	1.4
7	W	7.8	5.2	2	0.12	1.4
8	NW	6.6	5.2	22	0.41	3.1
9	Calms	6.5	-	-	-	-

Figure 21 Directional mean wind and probability of occurrence at Aeroparque on the coast of Buenos Aires City, directional fetch, heights and periods obtained by hindcasting. (From Barros 2005)

Effect of storm surge

Balay (1959 and 1961) suggests that sea levels in Buenos Aires are closely related to the winds over the outer estuary and its shelf. The largest increase in water level is caused by winds blowing along the channel axis from the southeast during high tide, while the largest depressions of the water level are caused by winds from the north at low tide. The strong winds from the southeast are called 'sudestadas'. The highest storm surge observed reached 3.25 meter above the tidal height predicted for that moment, which was 4.06 m above the Tidal Datum at Buenos Aires (D'Onofrio et al., 1999), see Figure 22 for distribution along the estuary).

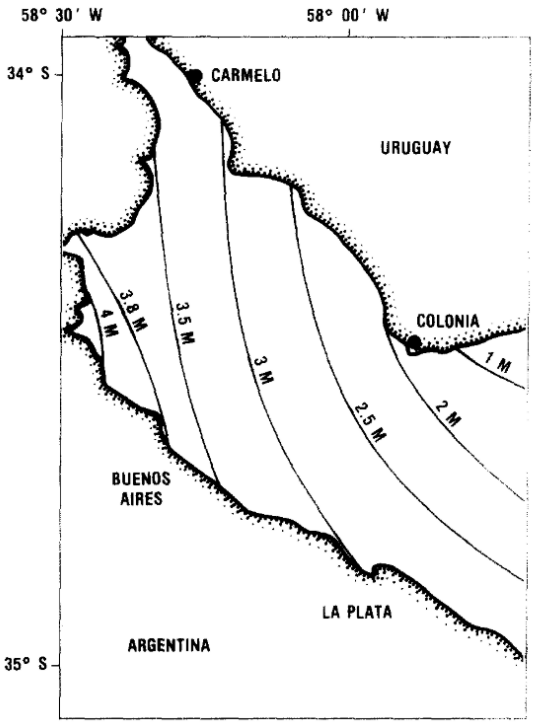

Figure 22 The sea level in meters at the time of maximum surge, 27 July 1958. (From Balay 1959)

The effect of the storm surges is largest at the area around Buenos Aires due to the long fetch over the water surface, the narrowing and shallowing shape of the estuary and the Coriolis deflection to the left. Balay (1959,1961) has studied the main flooding events in 1914, 1922, 1923, 1940, 1958 and 1959 which all had levels higher than 3 meter. This was caused by winds which had a velocity of at most 17 m/s at Buenos Aires.

The storm surges also change the current pattern in the estuary, tidal currents are usually in the order of 0.5-0.7 m/s, while during southeastern winds values ranging between 1.0 and 1.5 m/s are observed (Piedra-Cueva, 2003). This stresses the fact that winds have an important influence on the dynamics of the estuary.

Atmospheric forcing has considerable influence on the water levels, locally generated wind waves and the currents. Especially sudestadas (strong winds from the SE) lead to extreme deviations from the predicted tidal height. Around Canal Emilio Mitre the maximum expected wave height is around 1 m, and the deviation from the tidal predicted height can reach up to 3 m during extreme events.

2.7 Salinity and turbidity front

A distinctive feature of the Rio de la Plata estuary is the salinity front which is located in the vicinity of the Barra del Indio (see Figure 23 for location). The salinity front is the transition from the fluvial regime (fresh water) on the inner part to the saline water on the outer part of the estuary. The northern part of the estuary has a salinity less than 0.4 ppt while in the outer estuary the values range from 0 to 33 ppt. As described by Framinan the front shows strong seasonal and spatial variability affected by several physical forcings (Framiñan & Brown, 1996).

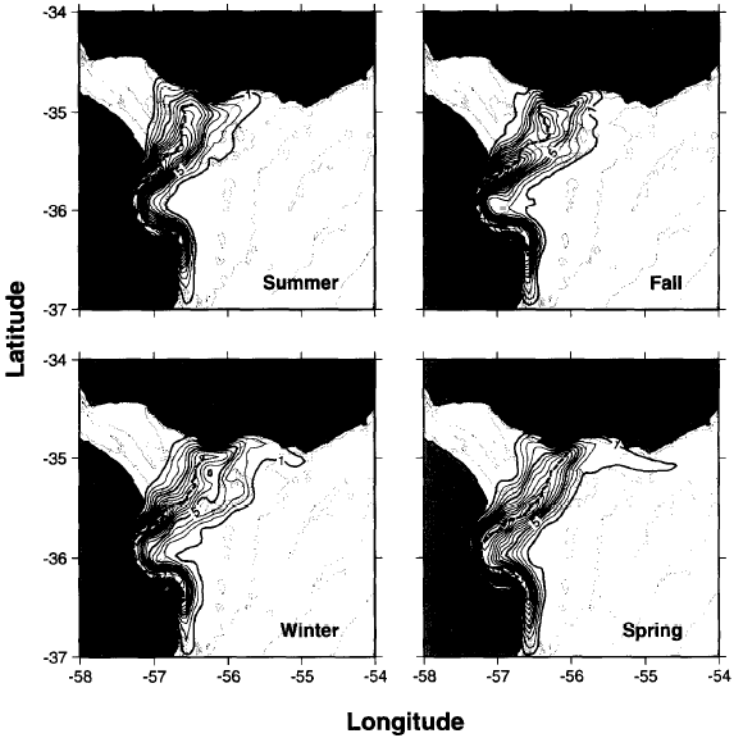

Figure 23 Frontal density distribution (contour interval 1x 10^{-5} km^{-2}) for the Rio de la Plata by season: (a), (b), (c) and (d) are plots for summer (January, February, March), fall (April. May June). winter (July, August, September) and spring (October, November, December),respectively (From Framinan and Brown 1996)

The main forcings of the surface salinity front are: a low seasonality in fresh water discharge, a strong seasonality in winds (fall and winter have winds which are balanced between onshore and offshore (N, NW,W, SW) and spring and summer winds which are onshore (NE, E, SE, S)), and a low tidal amplitude (0.3 to 1 m tidal range). In the bottom salinity the bathymetry has a leading role. This can also be seen in Figure 23, where a high standard deviation of the front is observed over the deeper channels (for example the plume along the Uruguayan coast in the Oriental Channel during spring). A relatively low spatial extent is found over the regions where channels do not exist. As described before, due to the extent and the shallowness of the system it is highly susceptible to the atmospheric forcing. Due to the winds the surface salinity front is located more towards the ocean (SW) during the fall and winter when there is high river discharge and a balance between the winds. While in the spring and summer the front moves towards the inner part of the estuary (NE) due to onshore winds and low river discharge (Guerrero et al., 1997).

As a result of the salinity front a strong turbidity front exists. During winter and fall it moves towards the ocean due to high river discharge and winds. While in summer it is located more inwards due to north-easterly winds and low freshwater discharge (Framiñan et al., 1996). The salinity front results in increased suspended sediment concentrations. During extreme onshore winds the salinity front still does not affect the salinities nor concentration near the Delta (Jaime & Menendez, 1999), therefore this process is not important to the sedimentation in Canal Emilio Mitre, but rather to the sedimentation in Canal Punto Indio.

Even during extreme conditions Canal Emilio Mitre is not affected by the salinity front, therefore flocculation due to increased salinity is not expected to play a role. Flocculation with for example organic material, is possible however.

2.8 El Niño

El Niño-Southern Oscillation (ENSO) is a phenomena on global scale related to the strong and complex ocean-atmosphere coupling over the tropical Pacific Basin. It is considered the main source of interannual climate and weather variability all around the globe. The phenomena has three phases: El Niño (warm phase), La Niña (cold phase) and the neutral phase. El Niño and La Niña refer to the oceanic components while Southern Oscillation refers to its atmospheric component.

El Niño is a naturally occurring event, it occurs generally every 2-7 years and can last up to 18 months (WMO, 2014). The World Meteorological Organization prepares forecasts of El Niño and La Niña episodes regularly, this is done based on observational modelling of the current, predictions through climate models and expert judgement. El Niño events typically starts with large scale warming of the surface waters in the central and eastern equatorial Pacific. Its peak is reached during November-January and then reduces in strength during the first half of the next year.

The ENSO phenomena has direct influence on the weather in the surrounding countries, this is called a teleconnection. An important feature of the phenomena is that the outcomes of each El Niño is different, it is dependent on the strength and timing of the El Niño event as well as the interaction with other climate patterns. However very clear trends can be distinguished, these should be interpreted as typical effects and not as forecasts (WMO, 2014). For the Rio de la Plata catchment basin this results in wetter conditions than normal, between December and February, as can be seen in Figure 24. La Niña events (cold episode) lead to dryer conditions between June and August.

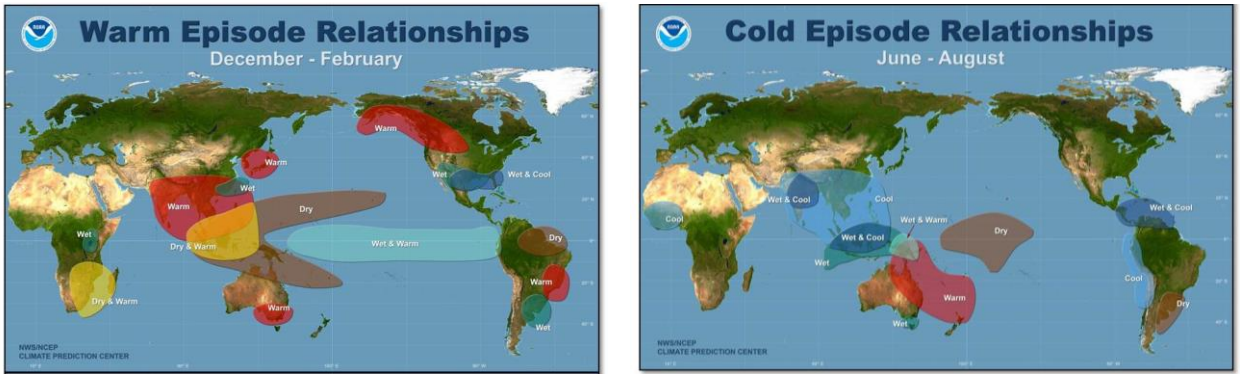

Figure 24 Maps of teleconnections affecting Rio de la Plata catchment basin (From NOAA National Weather Service Climate Prediction Center, year unknown)

The influence of ENSO leads both to an increase in frequency and intensity of extreme rain events over southeasthern South America in all seasons, causing consistent impacts on the discharge of the Rio Parana (A. M. Grimm & Tedeschi, 2009). The differences in space are shown in Figure 25. Since the precipitation anomaly is located over the catchment basin of the Rio Bermejo it is assumed that the sediment input per discharge unit stays constant, thus that the discharge is not diluted or gets more concentrated.

Next to the increased discharge Meccia et al. found that the ENSO cycles are also associated with surface wind anomalies over the Rio de la Plata (Meccia et al., 2009). During El Niño there is a dominant component from the east and during La Niña there is a dominant component from the west. This has an effect on the storm surge, which leads to high water levels in the Rio de la Plata estuary.

Barros et al. suggest that the increase in discharge in the main rivers in the Rio de la Plata basin is mainly due to the intensification of the El Niño events (see Figure 30 for long term trends of the discharge) (Barros, 2005). When analysing the 10 largest monthly discharge anomalies of the Parana River between 1904 and 2000, it is striking to see seven of them occurred during El Niño events and that four out of the five highest discharges occurred during the last 20 years (see Figure 26). Overall none of the high discharges occurred during a La Niña event. For the Paraguay River the same trend is seen with respect to the ENSO events, however with less strength (Barros, 2005). Since the discharge is considered an important forcer to the sediment discharge to the Rio de la Plata, the El Niño occurrences are considered an important forcer to the sedimentation in Canal Emilio Mitre. The trends in the strength and frequency of the ENSO events is discussed in paragraph 3.2.5.

The catchment basin of the Rio de la Plata estuary is highly influenced by the ENSO phenomena, main result is an increase in rainfall and discharge of the Rio Parana. Research also reveals a link with surface wind anomalies.

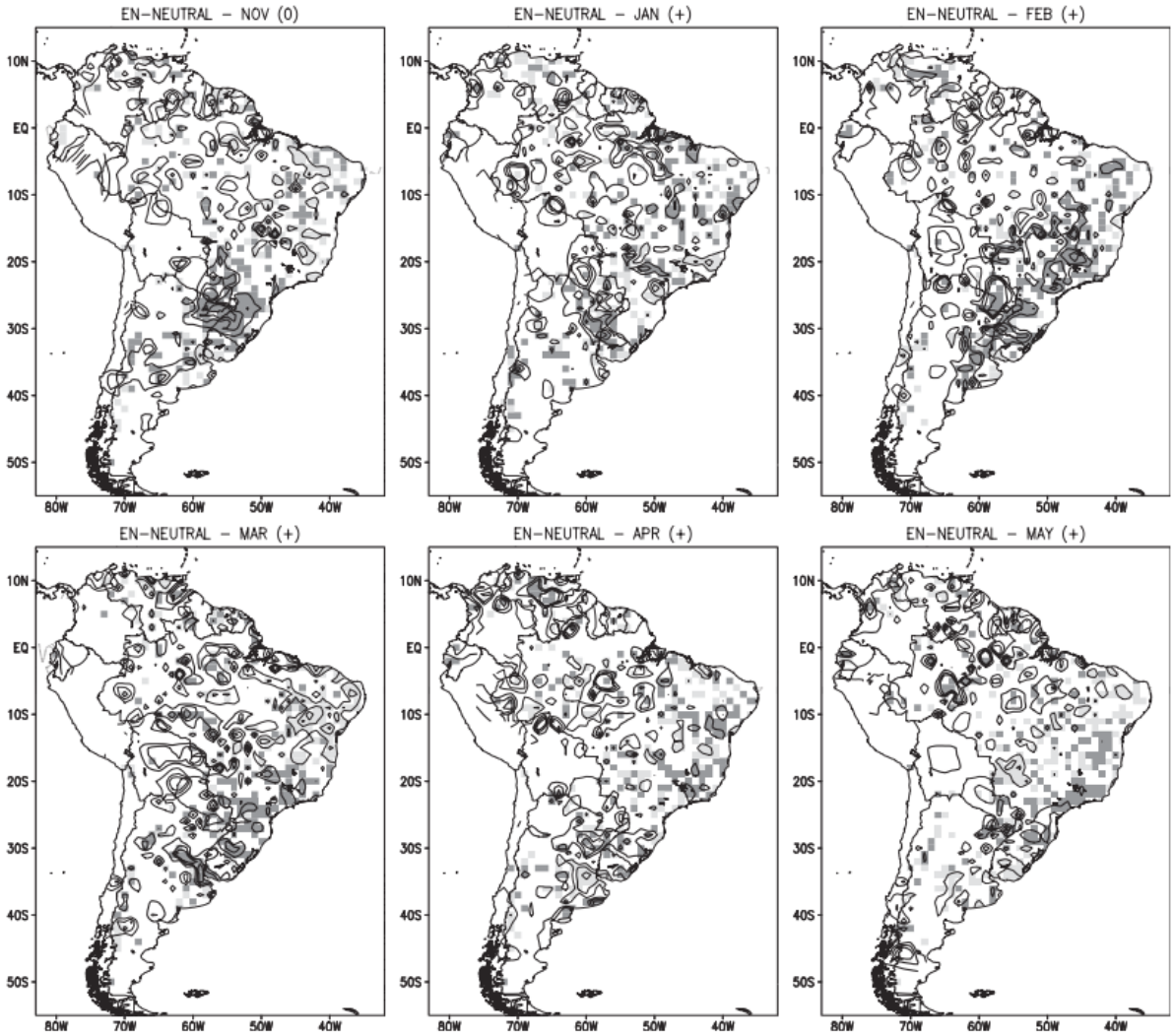

Figure 25 Differences between average daily rainfall during extreme events in El Niño years and neutral years. Contour interval is 2 mm day21. Positive (negative) differences significant over the 90% confidence level are dark (light) shaded (A.M. Grimm & Tedeschi, 2009)

Date	Season and ENSO phase	Discharge anomaly ($m^3 s^{-1}$)
June 1983	Autumn Niño (+)	38 300
June 1992	Autumn Niño (+)	26 800
December 1982	Summer Niño (0)	26 100
March 1983	Autumn Niño (+)	24 200
June 1905	Autumn Niño (+)	24 200
May 1998	Autumn Niño (+)	23 000
October 1998	Spring—neutral	21 000
October 1983	Spring—neutral	20 500
July 1992	Winter Niño (0)	18 800
February 1997	Summer—neutral	17 700

Figure 26 The largest 10 monthly discharge anomalies of the Parana River for 1904-2000 (From Barros et al. 2005)

2.9 Area of influence of physical forcers total system

Based on the findings in the previous paragraphs the area of influence of the various forcing mechanisms is visualised in Figure 27. Overall the estuary is divided into two regions by the Barra del Indio ; the shallow part upstream of the shoal is ruled by the fluvial discharge in combination with the micro-tidal regime. The part of the estuary downstream of the topographic feature exhibits micro-tidal estuarine dynamics, influenced more by the forcings on the estuary. This conclusion matches the work by M. Fossati and F. Cayocca (2014). Furthermore, from the literature it is concluded that the entire estuary is heavily influenced by the atmospheric forcing, affecting the water levels, currents and waves. This matches the observation of Officer that in large estuaries, the estuarine geometry, atmospheric and wind stress effects and the lateral effects also become important (Officer, 1992). Mainly the interaction between the complex bottom topography and the influence of tidal, atmospheric and fluvial forcing lead to high temporal as well as spatial variability of the estuarine processes (Fossati & Piedra-Cueva, 2008).

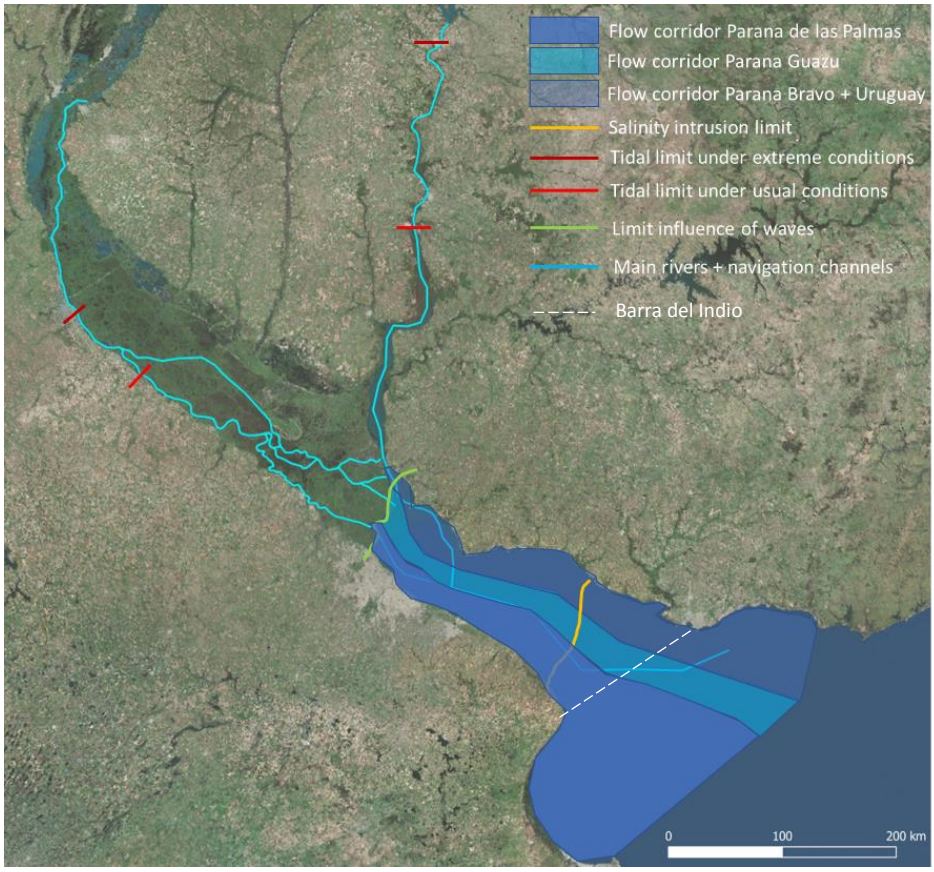

Figure 27 Conceptual model forcings total system

2.10 Conceptual model of physical forcers of sedimentation Canal Emilio Mitre

The sedimentation in Canal Emilio Mitre is forced by the following processes (see Figure 28 for visualisation):

1. Supply of sediment from upstream: The Rio Parana de las Palmas supplies suspended sediment (mainly silt, but also some clayey and sandy material, concentration = 250 mg/L). The discharge of the river has a pronounced peak around January and the dependence of the discharge on ENSO leads to interannual variability of the sediment supply to the system.
2. Infill from the flats: The channel with its depth of around 10 meters is affected by infill of sediments from the flats which have depths between 1 and 5 meters adjacent to the channel. The locally generated wind waves are responsible for the upstirring of the sediments and keeping it in suspension (up to 1 m wave height during extreme events). The tidal flow transports the sediment-rich water over the channel which has a lower transport capacity leading to sedimentation (tidal range ~0.5 m and tidal currents 0.5 m/s during regular circumstances). Especially highly energetic wind events are expected to lead to redistribution of the sediments in the system due to an increase in flow velocities (1-1.5 m/s).
3. Export of suspended of fine sediments: Clayey material in suspension is exported out of the system to the downstream part of the estuary. Since the salinity limit of the estuary is located far downstream of the area of interest (also during highly energetic events) salinity differences

are not taken into account and flocculation due to interaction with the saline water is not expected to play a role.

In this chapter data is gathered for modelling of the processes which force the sedimentation. The supply of sediment from upstream is an input of the model. The infill from the flats is modelled taking into account the tide and atmospheric forcing. The export of suspended sediments is also an output of the model.

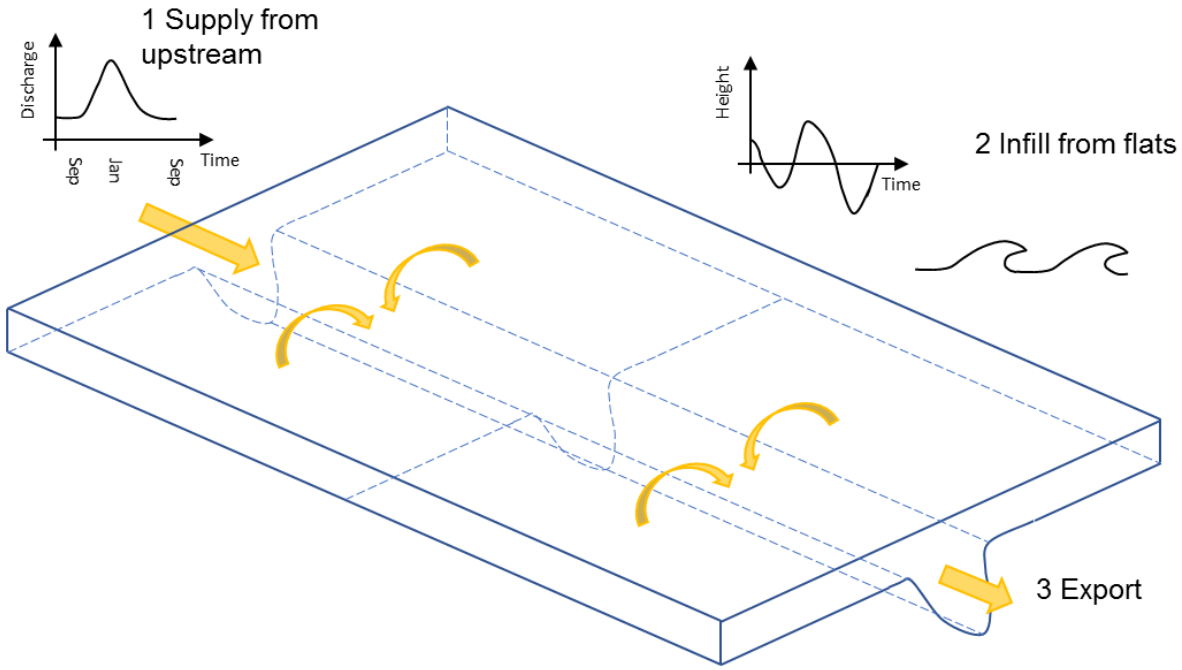

Figure 28 Forcing mechanisms sedimentation in Canal Emilio Mitre

3 Effect of climate change/variability on the physical processes

This chapter analyses the effect of climate change on the physical processes that affect the hydro- and sediment dynamics of the Parana delta. Paragraph 3.1 presents the effect of climate change on the hydrodynamics in coastal systems globally. The basis for the analysis is Chapter 5 of the IPCC Fifth Assessment Report (WGII AR5) with the title: *Coastal systems and low-lying areas* (Wong et al., 2014). This analysis is extended in paragraph 3.2 by presenting the local effects of climate change on the catchment basin of the Rio de la Plata and the estuary. Chapter 27 of the IPCC WGII AR5 report (Magrin et al., 2014) is used as a main source, it describes the effect of climate change on Central and Latin America. To conclude paragraph 3.3 presents two climate scenarios which are expected to have a major effect on the sedimentation of Canal Emilio Mitre.

3.1 Effect of climate change/variability on forcings of hydrodynamics of estuaries and deltas

According to IPCC the main climate-related drivers which affect coastal systems and low lying areas are: sea levels, storms, winds, waves, extreme sea levels, sea surface temperature, freshwater input and ocean acidity (Wong et al., 2014). However not all of these drivers (directly) affect the physical processes which force the hydrodynamics of estuaries and deltas. For those forcings mainly the sea levels, storms, winds, waves and freshwater input are important. Climate change in this section can be both climate-induced or human-induced. Both estuaries and deltas are investigated as the southern part of the system is clearly an estuary and the northern part of the system is a delta. The interaction between those entities also plays a large role as the boundary conditions from the delta influence the estuary and the other way around.

Observed impacts of (human- induced) climate change on the hydrodynamics of estuaries world-wide include:

- Changing human drivers such as dredging and channelization have led to change in sediment accumulation. Indirectly the sediment accumulation has also been also changed by habitat loss, changes in sea level, storminess and freshwater and sediment supply by the waterway (Syvitski et al., 2004).
- Change of the occurrence of floods and droughts, and sea level rise have led to change in the estuarine circulation, turbidity and tidal characteristics (Wong et al., 2014).

Projected impact of climate change on the hydrodynamics of estuaries include:

- Change in sea level may lead to sediment redistribution, change in salinity, tidal range and submergence periods (Anthony et al., 2009)
- Change in duration and strength of storm events may affect the sediment deposition-erosion balance of estuaries (Pilkey & Young, 2009)
- Change in precipitation regime and discharge distribution may lead to change in salinity in the estuary, eventually also leading to changes in the ecosystem (Jeppesen et al., 2007)

The IPCC report stresses that currently the most important drivers of change in estuaries are human-related changes over climate-induced changes.

Observed impacts of (human- induced) climate change on the hydrodynamics of delta's world-wide include:

- Widespread degradation of deltas due to decrease in sediment input from the rivers. Relative sea level rise, land use changes, river management concerning the banks and also

structures such as dams also play a role. This combined effect leads to degradation of various systems such as mangroves, subaqueous deltas and tidal flats.
- River floods and oceanic storm surge lead to flooding. Syvitski et al. found that 85% of the 33 investigated deltas have been subject to severe flooding (Syvitski et al., 2009).
- Sea level rise leads to coastal erosion, salt water intrusion into deltas and increased coastal flooding (Mcleod et al., 2010)

Projected impact of climate change on the hydrodynamics of deltas include:

- Extreme precipitation induced flows and sea level rise may result in coastal flooding, increased coastal erosion and increased salinization of cultivated land and groundwater (Mcleod et al., 2010). Syvitski et al. have estimate that using IPCC AR4 sea level rise for 2100 the flooding of the 33 previously mentioned deltas goes up with 50 percent (Syvitski et al., 2009).

The IPCC report states that during the last 50 years human-induced drivers (land use changes, sediment delivery) have affected the deltas more strongly than climate-induced forcers.

3.2 Effect of climate change/variability on the Rio de la Plata catchment basin

In this section the effect of climate change on the catchment basin of the Rio de la Plata is discussed, with the ultimate goal to find which forcers of the hydrodynamic system are affected by climate change. Both changes due to natural climate variability and anthropogenic drivers such as change in land-use are considered. The focus is on the effects which have been identified by the IPCC in the previous paragraph.

3.2.1 Temperature

Several studies have observed circulation changes on interannual and decadal scale since the 1960s, leading to changes in temperature over the Rio de la Plata catchment basin. As a result the number of cold days and nights went down, while the number of warm days and nights went up (Magrin et al., 2014). As the change in temperature does not have a direct effect on the hydrodynamics this effect is not considered further. However the indirect effect of changes in temperature might be severe, changes in the evaporation can lead to a change in land-use which in its turn my lead to a change in sediment production.

3.2.2 Precipitation and discharge

The variability and amount of precipitation in the Rio de la Plata basin has been studied extensively. Since the 1960s a clear increase in precipitation has been measured. Considering all the sub-continental regions over the globe, southern South America is even the region with the largest positive trend during the last century (Giorgi, 2003). Doyle et al. quantified the increase in precipitation as 5 mm per year on average over the entire basin after analysing data from 1960 until 1999 (Doyle et al., 2012). Note that for the north-eastern section of the drainage basin a negative trend concerning the precipitation amount is observed. Overall this has led to an increase of the total precipitation volume of 15% averaged over the basin from 1960 until 2000 (Berbery et al., 2002).

The distribution of the growth in precipitation over the area and the different ENSO stages has been investigated using a trend analysis (Silva & Berbery, 2006). The results are shown in Figure 29, they give information about which mechanisms caused the trends that were observed. Increasing rainfall over central and south-western Argentina are attributed mainly to the neutral years. The increasing rainfall over Uruguay, Paraguay and Brazil is mainly during El Niño years. Furthermore, it is striking to see that La Niña causes a trend of around 0 almost everywhere. Therefore when assessing changes in extreme discharges no extra attention needs to be given to the La Niña phase.

The combination of the warmer and wetter climate may have a positive influence on the crop yield in the western and southern region of the Pampas, located in Argentina (Magrin et al., 2014). This may

lead to extension of the area of agricultural land. Since crops lead to less evapotranspiration than the original vegetation this may lead to even higher discharges. Again also here the change in land-use may affect the sediment load and therefore the have an effect on the sediment input in the system.

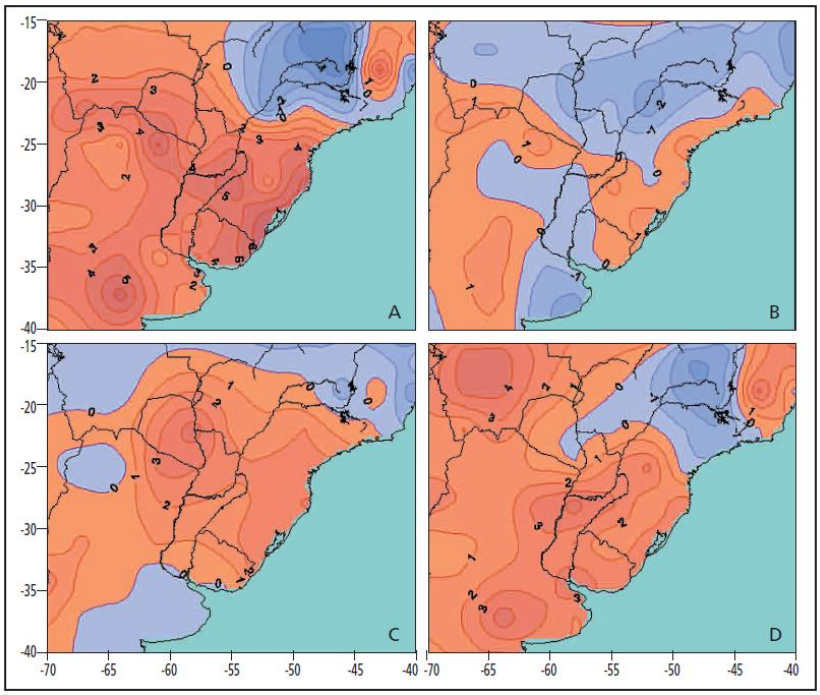

Figure 29 Precipitation trends for 1961-2000 in mm/year (a) annual precipitation (b) La Niña contribution (c) El Niño contribution and (d) neutral years contribution (From Berbery et al. 2006)

When considering the effect of climate change on river discharge a distinctive feature of the La Plata Basin has to be taken into account. Berbery and Barros (2002) found that the rate of change in precipitation in the basin leads to a rate of change of discharge which is generally two times higher. The previously mentioned 15% fractional change in precipitation led to a 36 % fractional change in discharge. This implies that before a larger part of the precipitation was evaporated or infiltrated, while during the latter period a larger part is transferred into streamflow. Berbery and Barros (2002) consider that on decadal time scale this could be partially due to change in land use and deforestation. However after comparing the percentage change between various years, this study comes to the conclusion that this feature cannot be attributed to the land use. It is an intrinsic and natural feature of the system that is important to take into account when assessing its behaviour as a reaction to climate change (Berbery et al., 2002). Doyle and Barros found that the increased discharge of the basin is attributed to three mechanisms. The first one is the increasing precipitation in most of the basin, followed by decreasing evaporation due to change in land use. A minor contribution is due to other climate variables (Doyle et al., 2011).

The increased amount of precipitation has led to increased river discharge, but also to greater severity and frequency of flooding. The increased discharge has also been observed in measurements since the 1970s (Figure 30). The alluvial valleys of the three rivers have been flooded more often since the seventies of the previous century. (As described in Chapter 2 no extremely low discharges occurred after the 1970s due to the construction of dams in the upper Rio Parana).

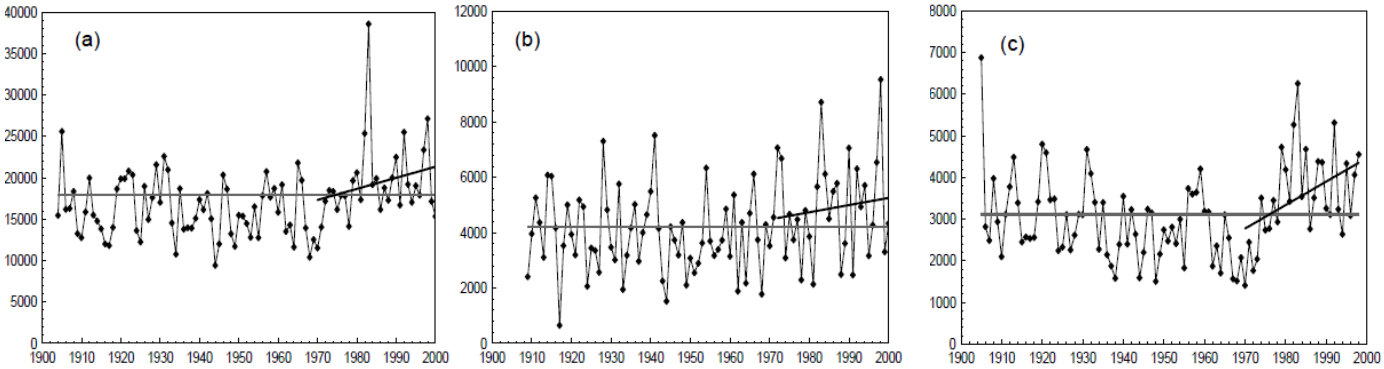

Figure 30 Annual discharge in m^3/s for (a) the Parana River at Corrientes (b) the Uruguay River at Paso de los Libres and (c) the Paraguay River at Asuncion (----- indicates the annual average and — the linear trend since 1972) (From Barros et al. 2005)

Figure 31 shows the monthly average discharge at Corrientes in time (Rio Parana) which confirms that since 1970 the average discharge has grown by around 40 percent. Before 1970 the average discharge was around 12,500 m^3/s, while since 1970 the average is around 17,500 m^3/s. When extrapolating this trend this leads to an expected 8.5 percent growth in the coming 10 years. Figure 31 shows the same trend when the average monthly discharge at Corrientes is chosen.

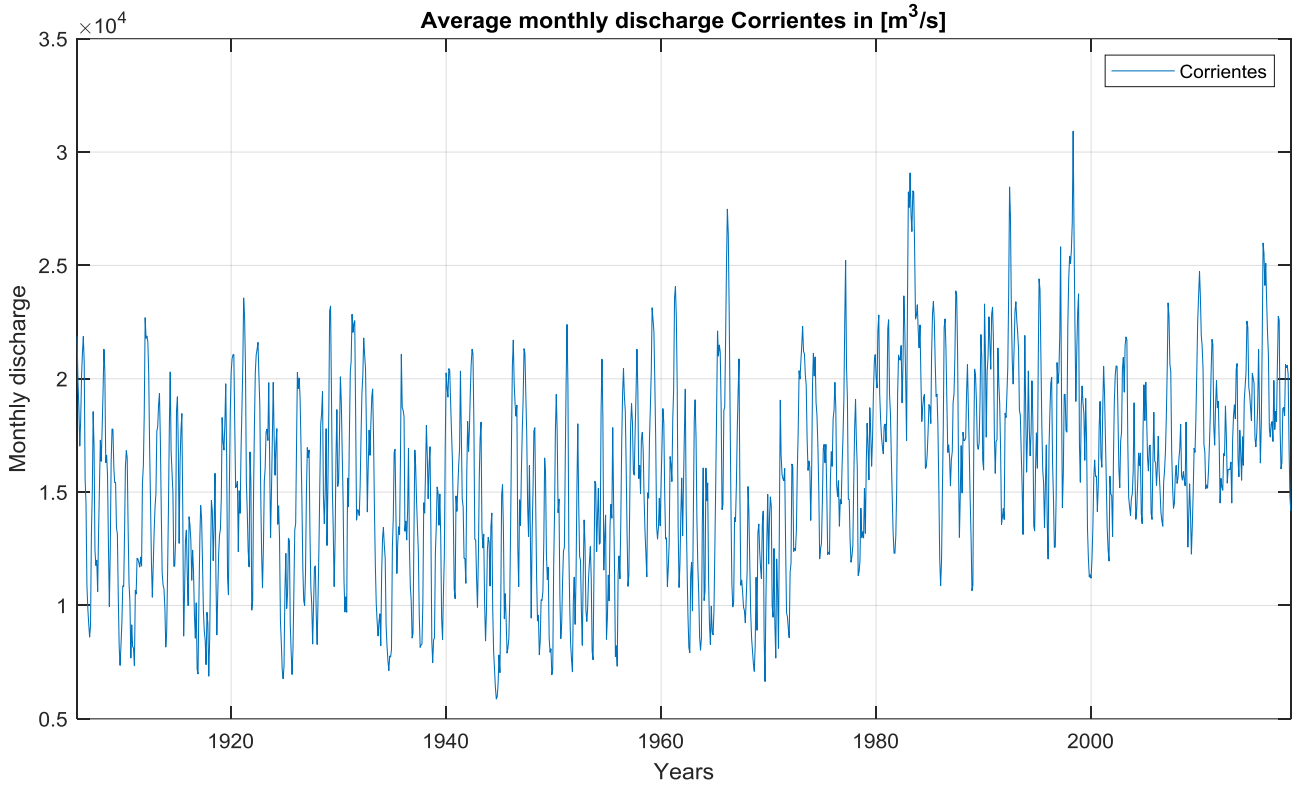

Figure 31 Average monthly discharge in Corrientes (Rio Parana), based on data from INA

3.2.3 Wind system and storm surges

Simionato et al. analysed the surface wind variability on interannual scales over the Rio de la Plata estuary (C. Simionato et al., 2006). The NCEP/NCAR reanalysis between 1948 and 1997 showed two distinctive and important modes of variability on interannual timescales (Figure 32). The first mode (47% of the variance) is a low-frequency modulation of the main seasonal pattern with periods around 2 years and is highly correlated with SST changes over the western tropical Pacific. This results in southeasterlies over the Rio de la Plata basin in case of negative sea surface temperature anomalies over the western tropical Pacific. During positive sea surface temperature anomalies this leads to northwesterlies. This phenomena is explained by the fact that changes in temperature over that tropical Pacific warm pool are known to introduce changes in the atmospheric convective systems. Due to these changes an atmospheric Rossby wave train (giant meander in high-altitude winds which have large influence on the weather) is known to travel from the tropical western Pacific, reflecting on the Antarctic Peninsula, in the end extending eastwards over the South Atlantic. This atmospheric wave train causes a anticyclonic anomaly over the western part of the Atlantic leading to southeasterlies at the Rio de la Plata. The relevance of the occurrence of southeasterlies is high since these lead to storm surge on the Rio de la Plata.

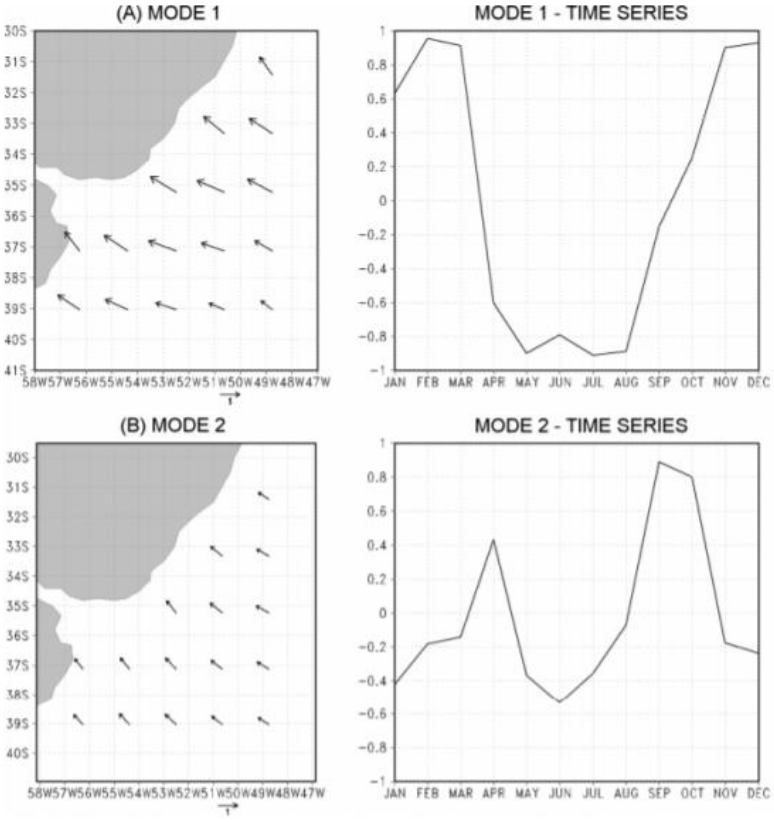

Figure 32 (A,B) Spatial patterns and (C,D) the related time patterns of the two first modes obtained by a principal component analysis on t-mode of surface wind climatological monthly means (From Simionato et al. 2006)

The shift of the wind system had a significant effect on the Rio de la Plata estuary. Especially around Buenos Aires positive storm surge and negative storm surge due to respectively south-easterly and northwesterly winds lead to problems of flooding in case of positive storm surge and difficulty with navigation and supply of drinking water in case of negative storm surge (D'Onofrio et al., 2008).

Next to the change in wind system also changes in the frequency and duration of storm surges have been observed in the Rio de la Plata. Fiore et al. looked at changes at Mar del Plata which is located outside of the estuary on the south (Fiore et al., 2009). D'Onofrio et al. (2008) looked at changes at Buenos Aires. Relative sea level rise is mentioned by both authors as a possible explanation, since an increase in water depth affects the generation, propagation and dissipation of storm surges. However also the southward shift of the South

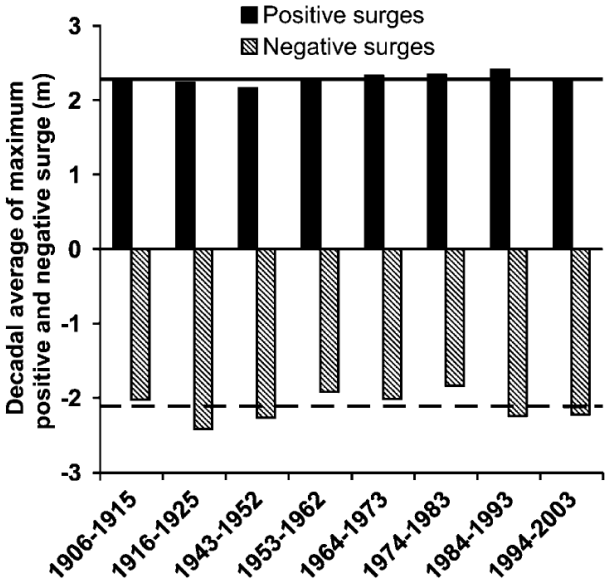

Figure 33 Decadal averages of the maximum positive and negative surges in each year. The solid and dashed lines represent the mean values for positive and negative surges, respectively. (From D'Onofrio 2008)

Atlantic high during the last decades of the twentieth century is mentioned (Barros, 2005). This would explain the increase of eastern winds leading to positive storm surges. The third possible reason mentioned is the southward shift of the regional atmospheric circulation over the southern portion of South America (A. Grimm et al., 2000).

Figure 34 shows the decadal averages of the maximum positive and negative surges in each year. Positive surge levels increased with +1.46 ± 0.8 mm/y and the negative storm surge increased with + 1.02 ± 0.09 mm/y. These trends are of the same order of magnitude as the relative sea level rise at Buenos Aires, which is estimated as 1.68 ± 0.05 mm/y. The duration of positive surges went up (+0.22 ±0.12 h/y) while the duration for negative storm surges went down (-0.23 ±0.12 h/y) (D'Onofrio et al., 2008).

The relevance of this change is illustrated by the IPCC report of South America (Magrin et al., 2014) which mentions the region of the Rio de la Plata specifically as a region where strong trends are found in storm surge extremes. It quotes a study by ECLAC on climate variability, dynamics and trends in south America which suggest a trend of 5 mm/year increase of storm surge level and a 3.6 meter high storm surge level for a return period of 50 years as of 2040 (Rodríguez & Mendeze Incira, 2015).

3.2.4 Sea level rise

Re concluded that when considering the water level in the Rio de la Plata estuary for the decades of 2030 and 2070 that mean sea level rise is a more important factor than the influence of wind and the discharge from the tributaries to the estuary as a whole (Re, 2005). Although the interest and spatial scale of this thesis is different, this is a clear indication that sea level rise has impact on the area.

When taking into account the effect of sea level rise it is important to look at the conditions at the specific site. Local sea level change differs significantly from the global average. Surface winds which shift, the addition of melting ice influencing the ocean currents, subsidence and the expansion of warming ocean water are all processes that can lead to differences over the globe. Especially with the melting of Antarctica which is located relatively close, this is important to take into account. Also local processes like sediment compaction and seismicity can play a role (Church et al., 2013).

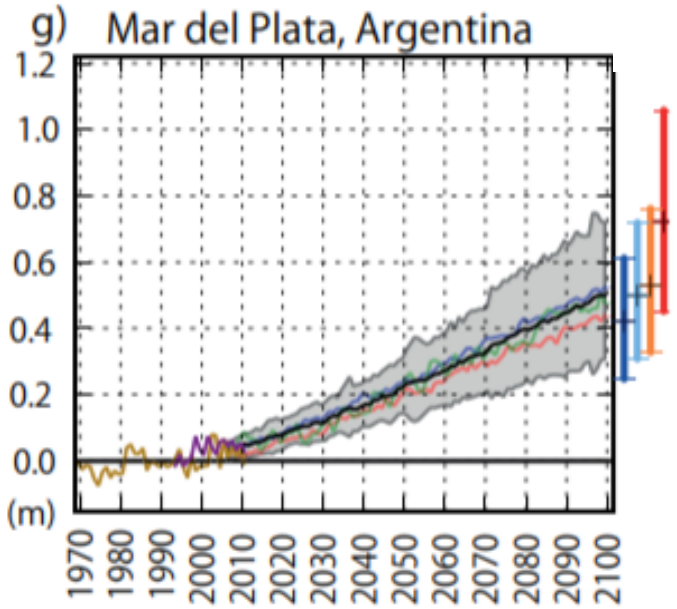

Figure 34 Observed and projected relative sea level change near Mar del Plata. Observations tide-gauge measurements since 1970 (yellow), satellite record since 1993 (purple), projected range from 21 CMIP5 RCP 4.5 scenario runs with 90% uncertainty for the period 2006-2100 (shaded region with bold line as ensemble mean), colored lines represent three individual climate mode realisations drawn randomly from three different climate models used in the ensemble. (From IPCC 2013)

The closest sea level rise forecast by the IPCC is located at Mar del Plata, Argentina (38.0 S, 57.5 W). This station is located south of the estuary on the Atlantic Ocean. The IPCC estimates a relative sea level rise of 4.8 mm/year until 2100 (see also Figure 34 for different scenarios).

Due to the wind rotation to the east the effect of the average sea level rise in the Rio de la Plata is expected to be higher than the sea level rise at the ocean. Also therefore the Uruguayan coast experiences higher levels than the Argentinian coast, especially closer to the delta (Barros, 2005).

A record of annual mean sea levels for 1905-2001 analysed by Barros (2005) found that the trend at Buenos Aires over those years was a sea level rise of 1.7 mm/year, resulting in a sea level rise of

around 17 centimetre during the twentieth century, about 50% of the rise occurred during the last 30 years of the record. This is the only long term sea surface elevation in the estuary so no comparison can be made between different stations.

The expected effect of sea level rise on the rivers is that a backwater curve comes to existence which in the end, due to the reduced discharge capacity of the river, leading to sedimentation over the part of the river where the backwater affects the river. If the water level goes up by half a meter, after a long time the bed level of the river also goes up by half a meter. This process of aggradation takes much longer than the rise of the water level in the estuary. The propagation of the backwater curve into the river is favoured by the low slope of the hinterland of 0.01 m/km (Barros, 2005).

The impact of relative sea level rise on the tidal propagation in shallow, well-mixed estuaries is hard to predict. Some estuaries flush more efficiently, while others silt up more quickly. Friedrichs et al. already mentioned this is his report in 1990 (Friedrichs et al., 1990). This subject has not been studied specifically for the Rio de la Plata estuary, but since the sea level rise may affect the tidal range and tidal wave propagation also the direction of the currents and the sedimentation pattern might be affected (Flather et al., 2001).

As mentioned in paragraph 2.7 change in precipitation/discharge may lead to changes in the salinity distribution in estuaries, which is in its turn important for where the turbidity front is located. No observations or research about the movement of the salt wedge due to climate change in the Rio the la Plata have been found.

3.2.5 El Niño-Southern Oscillation under the influence of climate change

The effect of the climate phenomena El Niño-Southern Oscillation on the physical forcers over the Rio de la Plata catchment basin was addressed in paragraph 2.8. This paragraph describes the changes in frequency and strength of the phenomena in history.

Several El Niño indices are available to assess the strength of the El Niño event, different metrics are used ranging from sea surface temperature to sea level pressure or out-going longwave radiation. In this research the Oceanic Niño Index (ONI) index by NOAA is used which is the running 3-month mean sea surface temperature anomaly for the Niño 3.4 region (5˚N-5˚S, 120˚-170˚W). Events are defined as 5 consecutive overlapping 3-month periods at or above the +0.5˚ anomaly for warm (El Niño) events and at or below the -0.5˚ anomaly for cold (La Niña) events, the strength of the event is determined based on the value which is exceeded for at least 3 months:

- Weak (with a 0.5˚ to 0.9˚ SST anomaly)
- Moderate (1.0˚ to 1.4˚ SST anomaly)
- Strong (1.5˚ to 1.9˚ SST anomaly)
- Very Strong (≥ 2.0˚ SST anomaly)

Figure 35 shows the ONI index since 1950, strong El Niño events are indicated by their year of occurrence. It is observed that the strength of the very strong El Niño since 1950 became higher. Additionally, the record shows that after a very strong El Niño it is not likely that a second very strong El Niño will occur within a few years. When applying statistics to this data it is found that the chance of a strong El Niño is 13.0% per year and the chance of a very strong El Niño is 5.8% per year. Table 1 shows the probability of occurrence of X number of El Niño events during the potential project duration of 10 years. Since the chances that one or more (very) strong El Niño event will occur during the project duration of 10 is large, this is considered an important source of climate variability. Next to the occurrence of the El Niño event, also the intensity is expected to have a significant effect on the increase of discharge and sediment input.

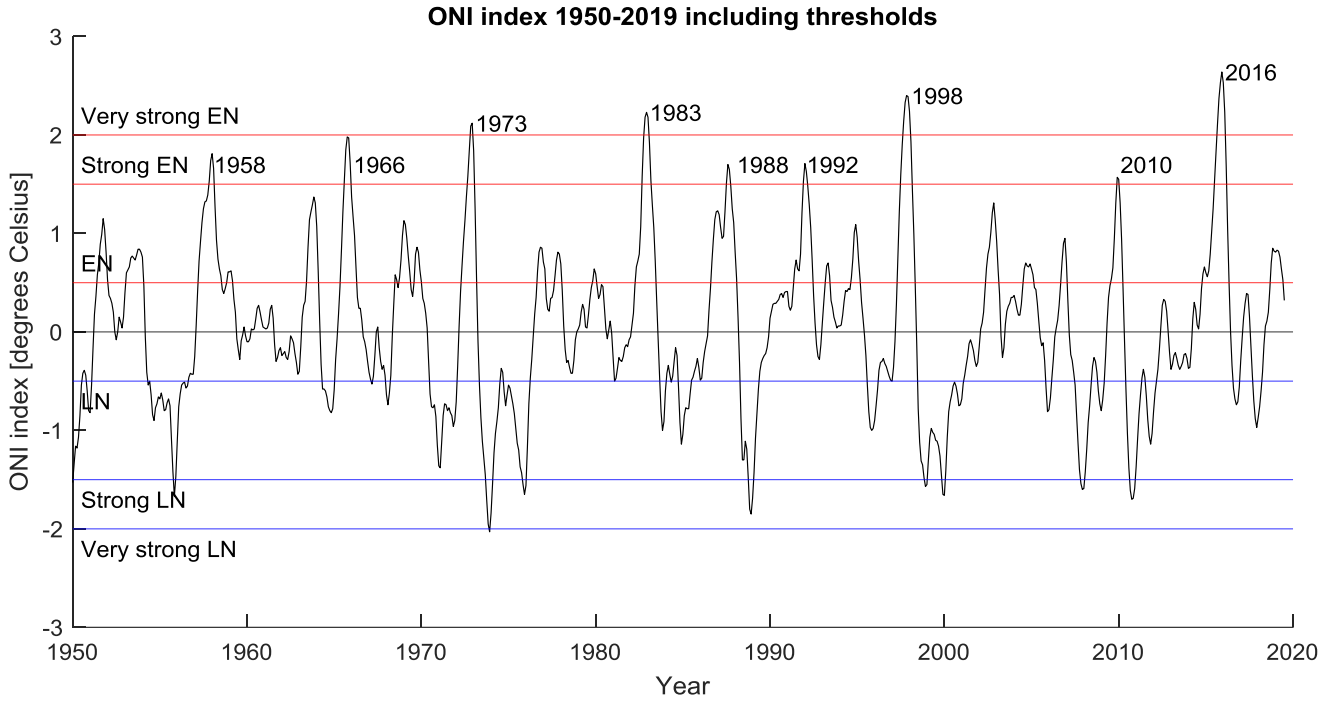

Figure 35 Oceanic Niño Index 1950-2019

	0 events	1 event	2 events	3 events	4 events
Strong El Niño (+1.5 ˚C)	27.1%	35.4%	23.1%	10.0%	3.3%
Very strong El Niño (+2.0 ˚C)	56.0%	32.5%	9.4%	1.8%	0.3%

Table 1 Probability of occurrence X number of strong or very strong El Niño events in 10 years

Until recently longer records were not available, however innovative research produced world's first 400-year long seasonal record of El Niño event by using samples from corals (Freund et al., 2019). The 400-year record showed a change in El Niño types, with an increase of the Central Pacific El Niño activity during the late 20th century and suggested future changes to the strength of the Eastern Pacific El Niño. The 1998-1999 and 2015-2016 events are mentioned as hints of the stronger Eastern Pacific category. Both according to the 100 year instrumental record of the NOAA and the record from the coral the previously mentioned, recent stronger Eastern Pacific El Niños were the strongest ever measured. The research also concludes that during the past four centuries, the most recent 30 years shows fewer, but more intense Eastern Pacific El Niño events. On the other side assessing whether the changes in ENSO are natural or anthropogenic is difficult to detect against a background of large internal variability (Cai et al., 2014).

There is no doubt that the ONI index is predictable, though the limits of its predictability are still a subject of considerable debate in science. As a result of over two-decades of intensive observational, theoretical and modeling efforts, El Niño's basic dynamics is now well understood and its prediction has become a routine practice at application centers all over the world (Chen et al., 2008). Currently the different kind of models have useful skills in predicting typical indices of El Niño at lead times of 6-12 months. At a 6 month lead, the model by Chen et al (2004) was able to predict most of the warm and cold events which occurred during this long period, especially the relatively large El Niños and La Niñas, though the model had difficulties with small events and no-shows. This kind of skill is representative of the current status of prediction.

3.2.6 Studies on influence of climate change on sedimentation

No research has been found which investigates the influence of climate change on sediment dynamics in the Rio de la Plata. Meccia suggested a relationship between changes in the estuarine

circulation and changes in the sedimentation regime, leading to modification of the dredging needs of the access channels in the system (Meccia et al., 2009), but no further specifications are given.

3.3 Climate scenarios

The climate- and human-induced changes discussed in the previous paragraphs include a wide spectrum of potential impacts to the system. Based on this knowledge, two climate scenarios are formulated which are expected to have the largest effect on the sedimentation in Canal Emilio Mitre and will be implemented in the numerical model in Chapter 5. This paragraph presents the projected effect of the scenario on the sedimentation, furthermore it explains why the other changes are not expected to have a large effect on the sedimentation.

1. **Climate change scenario: +8.5% discharge Rio Parana**

As explained in paragraph 2.10 the discharge of the Rio Parana de las Palmas is considered an important forcer to the sedimentation in Canal Emilio Mitre. Paragraph 3.2.2 explains that in 10 years the river discharge of the Rio Parana is expected to increase by 8.5% due to changes in the precipitation regime and changes in land-use. It is assumed that the 8.5% increase in discharge also leads to the same fractional increase in sediment input since the additional rain is spread quite evenly over the watershed and also occurs over the Rio Bermejo catchment which supplies a major part of the sediment (paragraph 2.4).

The increase in discharge is expected to lead to increased ebb velocities around the breakwaters where the Rio Parana de las Palmas flows into Canal Emilio Mitre. This increase is expected to result in a downstream shift of the sedimentation in space. Furthermore, the increased overall sediment input is expected to lead to an increase in the overall sedimentation volume. The 8.5% increase in projected to occur in 10 years, only this scenario is executed in the numerical model but it has to be kept in mind that this is a gradual effect occurring on a time scale of 10 years.

2. **Climate variability scenario: +20.7% discharge Rio Parana with pronounced flood peak**

Next to climate change, the discharge of the Rio Parana is also affected by climate variability linked to the ENSO phenomena. Considering the time scale of the project it is expected that an El Niño event occurs one or two times. During an El Niño event the yearly flood peak is much higher in magnitude and persists longer, an important aspect that this high discharge also leads to interaction of the river flow and sediments with the flood plains (Appendix 10.2). A climate variability scenario is specified using the 2015-2016 discharge of the Rio Parana which is 20.7% higher than the reference year 2013-2014. The same assumption is made as in the climate change scenario: the fractional increase in sediment load is expected to be the same as in discharge. This scenario is expected to also lead to a shift of the sedimentation downstream in space and an overall increase in volume. Furthermore, the temporal effect of the high sediment input during the flood peak around January is expected to lead to an increase in sedimentation speed around that period.

All in all, these two scenarios lead to the discharge signals as presented in Figure 36.

1. **Disregarded scenarios and explanation**

Sea level rise: Sea level rise is expected to affect the tidal propagation and currents. Thereby it affects the sediment dynamics in the area of interest. When considering the time scale of 10 years and taking into account the maximum projected sea level rise around the estuary of 4.8 mm/year this results in a sea level rise of around 0.05 m during the total duration of the project (paragraph 3.2.4). In case the reference levels and the minimum required depth remain constant this would lead to an estimated capital dredging volume on the estuary of 0.23 Mm^3 (100 m width channel*47.5 km length channel*0.05 m height of sediment). Due to the fact that sea level rise is a slow process no backwater is expected on the Rio Parana and the river is expected to adapt by sedimentation over the lower reach. The additional 0.05 m in 10 years has a very small impact compared to the increase of sediment input in the first two scenarios, therefore the sea level rise scenario is disregarded in this study.

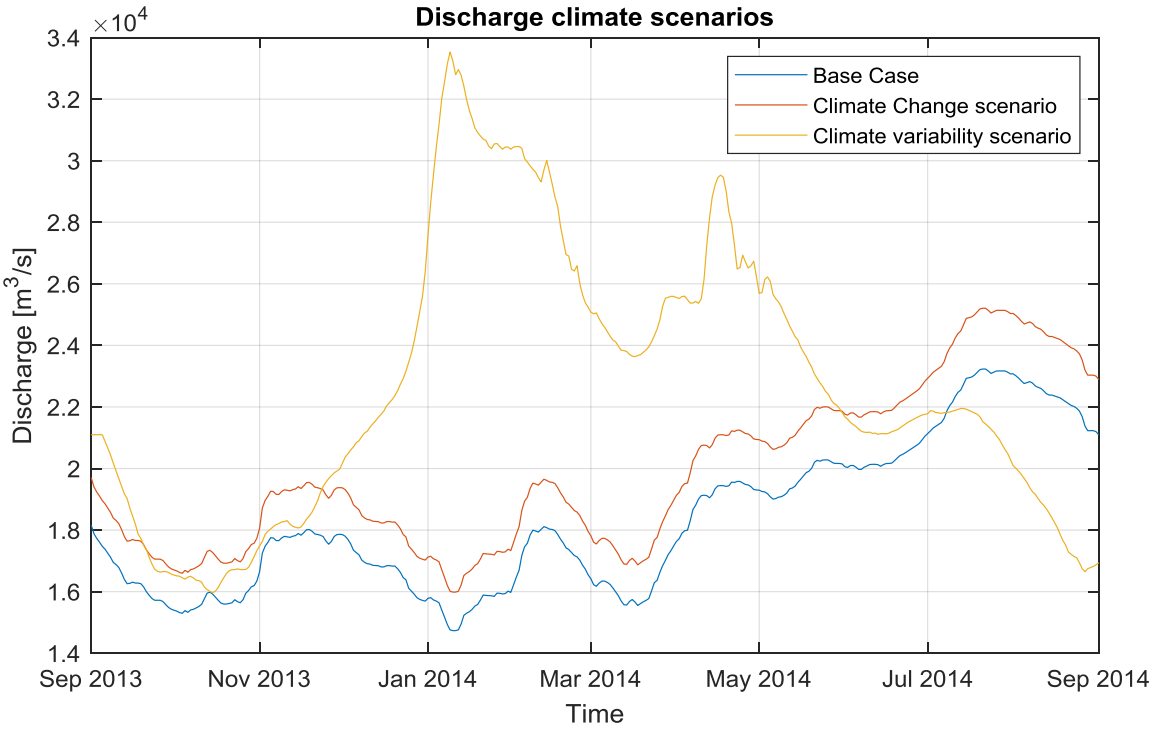

Figure 36 Discharge signal climate (variability) scenarios

Change in wind system: Interannual changes in the wind system have been observed, which lead to changes in duration and strength of storm surge events (paragraph 3.2.3). The persistent sudestadas lead to set-up which lead to backwater effects on the Parana river, due to the low slope of the delta of the Rio Parana (i_b=10^{-5}), the effects are known to propagate up until Rosario which is located around 300 kilometre upstream from the estuary. When using the backwater formulas with the empirical fit to Bresse a set-up of 3 m to a water depth of 15 and the slope of 10^{-5}, this leads to half-length of 450 kilometre which is even more than this distance. This difference is explained by the fact that the winds do not persist for a long period and the assumptions of the backwater that there is a rectangular uniform channel are violated. Furthermore, the slope of the delta increases towards the hinterland.

The increase in storm surge intensity is moreover expected to affect the availability of suspended sediment in the water column on the estuary due to the upstirring of sediments. The bed shear stresses in the shallow estuary are highly dependent on the intensity of the wind waves which are higher during storm surges. The high sediment concentrations are expected to result in higher sedimentation rates. The literature described storms as an important mechanism in the redistribution of sediment in the estuary (Fossati et al., 2014). The storm surges may also lead to changes in the current pattern.

Due to limited data on forecasts on this forcer, the choice is made to rather address the effect of temporally-varying wind compared to constant wind forcing. This is done in paragraph 6.4.

4 Dredging of Canal Emilio Mitre

The navigation channels through the Rio de la Plata estuary and the Rio Parana have a continuous need for maintenance dredging. This chapter presents the analysis of the dredging in Canal Emilio Mitre based on the dredging record, yearly bathymetries and documentation on the extraordinary sedimentation during the El Niño year of 2016 (Hidrovia SA, 2017). Paragraph 4.1 shows the dependence of the dredging volumes on the dredging strategy and the ONI index. Paragraph 4.2 elaborates on the current dredging strategy and paragraph 4.3 discusses the validity of comparing dredged volumes and simulated sedimentation. To conclude, paragraph 4.4 presents the deepening scenarios based on the interest of the Argentine government. More background on the history and the dredging in the rest of the waterway system is provided in Appendix 10.4.

4.1 Relation dredging volumes Canal Emilio Mitre and ONI index

Canal Emilio Mitre from this point in the report consists of the stretch of KP+41.5 to KP-30. Both CSD's (cutter suction dredger) and TSHD's (trailing suction hopper dredger) are dredging in this part of the waterway. Figure 37 shows the annual average dredging effort between 2007 and 2017 including and excluding the CSD in blue. On average of 4.5 Mm3 (excluding CSD) and 5.7 Mm3 (including CSD) is dredged from the navigation channel. This is around 1.2 m on average over the navigable width of 100 m of the channel (including CSD).

High interannual variability is observed in 2010 (~200%) and 2016 (~400%), this is partly linked to the dredging strategy with the buffer pits dredged by the CSD (elaborated on in paragraph 4.2). Next to this, the variability is highly related to the ENSO phenomena of which the ONI index is an indicator. Both during 2010 and 2016 the ONI index indicated at least a strong El Niño event (ONI index >1.5 ˚C), which coincides with a peak in dredging volume. In the literature study it was concluded that the El Niño events lead to an increase in discharge of the Parana de las Palmas and an increase in input of sediment on the upstream boundary of the navigation channel. It is concluded that the interannual variability of the dredging need of Canal Emilio Mitre is related to the ENSO phenomena.

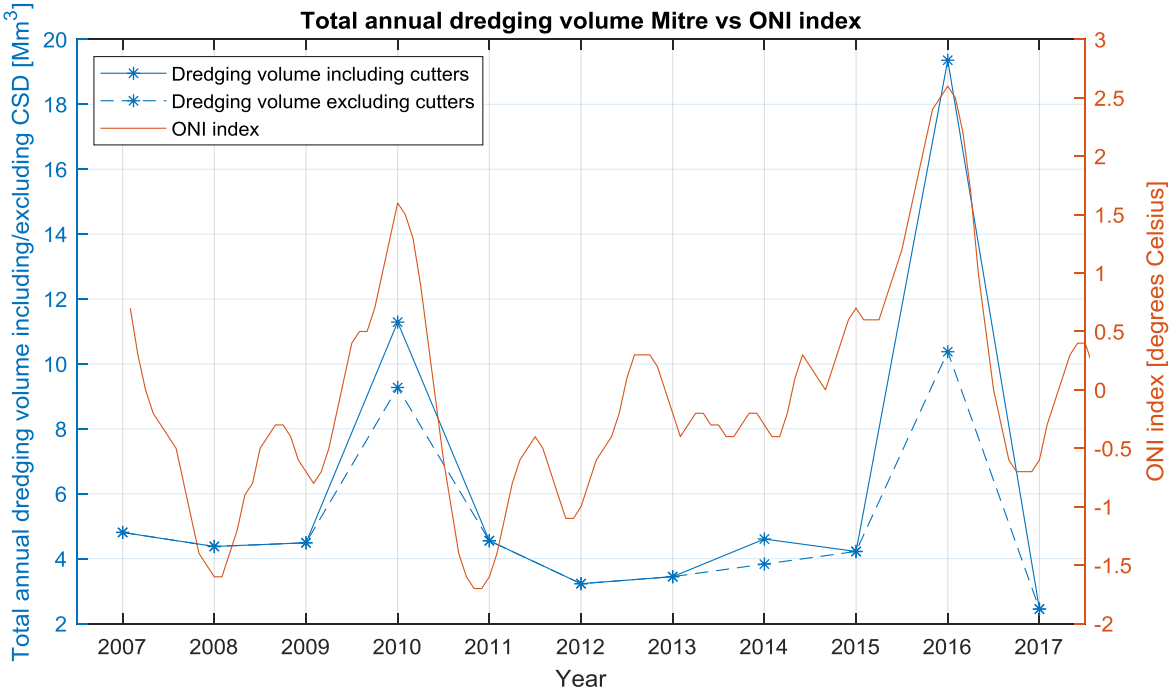

Figure 37 Total annual dredging volume Mitre vs ONI index

This matches the conclusion that during El Niño the input of fine sediments from the Rio Bermejo is high (Brea et al., 2010). Furthermore, the dredging in Canal Accesso and Canal Punto Indio does not show any relation with the ONI index showing that the additional sedimentation is not related to the hydrodynamics or the sediment concentration in the total estuary, but rather to forcing of the upstream supply of sediment.

4.2 Current dredging strategy Canal Emilio Mitre

Figure 38 shows the average annual dredging volumes around Canal Emilio Mitre between 2008 and 2017 by the two different type of dredging vessels. Understanding the dredging strategy is useful since it During non El Niño years the channel is dredged using several TSHD's. During El Niño years a CSD is used to dredge two large pits in the channel up to a depth of 20 meter below Cero Riachuelo (see Figure 40 and Figure 114 for location and depth of the pits in time). The CSDs dispose next to Canal Emilio Mitre on the flats (orange arrow). This area is not accessible for the TSHD due to the limited navigable depth. Therefore the TSHDs dispose the sediment downstream, south of Canal Acceso (KP-30) and partly in the pits created by the CSDs (blue arrows). Disposal of the dredged material by the TSHD in the buffer pits reduces their sailing time and therefore the costs.

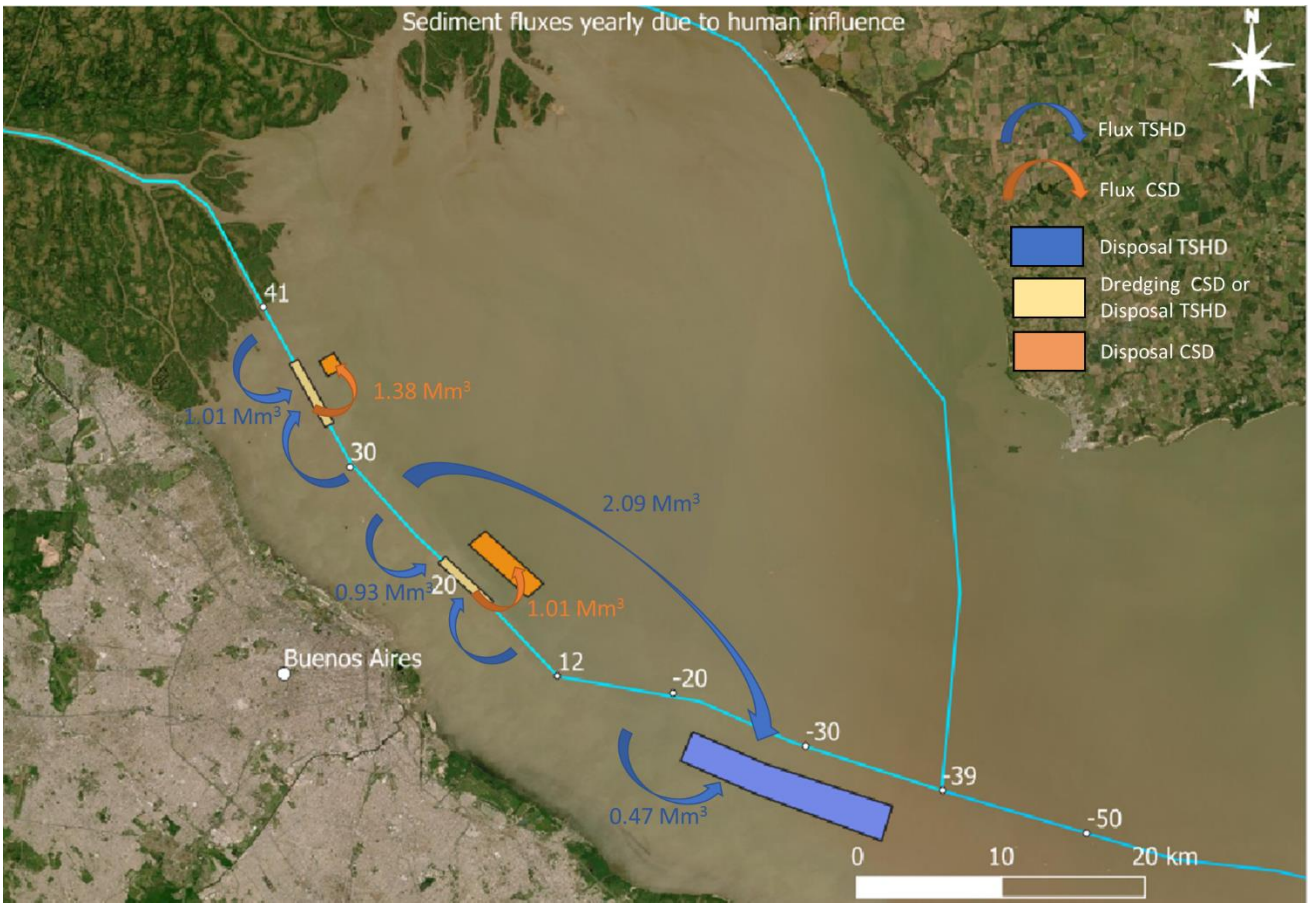

Figure 38 Sediment fluxes yearly due to human influence (average 2008-2017). Disposal areas are not to scale.

Further analysis of the dredging record shows that the upstream pit is mainly used as a sediment trap, it is only used as alternative disposal location in case of extreme sedimentation events. This is supported by the fact that the bathymetry of the pit shows infill only from the upstream side (Figure 40) and that modelling with a bathymetry without pits concludes that the pit is located at the location of maximum sedimentation (see paragraph 5.4.3). The downstream pit is mainly an alternative disposal location and is not used as sediment trap, furthermore the documentation on the extreme sedimentation in 2016 concludes that the downstream pit was not influenced by the El Niño event. This is supported by the bathymetries in time which show infill over the whole pit (Figure 40).

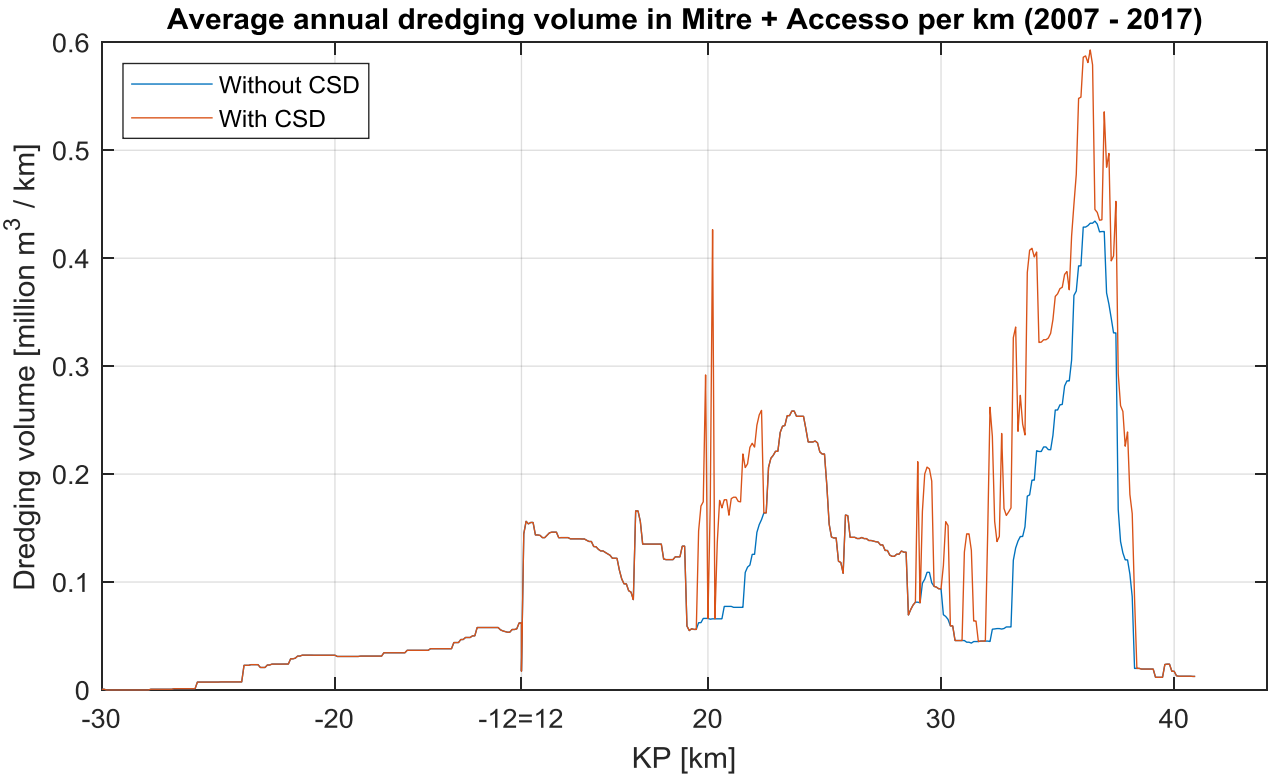

Figure 39 Average annual dredging volume in Canal Emilio Mitre per km (2007-2017). Right is upstream

Although Figure 38 creates a good picture of the dredging strategy in the navigation channel, this does not include information about the spatial distribution. The spatial distribution of the dredging in Canal Emilio Mitre and Canal Accesso is shown in Figure 39 and is discussed in detail, since in Chapter 6 these volumes are compared to the simulated sedimentation. Overall a downstream decrease in the dredging volume is observed, matching the expectations since at the mouth of the Rio Parana de las Palmas the transport capacity of the water goes down drastically leading to the settling of the suspended sediment. The details of the distribution are related to the dredging strategy with pits. The figure shows the high dredging volumes by the CSD between KP 37 and KP 33 (upper pit) and between KP 22 and KP 18 (lower pit). The difference between the dredging volumes without the cutter and with the cutter shows that between the pits the dredging is done only by the TSHDs and therefore gives a good indication of the trends in sedimentation. From upstream (KP41) to

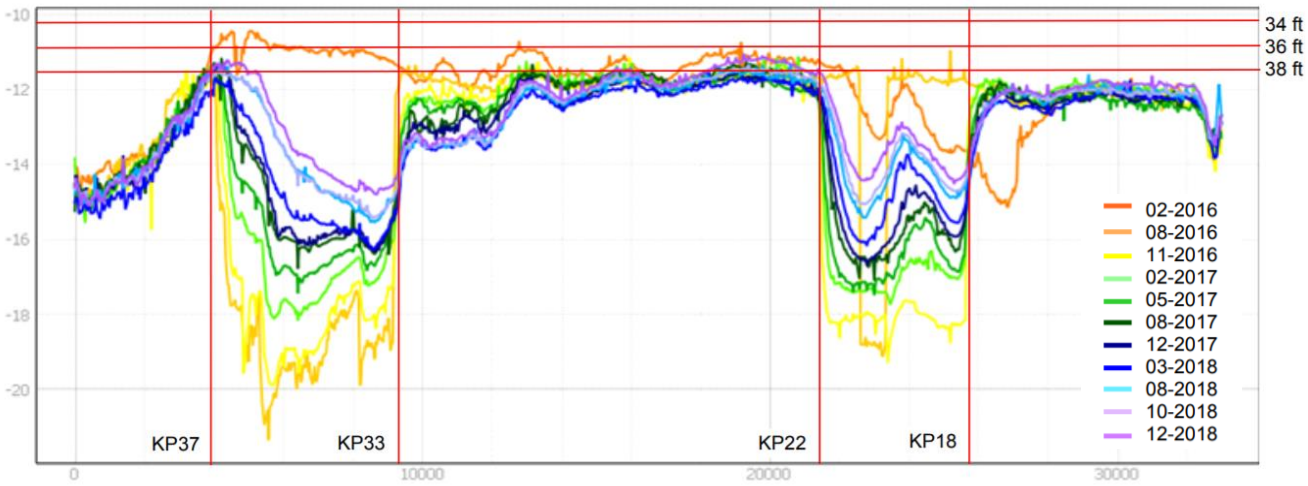

Figure 40 Depth profile Canal Emilio Mitre between 02-2016 (before CSD) and 12-2018. Left is upstream. Credits to Anne Waij, Boskalis (2019)

downstream it is striking to see that up to KP38 no dredging is done, the flow velocities are high enough to keep the sediment in suspension. Moreover, there is enough natural depth there, which implies that sedimentation does not immediately lead to additional dredging (Figure 40). From KP 37 the dredging amount increases drastically due to the presence of the sedimentation pit. The pit reduces the flow velocity and like this reduces the transport capacity of the flow leading to settling of the relatively coarse fraction which is in suspension. After the pit (KP33 until KP28) the dredging volumes are relatively low as the sediment already settled in the pit, the dredging volumes here are mainly reported during years when there are no pits. Between KP 28 and KP 12 the secondary pit has been present through the years. It is striking to see that after KP -30 in Figure 39 no dredging occurs anymore, this is probably related to an increase in depth of the flats.

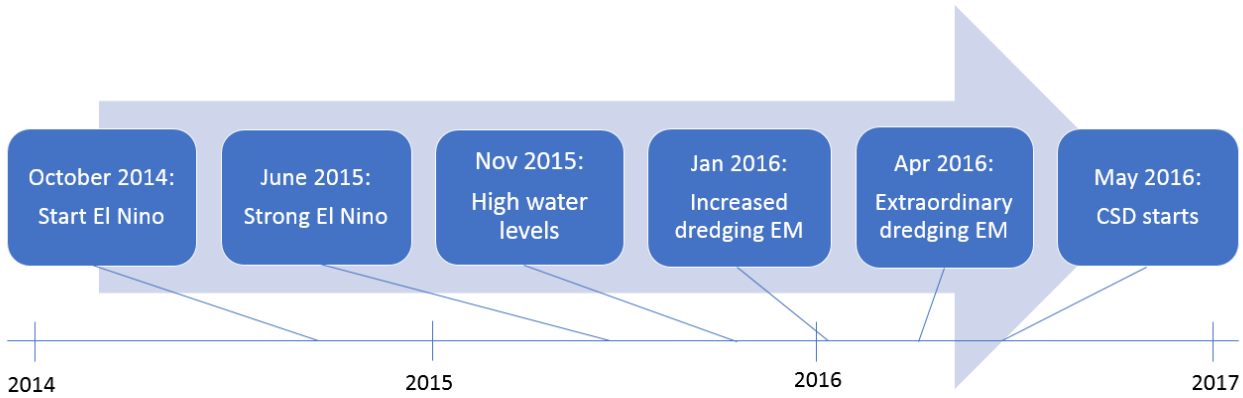

Figure 41 Time line extraordinary dredging 2015-2016 as result of El Niño

The time line leading to the 2016 extreme sedimentation event is presented in Figure 41. In short, 18 months after the onset of the El Niño event the CSD started dredging the pits. From this observation it is concluded that there is time to mobilize extra material and therefore anticipate on the effects of an El Niño event. All events in the time line are measurable, in October 2014 the ONI index exceeded 0.5 ˚C (El Niño threshold) and in June 2015 it exceeded 1.5 ˚C (strong El Niño). Then in November 2015 high water levels were measured at Corrientes (above 7 m to the local reference level which is the evacuation level). Only in April 2016 extraordinary dredging occurred (above 7.6 Mm^3 in 365 consecutive days) and in order to prevent interruption of the navigability, the CSD started in May 2016. For the 2010 event, 12 months passed between the onset of the El Niño event and the start of the CSD. The fact that the ONI index is predictable for the time span of 6-12 months (paragraph 3.2.5), grants at least 18 months for the contractor to anticipate on the effects of an El Niño event .

4.3 Validity of comparing dredged volumes and simulated sedimentation

In Chapter 6 the reported dredged volumes are compared to the simulated sedimentation from the model in order to verify whether the model is able to replicate the sediment dynamics around Canal Emilio Mitre. However this comparison assumes that the dredged volume is equal to the sedimentation, since the dredging in this system is only maintenance dredging (versus capital dredging) this is a valid assumption, however the following considerations have to be kept in mind:

- Dredging is not a continuous process it happens once every period, while sedimentation is continuous. Therefore it is important that the dredging record is long enough to average out the fact that dredging is not continuous.
- Areas which have enough navigational depth, which show some sedimentation do not need immediate dredging as long as the minimal navigational depth is not exceeded. This is the case in the stretch upstream of KP 40.
- In the dredging process the reported dredging volume is always larger than the sedimentation on the bed due to the addition of water during the dredging process.

- The density of the bed varies both in time and space, even if the density is known at some locations at a specific time this might vary due to the effect of consolidation and temporally and spatially varying forcers (such as flow, waves ect).
- The dredging record could be off for strategical or technical reasons. For example it is unknown whether the volumes have been determined by survey or are volumes in the dredger. In case the reported volumes are surveyed volumes there should be no difference between the simulated and reported volumes. In case the reported volumes are volumes in the dredger the simulated volumes are expected to be lower than the reported volumes. The factor is dependent on the dilution during the dredging process which is in its turn dependent on the dredging strategy and mainly on the duration of the overflowing. Although this uncertainty reduces the certainty of the comparison of the absolute values, this does not reduce the certainty of the comparison of spatial trends.

In order to minimize the effect due to the factors mentioned above a time period has been chosen in which the location of the pits was stable to get a spatial distribution which is not disturbed by the movement of the pits. Between 2015 and the end of 2017 both pits were stable in space (Figure 114), the spatial dredging pattern of those years is shown in Figure 42. Compared to Figure 39 the absolute values are significantly higher since 2015-2016 was a major El Niño year, therefore mainly the trend is relevant.

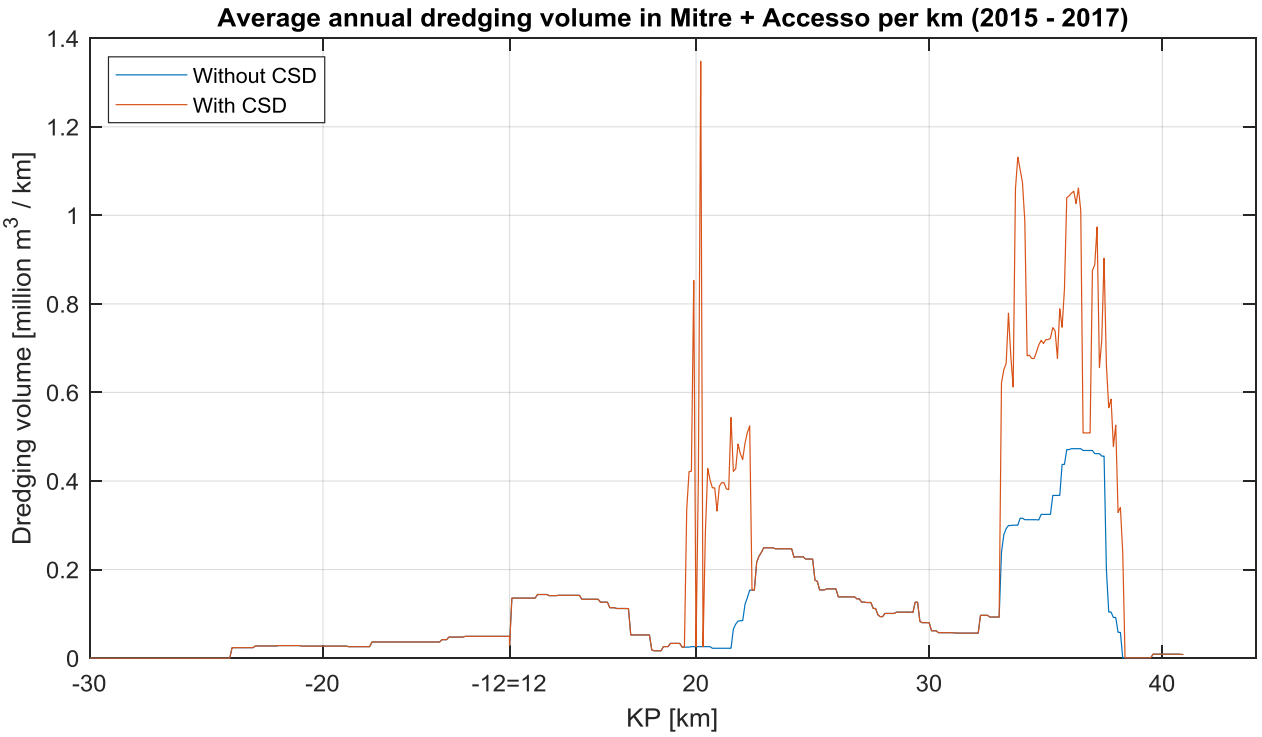

Figure 42 Average annual dredging volume in Canal Emilio Mitre per km (2015-2017). Right is upstream

The choice has been made to compare the dredged and simulated volumes between KP 41 upstream and KP -30 downstream. The upstream boundary is determined by the point where the river turns into a navigation channel on the estuary since the type of sediment and exact extent of the waterway system between the breakwaters (transition river to estuary) is unknown. Downstream the boundary is chosen where the maintenance dredging stops most due to the increase in depth of the flats around it.

4.4 Deepening scenarios

Currently navigation for ocean going vessels through Canal Emilio Mitre is only possible during the tidal window. In order to ensure constant navigation of a larger fraction of the ocean going vessels

the Argentine government is interested in the deepening of Canal Emilio Mitre (Argentine government, 2019).

Two possible deepening scenarios are introduced to investigate the effect of additional depth on the predicted sedimentation in the channel. Navigation is currently guaranteed for 34 feet and an additional 2 feet keel clearance. The first deepening scenario is 36 feet the second one is 38 feet. In the scenarios the full bathymetry from KP+41.5 until KP-39 is deepened, including the pits. The choice is made to also deepen the pits since the additional depth leads to further deviation from the natural depth and is thus expected to lead to more sedimentation. This in its turn leads to more dredging and thus more capacity is needed in the buffer pits.

The expected effect of the deepening of the navigation waterway is an increase in siltation due to decreased bed shear stresses in the channel due to the larger depth. A spatial shift is expected from the downstream stretch of the channel to the upstream stretch of the channel due to the larger reduction of the transport capacity of the water.

An estimation of the change in maintenance dredging volume is made using the 'volume of cut' method, which is a frequently used engineering rule (Trawle & Herbich, 1980). This rule is based on the assumption that the deposition in the channel is related to the volume of cut, which is the capital dredging. The increase in maintenance dredging is calculated by comparing the volume of cut of the old and the new situation.

$V_{new,\,md} = V_{old,\,md} + I_{cut}\,V_{old,md}$
with: $I_{cut} = (V_{new,cut}-V_{old,cut})/V_{old,cut}$
From the analysis of the dredging the following values are determined for Canal Emilio Mitre:

- $V_{old,cut}$ = 244.6 m^3 per meter width of channel
- $V_{new,cut}$ = 274.1 m^3 per meter width of channel
- I_{cut} = (274.1-244.65)/ 244.6= 0.12
- $V_{old,md}$ = 4.5 Mm^3
- $V_{new,\,md}$= 4.5 Mm^3+ 0.12* 4.5 Mm^3 = 5.04 Mm^3

$V_{old,cut}$ has been determined by comparing the current bathymetry and the bathymetry of the flats along Canal Emilio Mitre. From this it follows that an increase of the depth with 2 ft is expected to lead to 12% increase and that 4 ft is expected to lead to 24% increase of the maintenance dredging volume. In order to check the validity of this estimation the range of the proportionality factor is checked:
$V_d = \gamma * V_{cut}$ with:

- V_d= 4.5 Mm^3
- V_{cut} = 244.6 m^3 per meter width of channel* 200 m width = 48.92 Mm^3

$\gamma = V_d / V_{cut}$ =4.5/48.92 =0.09
This is in the range of silty/sandy nearshore to offshore conditions (van Rijn, 2013) and therefore confirms the estimate.

5 Model set-up and calibration

This chapter describes the choices and assumptions that have been made during the set-up of the numerical model. Paragraph 5.1 elaborates on the modelling approach, explaining which processes are included and why Delft3D is chosen. In paragraph 5.2 the model set-up is explained including the grid, time frame, boundary conditions and model parameters. The calibration of the hydrodynamics (discharge distribution, water levels and flow velocities) is presented in paragraph 5.3. Last but not least, the calibration of the sediment dynamics parameters is described in paragraph 5.4, the role of the physical processes identified in paragraph 2.10 is validated.

5.1 Modelling approach

5.1.1 Relevance of numerical modelling

Numerical modelling is a powerful tool to assess whether the physical processes that have been identified in Chapter 2 are indeed the relevant processes. Next to identifying the driving processes the assessment of the sensitivity of the model parameters provides further insight and understanding of the system. Last but not least, the calibrated and validated model is a quick and effective way of assessing the effect of scenarios on the sedimentation in Canal Emilio Mitre. With the goal of this thesis of assessing the effect of climate, dredging and wind scenarios, making use of a numerical model is thus an adequate approach. Therefore a numerical model is set up with the goal of checking the driving forces for the sedimentation in the channel and forecasting the effect of various scenarios.

5.1.2 Included processes and main assumptions

From paragraph 2.10 it followed that for the set-up of the hydrodynamic model for Canal Emilio Mitre the following drivers are most important: discharge and sediment input from the Rio Parana de las Palmas, infill from the flats under the influence of the tide and the locally generated wind waves. Therefore the following forcers are included in the numerical model:

- River discharge of the Rio Parana and Rio Uruguay, in order to ensure the right flow regime
- Tidal forcing, in order to ensure the movement of the sediment laden water over the channel
- Constant wind signal affecting the locally generated wind waves, set-up and currents, in order to ensure the (re)suspension of sediment

More information on how these processes are accounted for in the model is provided in paragraph 5.2.4. The main assumptions in the set-up of the numerical model are:

- The effect of wind is present in the offshore boundary, the effect of time-varying wind on the inner estuary in included in paragraph 6.4. In the rest of the scenarios a constant wind is applied only to generate waves (not affecting the currents and water levels).
- The sediment concentration of the rivers is assumed to be constant in time, therefore the sediment supply from upstream is only dependent on the discharge of the river. This assumption is addressed in the Discussion (paragraph 7.3).
- The Rio de la Plata estuary has a salinity front which is situated on the line between Montevideo and Punta Piedras over the Barra del Indio shoal, the location of this front is relatively stable in time (Fossati et al., 2008). From literature it followed that the area around Emilio Mitre Channel is not affected by the salinity.
- As described before the fluid is considered vertically homogeneous, the horizontal flow and concentration profile do not show significant variation in the vertical direction (Simionato et al., 2011), therefore a depth-averaged approach is valid. Flow distribution and sediment transport are mostly depending on the large-scale horizontal patterns and variations in bathymetry. Therefore Delft3D-FLOW is used in the 2DH mode (still referred to as Delft3D model in the rest of the report, although this specific model is not three dimensional).

5.1.3 Choice for Delft3D

To model the sedimentation in Canal Emilio Mitre both the hydrodynamics and the sediment dynamics have to be taken into account. Delft3D is a multi-dimensional (2D or 3D) hydrodynamic (and transport) open-source modelling system that is able to simulate the relevant dynamics with a sufficient level of detail. The core of Delft3D is the FLOW module which calculates non-steady flow and transport phenomena that result from the river, tidal and meteorological forcing. The hydrodynamic conditions calculated in this module are used coupled with the other modules of the program. The WAVE module uses the SWAN model to compute the evolution of random, short-crested waves. The WAVE module is used to include the effect of flow on the waves and the other way around. The online-coupling between the two modules arranges the information exchange during the computation. Next to the FLOW and WAVE module the sediment transport and morphology module supports both bedload and suspended transport of non-cohesive sediments and suspended load of cohesive sediments (Deltares, 2018). This module is integrated in the flow module and allows a direct coupling between morphological changes (erosion and sedimentation) and flow dynamics during the simulation.

The processes which were summarized in paragraph 5.1.2 can be incorporated in the FLOW and WAVE modules. The MOR module computes the sediment transport (both suspended and total bed load) and morphological changes for cohesive and non-cohesive fractions under the influence of waves and currents. Since all relevant physical processes can be included in the modelling software and Delft3D is also widely used within the TU Delft and Boskalis (which facilitates further research on this waterway system), this software was selected.

Because the status of the recently developed flexible mesh version (Delft3D-FM) of the Delft3D system at the start of this study (development and testing phase, 2019), it has been recommended to use the robust and often applied curvilinear version of Delft3D (Delft3D-4) when using the MOR module.

5.2 Model set-up

This paragraph describes the choices considering the model set-up based on the outcomes and literature study presented in the preceding chapters. In short all choices which have been made were aimed at modelling the hydro- and morphodynamics around Canal Emilio Mitre as accurate as possible. Outside the area of interest simplifications have been applied in order to reduce the computational effort of the model. The set-up of the model was thus mainly a consideration of spatial scale and resolution against computational effort.

5.2.1 Extent modelling domain and grid

The extent of the modelling domain is presented in Figure 43 and is based on the following considerations:

- The location of the upstream boundary conditions on the Rio Parana and Rio Uruguay are chosen based on the availability and reliability of the data (paragraph 2.3) and the fact that the boundary should not be affected by the water level at the Rio de la Plata, both due to the astronomical tide and the effect of extreme storm surge. Therefore the upstream boundaries on the Rio Uruguay and Rio Parana are located at the Salto Grande Dam and Timbues respectively.
- The downstream boundary condition is located on the line Montevideo (Uruguay) – Punta Piedras (Argentina) on the Barra del Indio shoal. An offshore boundary condition that is parallel to the bottom contours ensures that the boundary condition is not affected by the depth variation. Since the hydrodynamics around Canal Emilio Mitre is only affected by the tide (including wind effects) from the offshore boundary and not by specific current patterns the boundary is located close enough to minimize the computational domain, but large enough so that the boundary does not affect the hydrodynamics around Canal Emilio Mitre.
- River branches with a width of less than 200 meters have been left out, as they have no significant contribution to the discharge based on the flow partition along the branches (Bombardelli et al, 1995). These branches have an estimated discharge of less than 100 m^3/s

(0.5 % of the total discharge). This choice may however influence the distribution of the sediment transport to the estuary.

- The Rio Ibicuy (side branch of the Rio Parana) has been schematised into a channel-like branch, despite its meandering character, since its discharge is minor (1,600 m^3/s) and it does not affect the discharge of the Rio Parana de las Palmas significantly.
- Between Rosario and the bifurcation of the Parana de las Palmas and the Parana Guazu considerable flood plains exist. The flow capacity of these flood plains during extreme discharges is not taken into account as explained in Appendix 10.2, due to its complexity and lack of bathymetric data. The result is that during extreme discharges the flow velocities and water levels in the river branches may not be representative. Furthermore, this affects the sediment balance and the propagation of the flood wave. This is addressed in the Discussion (paragraph 7.3).

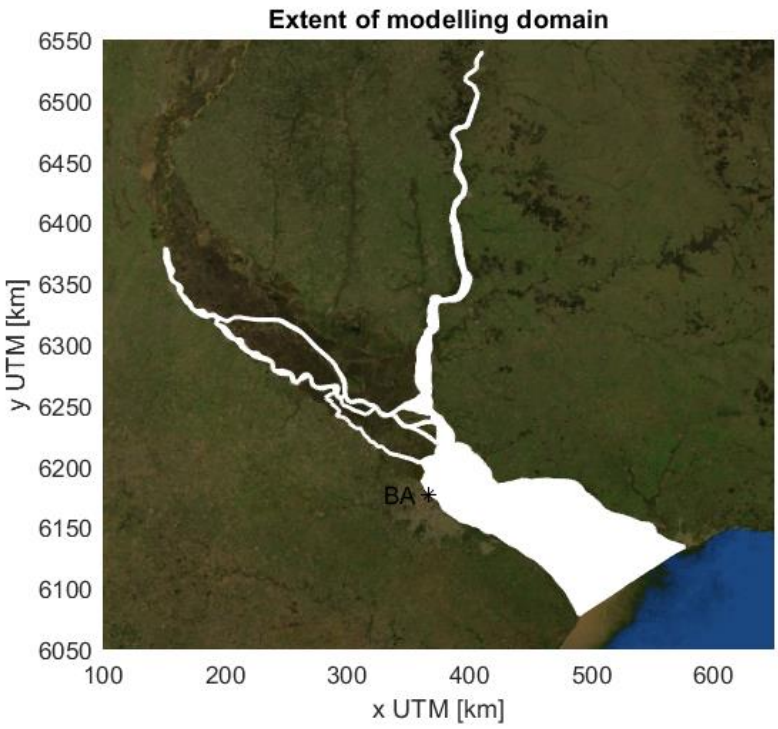

Figure 43 Extent of modelling domain with Buenos Aires (BA) for reference

A curvilinear grid is constructed using the Cartesian coordinate system (WGS 84/UTM zone 21S) (see Figure 43 and Figure 44). During the construction of the curvilinear grid the following considerations have been taken into account (which follow from the Delft3D FLOW manual (Deltares, 2018)):

- The horizontal resolution of the grid is based on the following considerations:
  - The characteristic length scale of the bathymetry: important bathymetrical features are covered by at least 5-10 grid cells, therefore Emilio Mitre channel is covered by around 15 grid cells in width to ensure good representation of the bathymetry.
  - Fit of the grid to the land boundaries: splines have been fitted to the land-water boundary and by choosing a reasonable grid size the grid more or less follows the river banks. At some locations the curves of the river were sharp, therefore the grid does not completely follow the land boundaries. In that case the course of the river was schematised keeping the overall length of the branch the same in order to prevent changes in water level gradients. This problem did not arise in the branch leading to the area of interest.
  - Characteristic length of the flow patterns that need to be resolved: in this case no features like local horizontal circulations (horizontal large eddies) are modelled thus this is not the ruling criteria.
- The other properties of the grid are based on orthogonality, aspect ratio and smoothness requirements. The requirements specified in the Delft3D manual are met in and close to the area of interest. Only the aspect ratio exceeds the prescribed value, which is justified since the flow is predominantly in one direction. Mainly in the area around Isla Martin Garcia the grid requirement of orthogonality is not met, and therefore the outcome of the model in that area has to be studied with care. The fact that the area of interest is only influenced by the corridor of flow of the Parana de las Palmas justifies this choice.

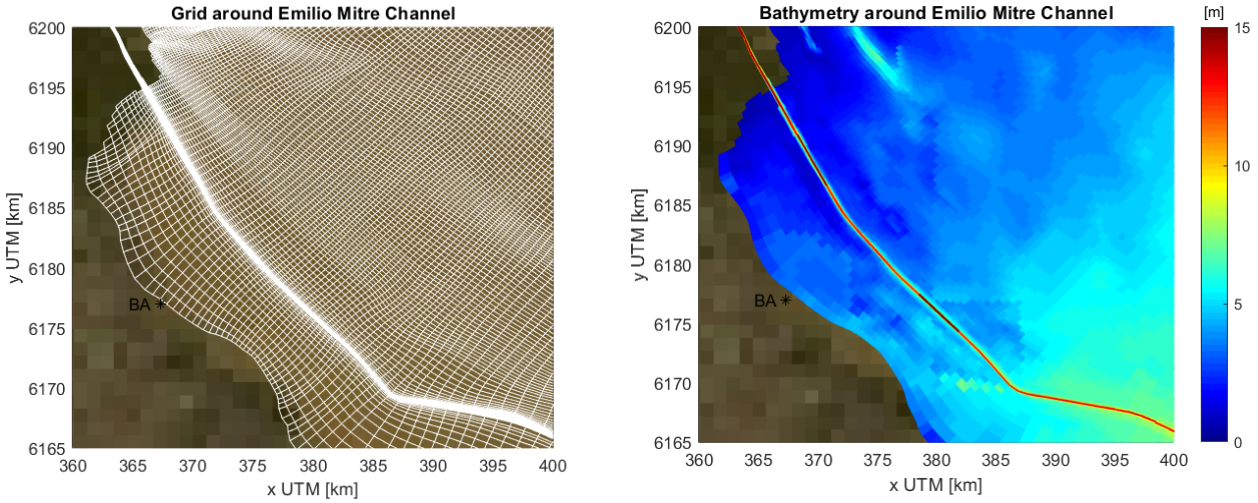

Figure 44 Grid and bathymetry around Canal Emilio Mitre

The fact that not all the requirements of the grid are met far away from the area of interest may have consequences. Although mass is conserved there might be problems with momentum conservation. Therefore during the validation the model has been tested on the sensitivity to this choice, as elaborated in paragraph 5.4.3.

These considerations and assumptions resulted in a grid for the FLOW computation with 136 cells in n-direction and 901 cells in m-direction which varying resolution. The cells in the Rio Parana and in the other rivers are relatively narrow and long while the cells in the outer Rio de la Plata are square and large. For example the cells inside Canal Emilio Mitre have a length of 650 meter and a width of approximately 15 meter. Outside the area of interest in the outer Rio de la Plata the grid size goes up to 2000 by 2000 m.

For the wave modelling with SWAN a separate grid is constructed which consists of the grid for FLOW with 3 extra rows of computational cells along the boundary at the outer Rio de la Plata estuary and does not include the Rio Parana and Rio Uruguay. Since only locally generated wind waves are present in the inner part of the estuary these are not expected to affect the rivers. Furthermore, by adding 3 rows of cells on the outer Rio de la Plata the boundary conditions do not affect the waves in the area of interest.

5.2.2 Bathymetry

Bathymetric data has been assigned as initial condition to all the cells in the grid, as shown in Figure 44. Various data sources have been used with different spatial quality and temporal availability (Appendix 10.5 provides sources). All data sets have been transferred to the reference level Cero Riachuelo and to the projection EPSG 32721 (WGS 84/UTM zone 21S). In order to prevent that the high quality data is contaminated by the low quality data, first the high quality data was included which was complemented by the low quality data in a later stage. Different interpolation methods have been used for the different parts of the domain, in the end resulting in a bathymetry that resembles the natural bathymetry as closely as possible. Special attention was given to the representation of the bathymetry of the channels around Emilio Mitre and the bifurcations upstream on the river. As mentioned before the river branches of the Parana Guazu were schematised in the grid, therefore also the bathymetry has been schematised. This has been done by estimating the conveying capacity and creating a bathymetry that matched the real conveyance capacity. Moreover, areas like the Martin Garcia Canal have a grid size that is too large to take into account the (narrow) deep channels, therefore some manual adjustments have been done to assure a representative flow capacity around that area. The validity of these simplifications is tested an verified in paragraph 5.4.3

Bathymetric data was used which was collected between 2013 and 2018. Since the bathymetry in the navigation channels varies in time due to the flow conditions, the use of bathymetric sources with

different sampling dates led to some uneven regions in the bathymetry. Especially the transition from the navigation channel to the flats showed significant spin-up. Therefore a simulation with 3.5 years of spin-up was performed to smoothen the bathymetry, after the smoothening the original bathymetry was retrieved in Canal Emilio Mitre by setting the depth in the navigation channel to the minimum navigational depth of 34 ft and the pits were set to a depth of 16 meter. For the deepening scenarios the bathymetry of Canal Emilio Mitre has been altered. Where this is the case, this is stated in the text.

5.2.3 Time frame and time step

The potential dredging project has a duration of 10 years, and the interest is mainly in the interannual variations. Therefore simulations are done with a duration of one year, and by using different forcers the interannual variability is addressed. Each simulation covers the period from the 1st of September until the 1st of September of the following year since that takes into account the whole flood peak (with its highest point in January). 2013-2014 is chosen for the Base Case since analysis of the forcers showed that this is an average year, also for the climate and deepening scenarios this year is used. For the climate variability scenario however 2015-2016 is chosen (paragraph 2.3 for explanation).

A time step of 30 seconds is used in the model, as the time step in Delft3D is based on accuracy rather than stability arguments since it uses the ADI scheme which is unconditionally stable. The accuracy is dependent on the Courant-Friedrichs-Lewy number, which should generally not exceed the value of $4\sqrt{2}$. However for problems which have rather small variations in space and time the Courant number can be substantially higher (Deltares, 2018). In Emilio Mitre Channel the highest Courant number is around 12, but due to the fact that the flow direction coincides with the direction of the cells this value is acceptable. Two cells at the bifurcation of the Rio Parana and the Rio Pavon give Courant messages due to the fact that the flow is not in the same direction as the orientation of the grid. However no strange flow patterns are observed and the discharge distribution matches reality. The influence of the time step on the stability and accuracy was checked by running the model with a four times smaller time step, this did not change the flow patterns and discharge distribution.

5.2.4 Boundary and initial conditions

Downstream boundary: Hourly water level time series including tide and set-up due to wind ocean
The downstream boundary condition is located on the line Montevideo (Uruguay) – Punta Piedras (Argentina). An hourly water level time series (including both the effect of the tide and wind over the ocean) is imposed between the coasts on 10 evenly spaced locations. The data at this boundary is provided by the calibrated and validated 3D hydrodynamic model by Pablo Santoro (IMFIA) which uses reanalysis wind data to simulate the water level elevation on the Rio de la Plata estuary (Santoro et al., 2018). Although the model has been calibrated especially against data on the Uruguayan side it also shows reasonable results for the Argentinian side. The water level on the boundary includes both the tidal signal and a non-tidal residual which is practically the surge due to wind on the ocean and outer estuary. The effect of the local wind field on the inner estuary is included in paragraph 6.4.

Upstream boundary condition: Daily discharge time series on both rivers
The upstream boundary conditions on the Parana and Uruguay rivers are daily discharge time-series. The upstream boundaries on the Rio Uruguay and Rio Parana are located at the Salto Grande Dam and Timbues respectively. Daily time-series of the discharge are imposed. Especially the discharge of the Parana River is considered an important forcer to the system, after an extensive study of the discharge data of the Parana the discharge signal of Timbues has been modified for high discharges (paragraph 2.3). The discharges at the Parana and Uruguay river are prescribed as total discharges over the whole cross-section. As the bathymetry changes considerably over the cross-section Delft3D distributes the discharge over the different grid cells based on the depth in that cross-section.

Wind forcing: simplified signal
As described in paragraph 2.6 the knowledge of wind and waves is limited, especially the variability over the estuary is uncertain. Therefore a simplified wind signal is imposed on the WAVE module. For the wind a constant speed of 5 m/s is imposed blowing along the estuary towards Buenos Aires (135 degrees). Furthermore, a small wave is sent into the estuary from the offshore boundary condition

(H_s=0.5 m, T_p=5 s) which is developed by the wind condition over the estuary. The characteristics are based on the data analysis of the wind and wave data at Pilote Norden which is a representative location for Canal Emilio Mitre. This results in locally generated wind waves. The wind is only imposed over the WAVE module and not over the FLOW module in order to not affect the water levels on the estuary.

Since the wave grid only extends over the estuary, waves can only develop there. Stationary wave computations are conducted by SWAN every 1440 minutes. At the same interval the hydrodynamic module and SWAN communicate. For the SWAN-computations, water level and velocity are taken from the results of the hydrodynamic computation.

Initial conditions: restart file from previous runs
The initial hydrodynamic conditions are determined from a run of 2 months with constant boundaries which match the domain at first instant, these include the water levels and the flow velocity components but also the suspended sediment concentrations of the different fractions.

5.2.5 Model parameters

Wind stress formulation
The wind stress formulation determines the wind drag coefficient which is an essential metric in the calculation of momentum exchange over the air-water interface. The coefficient is known to increase with the wind speed. The standard values of Delft3D give a wind drag coefficient of $1.3*10^{-3}$ which is reasonable for a wind speed of 5 m/s when compared to the values of Large and Pond (1981).

Bed roughness
The roughness formula of Manning is chosen as this formulation is used in open channel analysis. Calibration is described in paragraph 5.3.

Viscosity and diffusivity
The Delft3D manual mentions the eddy viscosity and eddy diffusivity as calibration parameters, however these are related to the dynamics of the flow. The value for the horizontal eddy viscosity is related to the grid size and the horizontal gradient in the depth averaged flow velocity. If the diameter of the circulation and the grid size (Δx) are much larger than the water depth (h) then the eddy generation is friction dominated and therefore the effect of sub-grid eddy viscosity is limited (Madsen et al., 1988). However when the horizontal grid dimension is equal or smaller than the water depth the eddy viscosity becomes very important in determining the flow pattern and therefore the choice of this parameter is important to accurately describe the effective shear stress in the momentum equation. Since the horizontal magnitude of the computational cells (15m) has the same magnitude as the water depth (order of meters) the value of the horizontal eddy viscosity significantly affects the flow pattern. To determine the horizontal eddy viscosity the Smagorinski eddy viscosity is used which is dependent on the gradient in flow velocity and the grid size (Madsen et al., 1988):

$$v_t = \left(0.5\,\frac{du_i}{dx_j}\right)^{1/2} * (C_s * \Delta x)^2 = \left(0.5\,\frac{0.6\frac{m}{s}}{100\,m}\right)^{\frac{1}{2}} * (0.8 * 15\,m)^2 \approx 8\,\frac{m^2}{s}$$

The chosen values have been determined for the area around the outflow of the Parana de las Palmas into Canal Emilio Mitre since this is the area where the viscosity affects the flow pattern the most. This value fits in the range for detailed models in which much of the details of the flow are resolved (grid size tens of meters), which results in an horizontal eddy viscosity or diffusivity between 1 and 10 m^2/s (Deltares, 2018). Therefore it is used as first value in the calibration process, described in paragraph 5.4. Using a uniform horizontal eddy viscosity over the whole domain is clear limitation of the chosen approach, since the characteristics of the flow and the grid size vary over the domain.

For all the other 'hydrodynamics' parameters the default settings specified by Deltares are used, the sediment and morphologic parameter are described in paragraph 5.4.1.

5.3 Calibration of the hydrodynamics

The main goal of the calibration of the hydrodynamics is to accurately represent the magnitude and timing of the discharge and tide through the Parana de las Palmas branch of the Rio Parana since this is considered one of the main forcers of the sedimentation in Canal Emilio Mitre. Calibration of the hydrodynamics was done in three steps. First the discharge distribution over the different branches was calibrated by adjusting the grid size and bathymetry over the different branches. Second the calibration of the water levels along the river and on the estuary was done by tuning the bed roughness parameter in the model. Lastly the sparse measured depth averaged flow velocity data was compared to the simulated depth averaged flow velocities.

5.3.1 Calibration of discharge distribution

Recently a study has been conducted by the INA which describes the discharge partition over the major bifurcations in the Parana delta under the influence of a range of discharges and a range of water levels on river (Gerbec et al., 2018). It shows that irrespective of the total discharge of the Rio Parana always around 23% of the discharge is diverted into the Parana de las Palmas which is the branch leading to Canal Emilio Mitre. Furthermore, the article also shows the discharge partition of the bifurcations downstream on the Parana Guazu. No calibration has been done on these distributions, as these partitions have minor influence on the area of interest since Canal Emilio Mitre is located completely in the flow corridor of the Parana de las Palmas as explained in paragraph 2.3.

The calibration of the discharge distribution over the different branches was done by adjusting the grid size and the bathymetry of the Rio Parana Guazu. The bathymetry was altered to represent the channel bathymetry on the local grid resolution. No changes have been made to the Rio Parana de las Palmas since the grid over that branch followed the land boundaries well and also the source of bathymetric data has a relatively high spatial resolution. The article by Gerbec et al. does not give information about the percentage of discharge that is diverted through the Ibicuy branch, contact with local experts (Sabarots Gerbec and Re, 2019) revealed that the Rio Ibicuy takes around 10% of the discharge of the Rio Parana. No information or measurements are available of this branch, so the temporal variation of this distribution is unknown. The discharge distribution from the article by Gerbec (upper percentage) and the output of the model (lower percentage) have been visualised in Figure 45. The average discharges and percentages are shown in Table 2. Runs with extreme discharges (30,000 m^3/s) showed approximately the same distribution, therefore the model is considered suitable to predict the discharge distribution both during average and extreme conditions.

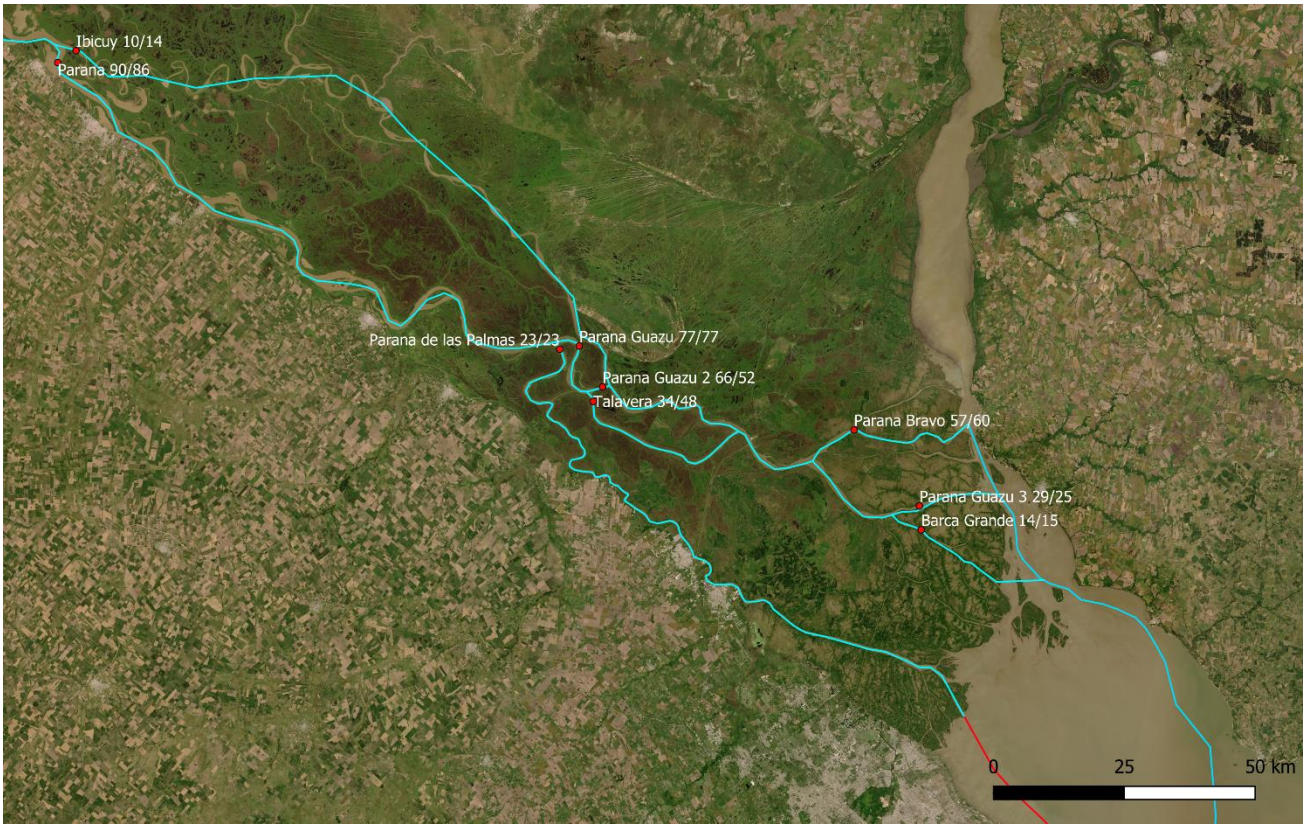

Figure 45 Discharge distribution Delta Rio Parana (Name of branch, upper % from article Gerbec (2018), lower % from Delft3D model with 'calibrated' grid and bathymetry)

	Gerbec (2018)		**Model without adjusting grid and bathymetry**		**Model with adjusting grid and bathymetry**	
	Percentage	m^3/s	Percentage	m^3/s	Percentage	m^3/s
Bifurcation 1						
Parana	**90%**	14,400	**85%**	13,600	**86%**	13,750
Ibicuy	**10%**	1,600	**15%**	2,400	**14%**	2,250
Bifurcation 2						
Parana Guazu	**77%**	11,088	**66%**	8,950	**77%**	10,600
Parana de las Palmas	**23%**	3,312	**34%**	4,650	**23%**	3,150
Bifurcation 3						
Parana Guazu 2	**66%**	7,318	**58%**	5,200	**52%**	5,500
Talavera	**29%**	3,216	**42%**	3,750	**48%**	5,100
Mercadal	**5%**	554	**not present in model, added to Talavera**		**not present in model, added to Talavera**	
Bifurcation 4						
Parana Bravo	**52%**	6,597	**58%**	6,600	**60%**	7,700
Parana Guazu 3	**29%**	3,679	**27%**	3,050	**25%**	3,200
Barca Grande	**14%**	1,776	**15%**	1,700	**15%**	1,950
Parana Mini	**5%**	634	**not present in model, added to Bravo**		**not present in model, added to Bravo**	

Table 2 Discharge distribution Delta Parana, discharge upstream of bifurcation Rio Parana-Rio Ibicuy: 16,000 m^3/s

5.3.2 Calibration of water levels

Calibration of the water levels on 10 stations is done by tuning the bed roughness coefficient. Appendix 10.6 elaborates on this calibration also presenting the details at all stations along the waterway. Conclusions of the calibration of the water levels at Braga are presented here since that station is located closest to Canal Emilio Mitre.

The roughness formula of Manning is chosen as this formulation is used in open channel analysis. The choice is made for a space-varying Manning value since the domain consist of water bodies with different properties. According to literature a value of Manning's n of 0.025-0.03 is suitable for a Parana like river (Chow, 1959), while on an estuary a value of 0.01-0.02 is more suitable dependent on the mud percentage (van Maren et al., 2015). Runs with different but spatially uniform roughness confirmed that these values were in the right range for those regions. Afterwards a space varying roughness was applied, resulting in a roughness of 0.015 on the estuary, 0.025 on the lower river and 0.027 on the river above the bifurcation of the Rio Ibicuy (Figure 87 for spatial pattern). The space-varying roughness coefficient showed the best behaviour overall, both for 2 months in 2013 and 2 months in 2016 (Figure 46 and Figure 47 respectively). In both figures the rapid fluctuations are related to tide, while the longer and larger fluctuations are related to influence of the offshore boundary affected by the wind.

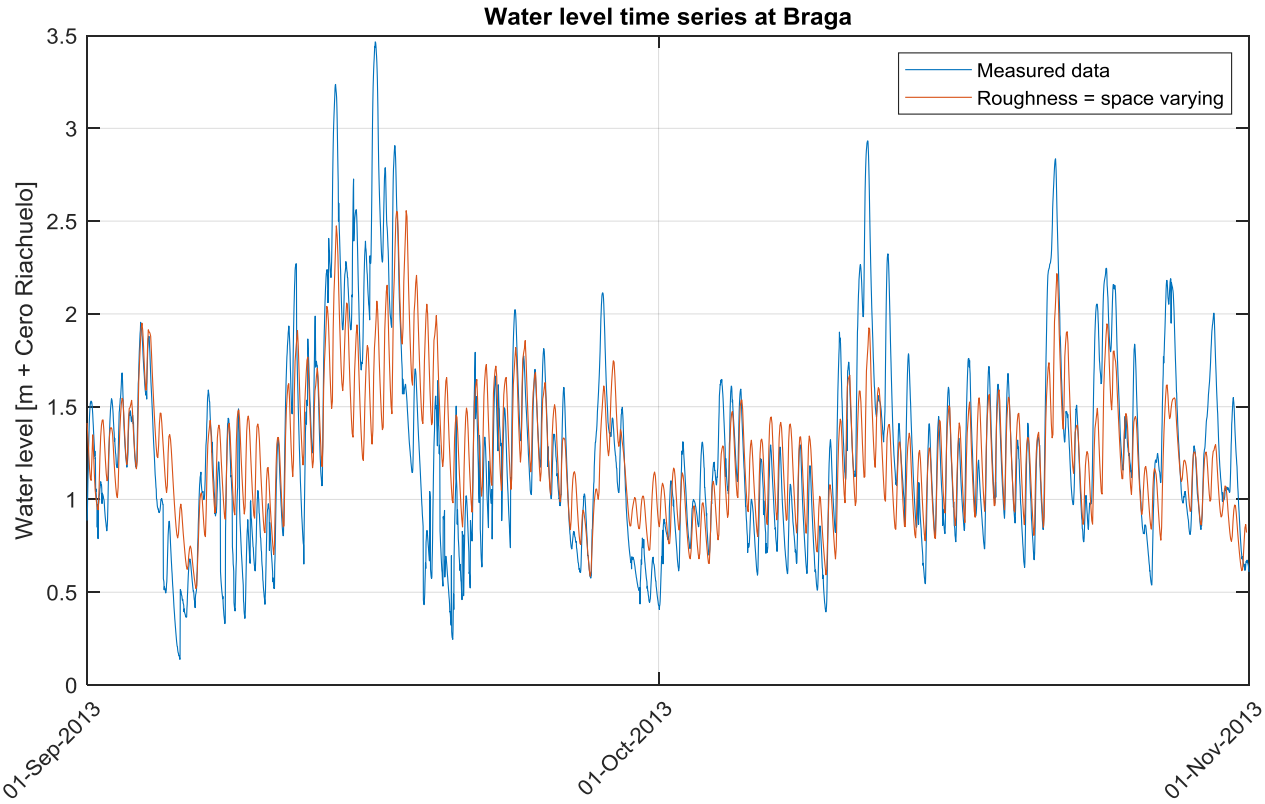

Figure 46 Water level time series at Braga (blue) and simulated water levels (orange) with space varying roughness (01-09-2013 until 01-11-2013)

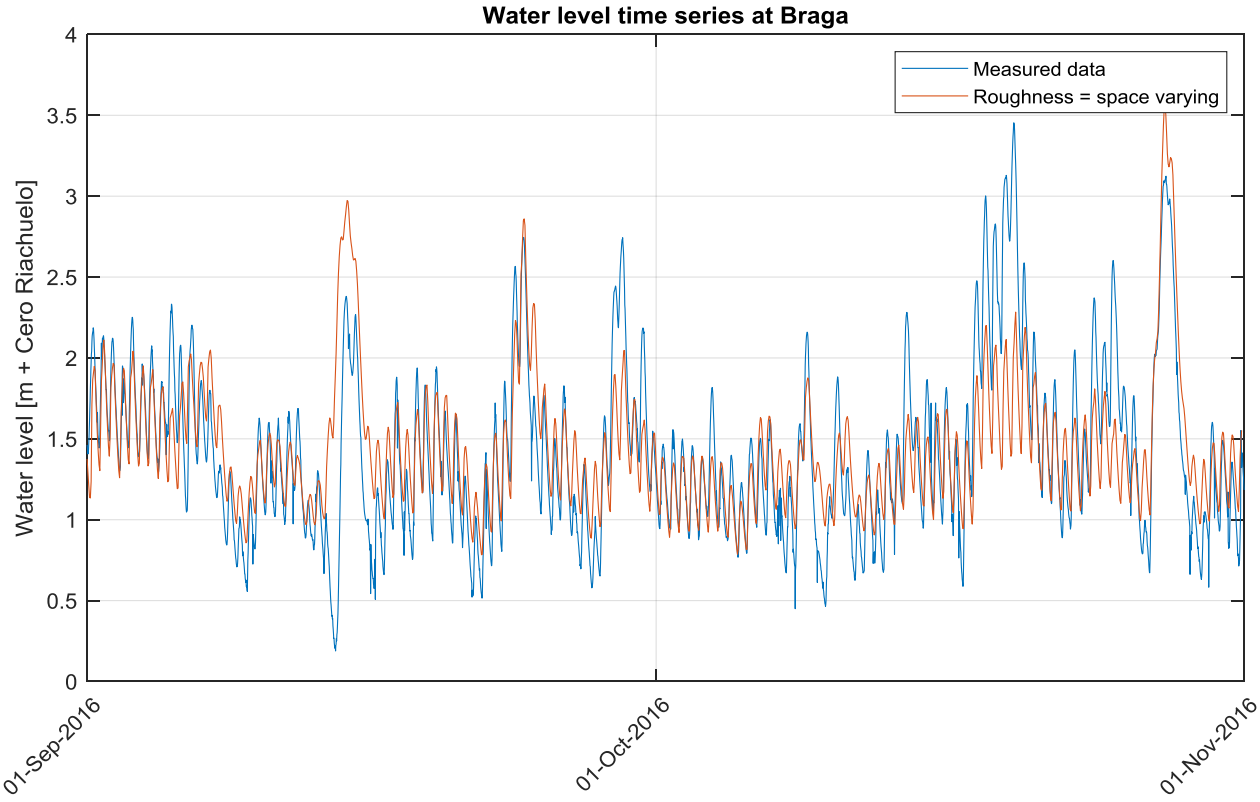

Figure 47 Water level time series at Braga (blue) and simulated water levels (orange) with space varying roughness (01-09-2016 until 01-11-2016)

These results illustrate that although the timing and amplitude of the tide is right, strong winds on the estuary lead to serious deviations in the water level. It shows that the main peaks in the water levels which cannot be explained by the tidal signal are however also presented in the model, due to the fact that the offshore boundary condition also includes the effect of wind on the ocean. However local wind effects on the inner estuary are not included.

Next to calibration of the roughness coefficient the calibration of the water levels provided the following insights:

- The amplitude and timing of the tidal propagation at all stations matches the measured time-series. In combination with a matching discharge distribution this gives confidence that the flow velocities are well represented in the model.
- The absolute value of the water levels differ up to 0.5 m at some stations (Ramallo or San Nicholas) with a constant deviation while at the next station it shows a good fit (San Pedro or Rosario). These differences are attributed to reference level errors and do not occur close to the area of interest.
- The water levels at Pilote Norden, Braga and Zarate show a significant influence of the wind. The signal produced purely by the tide at some instances show a good fit and at other times show large differences with the measured time series. This is an important limitation to the current set-up of the research.

After the calibration of the water levels the analysis of the calibration of the discharge was redone, no relevant changes were observed in the discharge distribution.

5.3.3 Calibration of flow velocities

During 2016 and 2017 several measuring campaigns of depth averaged flow velocities throughout the Parana Delta were performed by INA (Sabarots Gerbec et al., 2018). Although the measurements are sparse both in space and time they provide a good picture of the relative magnitude of the flow

velocities in the different branches. The absolute values are less relevant since they have been recorded mostly during high discharge periods. Overall the relative magnitude of the flow velocities matches the projected flow velocities. For example the high flow velocities (up to 1.5 m/s) at the bifurcation of the Parana Bravo and Parana Guazu were also measured during the campaign.

The flow velocities recorded on the Parana de las Palmas branch range between 0.8 and 0.95 m/s but were all recorded when the discharge at Timbues was above 21,000 m^3/s which is well above the average of 17.500 m^3/s which was used in the Base Case, this significantly affects the flow velocity. Therefore during regular flow conditions the flow velocities are estimated to be about 0.75 m/s (based on the difference in discharge) which matches the values of the Base Case in which the flow velocities range between 0.65 and 0.8 m/s depending on the tide.

Furthermore, the flow velocity data confirms that the cross branches in the delta do not contribute to the discharge of the Rio Parana since the flow velocities stay below 0.1 m/s. Therefore the choice of excluding these branches from the model is confirmed, although once again it may affect the transport of sediment to the estuary.

5.4 Calibration of sediment dynamics

5.4.1 Morphological settings

In order to gain understanding in the sediment dynamics of Canal Emilio Mitre three representative sediment fractions were selected. Modelling the sediment dynamics with one fraction was found to be a too large simplification as explained in Appendix 10.7. The three fractions were selected based on the knowledge about the sediment characteristics and dynamics presented in paragraph 2.4. Since the chosen fractions are specifically selected for Canal Emilio Mitre the erosion/sedimentation results are not representative for other regions of the estuary. The calibrated characteristics are presented in Table 3, the rest of this paragraph describes the initial selection and calibration of these parameters.

Fraction	D_{50} [µm]	W_s [mm/s]	$\rho_{specific}$ [kg/m^3]	ρ_{dry} [kg/m^3]	$\tau_{c,erosion}$ [N/m^2]	$\tau_{c,deposition}$ [N/m^2]	M [$kg/m^2/s$]	Used formula
1 Sandy	100	~8	2650	1650	-	-	NA	Van Rijn (1993)
2 Silty	~23	0.5	2650	1650	0.15	1000	8e-5	Partheniades-Krone (1965)
3 Clayey	~7	0.05	2650	1650	0.1	1000	6e-5	Partheniades-Krone (1965)

Table 3 Sediment properties Delft3D after calibration

The distribution of the fractions in space is shown in Figure 48. The first fraction is a sandy fraction, this fraction is the dominant fraction at the Parana de las Palmas with decreasing availability downstream. It is expected to settle directly after the reduction of the transport capacity. The second fraction is a silty fraction, this fraction is the dominant fraction in the bed from KP41 until KP12 of the navigation channel. It is expected to settle along the channel with peaks in volume in the pits and to be resuspended mainly during energetic events like storms. This fraction is expected to be responsible for a majority of the sedimentation in the waterway. The last fraction is clayey fraction, this fraction is expected to be present as suspended material, and partly as bed material from KP 41 and downstream. Downstream the energy for resuspension decreases leading slow deposition of this fraction, leading to a larger fraction of the clayey material in the bed. Although part of the clayey fraction is expected to settle, a part also stays in suspension downstream of Canal Emilio Mitre as the reported concentrations are around 100 mg/l there.

Paragraph 2.4 concludes that cohesive behaviour plays an important role, this is confirmed by the mud percentages found in the sieve curves, therefore water-bed exchange processes are modelled with the well-known Partheniades-Krone formulation (Partheniades, 1965) for the clayey and silty fraction. For the sandy fraction the formulation by Van Rijn is used (1993), implying that the cohesive fraction and non-cohesive fraction are not interacting. This is a suitable assumption since the area around the transition from the river to the estuary is ruled by non-cohesive behaviour and downstream the cohesive behaviour does play an important role.

The D_{50} of the sandy fraction is based on the average diameter of the sandy fraction in the sieve curve halfway Mitre. This material is expected to be deposited during highly energetic events and is therefore expected to match the sediment around the transition from river to estuary where energetic circumstances are present year-round due to the flow velocities of the Parana de las Palmas. The specific and dry density are constant for all fractions and have been determined based on yearly samples that are taken from about 10 points in the Emilio Mitre channel (Argentine Government, 2018), they are 2650 and 1650 kg/m^3 respectively. The measured data shows that these parameters vary both in time and in space, matching the expectations since they are dependent on processes like consolidation, hydrodynamic forcing and also dredging activity. Just like the chosen representative fractions these properties should also be interpreted as distributions.

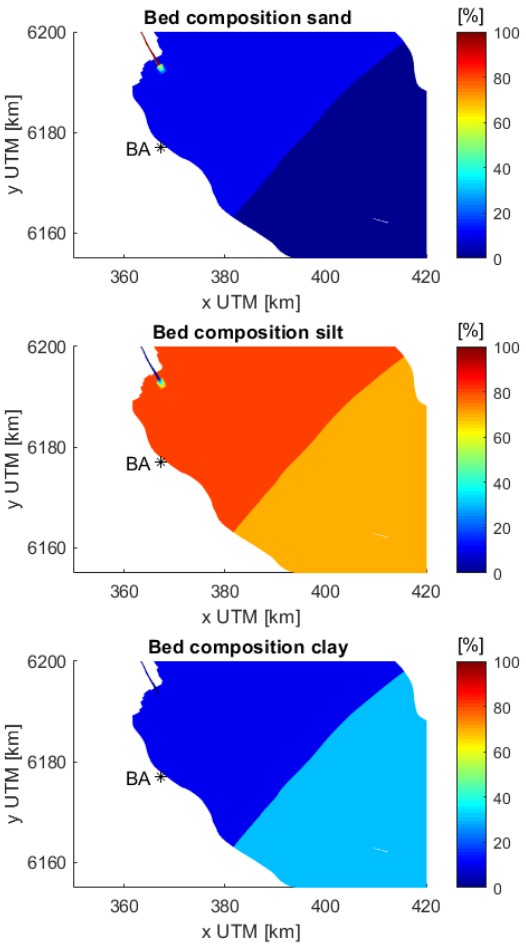

Figure 48 Bed composition different fractions

Defining the settling velocities for the cohesive fraction is difficult due to processes such as flocculation and hindered settling. No information has been found about the size of the sediment in suspension and the role of flocculation on the Rio de la Plata. On the middle Rio Parana flocculation is known to play a role in regions of low shear due to the presence of organics for the sediment fractions smaller than 15 µm (Mangini et al., 2003). On the Rio de la Plata estuary the shear however is higher and due to the lack of data the effect of flocculation on the particles is unknown. It is expected that flocculation processes are mostly relevant in the reaches with increased salinity, which are outside the region of interest. As an approximation the silty fraction is chosen to be somewhat finer than the average silt in the samples, with a settling velocity of 0.5 mm/s. This value matches with a diameter of 25 µm according to the approximation of Stokes for the settling velocity. In reality for the cohesive fraction using the Stokes approximation is not accurate since its assumptions do not apply. However this is used as a first approximation, as no other widely accepted formulation is available. For the clayey fraction the settling velocity is set at 0.05 mm/s.

A spatially varying critical bed shear stress for erosion for the clayey and silty fraction have been determined based on literature and the calibration is described in paragraph 5.4.2, yielding 0.2 N/m^2 (van Rijn, 2007) for the area around the transition from river to estuary which is expected to be sandy, to 0.15 N/m^2 at KP12/-12 to 0.1 N/m^2 at the silt-sand boundary suggesting a barely-consolidated, easily erodible sediment (Mengual et al., 2017). The values are displayed in Figure 49. All these values are in the range 0.1-0.3 N/m^2 which Van Rijn reported for weakly-consolidated mud beds with sizes ranging from 8-62 µm (van Rijn, 2007). The critical bed shear stress for deposition is set at 1000 N/m^2, which means in practice that deposition can always occur.

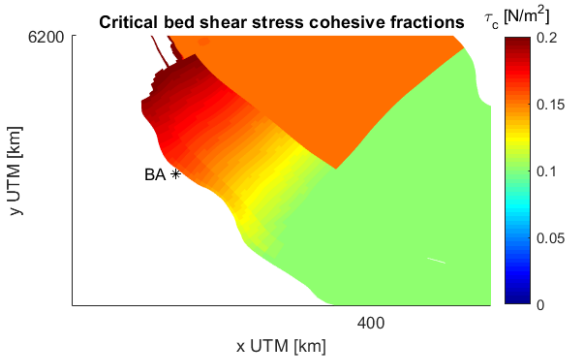

Figure 49 Critical bed shear stress for cohesive fractions [N/m^2]

5.4.2 Calibration sediment dynamics parameters

Before describing the Base Case in paragraph 6.1, first the calibration of the parameters of the sediment dynamics is described. The sensitivity of the model to the parameters mentioned in Table 4 have been tested in a simulation for 2 weeks, in order to reduce computational time. The default values have been determined based on physical grounds. The minimum and maximum value represent the range of physically realistic values as found in literature.

Parameter	Minimum value	Default value	Maximum value	Code scenario
v_T (horizontal eddy viscosity)	5 m^2/s (50%)	10 m^2/s (100%)	20 m^2/s (200%)	1+2
w_s silty (fall velocity)	0.25e-3 m/s (50%)	0.5e-3 m/s (100%)	1e-3 m/s (200%)	3+4
w_s clayey (fall velocity)	0.025e-3 m/s (50%)	0.05e-3 m/s (100%)	0.1e-3 m/s (200%)	5+6
D_{50} sandy (median diameter)	Not possible	100 µm (100%)	200 µm (200%)	8
M silty (erosion parameter)	4e-5 $kg/m^2/s$ (50%)	8e-5 $kg/m^2/s$ (100%)	16e-5 $kg/m^2/s$ (200%)	9+10
M clayey (erosion parameter)	3e-5 $kg/m^2/s$ (50%)	6e-5 $kg/m^2/s$ (100%)	12e-5 $kg/m^2/s$(200%)	11+12
$\tau_{cr\ silty}$ (critical bed shear stress erosion)	0.1 N/m^2 (67%)	0.15 N/m^2 (100%)	0.2 N/m^2 (133%)	13+14
$\tau_{cr\ clayey}$ (critical bed shear stress erosion)	0.05 N/m^2 (50%)	0.1 N/m^2 (100%)	0.15 N/m^2 (150%)	15+16

Table 4 Parameters for sensitivity analysis 1 (scenario 7 does not exist)

Calibration of the sediment dynamics parameters is performed by comparing the spatial pattern of the reported dredged volumes from 2015-2018 to the simulated sedimentation both in m^3/KP/year. After normalising both profiles the root mean square error (RMSE) is calculated in order to address which sediment dynamics parameters lead to the closest fit. The graphs and figures resulting from the calibration are given in Appendix 10.8, here the main findings are presented.

The main calibration parameters are the eddy viscosity, erosion parameter for the silty fraction and the critical shear stress for erosion for both fractions. The eddy viscosity influences the sedimentation around the transition from river to the estuary where the gradient in horizontal velocity are high, where a high value leads to more sedimentation in the upstream pit. The erosion parameter for the silty fraction can be considered a scaling parameter for the sedimentation over the entire channel This is due to the relation with the suspended sediment concentration. Therefore in this case the suspended sediment concentration was calibrated rather than the sedimentation pattern. The critical shear stress for erosion, as expected, turned out to be crucial for the sedimentation pattern. Especially around the upstream pit low values lead to unrealistic erosion. Downstream high values of the critical bed shear stress lead to low sedimentation volumes. Therefore the use of a spatially varying critical bed shear stress is adopted for both cohesive fractions, since they are known to interact. Furthermore, the variation also matches the varying sediment characteristics along the canal, with a more sandy character upstream and a muddy character downstream.

5.4.3 Sensitivity analysis: role of forcing mechanisms and assumptions

A sensitivity analysis (SA) is a formalized procedure to identify the impact of changes in model inputs and components on a model's output (Newham et al., 2003). It is helpful in assessing whether the model resembles the system or process under consideration and can distinguish parameters and data input which have considerable influence on the output and variables which are inconsequential. A

sensitivity analysis is essential for this research in order to test whether the identified physical processes indeed have the expected effects (as described in paragraph 2.10) and furthermore if the assumptions on the bathymetry do not affect the simulated sedimentation.

The outcomes of the sensitivity analysis are visualised in Figure 50, and are described in this paragraph per scenario:

- Excluding tide: Excluding the tide leads to a sedimentation profile which shows exponential decay of the sedimentation from KP 41 until around KP 30 where the sedimentation in the channel is close to zero. From this it can be concluded that when the tide is excluded the sedimentation profile is rule by the supply of sediment from upstream. Paragraph 2.10 concluded that the tide is responsible for the movement of the sediment laden water over the channel, leading to infill due to the reduced bed shear stresses in the channel. Indeed this scenario shows that the sediment concentration is not affected too much but that the sedimentation volume is much lower. Furthermore, it reveals also that in case the tide is absent also sedimentation is simulated around KP 40 which is around the transition from the river to the estuary. The absence of the tide leads to the reduction of the bed shear stresses, leading to more sedimentation. The observation that the sedimentation in the channel downstream of KP30 is close to zero shows that the sedimentation in that area is very sensitive to changes in the tidal regime.
- Excluding waves: Downstream of KP 25 excluding the waves leads to the same profile as excluding the tide. This provides confidence that in that region the sedimentation in the channel is indeed ruled by forcers on the estuary itselves in which the tide is responsible for the movement of the water with a high sediment concentration over the channel and in which the waves are responsible for the (up)stirring of the sediment. Upstream of KP 25 the trend of the profile looks similar to the regular trend, but has a lower magnitude. This matches the expectations as the sediment concentration is still high around the transition from the river to the estuary due to the input from the Parana de las Palmas, but as the tide is still present this does lead to infill due to reduced bed shear stresses in the channel.
- Increased wind speed: increasing the wind speed to 8 m/s (constant in time) compared to the 5 m/s in the regular forcings results in a large absolute increase in simulated sedimentation, while the spatial pattern in comparable. In paragraph 2.10 it was concluded that the wind leads to locally generated wind waves increasing the (up)stirring of sediment, indeed in the modelling results this scenario shows an increased sediment concentration. Since the forcing due to the tide is constant, this leads to increased infill from the flats. Between KP20 and KP30 this effect is larger than in the other regions, this is explained by the fact that the flats are still shallow there and the flow of the Parana de las Palmas is less dominant there.
- Bathymetry change Martin Garcia: As described in paragraph 5.2.2 the bathymetry in around Canal Martin Garcia (mouth of Rio Uruguay) was schematised since the grid was too coarse to accurately represent the navigation channels. This scenario is therefore rather a check of the validity of the assumptions rather than a forcing mechanism. The results of this scenario show that even if drastic bathymetric changes are applied in this area this does not affect the sedimentation in Canal Emilio Mitre. The model results did show drastic changes in the hydrodynamics around the Canal Martin Garcia, but this does not affect the area of influence (as expected, since this region is located in another flow corridor). Therefore it is concluded that this simplification has no relevant effect on the results.
- Excluding pits: excluding the pits from the bathymetry results in a shift of the maximum of the sedimentation downstream, this shows that the pit is effective in attracting sedimentation since the flow velocities are reduced more upstream. Also the spatial pattern deviates at the second pit, without the pits a continuous profile is observed.
- It is concluded that the tested forcing mechanisms show the expected effect on the simulated sedimentation profile, both in spatial and absolute sense, and that therefore the right forcing mechanisms were included. The model is however shown to be very sensitive to the wind forcing, especially the absolute trend but also the spatial trend. Therefore a temporally varying wind scenario is tested, the results of these simulations are discussed in paragraph 6.4

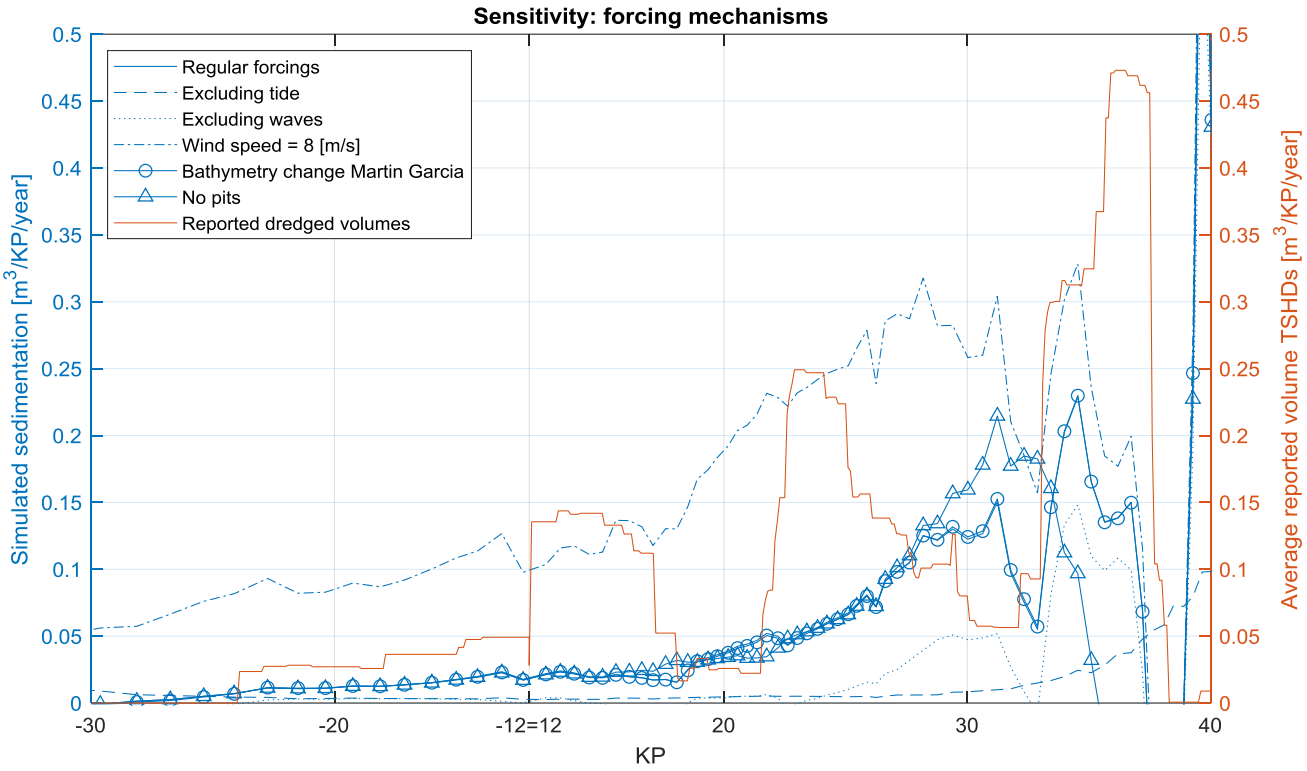

Figure 50 Sensitivity to forcing mechanisms and assumptions

6 Effect of scenarios on sediment dynamics

In the graphs on simulated sedimentation the left side of the figure is downstream (Rio de la Plata estuary) and the right side of the figure is upstream (Rio Parana de las Palmas), for example Figure 56.

This chapter presents the hydrodynamic and morphodynamic results of the numerical model. Paragraph 6.1 presents the Base Case, elaborating on the validation of the morphodynamics by comparing the reported dredged volumes and the simulated sedimentation by the model. In paragraph 6.2 the outcomes of the climate scenarios are presented, concluding that both scenarios lead to an increase in simulated sedimentation and a shift in the spatial pattern. Paragraph 6.3 presents the results of the deepening scenarios, concluding that without temporally varying wind deepening the model forecasts attraction of flow into the channel and thus a decrease in simulated sedimentation. In paragraph 6.4 the effect of temporally varying wind over the inner part of the estuary is added, leading to a considerable change in the absolute predicted values of the sedimentation as well as the conclusion that the deepened stretch attracts more sedimentation than the regular bathymetry.

6.1 Base Case

The Base Case is a computation with a duration of 1 year starting at 01-09-2013. This period in time is chosen as it represents an average year considering the forcings. It is therefore also used as the validation of the sediment dynamics of the model and compared against other scenarios in the following paragraphs. To illustrate the dynamics of the system first the wave characteristics, flow velocities, bed shear stresses and concentrations are presented both at rising and at falling tide (all parameters represent the same time step at which flow velocities are maximum or minimum).

Wave characteristics
Figure 51 gives the significant wave height over the domain which is almost constant in time due to the constant wind forcing (small differences due to tidal range). The wave height shows dependence on the water depth, around the transition from the river to the estuary (delta region) the wave height is low, while in the channel an increase in wave height is observed. Although no data is available to validate this behaviour the dependence on depth is physically sound. The mean wave period shows the same behaviour with lower values in shallower water.

Flow pattern
Figure 52 illustrates the flow pattern around the channel during rising and falling tide. During rising tide the flow velocities in the channel are a little lower than around the channel, which is as expected due to the opposing flow from the Parana de las Palmas. It also reveals that the flow velocities around the transition from the river to the estuary are never to the north. The discharge of the Parana de las Palmas is stronger than the tidal flow velocities. During falling tide the flow velocities are considerably higher as the discharge enhances the tidal flow, around the transition from the river to the estuary the velocities in the navigation channel are a higher than in the surrounding cells due to the lower resistance due to the larger water depth.

Bed shear stresses
The bed shear stresses at rising and falling tide are presented in Figure 53, which shows a background bed shear stress of around 0.05-0.1 N/m^2 induced by the small tidal velocities and the waves. During the falling tide the flow velocities are enhanced by the discharge of the rivers, the bed shear stresses go up to 0.25 N/m^2 in the navigation channel and 0.15 N/m^2 adjacent to it.

Suspended sediment concentration
The suspended sediment concentration shows the dependency on the suspended sediment concentration from the Rio Parana de las Palmas and the effect of waves in the shallow areas. Even

during low energetic conditions the suspended sediment concentrations is still rather high (see Figure 44 for bathymetry). This is explained by the bed shear stress due to waves which are constantly present in the model.

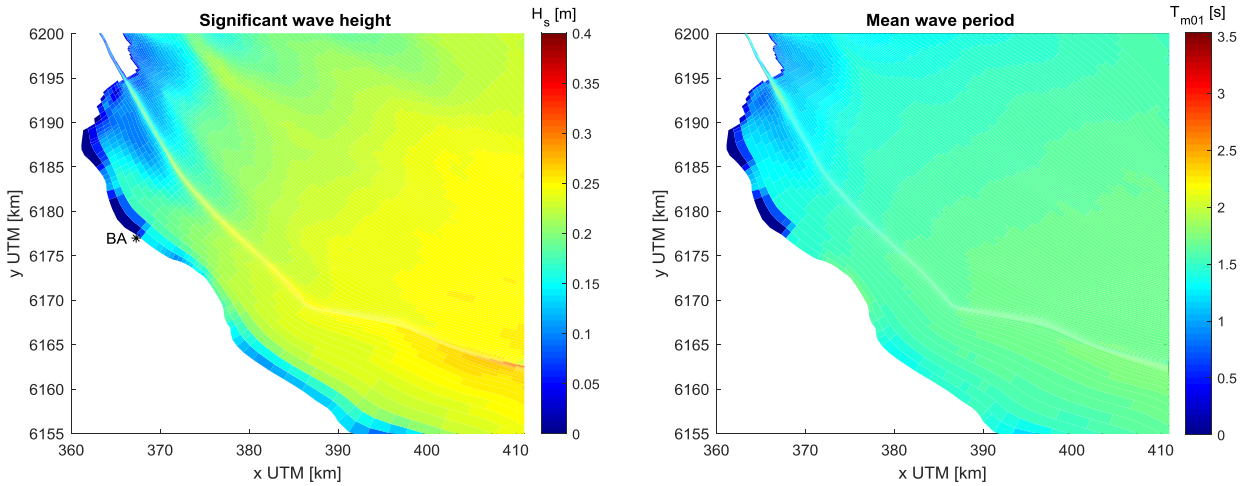

Figure 51 Base Case: significant wave height (left) and mean wave period (right) both during rising tide

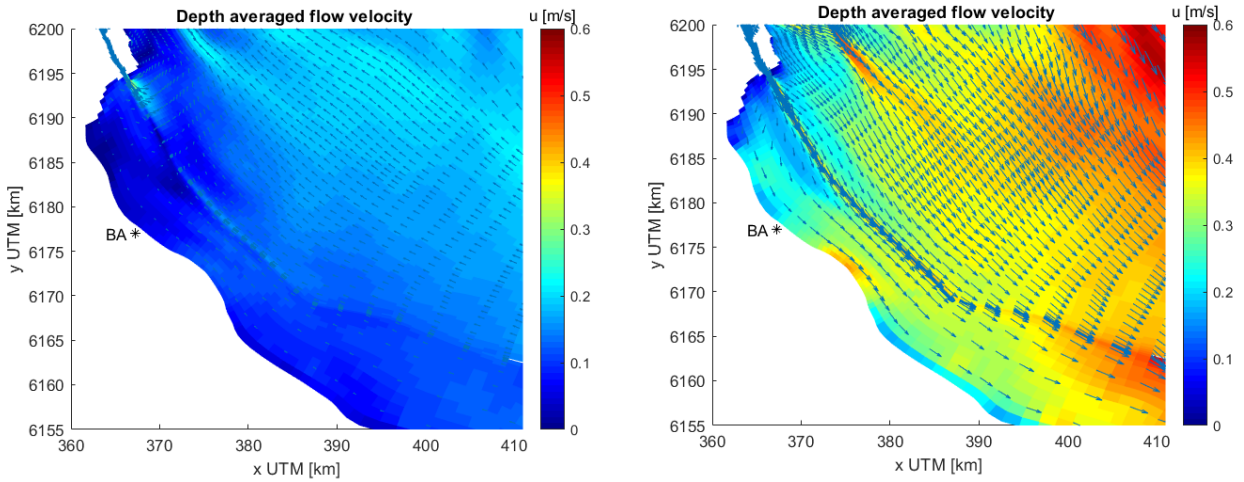

Figure 52 Base Case: Depth averaged flow velocity during rising (left) and falling (right) tide

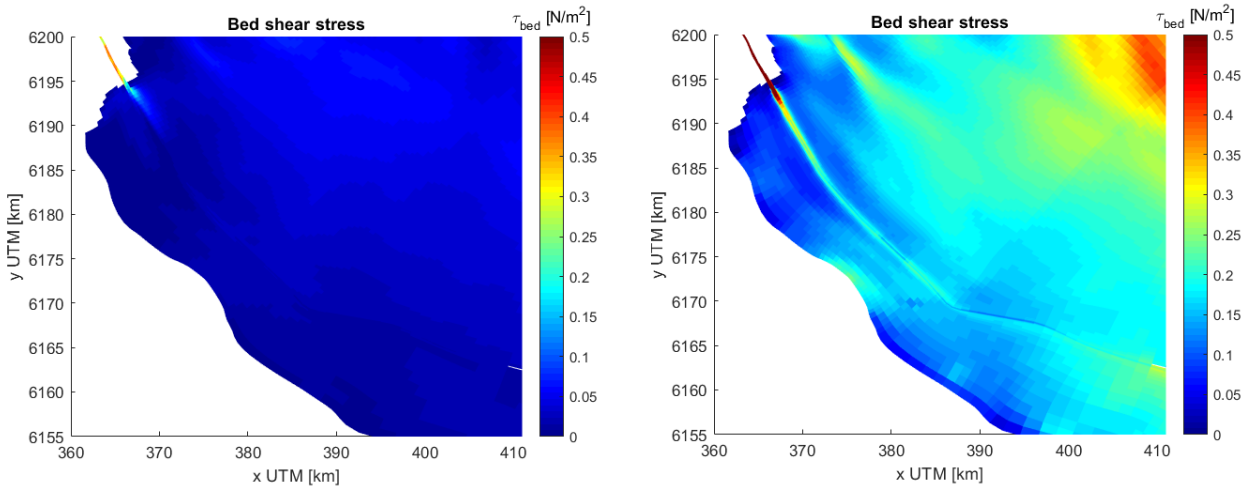

Figure 53 Base Case: bed shear stress during rising (left) and falling (right) tide

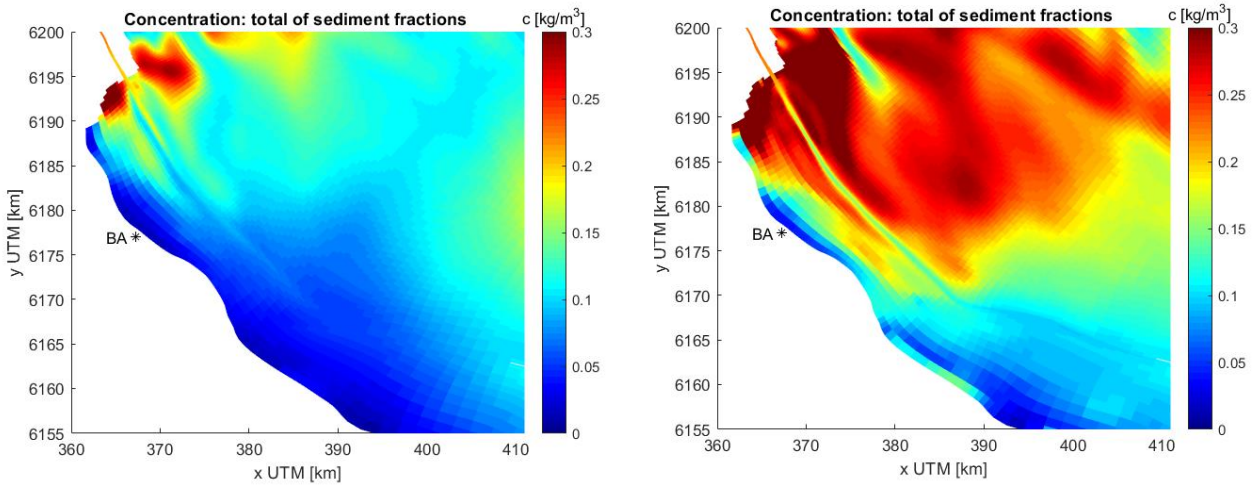

Figure 54 Base Case: concentration during rising (left) and falling (right) tide

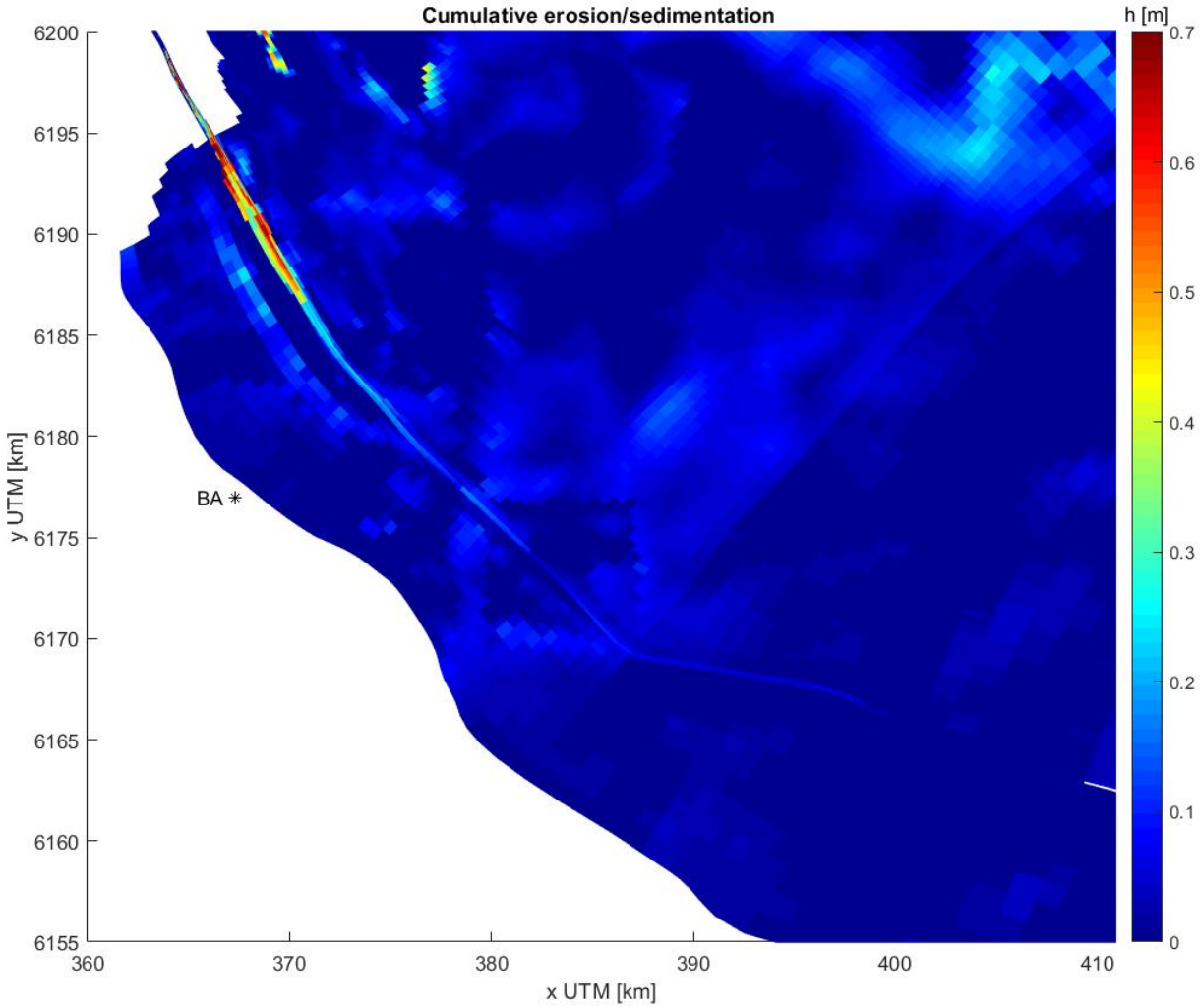

Figure 55 Base Case: cumulative erosion/sedimentation [1 year]

Figure 55 illustrates the cumulative erosion/sedimentation over the area of interest for the Base Case simulation with a duration of 1 year. It shows sedimentation in the navigation channel, decreasing in magnitude from upstream to downstream. The comparison between simulated sedimentation (black)

and the reported dredged volumes in 2015, 2016 and 2017 (blue) is presented in Figure 56. This figure was constructed by aggregating the simulated sedimentation between the 5 m depth isoline of the navigation channel in the numerical model. The x-coordinate indicates the kilometer points as used in the estuary, with the Rio de la Plata estuary on the left and the Rio Parana de las Palmas on the right (KPs indicated in Figure 38 on the map). The dredged pits are indicated in the upper panel and lower panel, the lower panel indicates the initial bathymetry of a transect through the navigation channel in the model. The dredging data of 2015, 2016 and 2017 is used since that bathymetry was used since the location of the pits was constant in time.

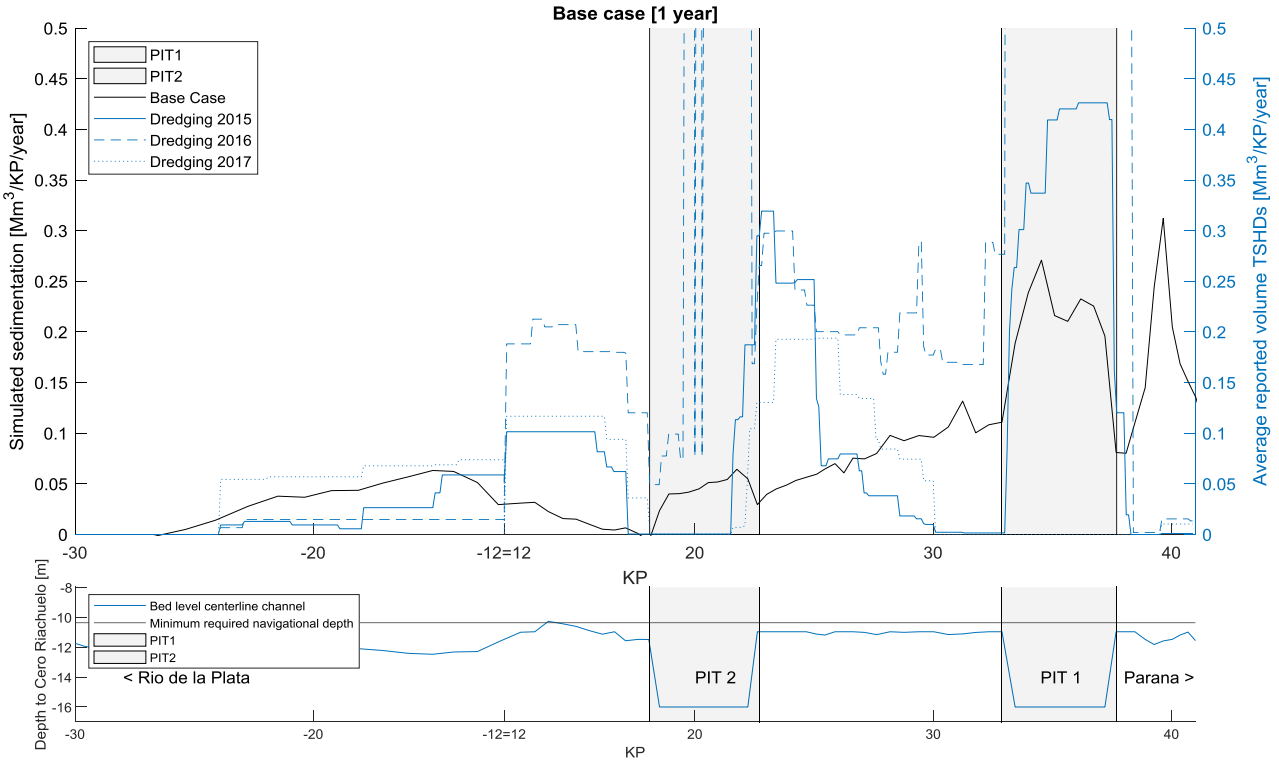

Figure 56 Base Case: Comparison simulated sedimentation vs reported dredging volumes different years (upper panel) and initial bathymetry in model (lower panel)

Comparison of the spatial distribution of the dredging and simulated sedimentation provides the following insights:

- Between KP 38 (upstream) and KP -25 (downstream) both trends show sedimentation/dredging with overall a decreasing trend in volume in the downstream direction. Both the onset of extreme sedimentation at KP 38 and the end of sedimentation at KP -25 match the reported dredging volumes.
- The peaks in reported dredging volumes in both pits (grey in the figure) are also recognised in the simulated sedimentation trend.
- The abrupt reduction of the reported dredging volumes downstream of pit 1 is also recognised in the simulated sedimentation.
- At KP 40 a peak in the simulated sedimentation is shown, at this location occasionally some dredging is also recorded but the magnitudes do not match. Although sedimentation is simulated here the natural water depth is still larger than the guaranteed navigational depth and therefore this does not lead to a direct dredging need (Figure 40). Furthermore, this location in the model also shows to be very sensitive to the discharge of the Parana de las Palmas and the effect of temporally varying wind on the inner estuary, as elaborated on in paragraph 6.2 and 6.4 respectively.

To conclude, the spatial pattern of the simulated sedimentation and the reported dredging volumes match to a global extent with a reduction of the trend downstream and peaks in the pits. However

when looking at the absolute volumes the reported volumes are larger than the simulated volumes. Possible reasons for this difference are summarized below:

1. The simulated sedimentation for 2013-2014 (3.38 Mm^3) is compared in the graph with the average annual dredged volume for 2015-2017 (8.68 Mm^3 on average→ factor 2.56) since that period showed a constant location of the pits. During 2015-2016 the major El Niño event took place which led to a larger reported dredging volume than is reported during 2013-2014 (3.83 Mm^3→ factor 1.13) or over the complete period (5.7 Mm^3 → factor 1.68).
2. Dredging does not occur gradually at all locations at the same time, once every year the dredging effort is performed after which the area is left. While the simulated sedimentation is a constant process. Also sedimentation can occur in regions where there is enough over depth, thus not leading to need for additional dredging (such as around KP40). This leads to deviations in time between reported dredging and simulated sedimentation.
3. Furthermore, the current set-up of the research assumes the reported dredging volumes are fully efficient, implying that one cube of sedimentation results in one cube of dredging in the reported volume. Since the measurement method of the reported dredged volumes is unknown (survey versus hopper volumes) this introduces a large uncertainty in the absolute volumes. In case the volumes are hopper and cutter volumes, these could even have been measured using a different method leading to even more uncertainty.
4. The sensitivity analysis looked into the effect of the different forcing mechanisms. This revealed that the higher wind speeds are very effective in stirring up the sediment resulting in high sedimentation volumes. Therefore excluding these high wind speeds in the model could have led to underestimation of the sedimentation, this uncertainty is addressed in paragraph 6.4.

To conclude, the model is considered an acceptable representation for the intended use, namely the analysis of the spatial and relative effect of the different scenarios on the sedimentation in Canal Emilio Mitre. In this paragraph it was shown that the predicted spatial pattern matches and paragraph 5.4.3 revealed that the model is able to show the effect of different physical forcers. Therefore it is also suitable to investigate the effect of different climate and dredging scenarios. The model shows a good match considering the absolute amount of dredging for the 2013-2014 year, but since dredging volumes are highly variable between years this has to be studied with care. Additional information on the consolidation of the bottom material and the way in which the reported dredging volumes were documented are needed for that analysis. The following paragraphs present the outcomes of the scenarios, the following structure is used in all paragraphs:

- Table which summarizes the absolute, spatial and temporal effect compared to the Base Case
- Explanation on the scenario
- Figure on spatial change of simulated sedimentation pattern in detail
- Figure on spatial change of simulated sedimentation per area*
- Figure on temporal change in sedimentation speed (if relevant)
- Explanation of observed differences linked to the hydrodynamics
- Main conclusions from this scenario

*The areas are defined as: Upstream of pit 1 (KP 41- KP 38.2), pit 1 (KP 38.2 – KP 33), between pits (KP 33 – KP 22.2), pit 2 (KP 22.2 – KP 18.2) and downstream of pit 2 (KP 18.2 – KP -32)

6.2 Climate scenarios

	Climate change	**Climate variability**
Absolute effect	3.59 Mm^3 (+ 6.2% to Base Case 1 year)	3.96 Mm^3 (+ 17.2% to Base Case 1 year)
Spatial effect	Shift from upstream to between pits	Shift from pit 1 to between pits
Temporal effect	None	Increase sedimentation speed during flood peak

Table 5 Summary absolute, spatial and temporal effect climate scenarios compared to Base Case

The climate scenarios consist of a modification of the discharge on the Rio Parana boundary condition. In the climate change scenario the discharge signal was increased by 8.5% over the whole year. In the climate variability scenario the discharge of the El Niño year 2015-2016 was imposed which exceeds the Base Case discharge with 20.7% on average and peaks in January (details on these scenarios and prediction of the effects are in paragraph 3.3).

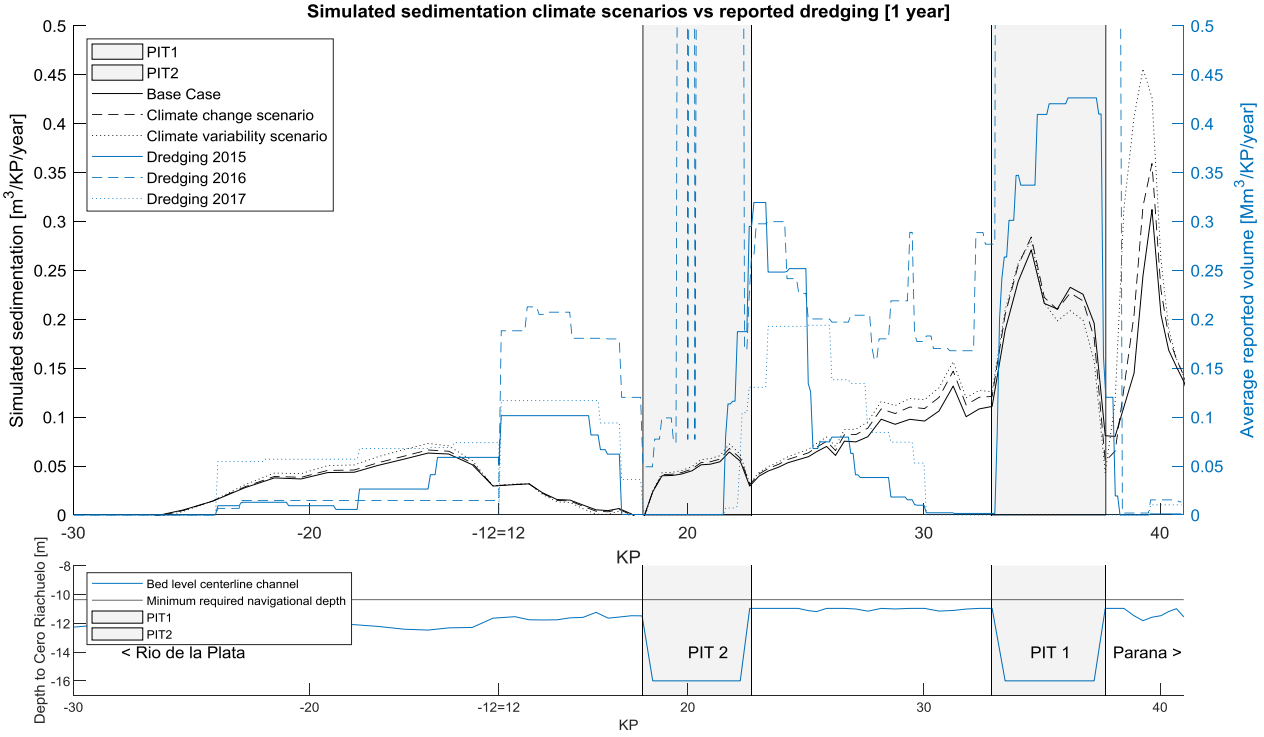

Figure 57 Climate scenarios: simulated sedimentation vs reported dredging [Mm^3/KP/year]

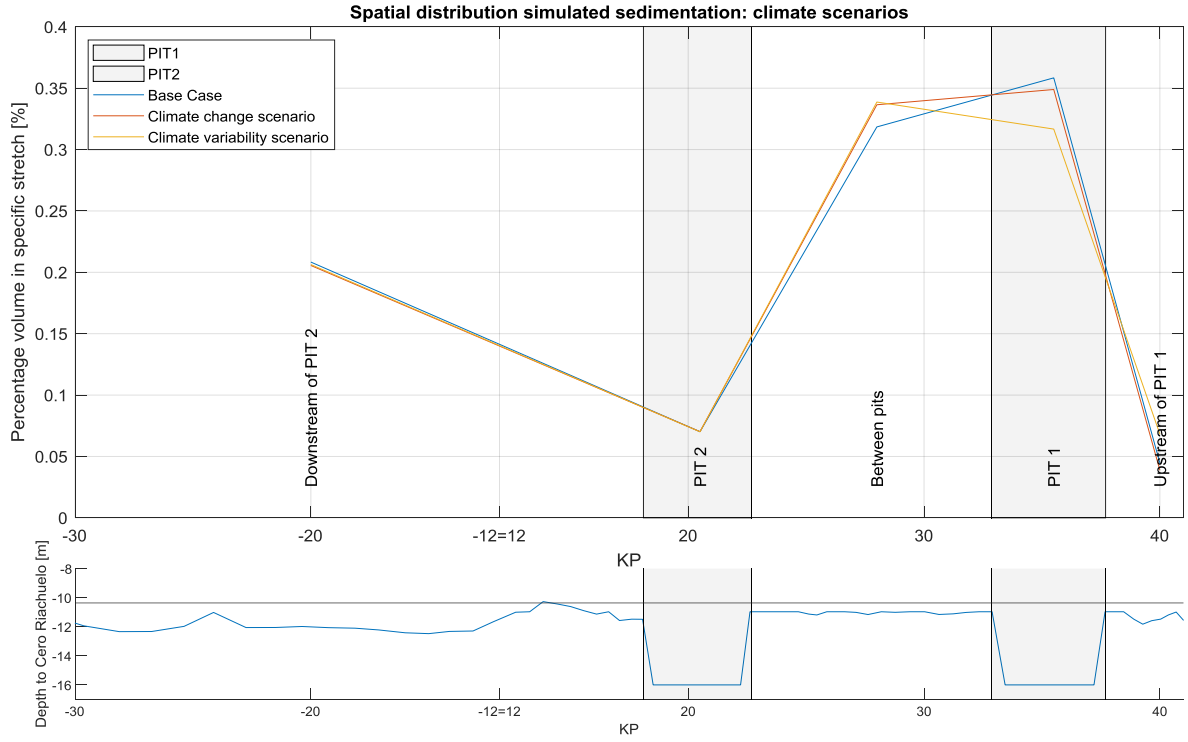

Figure 58 Climate scenarios: spatial distribution simulated sedimentation [%]

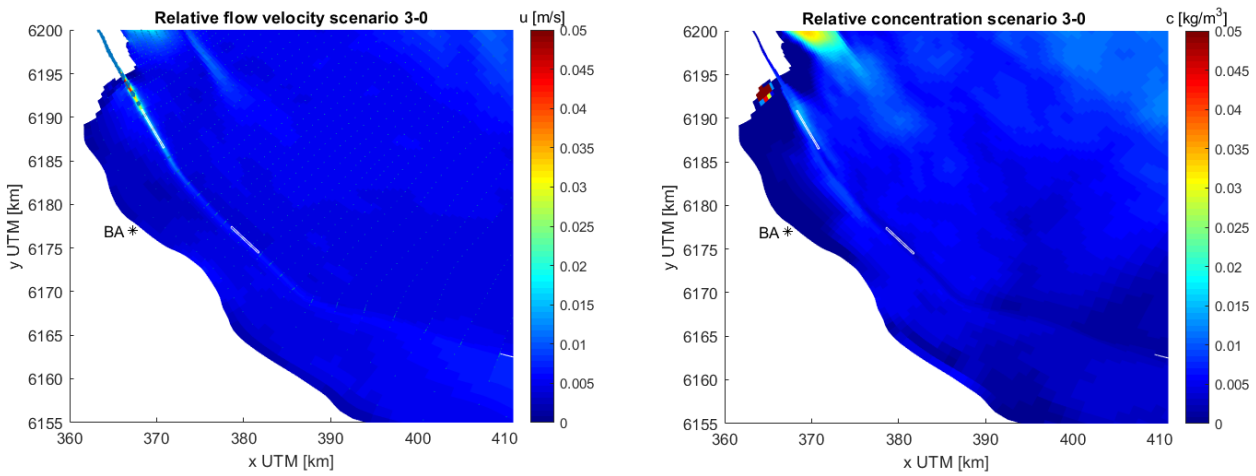

Figure 59 Relative flow velocity and concentration for scenario Climate Change - Base Case for falling tide (t=60)

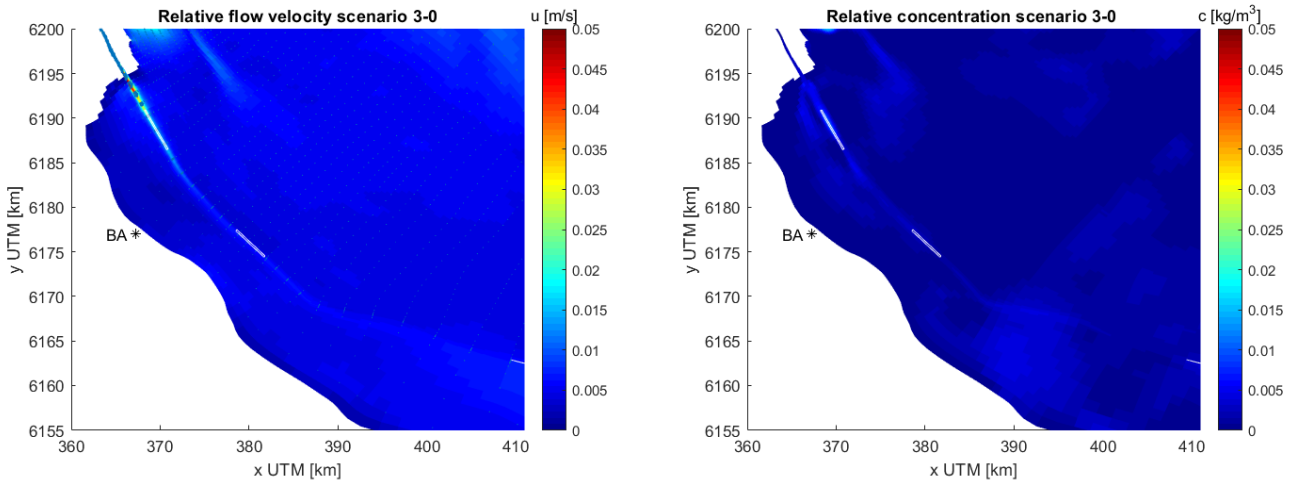

Figure 60 Relative flow velocity and concentration for scenario Climate change - Base Case for rising tide (t=12)

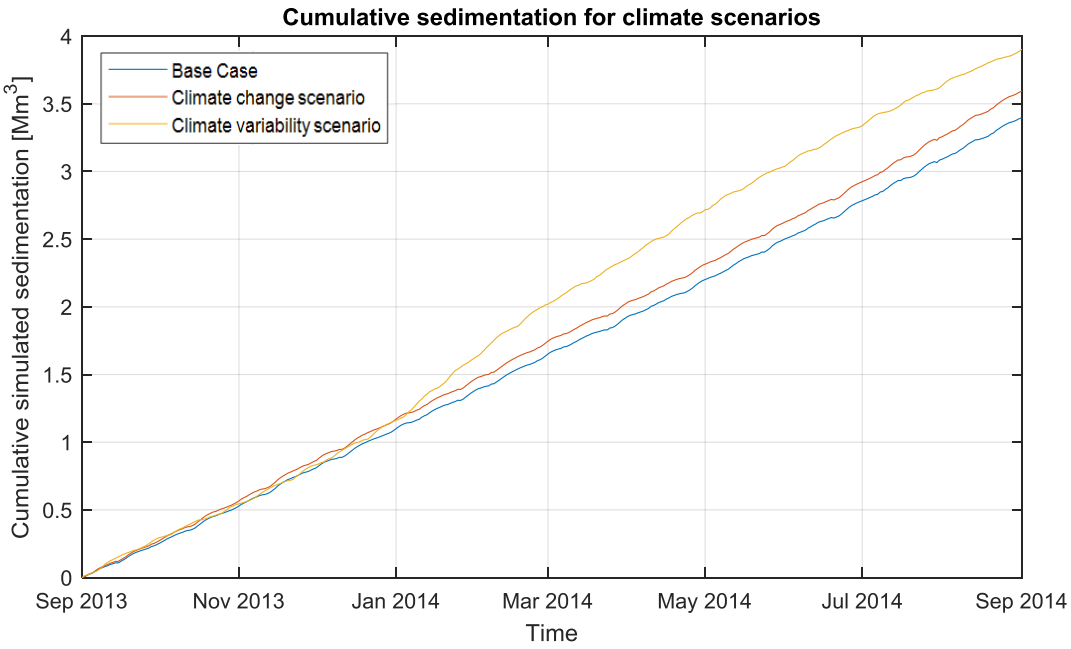

Figure 61 Climate scenarios: cumulative sedimentation in time

Comparison of the Base Case and the climate scenarios provides the following insights:

- The climate change scenario results in 6.2% additional sedimentation compared to the Base Case (Table 5). The spatial distribution is rather similar (Figure 57) but shows a shift from pit 1 and upstream of pit 1 to the area between the pits (Figure 58). Analysis of the flow velocities and suspended sediment concentration shows that due to the higher discharge close to the transition from the river to the estuary, the flow velocities are higher, resulting in a higher sediment concentration and settling of the sediment more downstream (Figure 59 and Figure 60). Since the absolute supply of sediment from upstream is still larger than in the Base Case, overall the sedimentation is higher over the whole profile and a spatial shift is visible from pit 1 to the area between the pits. In time the sedimentation speed for the climate change scenario is slightly higher than for the Base Case (Figure 61), which is as expected as the additional supply of sediment from upstream is also constant in time.
- The climate variability scenario results in 17.2% additional sedimentation compared to the Base Case (Table 5). The spatial distribution is similar (Figure 57) but shows more volume between the pits, less in pit 1 and more in the stretch upstream of pit 1 (Figure 58). Analysis of the flow velocities and sediment concentration shows that due to the higher discharge close to the transition from the river to the estuary, the flow velocities are higher, leading to the fact that the suspended sediment settles more downstream, and thus between the pits instead of in pit 1 (Figure 59 and Figure 60). Additionally Figure 58 shows a higher percentage upstream of pit 1 than the Base Case, this is explained by the low discharge at the end of the simulation (see Figure 36). It shows that the sedimentation in the area upstream of pit 1 is very sensitive to the discharge of the Parana de las Palmas at that moment. The discharge peak around January is clearly recognised in the sedimentation speed of the climate variability scenario (Figure 61), which also peaks around January.

It is concluded that the model is able to represent the phenomena that an increase of discharge leads to an increase in sedimentation. The effect is recognised in the absolute sense, but also the spatial and temporal effect matches the expectation. The sedimentation in pit 2 and downstream of pit 2 is shown not to be affected by the increased discharge of the Parana, this matches the conclusion that the dredging volumes in pit 2 are not affected by extreme event of the 2016 El Niño (Hidrovia SA, 2017).

The analysis of the dredging record revealed that during the 2016 El Niño year the dredging volume of the TSHD is about twice as high during non El Niño years (Figure 37, CSD volume is excluded here since this is also buffer for the coming years). The cumulative sedimentation in the climate variability scenario however only went up by 17 % (Table 5). Although the temporal and spatial effect match the expectations and knowledge about the system, the prediction of the absolute effect deviates from the observations. Possible reasons for this deviation are addressed in the Discussion (paragraph 7.3).

Furthermore, it is observed that the temporal variation in the sedimentation speed during the base case is very low, it is almost a linear trend. Although no validation of this trend can be done it is expected that this variation is higher in reality due to the effect of storms leading the resuspension of bed material. Since the temporal variation of the wind forcing is not included in the model this is an expected outcome. This forcer is addressed further in paragraph 6.4.

6.3 Deepening scenarios

	Deepening 36 ft	**Climate variability 38 ft**
Absolute effect	0.368 Mm^3 (- 7.8% to Base Case 2 months)	0.380 Mm^3 (- 4.8% to Base Case 2 months)
Spatial effect	Shift downstream to pit 1	Shift downstream to pit 1

Table 6 Summary absolute, spatial and temporal effect deepening scenarios compared to Base Case (temporal not relevant)

For both the deepening and the wind scenarios the computations were done for 2 months instead of 1 year in order to save computational effort (justified since temporal trend of sedimentation is linear).

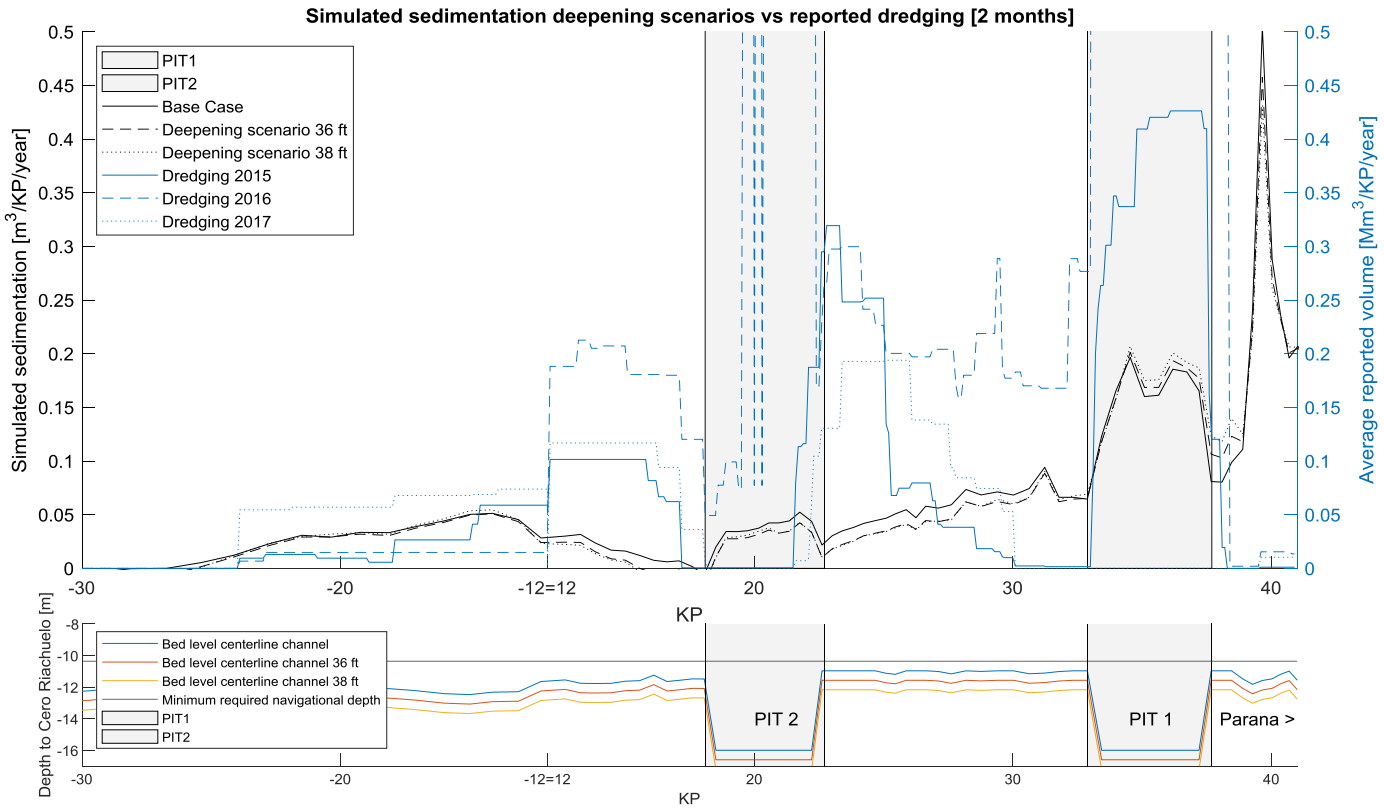

Figure 62 Deepening scenarios: simulated sedimentation vs reported dredging [Mm^3/KP/year]

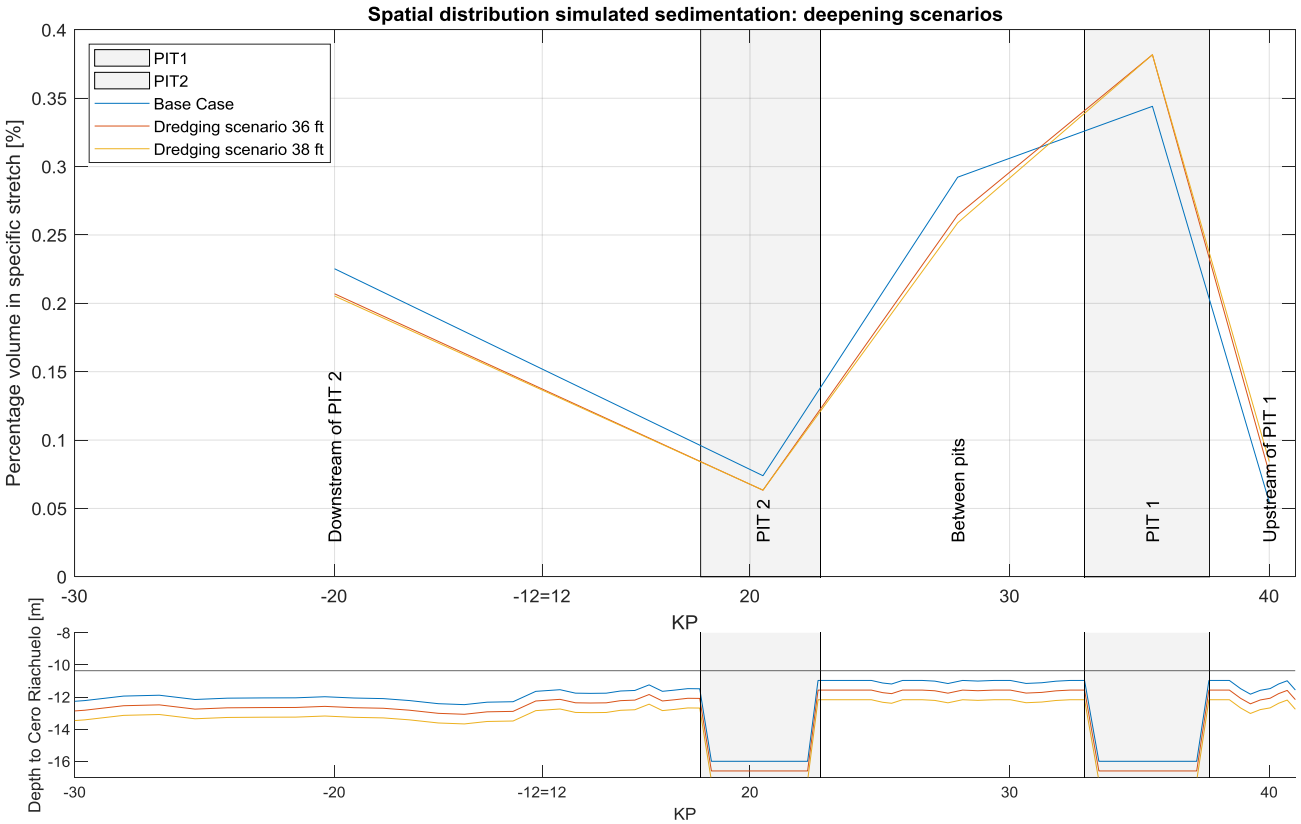

Figure 63 Deepening scenarios: spatial distribution simulated sedimentation [%]

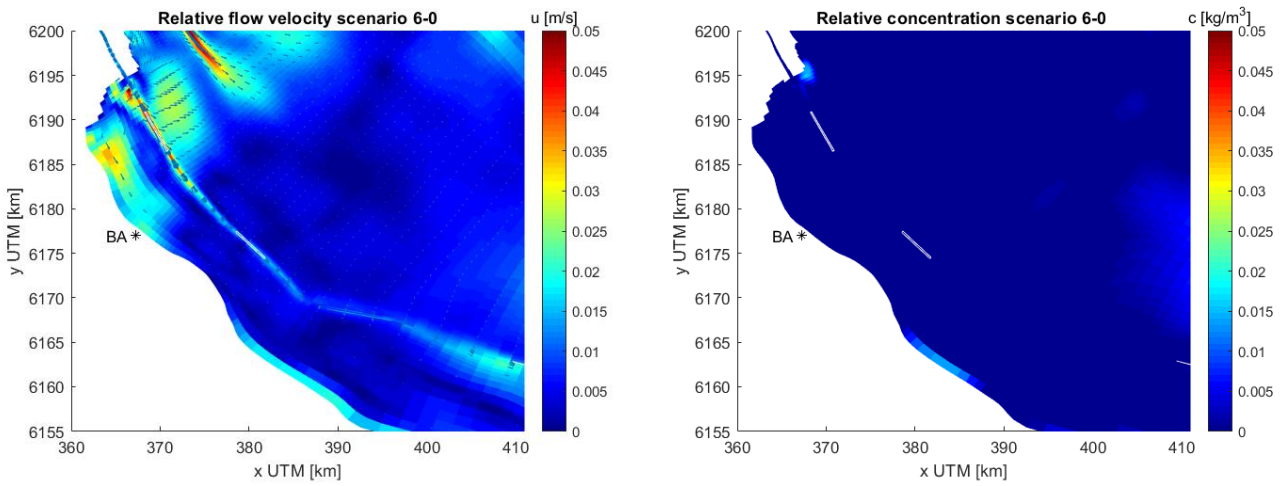

Figure 64 Relative flow velocity and concentration for scenario Dredging 38ft - Base Case for rising tide

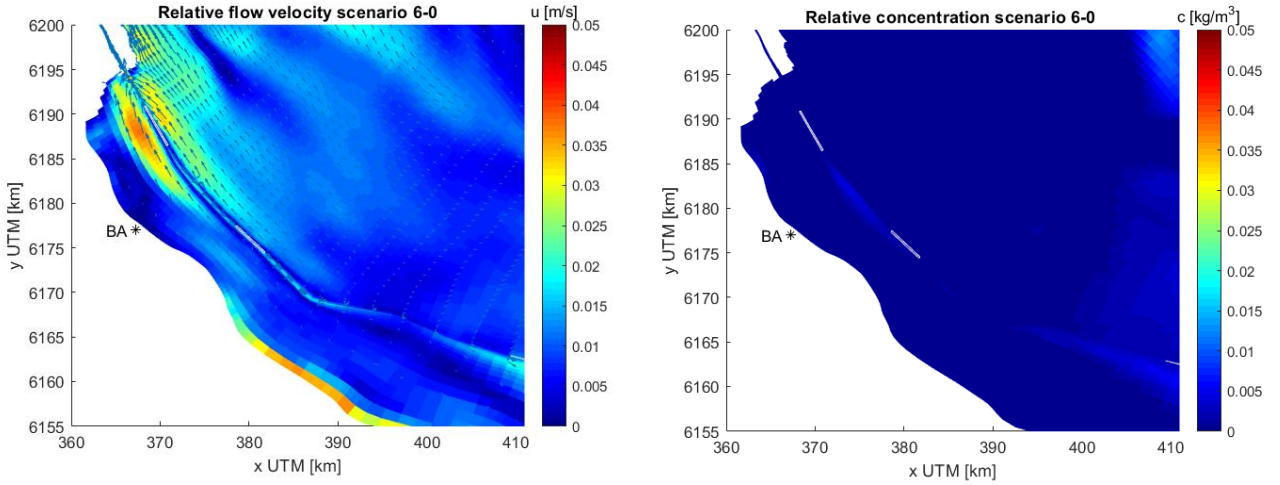

Figure 65 Relative flow velocity and concentration for scenario Dredging 38 ft - Base Case for falling tide

The deepening scenarios consist of a modification of the initial bathymetry between the toe line of the channel by deepening it by 2 and 4 feet respectively (details on scenarios and prediction of the effects are in paragraph 4.4).

Comparison of the Base Case and the deepening scenarios provide the following insights :

- The first deepening scenario results in an overall 7.8% decrease in sedimentation volume compared to the Base Case (Table 6). The spatial distribution is similar to the Base Case (Figure 62) but shows more sedimentation percentage-wise in the upstream pit and at the stretch before the upstream pit (Figure 63). The stretch between the pits, pit 2 and the stretch downstream of pit 2 show less sedimentation percentage-wise compared to the Base Case. Analysis of the flow velocities and suspended sediment concentration show that the deepened channel attracts discharge resulting in larger flow velocities in the channel compared to the Base Case. This results in higher suspended sediment concentration between the pits (Figure 64 and Figure 65).
- The second deepening scenario results in an overall 4.8% decrease in sedimentation volume compared to the Base Case (Table 6). The spatial distribution of the 38 ft scenario deviates in the same way as 36 ft scenario due to the attraction of discharge (Figure 62). Additionally it has more sedimentation at the start of the stretch (Figure 63) as the flow reduction at the start of the channel is more extreme than for the scenario of 36 ft.

To conclude, the deepened channel attracts flow both during rising and falling tide. All in all it leads to an overall reduction of the sedimentation volume in combination with an upstream shift of the percentage-wise trend. The 38 ft scenario leads to a smaller reduction of the sedimentation volume than the 36 ft scenario, suggesting that the economic optimum of the navigational depth is around 36 ft. However further variations of dredging depth, and its spatial distribution are needed to substantiate this since this outcome is against the expectations.

From numerical modelling it is concluded that deepening leads to attraction of flow into the channel leading to a reduction in the simulated sedimentation volume. This result deviates from the prediction based on volume of cut engineering rule (paragraph 4.4). In paragraph 6.4 the effect of temporally varying wind is added to this analysis.

6.4 Effect of temporally varying wind on deepening scenarios

	Base case with wind	**38 ft with wind**
Absolute effect	0.820 Mm^3 (+125% to Base Case 2 months)	0.884 Mm^3 (+160% to 38 ft 2 months)
Spatial effect	Shift from upstream to between pits	Shift upstream to downstream of pit 1
Temporal effect	Peak during energetic events	Peak during energetic events

Table 7 Summary absolute, spatial and temporal effect temporally varying wind scenarios compared to Base Case

In the previous simulations a temporally constant wind was applied over the inner estuary and the influence of extreme wind from the ocean was only included in the offshore boundary. This paragraph addresses the effect of the addition of temporally varying wind over both the FLOW and WAVE module of Delft3D, affecting the currents, water levels and waves. Appendix 10.9 concludes that using reanalysis wind provides the best fit (using RMSE analysis) of the simulated and measured water levels at Braga (closest station to the area of interest). Since addition of this temporally varying wind leads to a better representation of the water levels, it is expected to better predict the sediment dynamics.

Comparison of the Base Case and the temporally varying wind scenarios provides the following insights:

- Addition of temporally varying wind to the Base Case leads to an increase of 125% in sedimentation (Table 7). In space it leads to a shift to the area between the pits (Figure 67). In time the higher sedimentation speeds coincide with extreme wind events over the estuary (Figure 68). Analysis of the flow velocities and concentration during the highly energetic events (14 September) shows an increase of the flow velocities of up to 1 m/s and an increase of the suspended sediment concentration of up to 0.6 kg/m^3 (Figure 69). The increase of the currents with around 1 m/s matches with literature (Piedra-Cueva, 2003). While during the non-energetic circumstances almost no deviations in the currents and suspended sediment concentration are observed (Figure 70).
- Addition of temporally varying wind to the deepened scenario (38 ft) has a relatively larger effect of 160% compared to the deepened scenario without temporally varying wind (Table 7). In space it leads to a shift from upstream to the downstream region (Figure 67), this is explained by the attraction of flow due to the deepening (as explained in paragraph 6.3). In time once again the highly energetic events result in an increase of the sedimentation speed (Figure 68).

It is concluded that the local time-varying wind has large effects on the water levels and currents around the area of interest. Adding the reanalysis wind data leads to a better representation of the water levels, furthermore it leads to an increase of the simulated sedimentation with more than a factor 2. The results show that the effect on the deepened scenario is even larger than on the regular bathymetry. In the end it follows from numerical modelling that with time-varying wind the deepened channel experiences 7.8% more sedimentation than the regular bathymetry. When comparing this 7.8% to the outcomes of the volume of cut method in paragraph 4.4 it is concluded that the model

predicts a smaller increase than the engineering rule (paragraph 4.4), which predicts an increase of 24%. This difference is attributed to the fact that the channel is located along the direction of the tidal flow leading to the attraction of discharge and the fact that part of the sedimentation is caused by the upstream supply of sediment which is not affected by deepening of the channel.
Although addition of time-varying wind is expected to have a large effect on the sedimentation volume, an increase of more than 100% was not expected. Therefore it is recommended to recalibrate the morphological setting of the model including temporally-varying wind.

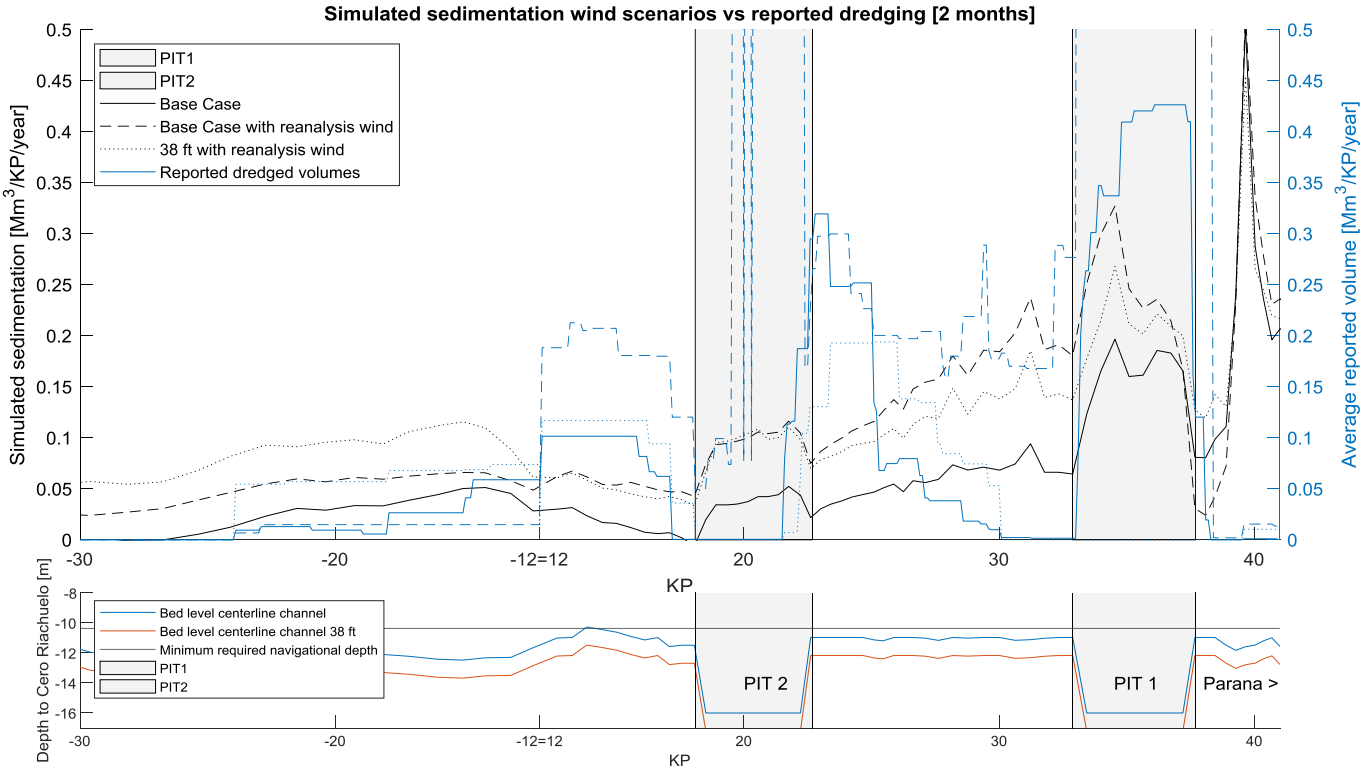

Figure 66 Wind scenarios: simulated sedimentation vs reported dredging [Mm^3/KP/year]

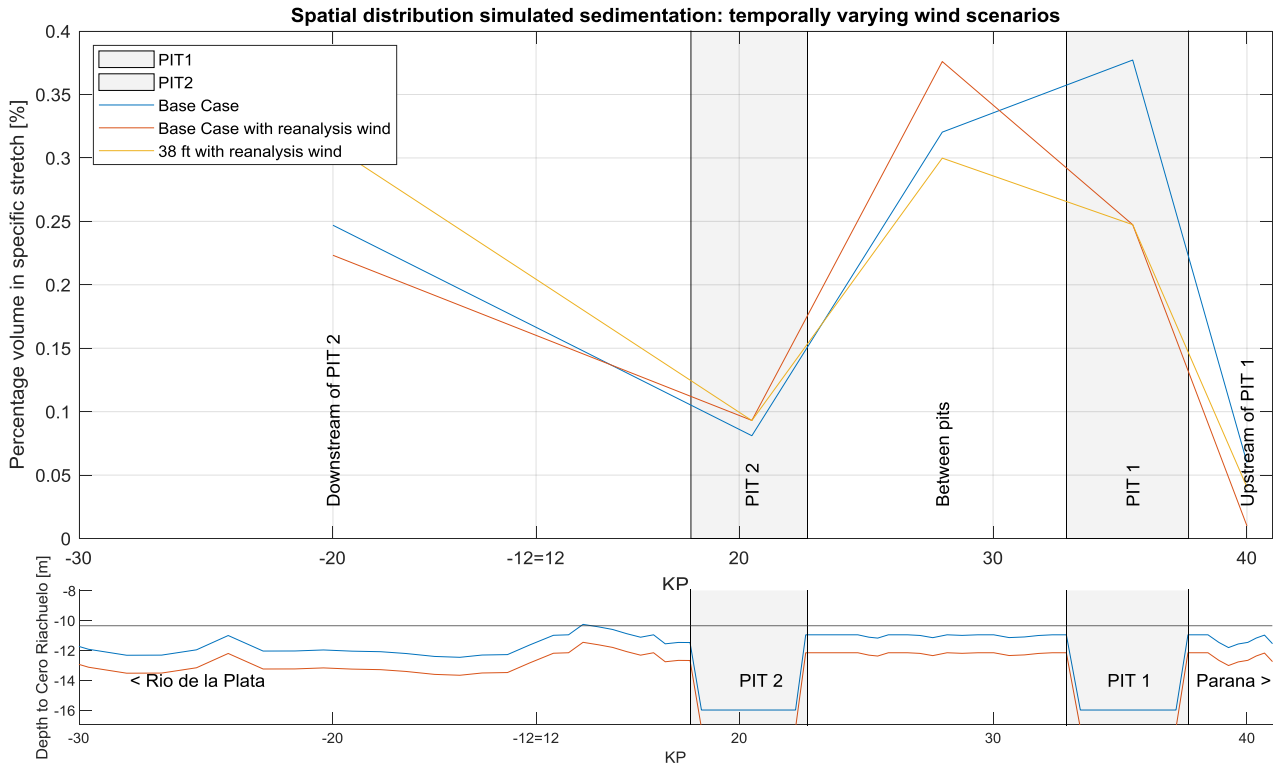

Figure 67 Wind scenarios: spatial distribution simulated sedimentation [%]

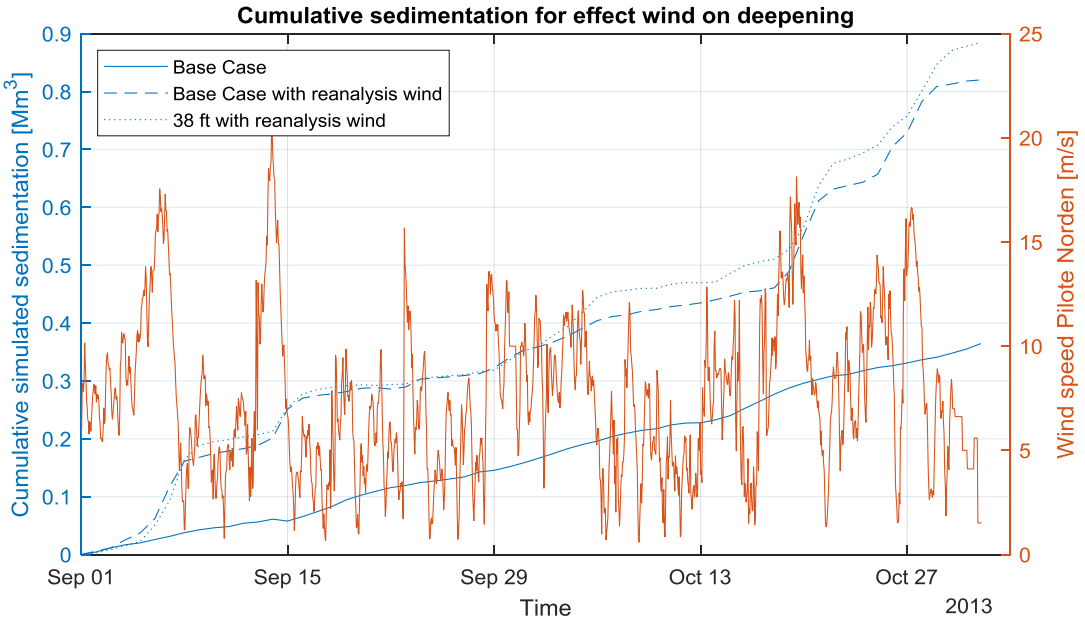

Figure 68 Wind scenario: temporal effect

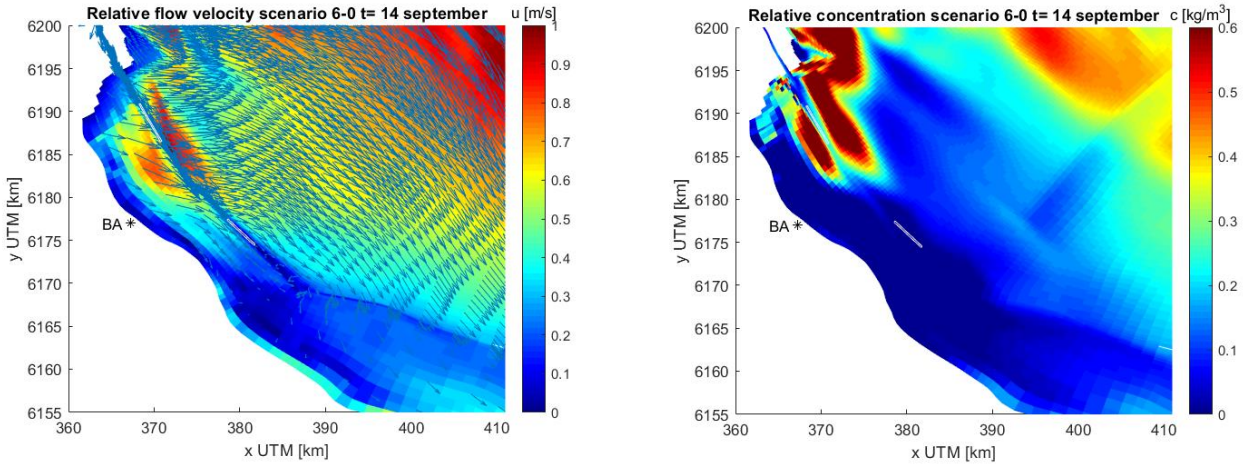

Figure 69 Relative flow velocity and concentration for scenario 6-0 for energetic conditions (38 ft with reanalysis wind - Base Case) t=14 September 00:00

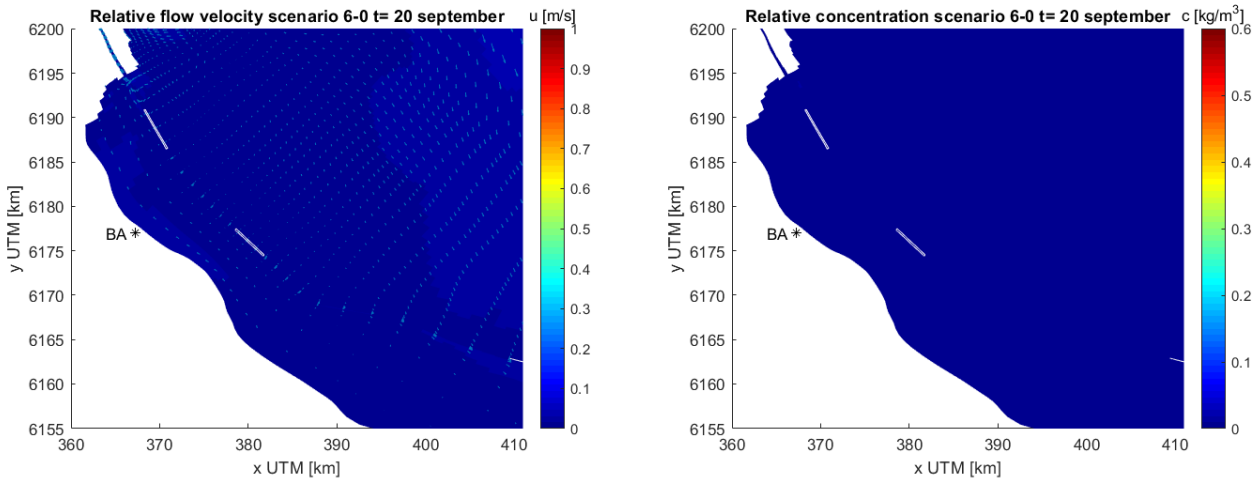

Figure 70 Relative flow velocity and concentration for scenario 6-0 for non-energetic conditions (38 ft with reanalysis wind - Base Case) t=20 September 00:00

7 Discussion: including variability in the dredging strategy

Analysis of the dredging record revealed that the annual average dredging effort in Canal Emilio Mitre is 5.7 Mm^3 per year, with peaks to 9.2 and 17.4 Mm^3 in the El Niño years 2010 and 2016 respectively. The upstream supply by the Rio Parana de las Palmas river branch and the infill from the sides are the main forcers affecting the sedimentation of the navigation channel. The infill from the sides is affected by the tide and the locally generated wind waves. Sediments from marine origin have a negligible contribution to the sedimentation. The infill from the sides is expected to have low interannual variability, while on the other hand the sediment supply from the Parana de las Palmas is shown to be highly variable between El Niño and non-El Niño years. The processes that were identified in the literature research as main forcers were validated in the numerical model and the identified processes indeed showed the expected effect on the sedimentation in the channel.

The main sources of variability in the dredging effort are climate variability and possible deepening scenarios. The effect of climate variability is linked to the ENSO phenomena and also partially linked to the dredging strategy with the incidentally dredged buffer pits. The conclusion from the numerical modelling with climate scenarios matches the analysis of the dredging record and the information provided by local scientists. The model can therefore be used as a forecasting tool for the effect of an increase in sediment input from the river system on the spatial sedimentation pattern. The observation in the report by the current dredging company that the extreme sediment input of the El Niño year 2016 only led to additional sedimentation in the upstream pit (and not in the downstream pit) provides confidence that also the spatial effect of additional sediment input is predicted correctly by the model.

From the numerical modelling, the chosen navigable depth is identified as a second factor leading to variability in the dredging effort. Engineering rules predict increased sedimentation in case of increased depth of the channel. Indeed numerical modelling shows roughly the same results, namely an increase of around 8% in simulated sedimentation for deepening from 34 to 38 feet allowing for navigation also during low tide. Simulating time-varying wind (instead of a constant wind in time) leads to a serious increase in predicted sedimented volume. This result provides support to the conclusion that the upstream part of the channel is mainly influenced by the upstream river supply while the downstream part of the channel is sensitive to the offshore forcings on the estuary, such as the wind.

Including the understanding which was gained in answering the first two research questions results in recommendations on how to include the risks and opportunities due to variability in the dredging strategy for Canal Emilio Mitre, which will be elaborated in the following paragraphs.

7.1 Optimization of current dredging strategy

Analysis of the dredging record showed that the upstream pit is mainly a sediment trap, while the downstream pit is an alternative disposal location for the TSHDs. During the analysis of the simulated sedimentation this was confirmed. Furthermore, the pits result in focussing of the sedimentation in space, as a decrease in sedimentation volume is observed downstream of the pits.

The location of the pits during 2016 (included in the Base Case bathymetry) is ideal. The upstream pit is located at the peak of the sedimentation, therefore attracting as much sediment as possible. The focusing of the sedimentation leads to more efficient dredging: it is suitable to be dredged by a CSD. Furthermore, the dredged material from the pit is expected to be more consolidated due to the low energetic circumstances in the pit (compared to its surroundings). The location of the downstream pit is optimal concerning the disposal of dredged sediment from other parts of the waterway, being located between the upper pit and the disposal location downstream of Canal Accesso (see Figure 38 for locations). This way it reduces the sailing time of the TSHDs in order to reduce operational hours.

From this analysis it is concluded that the location is optimal in the 2016 configuration. When considering the size of the pits three considerations have to be taken into account:

1. The development and statistics of the ONI index and the effect on the supply of sediment input from upstream
2. The selected navigational depth of the channel and the effect on infill from the flats
3. Mobilisation time of a CSD

The optimal size of the upstream pit is dependent on the first and third consideration since the sedimentation is shown to be mainly dependent on the strength of the ENSO event. The analysis of the events in time which lead to extreme sedimentation, showed that the El Niño started between 12 and 18 months before the CSD started working. Furthermore, the ONI index is predictable for around 6 months, leading to at least 18 months for anticipation. In case an extreme El Niño event is expected, it is recommended to dredge deeper pits in order to avoid excess costs due to mobilisation of additional material.

The optimal size of the downstream pit is dependent on the second and third consideration, since the pit is mainly used as alternative disposal location. The optimal size is therefore dependent on the selected navigational depth of the channel as both engineering rules and numerical modelling conclude that the total dredging effort is dependent on this.

To conclude, the current dredging strategy is suitable to mitigate the risks posed by the variability of the dredging effort in the system. The strategy should be optimised by forecasting the predicted dredging effort due to different scenarios, and adapting the size of the pits to these forecasts.

7.2 Alternatives for the waterway system

When looking at the Parana-Paraguay waterway system from a broader perspective it is striking to observe that Canal Emilio Mitre is used as the main route from the ocean to the river. The alternative route from the estuary to the river system is via Canal Martin Garcia and the BGT rivers (Bravo, Guazu, Talavera and indicated in Figure 71). This waterway has major advantages. Firstly, it has more natural navigational depth, being the main branch of the Rio Parana. Secondly, it is accessible to longer ships as the curves are less extreme (International transport and logistics legal consultants, 2019).

Figure 71 Alternative navigation route: BGT and Canal Martin Garcia

The bottleneck now is the navigation over BGT, but the Argentine government initiated dredging of this part until 34 feet as well in the near future. If both of these channels are open they can complement each other. A possible optimization of the system is using BGT for the large vessels and let the smaller vessels pass through Canal Emilio Mitre, this provides extra capacity to the waterway system and may reduce the dredging need in Canal Emilio Mitre.

Dredging of BGT might also affect the dredging effort in Canal Emilio Mitre. At first sight deepening of BGT leads to attraction of flow into the Parana Guazu, leading to less sediment supply into Canal Emilio Mitre (via the Parana de las Palmas). On the other hand, the decrease in discharge through the Parana de las Palmas leads to a reduced transport capacity and more material may settle in Canal Emilio Mitre. Further research is needed to address the effect of the deepening of BGT on the dredging in Canal Emilio Mitre.

7.3 Further research

The literature study, in combination with the analysis of the (dredging) data and the outcomes of the numerical model improved the understanding of the effect of variability on the dredging effort in the system. The combination of the results from data analysis and the outcomes of the numerical model

have resulted in confidence that the numerical model has the ability to predict the effect scenarios. This chapter elaborates on the effect of the assumptions and simplifications on the outcomes. Also, it suggests what practical actions or scientific studies are outside the scope of this study, but would enhance the reliability of the forecasts by the model.

1. Along the middle Rio Parana, extensive plains exist of up to 60 km in width. In the numerical model these flood plains are excluded. During very extreme discharges these flood plains are inundated as explained in Appendix 10.2. The effect of these extreme events on the sediment load of the Rio Parana is unknown, also to local specialists. Inundation might add sediment to the river due to erosion, but due to the fine sediment, low gradient, vegetation and meandering river course it is more likely that sediment will settle on the plains (Hupp et al., 2008). Due to this uncertainty it is unknown whether the sediment supply in the model on the upstream boundary during extreme circumstances (such as El Niño events) is realistic. Currently INA takes sediment samples once every two months, more frequent sampling (both Rio Parana and Rio Bermejo) contributes on the understanding of the role of the flood plains on the inter- and intra-annual variation of the sediment supply from upstream into the region of interest.
2. The combination of the fact that the sediment characteristics are highly variable in the region of interest and the limited knowledge on the consolidation of the cohesive material introduces uncertainty. Modelling with three sediment fractions revealed that the spatial sedimentation pattern fit the observations, but comparison of the simulated sedimentation and reported dredging in the pits shows an underestimation. It is uncertain whether there is a layer of barely consolidated material present in the estuary which is resuspended during highly energetic conditions. When looking from a scientific perspective, the conditions are favourable for the occurrence of a layer of fluid mud (van Rijn, 2016), however no sources have been found which mention this. Also the fact that pilots on the estuary get incorrect information from their echosounder implies that there is an unconsolidated layer of mud present (Gilardoni, 2018). The occurrence of fluid mud would possibly explain the extreme sedimentation in the pits, due to the steep slopes and high suspension rates on the shallow flats during energetic events. Research on the occurrence of fluid mud is highly advised in order to gain understanding of the sediment dynamics around the pits.
3. Partly coupled to the occurrence of fluid mud, is the sensitivity of the simulated concentration and sedimentation to the time varying wind/wave forcing. This followed from literature (Santoro et al., 2017 and M. Fossati, F. Cayocca, 2014) and was also confirmed by the sensitivity tests in the numerical model. In order to get a better idea of the effect of the wind/wave system on the suspended sediment concentration measurements have to be done both during regular and storm conditions. Furthermore, recalibration of the morphological parameters in the model with time-varying wind is recommended.
4. As described in paragraph 4.3 the reported dredging volumes may be inaccurate for technical and commercial reasons. Therefore extensive monitoring of the dredging record is recommended in case the project is rewarded. Using the fully reliable dredging data, an update of the numerical model can be made. The same is true for the assumed density of the simulated sedimentation, in case samples are taken this knowledge can be incorporated in the updated model. Adding this knowledge to the model will enhance the reliability of the forecasts of the sedimentation.
5. After all, a nested Delft3D model with boundary conditions from a larger model is very suitable to reduce the computational time of the model. This also yields computational effort for smaller grid cells on the slopes of the channel as the slopes are steep.

7.4 Effect of variability on other dredging projects

This study highlights the relevance of taking into account the effect of climate variability on long-term dredging projects. In the case of Canal Emilio Mitre the El Niño phenomena results in excessive additional dredging (up to 400% of annual average in 2016, also linked to the dredging strategy). Although in this system mainly the discharge of the river in combination with the sediment input is affected by the climate variability, in other regions ENSO has different effects. World-wide ENSO is the main source of climate variability, forced by the coupled ocean-atmosphere interactions in the tropical Pacific. Major ENSO events affect weather patterns over many parts of the globe through teleconnections (see Figure 72).

The effect of ENSO on the dredging industry is more extensive than the increase or decrease of sediment input. ENSO leads to changes in wind patterns, for example affecting the wave climate and therefore the workability. A study has been conducted on the effect of ENSO on the wave climate in Brazil, in order to address the interannual variability on the coastal management and coastal hazards policies related to those events (Da Silveira Pereira & Klumb-Oliveira, 2015). It shows that both El Niño and La Niña significantly affect the wave climate. Next to the wave climate, also turbidity and ecology can be affected. An example of anticipating on the effects of El Niño is advising when to execute dredging works that have strict environmental regulations, taking into account the chances of an ENSO event. An example is a dredging project close to a region with coral, its quality is known to be affected by ENSO events (Claar et al., 2018), so therefore the dredging should be planned so that it does not occur at the same time as the negative effect of the ENSO event. In this way the knowledge of the contractor about the effects and chances of ENSO events contributes to economical and sustainable solutions.

In order to take into account the effect of climate variability, the statistics of the effect of climate variability on the main forcers provide further insight in the effect on the specific project. Furthermore, during the project the predictions of the ONI index are a good basis to anticipate on. The fact that there is a delay in time between the start of the El Niño event and the effect on the system, moreover makes it possible for companies and governments to anticipate. In case new projects are awarded, it is essential to take into account the risks and chances due to El Niño in the tender phase since that makes it possible to include this uncertainty in the contract.

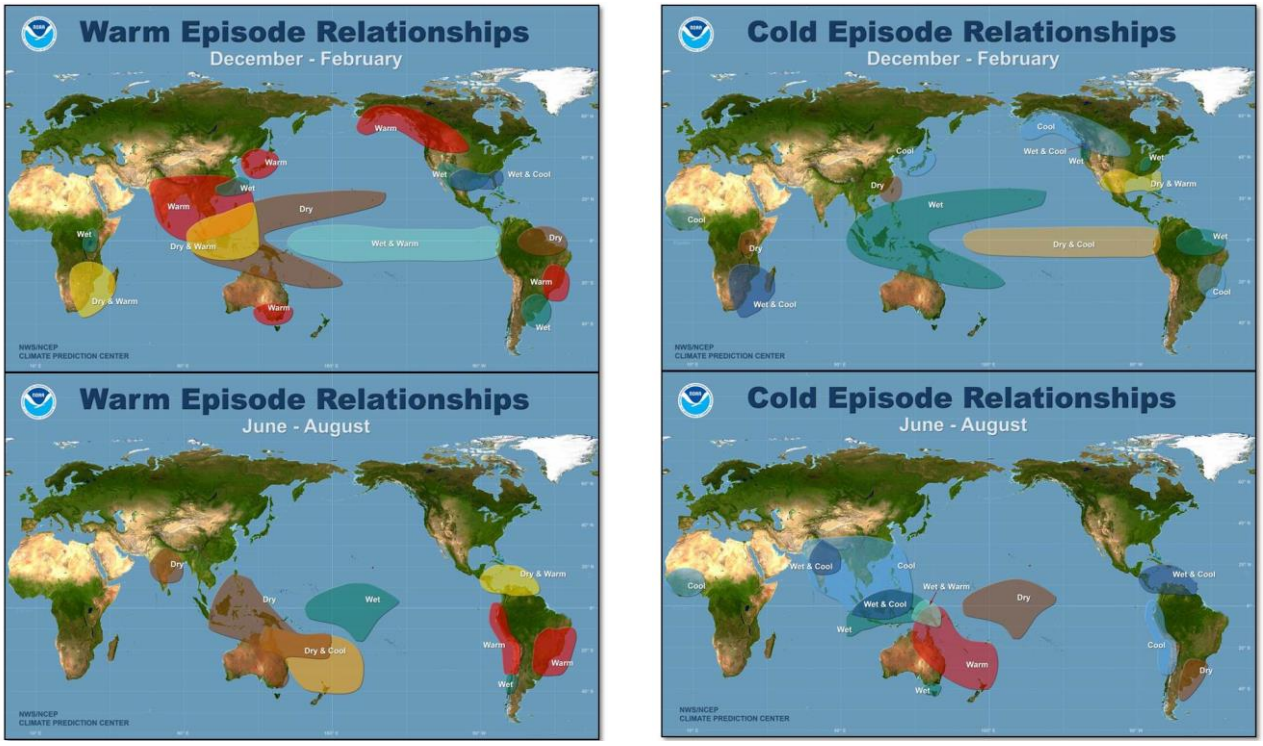

Figure 72 Teleconnections: world-wide effects of ENSO warm (El Niño) and cold (La Niña) events

8 Conclusion

Canal Emilio Mitre is a navigation channel through the shallow Rio de la Plata estuary between Uruguay and Argentina. The channel grants access to the Parana-Paraguay waterway system, which is the second largest inland system of South America. The waterway has large potential, both in the development of the hinterland and the reduction of emission of greenhouse gases due to a shift in transport mode. The waterway system has a need for continuous maintenance dredging, especially in Canal Emilio Mitre the dredging effort is large and moreover it is heavily influenced by interannual variability. The interannual variability is linked to the ENSO phenomena. Furthermore, the Argentine government is interested in deepening, since access from the Rio de la Plata estuary to the Rio Parana for ocean going vessels through Canal Emilio Mitre is currently only guaranteed during high tide. The goal of this thesis is to assess the dredging effort and its variability, the ultimate goal being to reduce the risk in the 10-year dredging contract.

1 What is, and what influences, the dredging effort in the navigation channel?

Analysis of the dredging record and bathymetries showed that an annually average amount of 4.5 Mm^3 (excluding CSD) and 5.7 Mm^3 (including CSD) is dredged from the navigation channel between KP 41 upstream and KP -30 downstream. This is around 1.2 m on average over the navigable width of 100 m of the channel (including CSD). Continuous maintenance dredging is performed by TSHDs which dispose either in the channel in buffer pits or downstream of the channel in deeper areas. Once every three to four years a CSD creates two pits in the channel in which the TSHDs dispose in order to reduce their sailing time. Next to being an alternative disposal location, the upstream pit is also used as sediment trap.

The physical processes which influence the dredging effort are (visualised in Figure 28):

1. Upstream supply of sediment (mainly fine sediment) from the Rio de las Palmas river branch, which peaks around January.
2. Infill from the flats due to a combination of wind (waves and currents) and the micro-tidal environment. The wind has major effect on the resuspension of sediment on the shallow flats. The tidal flow transports the sediment rich water over the channel in which the transport capacity is reduced resulting in sedimentation.
3. Small export of fine suspended sediment to the downstream region, no marine sediment is imported into the system.

The effect of climate variability is mostly recognised in the discharge of the Parana de las Palmas affecting the sediment supply from upstream (correlated to ENSO). The infill from the flats is dependent on the wind and tide in which the effect of climate variability and change is not evident. The variability of the infill from the flats however is affected by the selected navigational depth of the channel.

A depth-averaged Delft3D model is set-up in order to model the sedimentation in the channel. The effect of the identified forcing mechanisms of the sedimentation is studied and shows the expected results in the model (paragraph 2.10). The Base Case scenario is set-up to compare the spatial, temporal and absolute sedimentation trend of the model to the reported dredged volumes. The Base Case scenario shows that the spatial trend of simulated sedimentation matches the reported dredging. Overall a decrease is expected in sedimented volumes in the downstream direction with peaks in the pits and a reduction after the pits. Also the location where the simulated sedimentation ends, matches the location where the dredging ends. Regarding the absolute values, the reported volumes are a factor 1.13 to 2.6 higher than the simulated volumes (depending on the period of the dredging record which is selected). This systematic offset could be for various reasons, including the measurement method of the reported dredging volumes, the chosen density of the sedimented material in the numerical model, and the sensitivity of the simulated sedimentation to the temporally varying wind forcing.

2 What is the effect of variability on this effort, both due to climate variability and deepening scenarios?

Based on the IPCC reports, on the time scale of the project duration (10 years) mainly the interdecadal and interannual variability of the discharge of the Parana de las Palmas are the climate forcers that are expected to have a large effect on the sedimentation. The effect of SLR is minor on this time scale and no clear trend was observed in the wind signal. From this analysis two climate scenarios were set up:

- Climate change scenario: 8.5% discharge increase over the whole year. This is based on the analysis of the discharge record; the difference is attributed to changes in the precipitation regime and land use changes in the catchment.
- Climate variability scenario: El Niño discharge of 2016, which is overall 20.7% higher and has a pronounced peak around January which persists longer. This interannual variation is linked to ENSO.

The effect of climate variability is clearly recognised in the dredging record (available since 2007). It reveals a pronounced relation between the ONI index and the reported volumes. Analysis of the dredging record revealed that this is also due to the work method with the CSD which is operational only during El Niño years, but also without the CSD the dependence on the ONI index is still very pronounced. In time, the increase of the ONI index at the start of an El Niño event precedes the start of additional dredging by between 12 and 18 months, which implies that there is time for mobilisation of additional material.

Next to the effect of an El Niño on the dredging effort also the probability of the occurrence of such an event is essential in the analysis. Using the ONI index record since 1950, the chance of a strong El Niño is 13.0% per year and of a very strong El Niño is 5.8% year. Taking into account the project duration of 10 years this leads to 72.9% chance of *at least one* strong El Niño and 44% chance of *at least one* very strong El Niño. The trend of the ONI index is partially predictable, for a lead of 6 months the warm (El Niño) and cold events (La Niña) can be predicted, especially the very warm and very cold events.

The effect of variability due to climate, deepening and wind scenarios is assessed by executing scenarios in the numerical model. The climate variability scenarios show that the spatial, temporal and absolute trend of the sedimentation are affected. The climate change scenario, with an increase of 8.5% in discharge shows 6.2% increase in sedimentation. In space it leads to a shift from the region upstream of pit 1 into pit 1 and the stretch between the pits. The reason for this shift is the increase in flow velocities before pit 1 which leads to a smaller reduction of the transport capacity, leading to a delay in the settling of the sediment along the channel. The climate variability scenario (20.7% discharge increase) shows 17.2% extra sedimentation compared to the Base Case. The spatial changes in the sedimentation pattern are similar to the climate change scenario, apart from the fractional increase upstream of pit 1; this can be explained by the low discharge at the end of the scenario compared to the Base Case. This reveals that the area around the transition from the river to the estuary is sensitive to the discharge, which is also recognised when analysing the bathymetry through the years. Last but not least, the climate variability scenario also shows the pronounced effect of the increase in discharge in the simulated sedimentation speed, which peaks around January. Both climate scenarios show minor effects downstream and in pit 2. This matches the conclusion by the current contractor that the dredging volumes in pit 2 are not affected by the 2016 El Niño event. This leads to the overall conclusion that the climate variability is indeed mainly due to the upstream supply of sediment and that the second half of the channel is affected rather by offshore phenomena like wind and storms.

Engineering rules predict that deepening of the navigation channel leads to additional sedimentation, due to further reduction of the bed shear stresses. On the other hand the channel may also attract

discharge due to the reduced friction in combination with its orientation in the direction of the tidal flow. The deepening scenarios show that without time-varying wind the effect of the attraction of flow is dominant over the effect of reduced bed shear stresses. Deepening by 4 feet leads to a 4.8% decrease of the overall sedimentation compared to the Base Case. The spatial pattern changes considerably; as expected deepening leads to a shift of the sedimentation to pit 1 and the region upstream of pit 1, while the fractional sedimentation in the downstream reach reduces. This is due to both the reduction of the flow velocities directly after the transition from river to estuary and the attraction of discharge of the stretch between the two pits.

Addition of time-varying wind to the computations has a larger effect on the deepened channel (+4 feet) than on the regular channel, since this does lead to a larger difference in bed shear stress and does not lead to attraction of discharge. Especially during highly energetic events, the increase in currents leads to increased suspended sediment concentrations which matches literature. Overall, the deepened channel shows 7.8% more sedimentation than the regular bathymetry when temporally varying wind is added to both scenarios. This outcome shows that the model is sensitive to wind forcing, which also matches the behaviour of the system as described in literature. In order to improve the predictive skill of the model, recalibration of the model including temporally-varying wind is recommended.

3 What are possible strategies to reduce the risk due to variability?

The current dredging strategy with the pits is effective to reduce the risks due to variability. The pits which are used both as sediment traps and alternative disposal location are located in the optimal location. The upstream pit is located at the optimal location to attract sedimentation from the upstream supply and the downstream pit is located ideally to reduce the sailing time of the TSHDs. In the determination of the size of the pits three considerations should be taken into account: the development and statistics of the ONI index and the effect on the supply of sediment input from upstream, the selected navigational depth of the channel and the effect on infill from the flats and the mobilisation time of a CSD.

The ONI index will affect the sediment supply from upstream and will therefore mostly affect the sedimentation in the upstream half of the navigation channel as followed from the climate scenarios analysis. The chosen depth will affect the total dredging volume and will therefore mainly affect the optimal size of the downstream pit, since that pit is used as a buffer. Next to these two considerations the mobilisation time of a CSD plays a central role in the strategy, considering the sequence of events leading to extreme sedimentation a CSD should be available within around 12-18 months. The responsibility for extreme sedimentation as a result of climate variability should be assigned in the contract in order to avoid unexpected costs. Various options are possible, such as compensation for volumes over a certain threshold by the client, or the transferal of this risk to the users by an increase of the toll rates.

Next to the specific dredging strategy for Canal Emilio Mitre, the waterway system should be seen in a broader perspective. The major branch of the Rio Parana is the Rio Parana Guazu, this alternative route has major advantages for vessels, including being accessible to longer vessels and avoiding the queuing at Canal Emilio Mitre due to the tidal window. The opening of this alternative routes is expected to have major effects on the use of Canal Emilio Mitre. Furthermore, the deepening of this waterway may also affect the dredging effort of Canal Emilio Mitre.

This study highlights the importance of taking into account the effect of climate variability on dredging projects with a duration of around 10 years. In the case of Canal Emilio Mitre, this leads to additional dredging as a result of increased discharge, but in other regions ENSO might affect workability or turbidity. It is recommended for dredging projects in regions affected by the teleconnections of ENSO to examine which physical forcers of the system are affected by climate variability and if statistics are available on this variability. These statistics in combination with the forecast of the ONI index provide a good basis to take the effect of climate variability into account in the tender phase. Climate variability results in both risks and chances for dredging projects, and it is essential to determine to which party those are attributed.

9 Bibliography

Amsler, M. L., & Drago, E. C. (2009). A review of the suspended sediment budget at the confluence of the Paraná and Paraguay Rivers. *Hydrological Processes*, *23*(22), 3220–3235. https://doi.org/https://onlinelibrary.wiley.com/doi/abs/10.1002/hyp.7390

Anthony, A., Atwood, J., August, P., C., B., S., C., Foster, C., … Lellis-Dibble, K. (2009). Coastal lagoons and climate change: ecological and social ramifications in U.S. Atlantic and Gulf Coast ecosystems. *Ecology and Society*, *14*(1).

Argentine Government. (2018). *Sedimentos 2006a2017*.

Badano, N. D., Sabarots Gerbec, M., Re, M., & Menendez, A. N. (2012). A coupled hydro-sedimentologic model to assess the advance of the Parana River Delta Front. *River Flow 2012, Vols 1 and 2*, (September), 557–564.

Balay, M. (1958). *CAUSES AND PERIODICITY OF LARGE FLOODS IN RIO DE LA PLATA (FLOOD OF 27 AND 28 JULY 1958)*.

Balay, M. (1961). *El Rio de la Plata entre atmosfera y el mar*.

Barros, V. R., Boninsegna, J. A., Camilloni, I. A., Chidiak, M., Magrín, G. O., Rusticucci, M. (2015). Climate change in Argentina: trends, projections, impacts and adaptation. *Wiley Interdisciplinary Reviews: Climate Change 6*, *2*, 151–169.

Barros, V. (2005). *Global Climate Change and the Coastal Areas of the Rio de la Plata*.

Barros, V., Doyle, M., & Camilloni, I. (2005). Potential impacts of climate change in the Plata basin. *Regional Hydrological Impacts of Climate Variability and Change*, *295*(April), 2005. https://doi.org/10.1175/2007BAMS2476.1

Berbery, E. H., & Barros, V. R. (2002). The Hydrologic Cycle of the La Plata Basin in South America. *Journal of Hydrometeorology*, *3*(6), 630–645.

Bosboom, J., & Stive, M. (2015). *Coastal Dynamics I: Lectures Notes CIE 4305*. VSSD.

Brea, J. D., & Spalletti, P. (2010). *Generación y transporte de sedimentos en la Cuenca Binacional del Río Bermejo. Caracterización y análisis de los procesos intervinientes*. Buenos Aires.

Cai, W., Borlace, S., Lengaigne, M., Rensch, P. van, Collins, M., Gabriel Vecchi, Axel Timmermann, A. S., … Jin, F.-F. (2014). Increasing frequency of extreme El Niño events due to greenhouse warming. *Nature Climate Change*, *4*, 111–116.

Chow, V. T. (1959). *Open Channel Hydraulics*. New York: McGraw-Hill Book Co.

Church, J.A., P.U. Clark, A. Cazenave, J.M. Gregory, S. Jevrejeva, A. Levermann, M.A. Merrifield, G.A. Milne, R.S. Nerem, P.D. Nunn, A.J. Payne, W.T. Pfeffer, D. S., Unnikrishnan, A. S., Germany, D. S., Box, J. E., Carson, M., Uk, W. C., … Good, P. (2013). *Sea Level Change. In: Climate Change 2013: The Physical Science Basis. Contribution of Working Group I to the Fifth Assessment Report of the Intergovernmental Panel on Climate Change*.

Claar, D. C., Szostek, L., McDevitt-Irwin, J. M., Schanze, J. J., & Baum, J. K. (2018). Global patterns and impacts of El Niño events on coral reefs: A meta-analysis. *PLOS ONE*, *13*(2), 1–22.

https://doi.org/10.1371/journal.pone.0190957

D'Onofrio, E. E. D., Fiore, M. M. E., & Romero, S. I. (1999). Return periods of extreme water levels estimated for some vulnerable areas of Buenos Aires. *Continental Shelf Research*, *19*, 1681–1693.

D'Onofrio, E. E., Fiore, M. M. E., & Pousa, J. L. (2008). Changes in the Regime of Storm Surges at Buenos Aires, Argentina. *Journal of Coastal Research*, *1*, 260–265. https://doi.org/10.2112/05-0588.1

Da Silveira Pereira, N. E., & Klumb-Oliveira, L. A. (2015). Analysis of the influence of ENSO phenomena on wave climate on the central coastal zone of Rio de Janeiro (Brazil). *Journal of Integrated Coastal Zone Management*, *15*(3), 353–370. https://doi.org/10.5894/rgci570

Deltares. (2018). *Delft3D FLOW manual*. Delft.

Depetris, P. J. (2007). The parana river under extreme flooding: A hydrological and hydro-geochemical insight. *Interciencia*, *32*(10), 656–662. https://doi.org/10.1039/C5CC01087J

Deursen, van P. P. (1993). *Investigation of sediments Ruta de navigation de ultramar San Martin - Oceano*.

Doyle, M. E., & Barros, V. R. (2011). Attribution of the river flow growth in the Plata Basin. *INTERNATIONAL JOURNAL OF CLIMATOLOGY*, *2248*(September 2010), 2234–2248. https://doi.org/10.1002/joc.2228

Doyle, M. E., Saurral, I., & Barros, V. R. (2012). Trends in the distributions of aggregated monthly precipitation over the La Plata Basin. *International Journal of Climatology*, *32*(14), 2149–2162. https://doi.org/10.1002/joc.2429

Fiore, M. M. E., D'Onofrio, E. E., Pousa, J. L., Schnack, E. J., & Bértola, G. R. (2009). Storm surges and coastal impacts at Mar del Plata, Argentina. *Continental Shelf Research*, *29*(14), 1643–1649. https://doi.org/10.1016/j.csr.2009.05.004

Flather R., Baker T., Woodworth P., V. I. and B., & D. (2001). *Integrated effects of climate change on coastal extreme sea levels.*

Fossati, M, Cayocca, F., & Piedra-Cueva, I. (2014). Fine sediment dynamics in the Río de la Plata. *Advances in Geosciences*, *39*, 75–80. https://doi.org/10.5194/adgeo-39-75-2014

Fossati, Mónica, & Piedra-Cueva, I. (2008). Numerical modelling of residual flow and salinity in the Río de la Plata. *Applied Mathematical Modelling*, *32*(6), 1066–1086. https://doi.org/10.1016/j.apm.2007.02.034

Framiñan, M. B., & Brown, O. B. (1996). Study of the Rio de la Plata turbidity front. Part I: Spatial and temporal distribution. *Continental Shelf Research*, *16*(10), 1259–1282. https://doi.org/10.1016/0278-4343(95)00071-2

Framiñan M.B., Etala M.P., Acha E.M., Guerrero R.A., Lasta C.A., B. O. B. (1999). Physical Characteristics and Processes of the Río de la Plata Estuary. In P.-Q. M. Perillo G.M.E., Piccolo M.C. (Ed.), *Estuaries of South America* (pp. 161–194). https://doi.org/10.1007/978-3-642-60131-6

Freund, M. B., Henley, B. J., Karoly, D. J., McGregor, H. V., Abram, N. J., & Dommenget, D. (2019).

Higher frequency of Central Pacific El Niño events in recent decades relative to past centuries. *Nature Geoscience*.

Friedrichs, C., Aubrey, D. G., & Speer, P. E. (1990). *Impact of relative sea-level rise on evolution of shallow estuaries*.

G. Anschütz, R. S. E. (2000). Measurements of wave action in the oceanic limit of Río de la Plata estuary. *Marine Meteorology and Related Oceanographic Activities*, 107–116.

Gerbec, M. S., Re, M., Storto, L., & Morale, M. (2018). Analisis de reparticion de caudales en bifurcaciones del delta del rio Parana. *Congreso Latinoamericano de Hidraulica*, 2. Buenos Aires.

Gilardoni, C. U. . (2018). *Problemática de la navegación en los canales del Río de la Plata*.

Giorgi, F. (2003). Variability and trends of sub-continental scale surface climate in the twentieth century. Part I: Observations. *Climate Dynamics*, *18*, 675–691.

GRDC. (2019). Discharge data Uruguay Basin Palmar station. Retrieved from http://www.grdc.sr.unh.edu/html/Polygons/P3469100.html

Grimm, A., Barros, V., & Doyle, M. (2000). Climate Variability in Southern South America Associated with El Nino and La Nina Events. *Journal of Climate*, *1*. https://doi.org/10.1175/1520-0442(2000)013<0035:CVISSA>2.0.CO;2

Grimm, A. M., & Tedeschi, R. G. (2009). ENSO and extreme rainfall events in South America. *Journal of Climate*, *22*(7), 1589–1609. https://doi.org/10.1175/2008JCLI2429.1

Guerrero, R. A., Acha, E. M., Framin, M. B., & Lasta, C. A. (1997). Physical oceanography of the Río de la Plata Estuary, Argentina. *Continental Shelf Research*, *17*(7), 727–742. https://doi.org/10.1016/S0278-4343(96)00061-1

Hidrovia SA. (2017). *Sedimentacion Extraordinaria en Canal Emilio Mitre 2015-2016*.

Hupp, C. R., Noe, G., & Schenk, E. (2008). Floodplain Geomorphic Processes, Sedimentation, and Ecological Impacts of Hydrologic Alteration along Coastal Plain Rivers. In *2nd Joint Federal Interagency Conference, Las Vegas*.

International transport and logistics legal consultants. (2019). Operative Advantages of Martín García Canal due to New Depth Limits. Retrieved from http://itl-legalconsultants.com/news_eng/operative-advantages-of-martin-garcia-canal-due-to-new-depth-limits/

Jaime, P., & Menendez, A. (1999). *MODELO HIDRODINÁMICO "RÍO DE LA PLATA 2000" Informe*.

Jaime, P., & Menendez, A. (2002). *Analisis del regimen hidrologico de los rios Parana y Uruguay*.

Jeppesen, E. M., Sondergaard, A. R., Pedersen, K., Jurgens, K., Strzelczak, A., Lauridsen, T. L., & Johansson, L. S. (2007). Salinity induces regime shift in shallow brackish laoons. *Ecosystems*, *10*, 47–57.

Madsen, P. A., Rugbjerg, M., & Warren, I. R. (1988). Subgrid modelling in depth integrated flows. *Coastal Engineering*, (21), 505–511.

Magrin, G. O., Marengo, J. A., Boulanger, J.-P., Buckeridge, M. S., Castellanos, E., Poveda, G., …

Vicuña, S. (2014). *Central and South America. In: Climate Change 2014: Impacts, Adaptation, and Vulnerability. Part B: Regional Aspects. Contribution of Working Group II to the Fifth Assessment Report of the Intergovernmental Panel on Climate Change*.

Mangini, S. P., Prendes, H. H., Amsler, M. L., & Huespe, J. (2003). Importancia de la floculación en la sedimentación de la carga de lavado en ambientes del río Paraná, Argentina. *Ingenieria Hidraulica En Mexico*, *XVIII*(3), 55–69.

Mcleod, E., Poulter, B., Hinkel, J., Reyes, E., & Salm, R. (2010). Se-level rise impact models and environmental conservation : a review of models and their applications. *Ocean and Coastal Management*, *53*(9), 507–517.

Meccia, V. L., Simionato, C. G., Fiore, M. E., D'Onofrio, E. E., & Dragani, W. C. (2009). Sea surface height variability in the Rio de la Plata estuary from synoptic to inter-annual scales: Results of numerical simulations. *Estuarine, Coastal and Shelf Science*, *85*(2), 327–343. https://doi.org/10.1016/j.ecss.2009.08.024

Menendez, A., Kazimierski, L. D., & Re, M. (2017). *Sedimentación extraordinaria en los canales de navegación de Martín García*. 1–11.

Mengual, B., Hir, P. Le, Cayocca, F., & Garlan, T. (2017). Modelling fine sediment dynamics: Towards a common erosion law for fine sand, mud and mixtures. *Water*, *9*(8), 1–23. https://doi.org/10.3390/w9080564

Milana, J. P., & Kröhling, D. (2015). Climate changes and solar cycles recorded at the Holocene Paraná Delta, and their impact on human population. *Nature*, *5*(August). https://doi.org/10.1038/srep12851

Newham, L. T. H., Norton, J. P., Prosser, I. P., Croke, B. F. W., & Jakeman, A. J. (2003). Sensitivity analysis for assessing the behaviour of a landscape-based sediment source and transport model. *Environmental Modelling and Software*, *18*(8–9), 741–751. https://doi.org/10.1016/S1364-8152(03)00076-8

Officer, C. B. (1992). Physics of estuarine circulation. *Estuaries and Enclosed Seas. Ecosystems of the World*, *26*, 15–41.

Partheniades, E. (1965). Erosion and Deposition of Cohesive Soils. *Journal of the Hydraulics Division, ASCE*, *91*(January), 105–139.

Piedra-Cueva, I. (2003). Finite element modeling of the rio de la plata. *International Conference on Estuaries and Coasts*, *1*, 872–878.

Piedra-Cueva, I., & Fossati, M. (2007). Residual currents and corridor of flow in the Rio de la Plata. *Applied Mathematical Modelling*, *31*(3), 564–577. https://doi.org/10.1016/j.apm.2005.11.033

Pilkey, O. H., & Young, R. (2009). *The rising sea*. Washington DC: Islands Pres/Shearwater Books.

Prario, B. E., Dragani, W., Mediavilla, D. G., & D'Onofrio, E. (2011). Hydrodynamic numerical simulation at the mouths of the Parana and Uruguay rivers and the upper Rio de la Plata estuary: A realistic boundary condition. *Applied Mathematical Modelling*, *35*(11), 5265–5275. https://doi.org/10.1016/j.apm.2011.04.013

Re, M. (2005). *Impacto del Cambio Climático Global en las Costas del Río de la Plata*.

Rodríguez, L., & Mendeze Incira, J. (2015). *Climate variability, dynamics and trends. The effect of climate change on the coasts of Latin America and the Caribbean*. Cantabria.

Sabarots Gerbec, M., Gatti, G., Irigoyen, M., Storto, L., Morale, M., & Re, M. (2018). *Campañas de aforos líquidos Delta del río Paraná 2016-2017*. Buenos Aires.

Santamaria-Aguilar, S., Schuerch, M., Vafeidis, A., & Carretero, S. (2017). Long-Term Trends and Variability of Water Levels and Tides in Buenos Aires and Mar del Plata, Argentina. *Coastal Ocean Processes*, *4*(November), 1–15. https://doi.org/10.3389/fmars.2017.00380

Santoro, P., Fossati, M., Tassi, P., Huybrechts, N., Pham Van Bang, D., & Piedra-Cueva, J. C. I. (2017). A coupled wave–current–sediment transport model for an estuarine system: Application to the Río de la Plata and Montevideo Bay. *Applied Mathematical Modelling*, *52*, 107–130. https://doi.org/10.1016/j.apm.2017.07.004

Santoro, P., Solari, S., Fossati, M., & Jackson, M. (2018). *PRONÓSTICO RESTROSPECTIVO (HINDCAST) DE NIVEL DE MAR EN LA COSTA DE URUGUAY*.

Sarubbi, A., Pittau, M., & Menendez, A. (2004). *Delta del Parana: Balance de sedimentos*. Buenos Aires.

Sarubbi, A. (2007). *Analisis del advance del frente del delta del Rio Parana*. Universidad de Buenos Aires.

Sarubbi, Alejo. (2007). *Análisis del Avance del Frente del Delta del Río Paraná*. 145.

Schuerch, M., Scholten, J., Carretero, S., García-Rodríguez, F., Kumbier, K., Baechtiger, M., & Liebetrau, V. (2016). The effect of long-term and decadal climate and hydrology variations on estuarine marsh dynamics: an identifying case study from the Río de la Plata. *Geomorphology*, *269*, 122–132.

Silva, V., & Berbery, E. (2006). Intense Rainfall Events Affecting the La Plata Basin. *Journal of Hydrometerology*, *7*, 769–787.

Simionato, C., Berasategui, A., Meccia, V., Mianzan, H., & Acha, M. (2006). The potencial role of wind variability on plankton retention in the Rio de la Plata Estuary: a numerical study. *Proceedings of 8 ICSHMO (International Conference on Southern Hemisphere Meteorology and Oceanography)*, (1), 1383–1391.

Simionato, C. G., Meccia, V. L., Guerrero, R., Dragani, W. C., & Nunez, M. (2007). Rio de la Plata estuary response to wind variability in synoptic to intraseasonal scales : 2 . Currents ' vertical structure and its implications for the salt wedge structure. *Journal of Geophysical Research: Oceans*, *112*, 1–15. https://doi.org/10.1029/2006JC003815

Simionato, C. G., Moreira, D., Re, M., & Fossati, M. (2011). *Estudio de la dinámica hidro-sedimentológica del Río de la Plata: observación y modelación numérica de los sedimentos finos*.

Syvitski, J. P. M., Kettner, A. J., Overeem, I., Hutton, E. W., Hannon, M. T., Brakenridge, C. R., … Nicholls, R. J. (2009). Sinking Deltas due to human activities. *Nature Geosciences*, *2*(10), 681.

Syvitski, J., Vörösmarty, C., Kettner, A., & Green, P. (2004). *Impact of Humans on the Flux of Terrestrial Sediment to the Global Coastal Ocean*.

Tossini, L. (1959). El sistema hidrografico de la Cuenca de Rio de la Plata. *Anales Sociedad Cientifica*, *167*, 41–64.

Trawle, M. J., & Herbich, J. B. (1980). *Prediction of shoaling rates in offshore navigation channels.*

Urien, M. (1972). Rio de la Plata Estuary environments. *Geological Science of America*, *133*, 213–234.

van Maren, D. S., Winterwerp, J. C., & Vroom, J. (2015). Fine sediment transport into the hyper-turbid lower Ems River: the role of channel deepening and sediment-induced drag reduction. *Ocean Dynamics*, *65*(4), 589–605. https://doi.org/10.1007/s10236-015-0821-2

van Rijn, L. C. (2007). *A unified view of sediment transport by currents and waves, part 1: initiation of motion, bed roughness and bed load transport*.

van Rijn, L. C. (2013). *Basics of channel deposition/siltation* (Vol. 01).

van Rijn, L. C. (2016). *Fluid mud formation*.

Vieira, J. R., & Lanfredi, N. W. (1996). A hydrodynamic model for the Rio de La Plata, Argentina. *Journal of Coastal Research*, *12*(2), 430–446.

Wong, P. P., Losada, I. J., Gatusso, J. P., Hinkel, J., Khattabi, A., McInnes, K. L., … Sallenger, A. (2014). *Coastal systems and low-lying areas. In: Climate Change 2014: Impacts, Adaptation, and Vulnerability. Part A: Global and Sectoral Aspects. Contribution of Working Group II to the Fifth Assessment Report of the Intergovernmental Panel on Climate Change*.

World Bank. (2010). *Southern Cone Inland Waterways Transportation Study The Paraguay-Paraná Hidrovía: Its Role in the Regional Economy and Impact on Climate Change*.

10 Appendices

10.1 Appendix 1: Location measurement stations

Figure 73 shows the locations of the measurement locations of the water levels, waves and discharge.

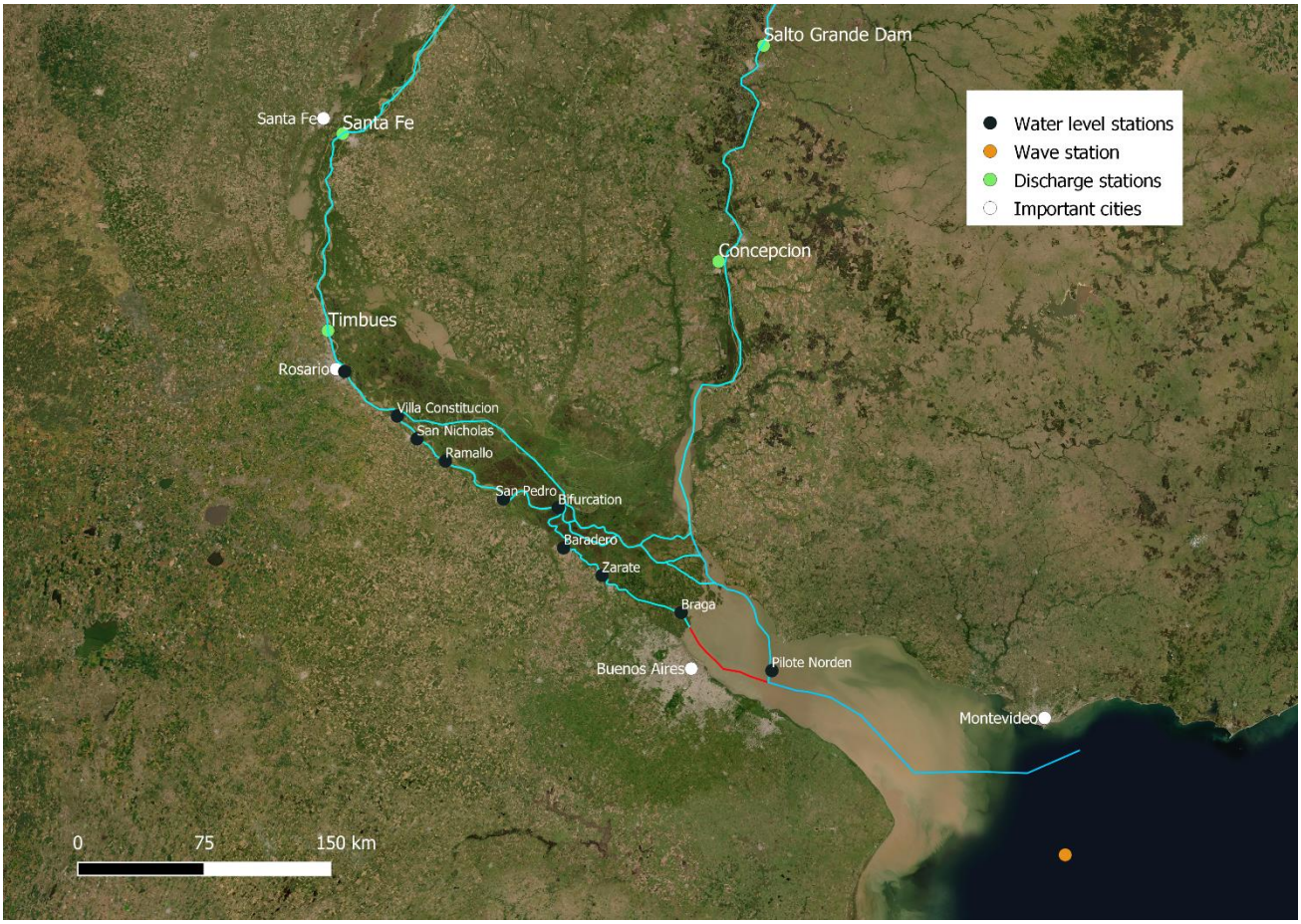

Figure 73 Location of measurement stations

10.2 Appendix 2: Relevance of modelling flood plain

Satellite imagery of the period from 2016-2018 was analysed to investigate whether the flood plains have to be taken into account in the numerical model, both looking at extreme discharges of the Rio Parana and water levels due to wind set-up. It is concluded that the flood plains will not be modelled, but that above discharges of 25.000 m^3/s they do interact.

Extreme discharges

The satellite imagery is shown in Figure 74 until Figure 81, with ascending discharge and water levels measured at Timbues. The orange dots in the figures indicate Rosario (south) and Victoria (north), which are two cities between which the highway is located that connects the two sides of the delta and are separated around 60 kilometre. The literature review showed that the influence of moderate floods is limited to the ponds and lagoons close to the river while major floods inundate the whole flood valley (Depetris, 2007). The data analysis confirmed this conclusion. Until a discharge of around 25,000 m^3/s and a water height of 4.30 m there is considerable storage of water on the flood plains but the main discharge is through the Parana river. There is interaction between ponds close to the main branch but the plains do not contribute to the discharge and the flow velocities are very low due to the extensive vegetation. Above a discharge of 30,000 m^3/s and a water height of around 5 meter the flood plains contribute to the transfer of the discharge. (Since not the complete discharge is measured at Timbues (due to presence of flood plains), the discharge of Corrientes 5 days before the data of the aerial picture is chosen This time is based on an educated guess using the diffusive approach for the speed of the flood wave and by considering the discharge signal during a regular period.).

Next to the Rosaria-Victoria stretch, also the downstream part of the delta was examined. Figure 78 and Figure 79 show the lower delta during regular discharge 19,000 m^3/s and during very high discharge (37,000 m^3/s). The imagery shows that even though the significant difference in course of the river in the upper delta during different discharges this does not have a significant effect on the downstream part of the delta. Therefore the distribution of the discharge over the different branches is not expected to differ too much when considering a range of discharges.

To conclude, for the downstream part of the delta not taken into account the flood plains is a reasonable choice. For the upstream part of the delta (around Rosario-Victoria) this is a simplification. Therefore the hydrodynamic results of the numerical model around that area do not give a representation of reality. Next to its effect on the hydrodynamics also an effect is expected on the sediment load of the river. This is discussed in paragraph 7.3.

Extreme water levels due to wind

Local knowledge also stresses the effect of strong winds from the south east on the water levels in the inner part of the estuary. In order to look at the effect of these winds on the amount of water on the flood plains the water levels in Buenos Aires were analysed, hourly water level measurements of Buenos Aires are available from 01-08-2018 until 01-04-2018 (SHN, 2019). During that period the satellite images of the lowest water level and highest water level are shown in Figure 81 and Figure 80. Both the report by Mariano Re et al (2015) on the inundations at Buenos Aires and the report by Menendez and Kazimierski (2019) on the analysis of extreme water levels at the city show that the high water levels at Buenos Aires are mainly related to the winds and not to other factors such as discharge or rain. Therefore using the water level at Buenos Aires as an indicator of the strength of the wind is a reasonable choice.

From the analysis it shows that the there is a clear influence of the water levels in the inner part of the estuary on the flooding of the islands in front of the delta (Martin Garcia and others). However when considering the channels and their extent, no changes are observed.

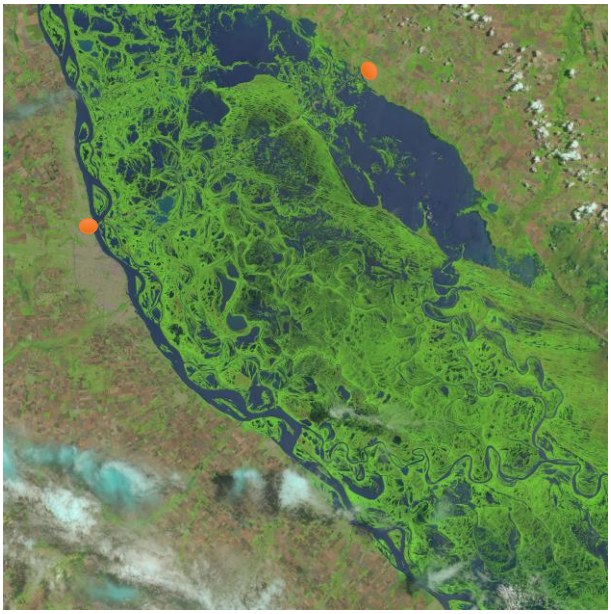

Figure 74 2016-11-28, Q~17,000 m^3/s, h=3.52 m

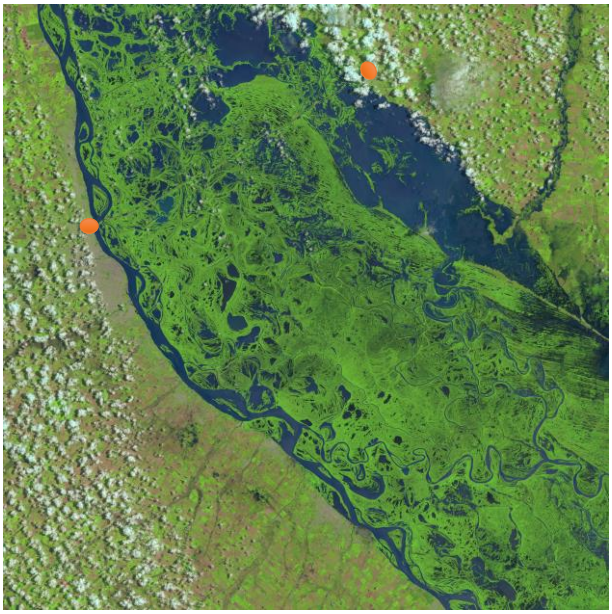

Figure 75 2017-01-07, Q~20,000 m^3/s, h=4.30 m

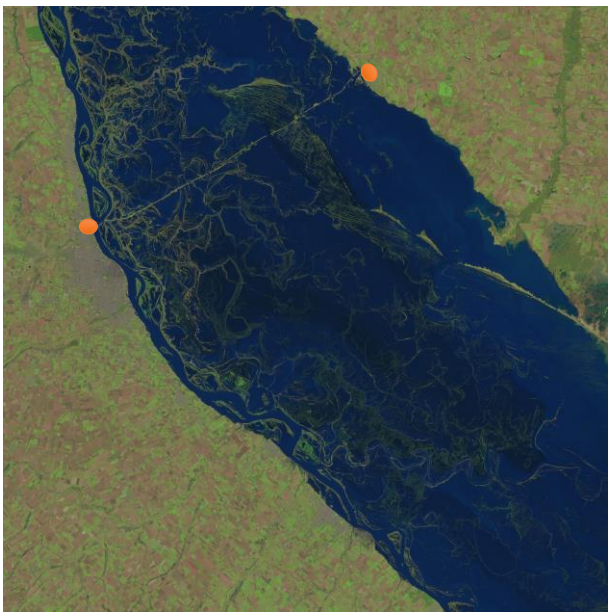

Figure 76 2016-07-21, Q~27,000 m^3/s, h=4.68

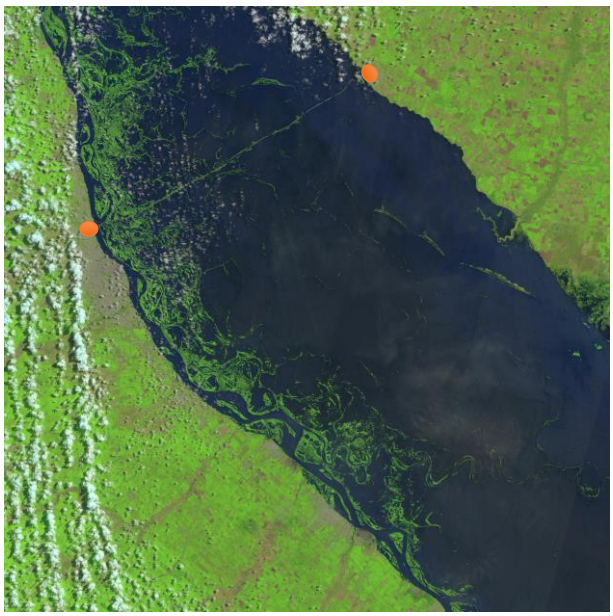

Figure 77 2016-02-12, Q~35,000 m^3/s, h=5.84 m

Figure 78 2016-09-26 Q=19,000

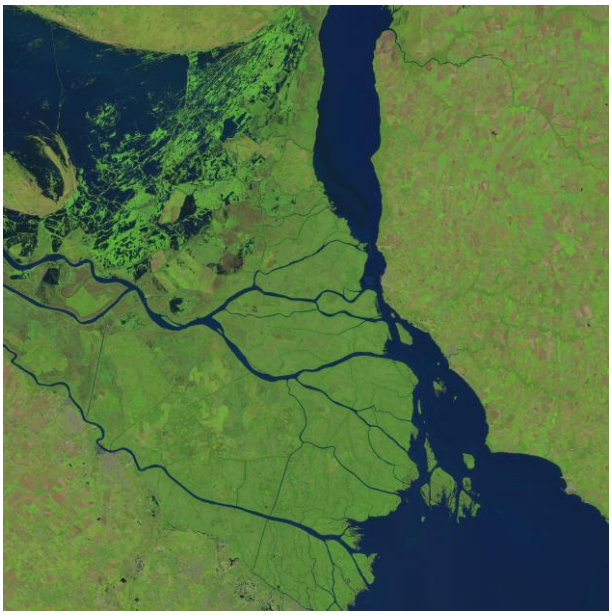

Figure 79 2016-01-20 Q=37,000

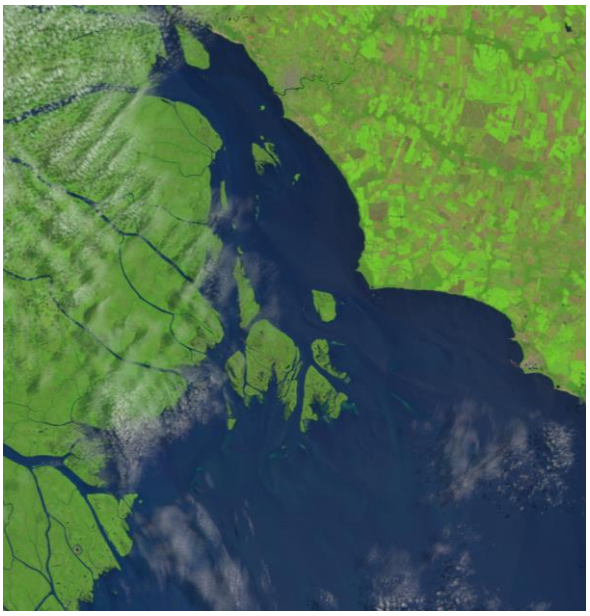

Figure 80 2019-02-18 H = 0.37 m

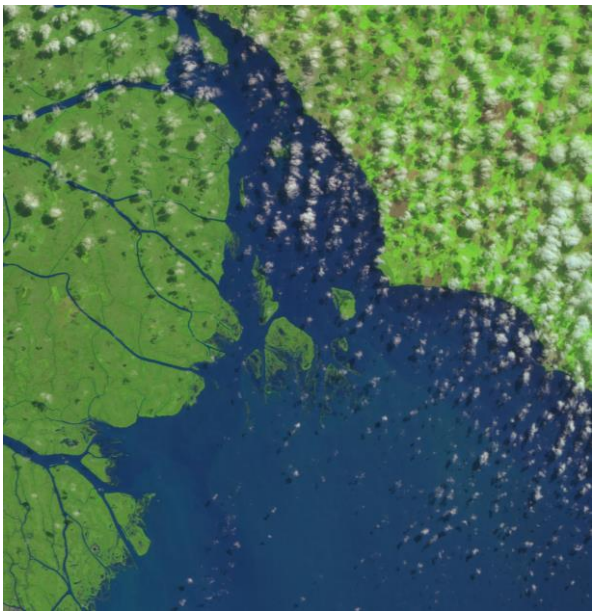

Figure 81 2019-03-25 H = 2.48 m

10.3 Appendix 3: Analysis sediment load Rio Parana and sieve curves Canal Emilio Mitre

First the sieve curves of Canal Emilio Mitre (KP 20.7) and Canal Accesso (KP-12,-16,-20,-27,-35) are presented. In Canal Emilio Mitre mainly silt is present, the transition from silt to clay dominated is around KP26. Additional analysis of the sediment load data of the Rio Bermejo shows that intense rain events are followed by high concentrations of the Rio Bermejo. Furthermore the analysis shows that if the concentration of the Rio Parana is high that this load comes from the Rio Bermejo, during low concentrations of the Rio Parana the sediment comes from different sources.

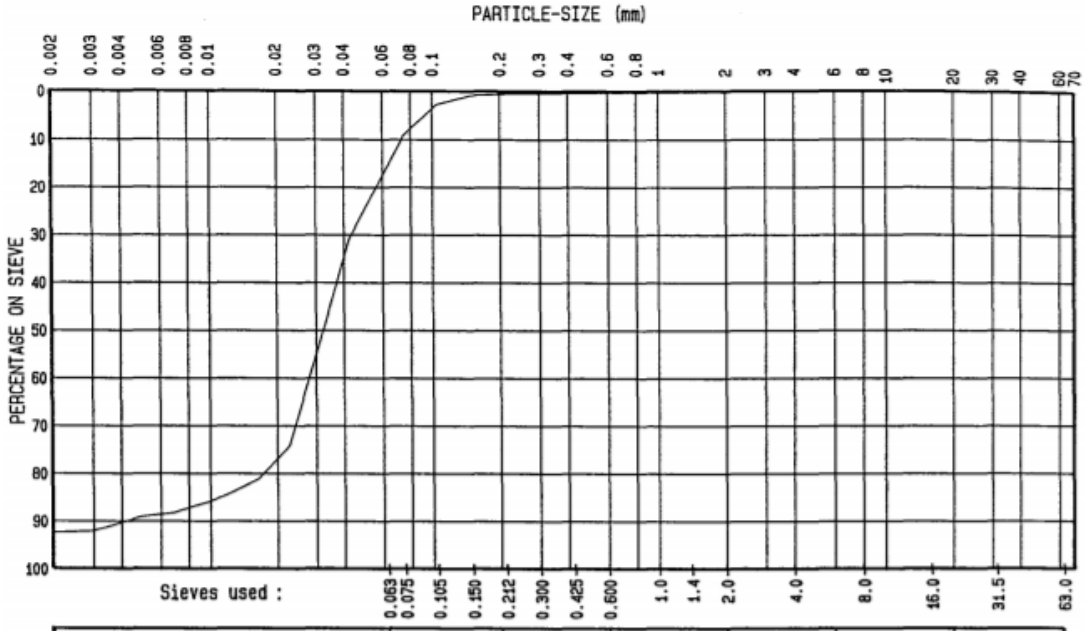

	BORING No.	SAMPLE No.	DEPTH	LEGEND	PERCENTAGE < ...um. 63	50	16	2
1	#12	5+6		———	84.4	75.7	18.7	7.6

	d10	d20	d30	d40	d50	d60	d70	d80	d90	d90/d10	d60/d10	dmf
1	0.004	0.017	0.024	0.028	0.032	0.037	0.043	0.056	0.073	17.5	8.9	0.035

	CUMULATIVE PERCENTAGES ON SIEVE															
	63.0	31.5	16.0	8.0	4.0	2.0	1.4	1.0	0.600	0.425	0.300	0.212	0.150	0.105	0.075	0.063
1							0.0	0.1	0.1	0.2	0.2	0.4	0.7	2.6	8.9	15.6

PARTICLE-SIZE DISTRIBUTION CURVE

Project : ARGENTINIE - RIO DEL PLATA Mitre KP 20.7 Contract nr. : C 30.004
Annex : 1

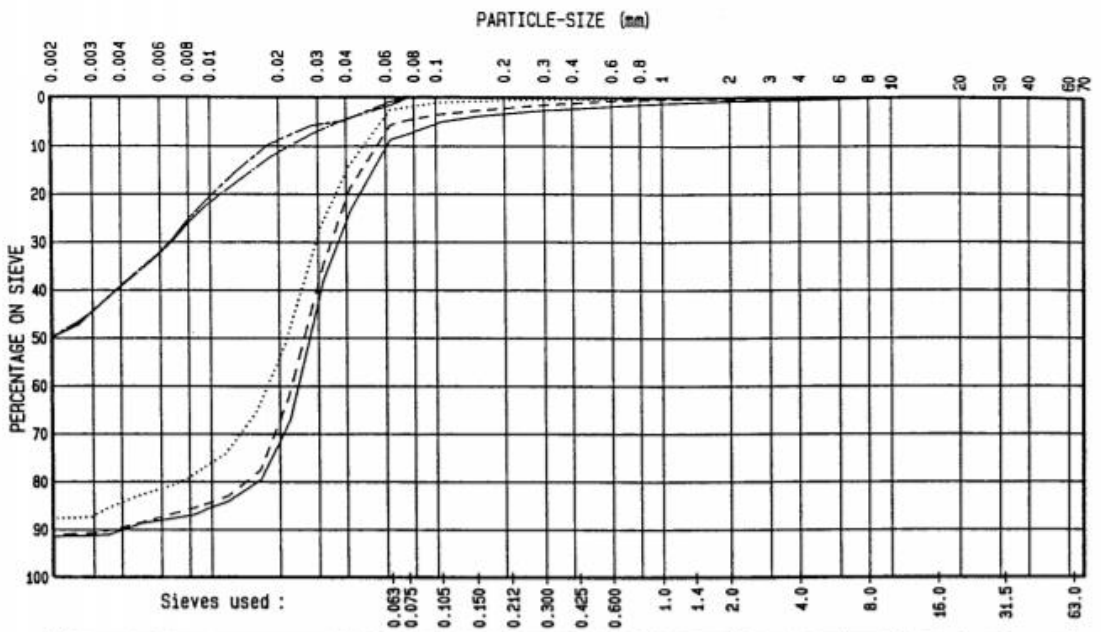

	BORING No.	SAMPLE No.	DEPTH	LEGEND	PERCENTAGE < ...um. 63	50	16	2	
1	#1	1 - 2		———	91.2	83.0	20.1	8.6	KP–12
2	#2	5		- - - - -	94.3	87.0	22.1	8.9	KP-16
3	#4	2 - 4	0.15 - 0.40 -GL	.....	97.4	91.1	35.3	12.3	KP-20
4	#4	2 - 4	0.40 - 0.60 -GL	—·——·—	98.4	97.0	85.6	50.2	KP-27
5	#6	TOP		—··—··—	99.2	97.2	88.2	50.3	KP-35

	d10	d20	d30	d40	d50	d60	d70	d80	d90	d90/d10	d60/d10	dmf
1	0.004	0.016	0.021	0.024	0.027	0.031	0.037	0.046	0.061	15.1	7.6	0.030
2	0.004	0.014	0.019	0.023	0.026	0.029	0.034	0.041	0.055	15.3	8.2	0.027
3		0.007	0.013	0.018	0.022	0.025	0.029	0.036	0.048			
4					0.002	0.004	0.007	0.011	0.023			
5					0.002	0.004	0.007	0.010	0.018			

	CUMULATIVE PERCENTAGES ON SIEVE 63.0	31.5	16.0	8.0	4.0	2.0	1.4	1.0	0.600	0.425	0.300	0.212	0.150	0.105	0.075	0.063
1					0.5	0.6	0.9	1.2	1.8	2.2	2.6	3.3	3.9	5.1	7.6	8.8
2						0.1	0.2	0.3	0.6	1.0	1.4	2.1	2.7	3.4	4.7	5.7
3								0.1	0.1	0.3	0.3	0.5	0.7	0.9	2.0	2.6
4																1.6
5																0.8

PARTICLE-SIZE DISTRIBUTION CURVE

Project : ARGENTINIE - RIO PLATA - CANAL DE ACCESO

Contract nr. : C 30.004
Annex : 1

Additional data analysis on the relation between the rain data in the Bermejo catchment area and the fine sediment load in the Rio Bermejo shows that periods of intense rainfall in the Upper Bermejo river basin are followed by periods of high suspended fine sediment loads at El Colorado in the Lower Bermejo river (Latitude: 26º 20' 03.40" Longitude: 59º 21' 44.70") (Figure 82).

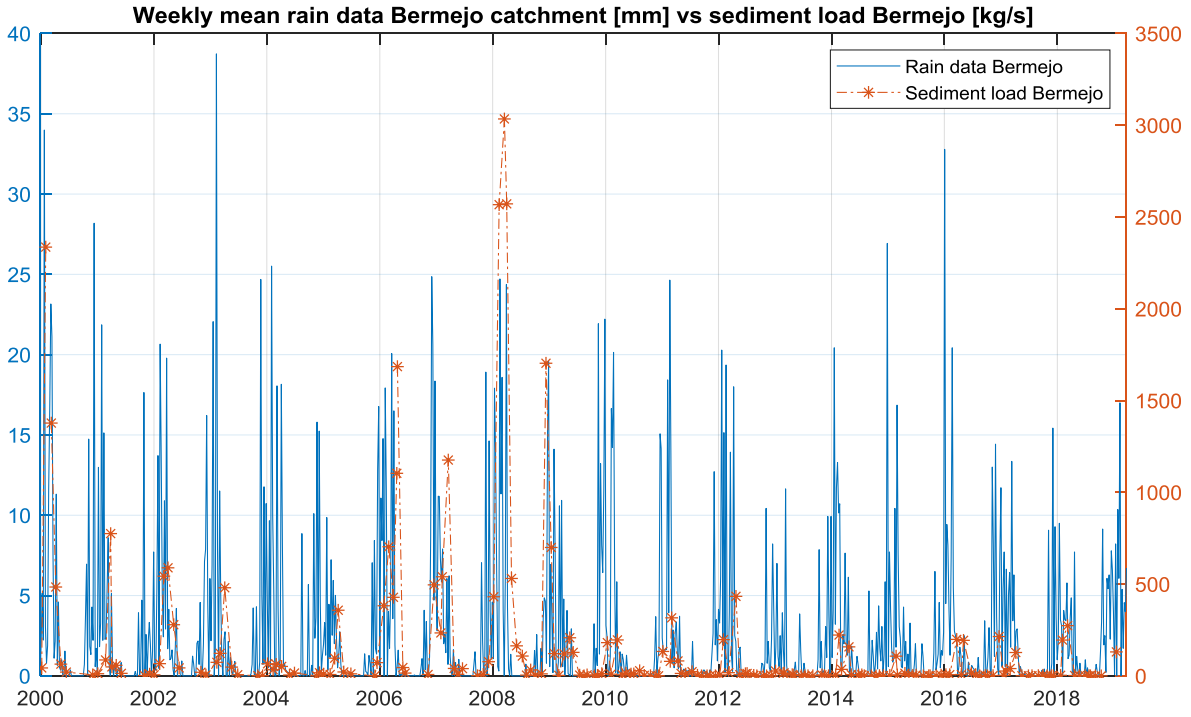

Figure 82 Weekly mean rain data Rio Bermejo (station: Pozo Sarmiento) vs sediment load Rio Bermejo (station: El Colorado)

Figure 84 illustrates the dependence of the sediment load at Zarate (Parana de las Palmas) on the sediment load of the Rio Bermejo. All the peaks in the concentration at Zarate are preceded by peaks in the concentration in the Rio Bermejo. The absolute values however do not match the data of the Rio Bermejo since downstream of the measuring location some other tributaries add extra sediment load. Furthermore, the sediment load in the Rio Parana does not follow the trends at the Rio Bermejo during low flow. This is due to the fact that the Rio Bermejo is not the only sediment sources in the system. Menendez, Kazimierski, & Re (2017) also concluded that at high suspended sediment concentrations (>100 mg/L) at the Rio Parana the load comes from the Rio Bermejo (Figure 83).

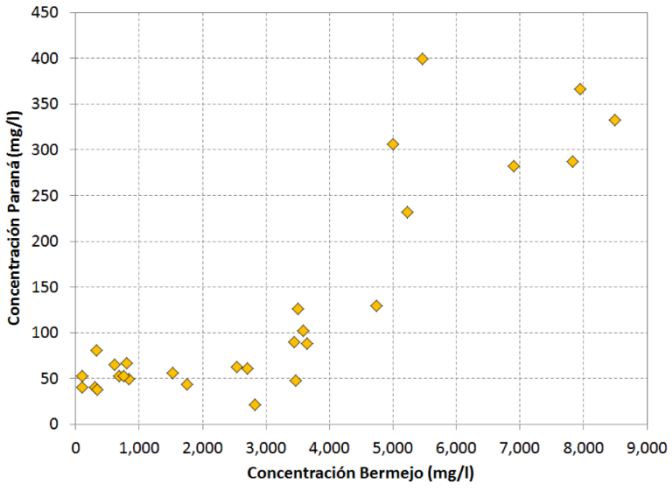

Figure 83 Correlation between concentration of sediment in suspension of the Rio Parana and Rio Bermejo between august 2013 and march 2016. From Menendez, Kazimierski, & Re, 2017

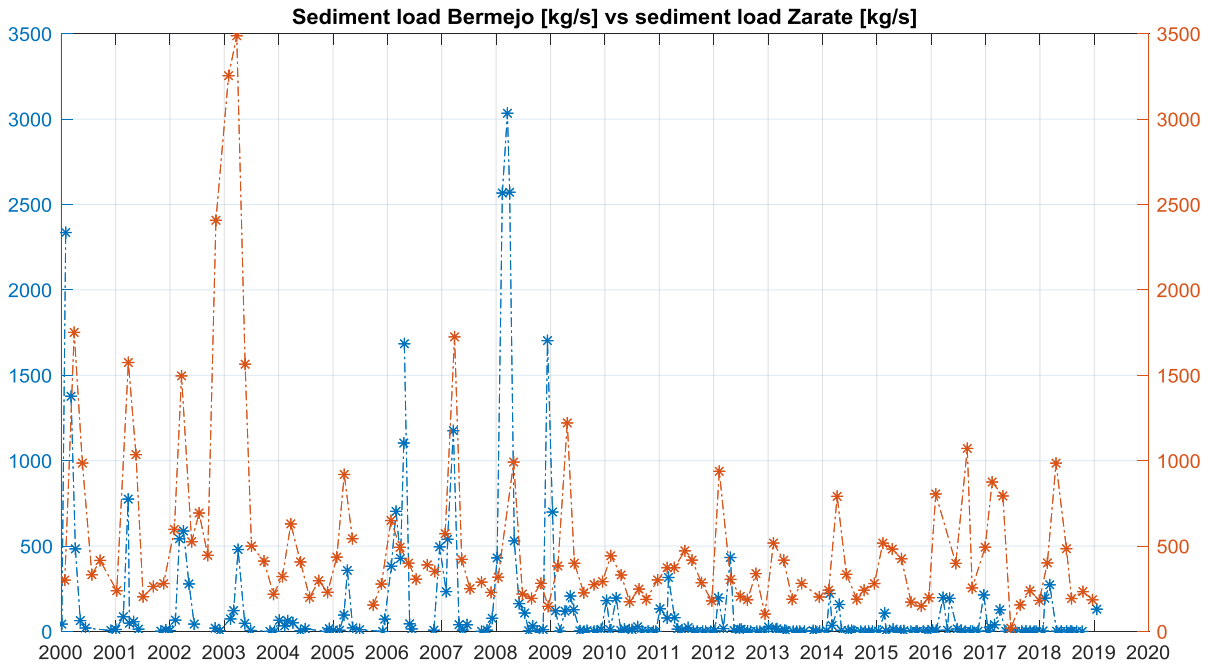

Figure 84 Sediment load Bermejo (station: El Colorado) vs sediment load Rio Parana de las Palmas (station: Zarate)

10.4 Appendix 4: Analysis dredging in the total waterway system

Currently the waterway between Punto Indio (Rio de la Plata) and Rosario (Rio Parana) is maintained at 34 feet and the stretch between little north of Rosario (Rio Parana) and Santa Fe (Rio Parana) is kept at 25 feet. Upstream of Santa Fe the navigational depth is 8 ft (World bank, 2010). A private concessionaire is responsible for the maintenance of the waterway and the Argentine government is the client. The overview of the area and the names of different channels are presented in Figure 85.

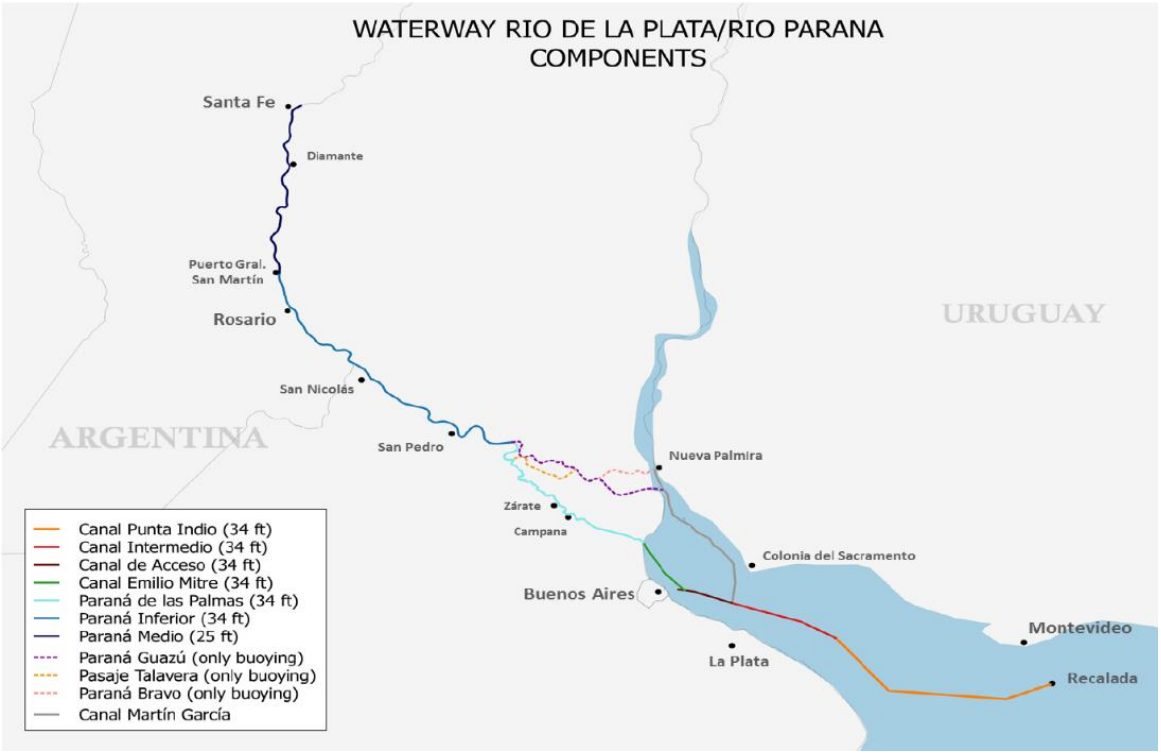

Figure 85 Dredged waterway components Rio de la Plata -Rio Parana and the major cities

The dredging record of the waterway system between 1995 and 2018 has been provided by the government. The current dredging company supplied this data to the government, and therefore it has been studied with care. A rough check between the AIS data (automatic identification system for ships) and the record did not show differences.

Figure 86 presents the spatial trend of the annually dredged volumes per kilometre between 2007 up and until 2017. This period is chosen since the dredging depths stayed the same in that period. Spatially the figure ranges from Santa Fe (right, upstream KP 600) to Punto Indio (left, downstream KP -200). The outer line of the plot represents the dredged volume per kilometre, although it does not give exact values, it creates a good impression of where dredging takes place. Three zones can be distinguished. On the Parana Medio, Parana Inferior and Parana de las Palmas the peaky signal is caused by sedimentation around bifurcations of river branches and bifurcations around islands. The dredged material is disposed within a distance of mostly 10 kilometre and sometimes up to 20 km. In the Canal Emilio Mitre section dredging occurs over a relatively long section from around KP 40 to KP 12, extending into Canal Accesso from KP -12 to KP -30. The high volumes are explained by the decrease in transport capacity for sediment in Canal Emilio Mitre compared to the Parana de las Palmas, which results in settling of the sediment in suspension. The peaks in the dredging volumes do not coincide with bathymetric features but are caused by the dredging strategy with pits.The numbering of the kilometre points at the end of Canal Emilio Mitre is KP 12 while the start of Canal Punto Indio is KP -12, this explains the gap in dredging volumes between those values. Downstream of Canal Emilio Mitre the dredging volumes are low, but they increase again in Canal Punto Indio. Possible explanations for this phenomena are the orientation of the channel which is perpendicular to the main direction of flow and the presence of the limit of the turbidity maximum.

The annually averaged dredging volume is 33.7 Mm^3, of which 21.8 Mm^3 (0.04 Mm^3/km) is dredged on the Rio Parana, 6.6 Mm^3 (0.14 Mm^3/km) in Canal Mitre and Accesso and 5.3 Mm^3 (0.03 Mm^3/km) is dredged in the rest of the Rio de la Plata estuary. This illustrates that the sedimentation per kilometre in Canal Mitre+ Accesso is particularly high.

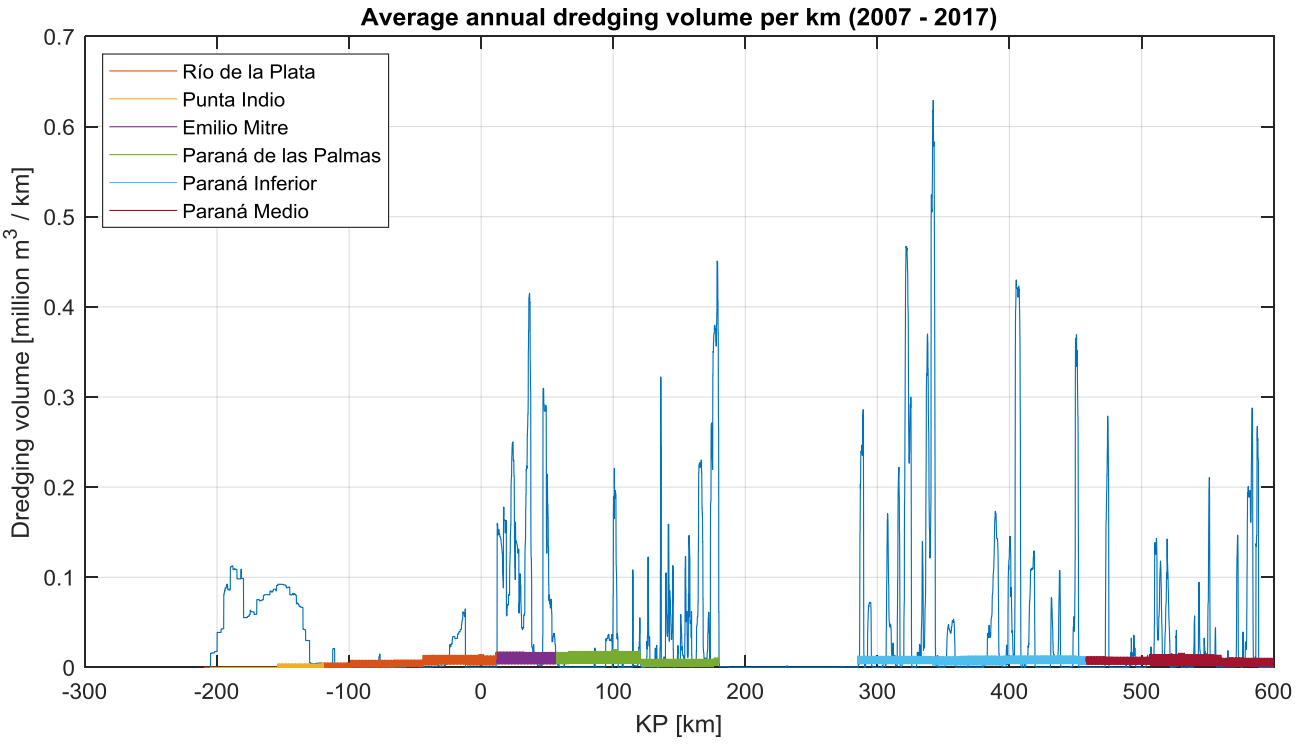

Figure 86 Average annual dredging volumes per km (2007-2017) whole waterway system

10.5 Appendix 5: Sources of bathymetric data

This appendix provides the sources and specifications of the bathymetric data which is used to construct the bathymetry of the numerical model as described in paragraph 5.2.2.

Organization	Type of data	Location	Spatial resolution	Date	Reference Level	No of data points
Argentine government	Bathymetric survey	Santa Fe – Atlantic ocean	Centreline navigation channel and cross-sections	Feb 2016 used + other years	Local Zero per stretch	170000
Argentine government	Bathymetric survey	Emilio Mitre - Atlantic Ocean	Centreline navigation channel and cross-sections	Feb 2016 + other years	Cero Riachuelo	96000
SOHMA + IMFIA	Navigation Charts	Uruguay River: Salto Grande Dam - Nueva Palmira	Bank to bank, 150 meter by 150 meter	2013 to 2015	Cero Wharton	90000
Boskalis	Bathymetric survey	Martin Garcia Channel	Cross sections along navigation channel	2019, different dates	LIMB	5700000
INA	Combination	Delta Parana: Santa Fe - Colonia del Sacramento	10 by 10 meter over the whole delta	Different years	IGN	A lot
SOHMA + IMFIA	Navigation Charts	Rio de la Plata estuary + continental shelf	2 km by 2 km	Different years	Cero Wharton	7000

Table 8 Sources of bathymetric data for numerical model

10.6 Appendix 6 Calibration of roughness coefficient

Calibration of the roughness coefficient is done by comparing the simulated water levels to the 10 water level stations on both the river and the estuary. This results in a space-varying roughness coefficient. This appendix described how this value was calibrated. The water level stations which were compared in the analysis are shown in Figure 88. The river stretch is expected to have a different roughness than the estuary, therefore per station the analysis has been done which value fits best. From that analysis a space-varying roughness was constructed. The main goal is calibration of the water levels at Braga since that station is located close to Canal Emilio Mitre and therefore it is a good indication of whether the flow velocities around Mitre are well represented by the model. This in its turn is expected to affect sedimentation.

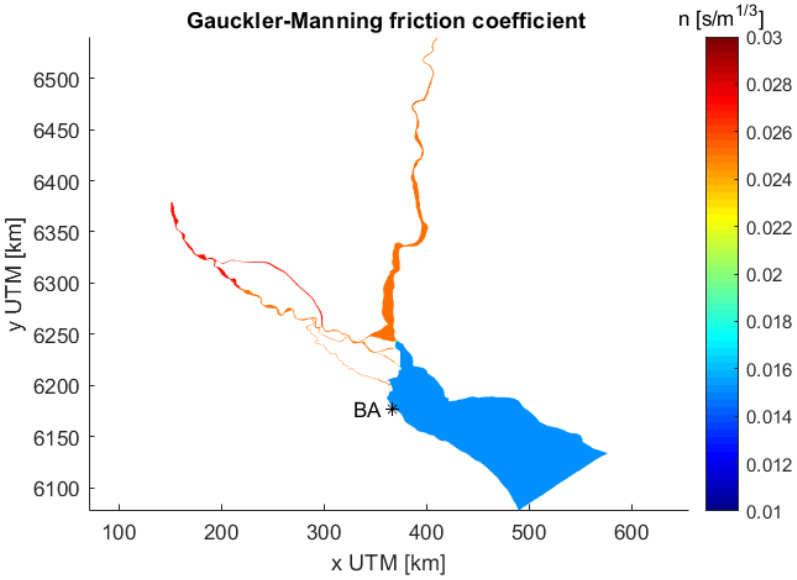

Figure 87 Spatial variation of roughness coefficient over modelling domain

The roughness formula of Manning is chosen as this formulation is used in open channel analysis. The choice is made for a space-varying Manning value since the domain consist of water bodies with different properties. According to literature a value of Manning's n of 0.025-0.03 is suitable for a Parana like river (Chow, 1959), while on an estuary a value of 0.01-0.02 is more suitable dependent on the mud percentage (van Maren et al., 2015). Runs with a uniform roughness confirmed that these values were in the right range. Afterwards a space varying roughness was applied, resulting in a roughness of 0.015 on the estuary, 0.025 on the lower river and 0.027 on the river above the bifurcation of the Rio Ibicuy (Figure 87). These values fit the values specified in the literature.

Figure 90 until Figure 99 show the measured water levels versus the simulated water levels under the influence of roughness coefficients. At Pilote Norden and Braga the simulation with a roughness of 0.015 shows the closest match. A low roughness was also expected here since these are located on the estuary, a value of 0.01 is expected in a mud-dominated estuary and 0.02 is expected on a sand-dominated estuary (van Maren et al., 2015). Therefore 0.015 is very reasonable for a silty estuary. At Zarate, Baradero, Bifurcacion, San Pedro and Ramallo the simulation with a roughness of 0.025 shows the closest match. This is a value that matches the typical value by Chow (1959). Further upstream at San Nicholas, Villa Constitucion and Rosario the value of 0.027 provides the best fit.

A clear trend can be distinguised in the roughness from high values in the upper stretches of the river to lower values on the estuary. Therefore a space-varying roughness is used varying from 0.027 at Rosario, Villa Constitucion and San Nicholas, to 0.025 at Ramallo, San Pedro, Bifurcacion, Baradero and Zarate. At Braga and on the estuary a value of 0.015 is used.

Next to calibration of the roughness coefficient the analysis of the water levels also provided the following insights:

- The amplitude and timing of the tidal propagation at all stations matches the measured time-series. This shows that the offshore boundary condition has enough resolution and protrudes in the right way into the river branches.
- The absolute value of the water levels differs up to 0.5 m at some stations (Ramallo or San Nicholas) with a constant deviation while at the next station it shows a good fit (San Pedro or

Rosario). These differences are attributed to reference levels errors and do not occur close to the area of interest.

- The water levels at Pilote Norden, Braga and Zarate show a significant influence of the wind. The signal produced purely by the tide at some instances shows a good fit and at other times it shows differences with the measured time series. Figure 89 shows that when the wind direction is directed into the estuary (120 to 160 degrees) the measured water levels are higher than the simulated water levels. The opposite is true when winds blow from the land towards the estuary. This is a limitation of the current set-up of the model, mostly because the extreme water levels cause high flow velocity which lead to resuspension of sediments around the delta where the channel is very sensitive to sedimentation. This is addressed in paragraph 6.4.

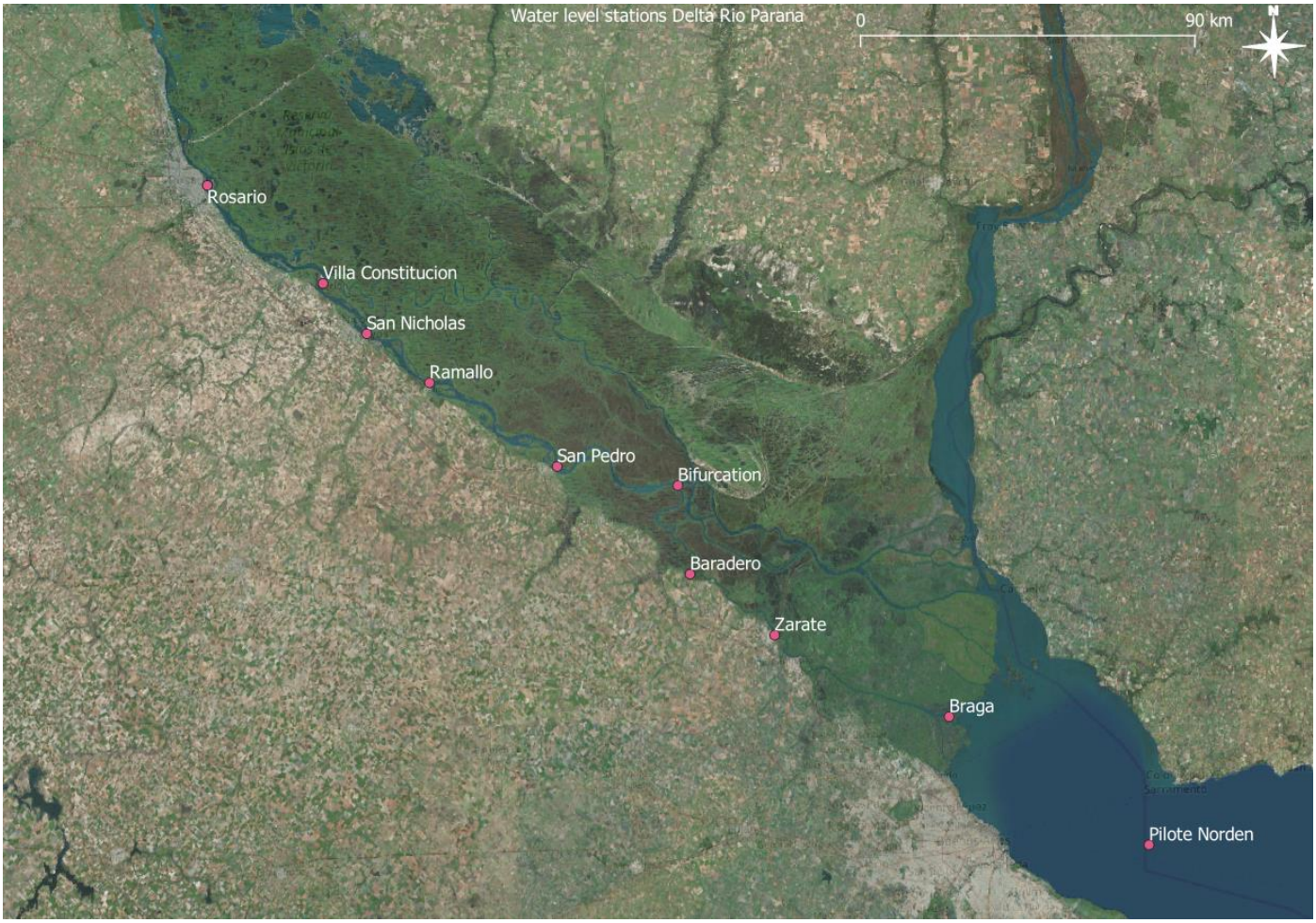

Figure 88 Water level station Delta Rio Parana

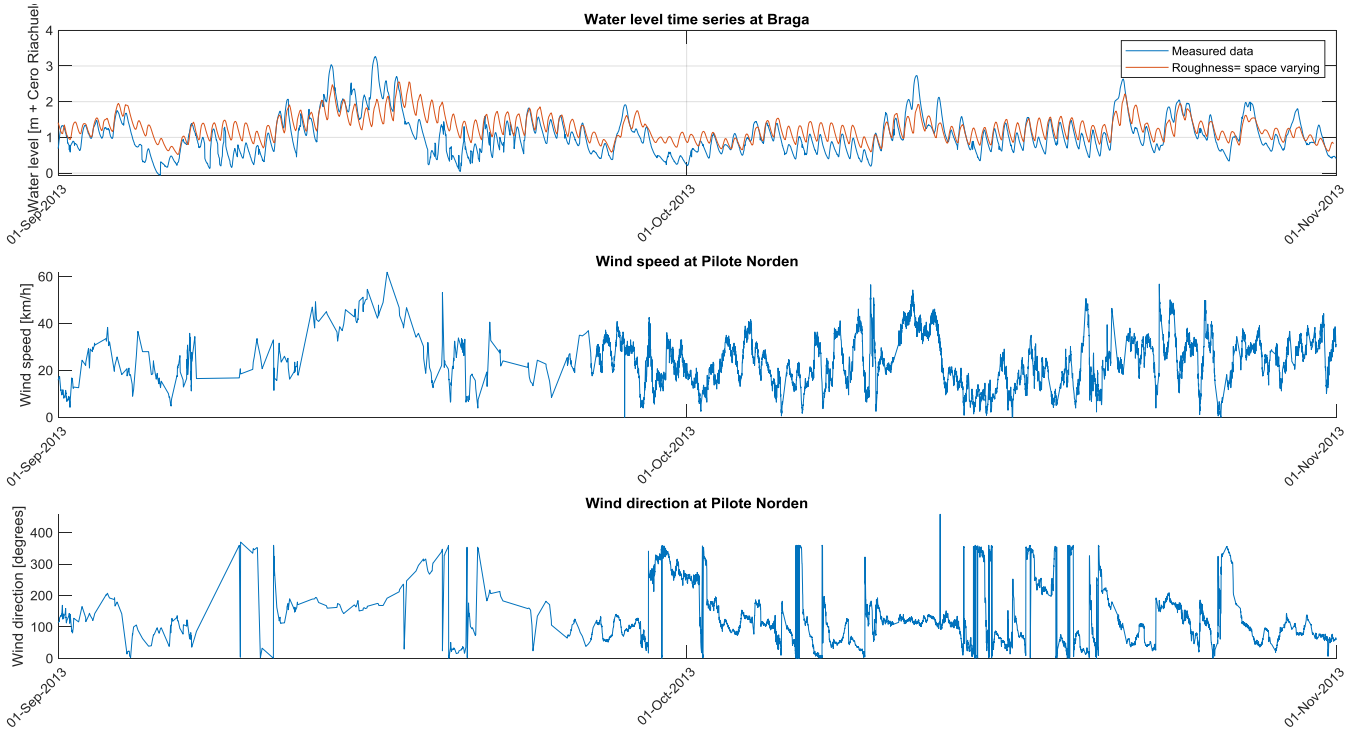

Figure 89 Dependency water levels Barga on wind direction and speed

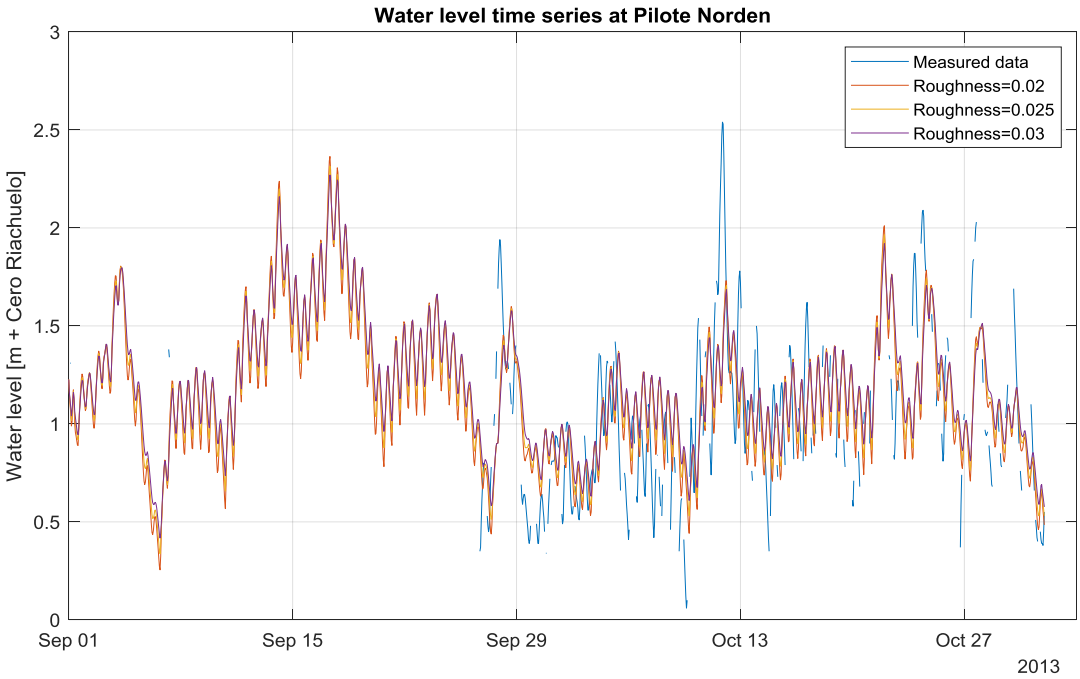

Figure 90 Calibration roughness: station Pilote Norden

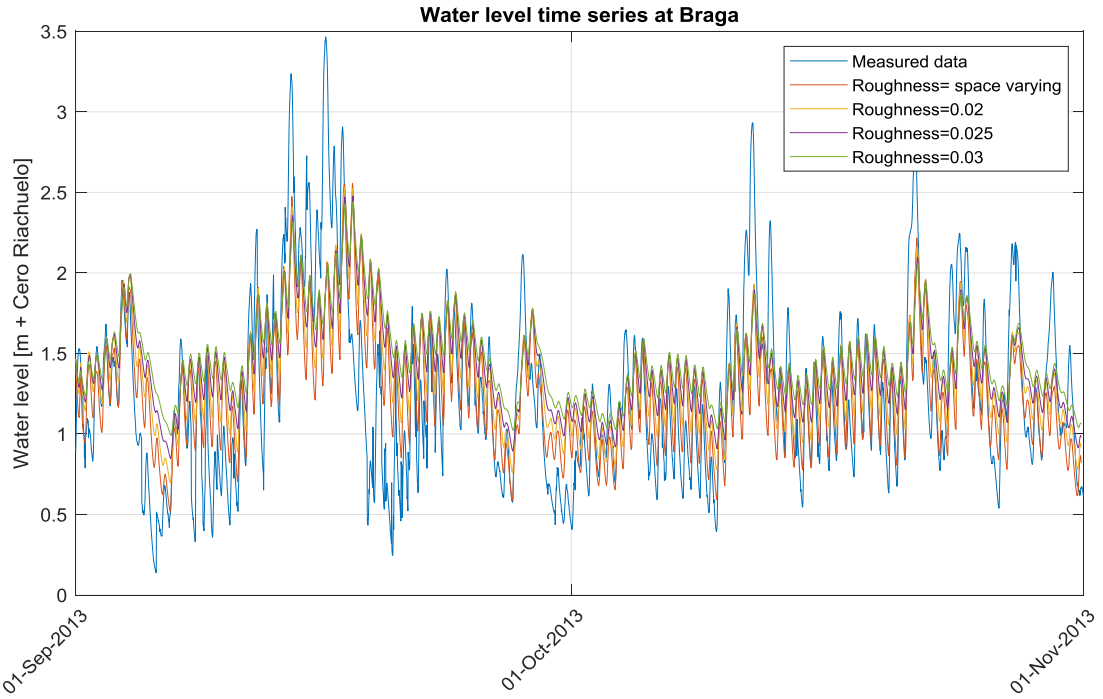

Figure 91 Calibration roughness: station Braga

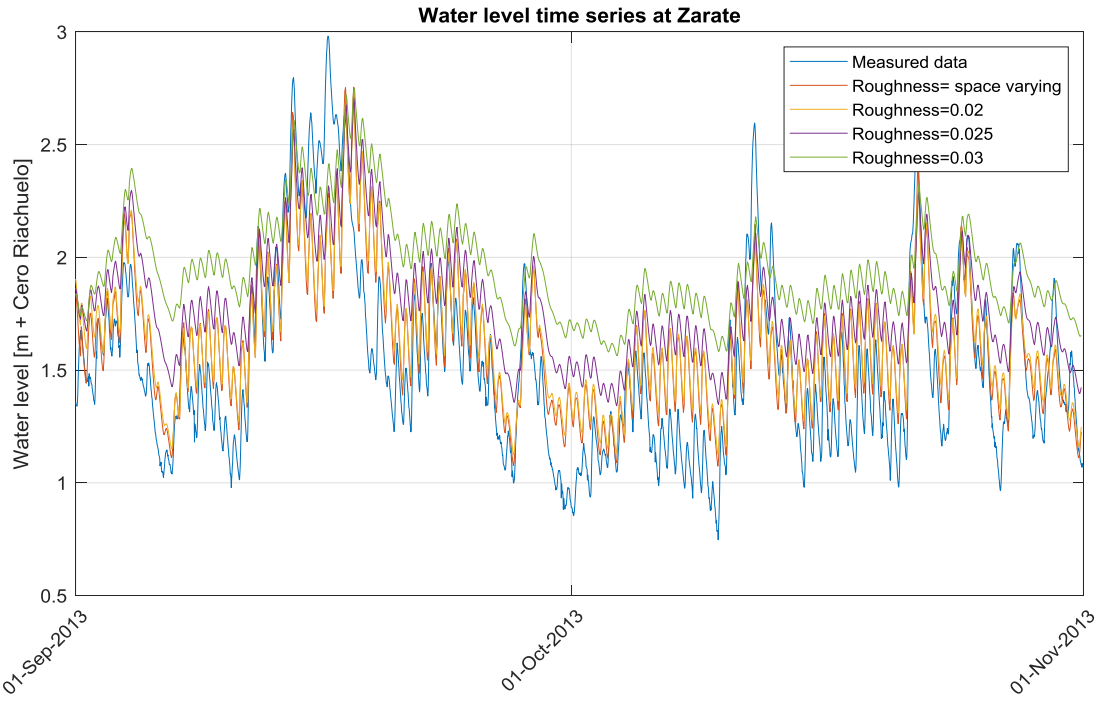

Figure 92 Calibration roughness: station Zarate

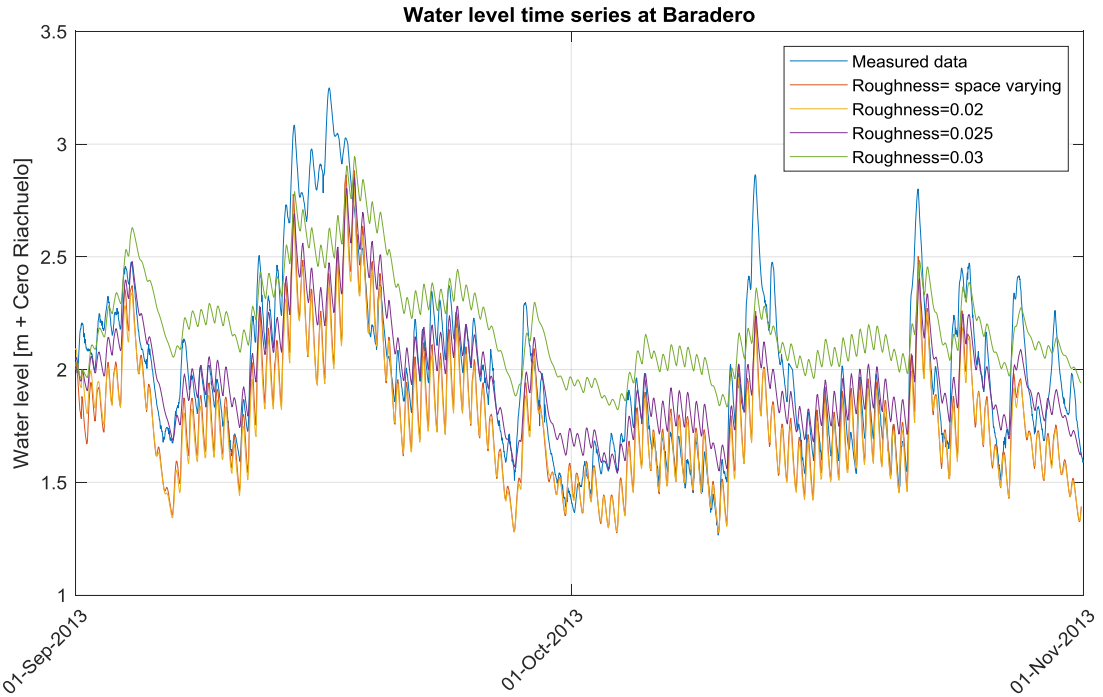

Figure 93 Calibration roughness: station Baradero

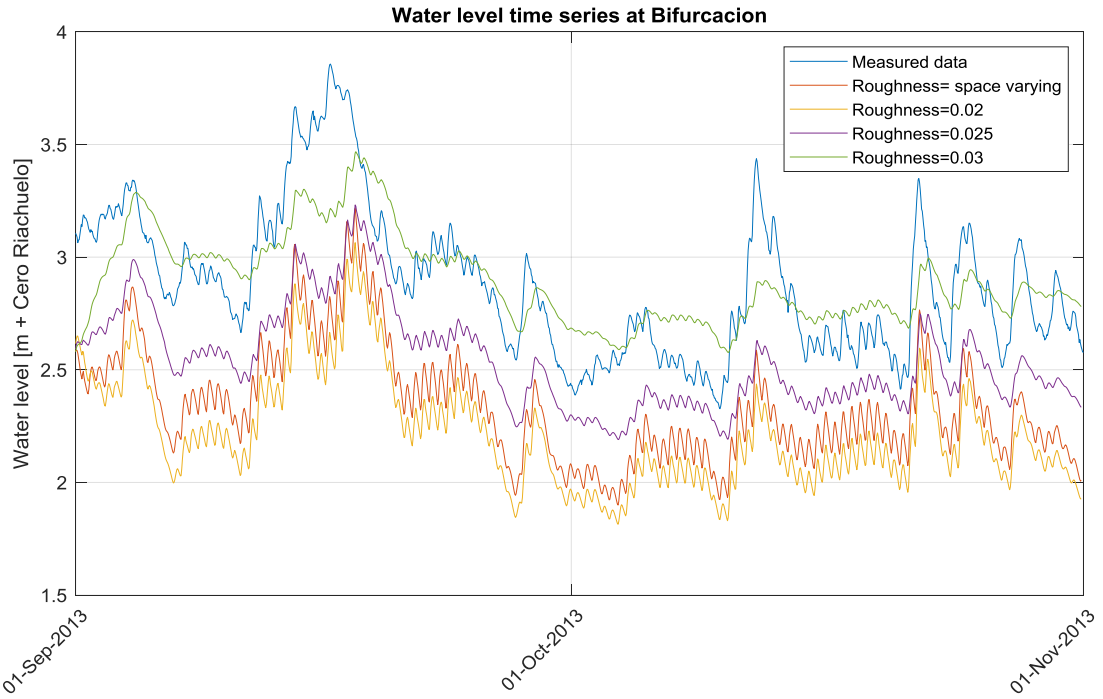

Figure 94 Calibration roughness: station Bifurcacion

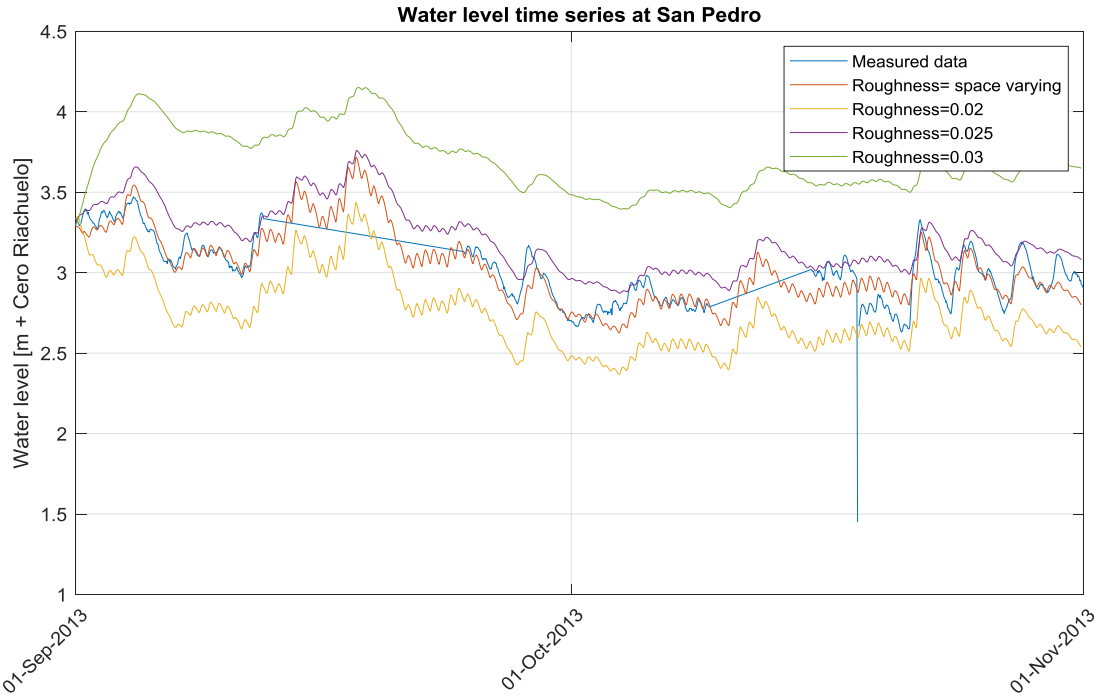

Figure 95 Calibration roughness: station San Pedro

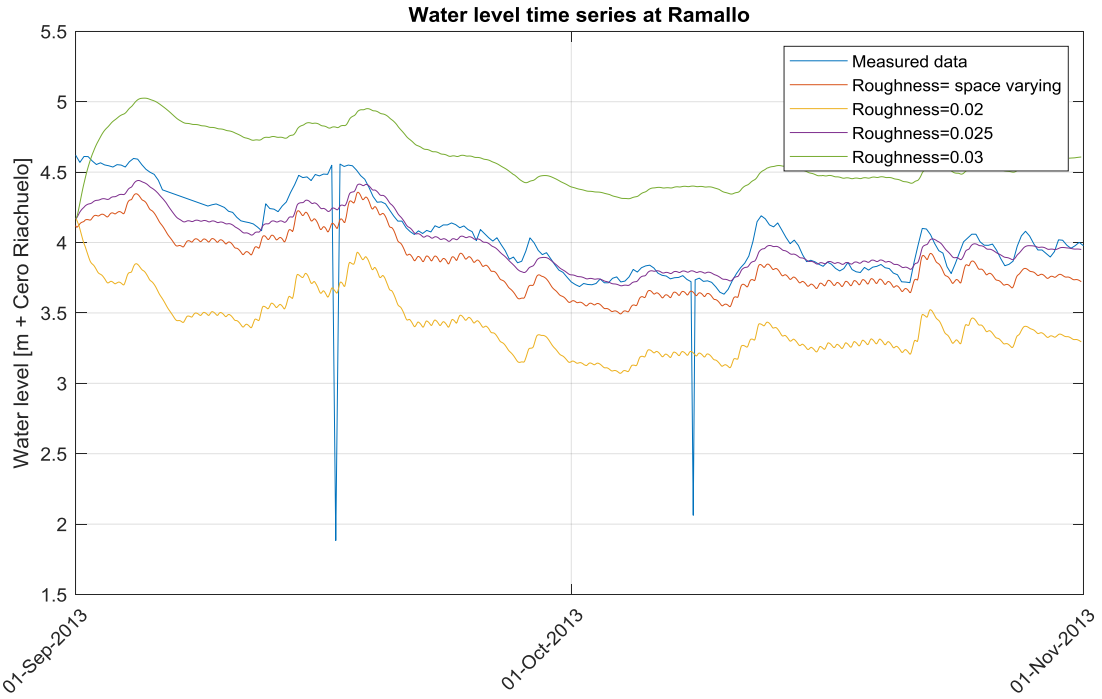

Figure 96 Calibration roughness: station Ramallo

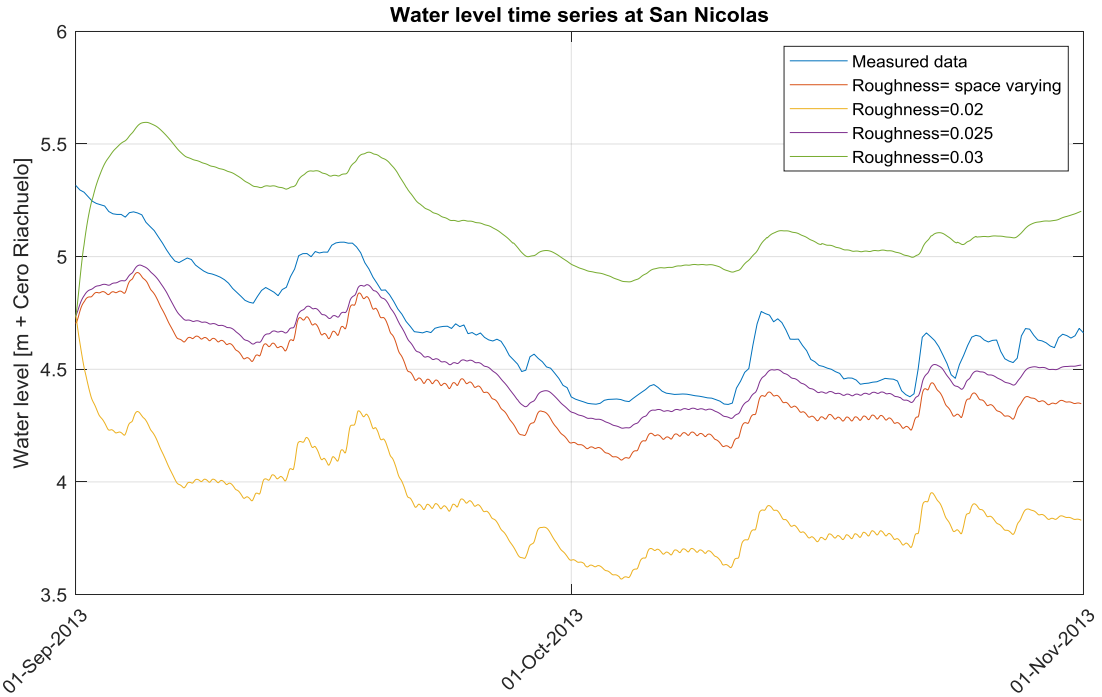

Figure 97 Calibration roughness: station San Nicholas

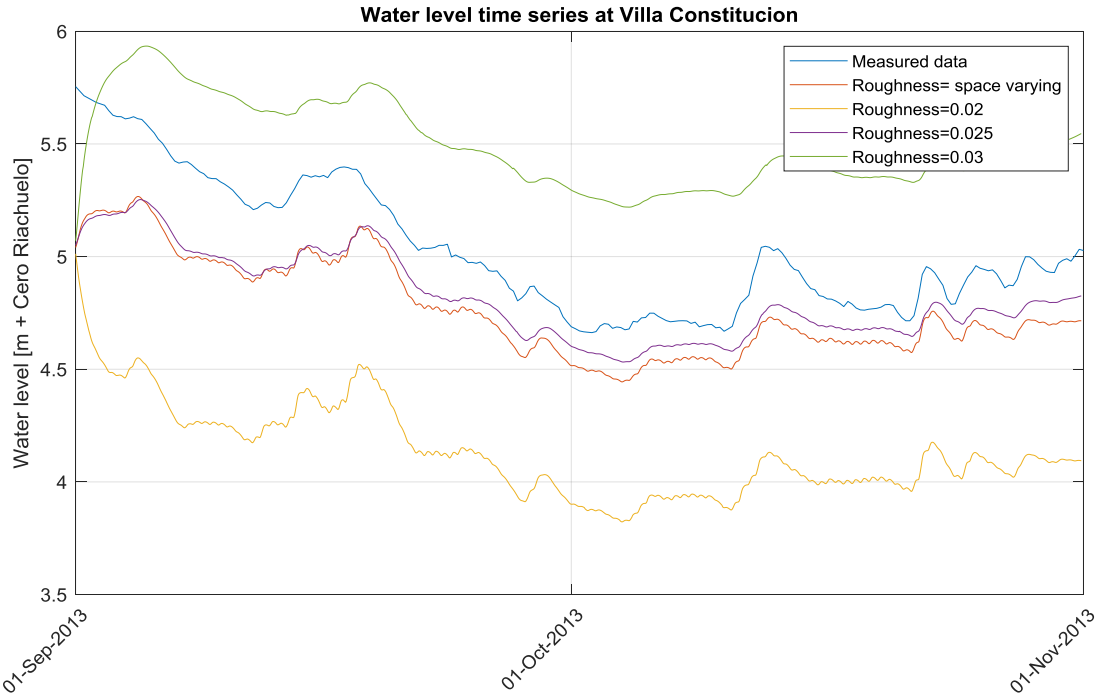

Figure 98 Calibration roughness: station Villa Constitucion

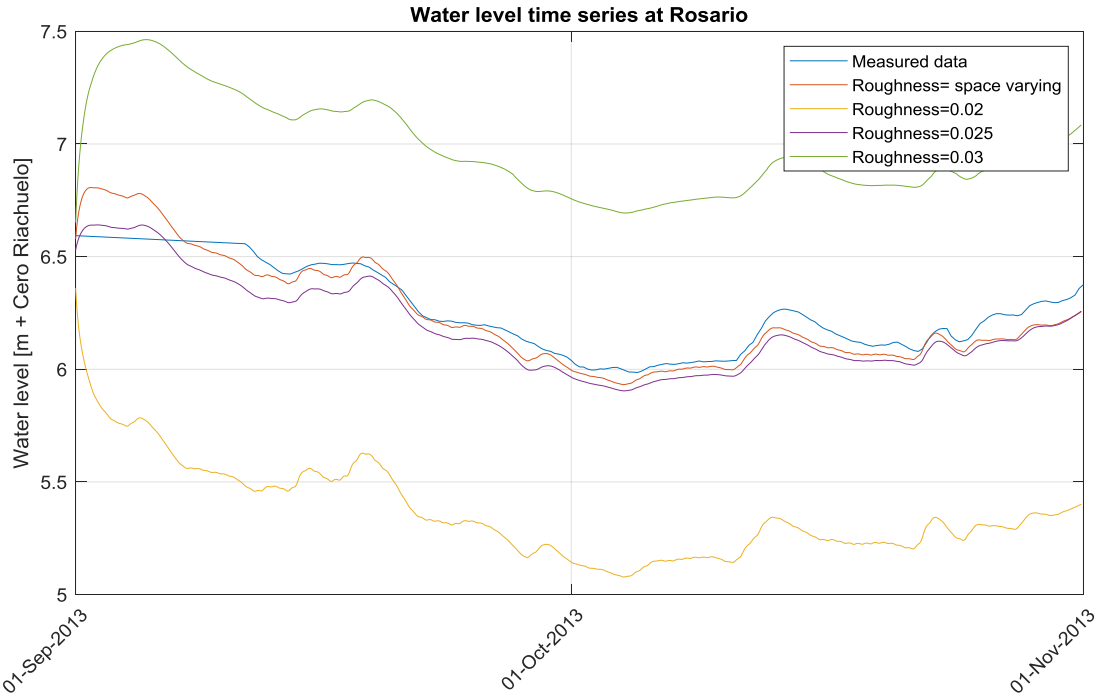

Figure 99 Calibration roughness: station Rosario

10.7 Appendix 7: Relevance of modelling more than one sediment fraction

This appendix describes the relevance of modelling with more than one sediment fraction, as shown in paragraph 2.4 the supply of sediment into the system is mainly silt, but also some clay and some sand. In the literature it is found that these different fractions lead to different behaviour (Sarubbi, 2007). The sandy fraction is deposited directly to the delta (which is the first part of the channel of interest), resulting in the advance of the delta front in length. While the silty material is responsible for the growth of the delta in the vertical direction, and is deposited further in the estuary (as confirmed by the bottom composition in Figure 100). The clayey fraction is the fraction which is in suspension and leads to the high suspended sediment concentrations on the estuary until the water reaches the Barra del Indio (topographic feature halfway the estuary) where the salinity limit is located.

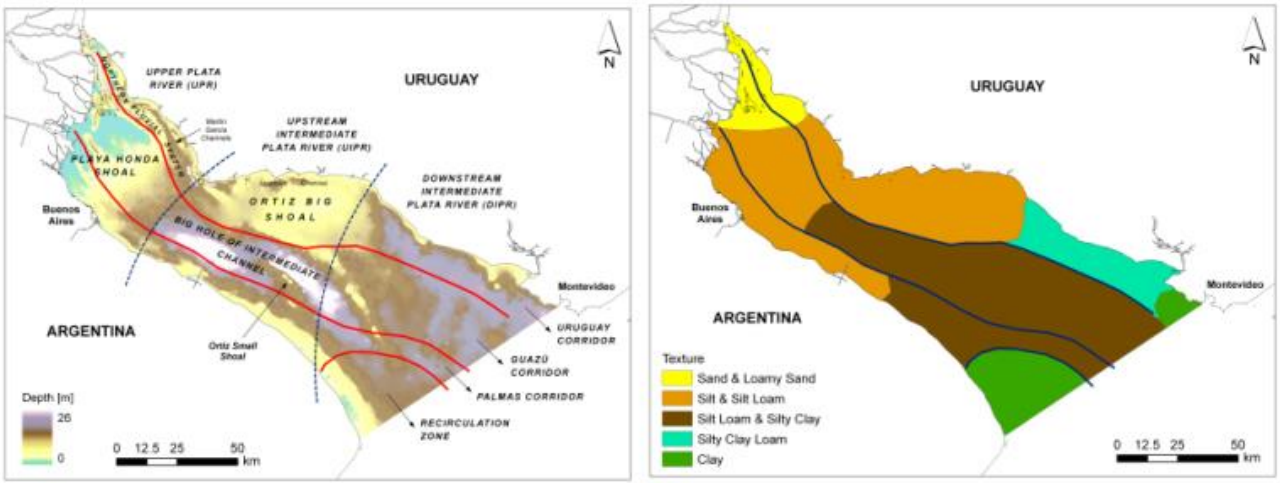

Figure 100 Schematic depth and bottom composition Rio de la Plata estuary

The concentration of the different fractions in the model indeed shows the same behavior, the sand settles close to the delta, the silt settles in Canal Emilio Mitre and the clayey fraction stays in

suspension (Figure 101). Since the sand is responsible for the sedimentation in the upstream part of the channel, the silt is responsible for the middle part and the clay starts playing a role in the lower part of the channel, all of these fractions are relevant. Moreover modelling with only silt, also lead to erosion in the upstream stretch since in reality sand is expected there, which is more resistant to erosion.

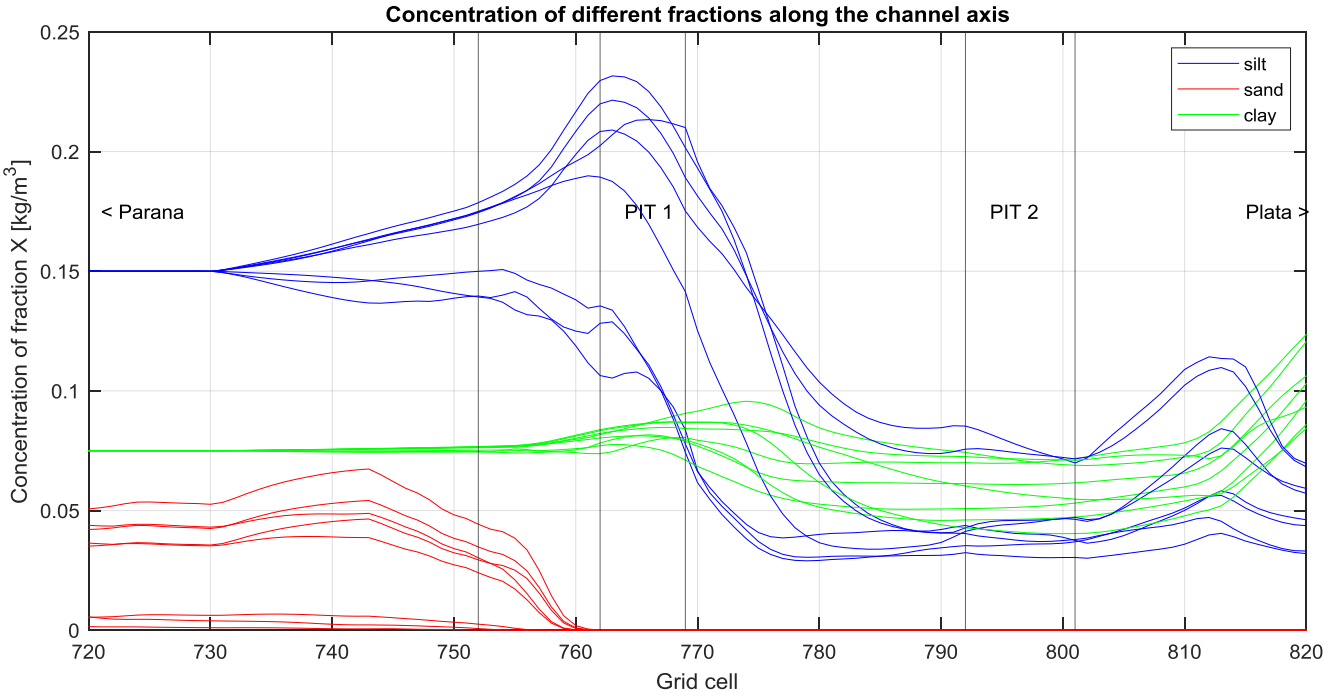

Figure 101 Concentration of different fractions along the channel axis from Base Case of model (different time steps)

10.8 Appendix 8: Calibration of sediment dynamics

In paragraph 5.4.2 the conclusions and set-up of the calibration of the sediment dynamics is presented, this appendix presents the supporting graphs and further explanation per calibration parameter.

The outcomes of the RMSE analysis and absolute value analysis are presented in Table 9 and Table 10. The higher the normalising factor the closer the absolute value of the simulated sedimentation is to the reported dredged volumes. Since the volumes were compared to the addition of the reported volumes of 2015,2016 and 2017 it looks like these values are far off, so it is rather important to look at the relative differences between the scenarios. The RMSE should be as low as possible, for the Base Case this was 0.293. From these table it is concluded that compared to the Base Case only the scenario 2 and 6 have a positive effect both on the RMSE and the absolute value. However increasing the horizontal eddy viscosity is not sound from a physical perspective, as described in paragraph 5.2.5. The other parameter which has a positive effect on both is the increase of the erosion parameter of the clayey fraction, however when taking a close look at the changes in the spatial profile in Figure 109 it is recognised that this leads to a clear underestimation of the sedimentation in the upstream pit. The only other parameter which requires special attention is the diameter of the sand, scenario 8 revealed that if this parameter is increased the peak which is visible in the model and not in the reported dredging reduces in size. It shows that the actual size of the sediment around that reason might be larger than the 100 micrometre. Since this parameter does not affect the profile over majority of the region of interest this is left for now. From these two tables and the corresponding graphs in this Appendix it is concluded that the calibration of the sediment dynamics is finished.

	0 basecase	1 vismin	2 vismax	3 minsilt	4 maxsilt	5 minclay	6 maxclay	8 maxsand
Normalising factor	0.330	0.239	0.377	0.284	0.295	0.294	0.345	0.282
RMSE	0.293	0.347	0.270	0.312	0.327	0.305	0.283	0.257

Table 9 Results RMSE and absolute value analysis part 1

9 Msiltmin	10 Msiltmax	11 Mclaymin	12 Mclaymax	13 tausiltmin	14 tausiltmax	15 tauclaymin	16 tauclaymax
0.311	0.332	0.325	0.303	0.363	0.303	0.276	0.324
0.299	0.324	0.294	0.299	0.319	0.301	0.322	0.295

Table 10 Results RMSE and absolute value analysis part 2

As observed in Figure 102 the silty fraction the minimum settling velocity leads to higher sedimentation rates in the middle part of the channel (around KP 20), however this leads to underestimation of the siltation in the upstream as the material stays in suspension. The maximum settling velocity leads to higher sedimentation in the upstream pit and lower value afterwards. This sensitivity test is very illustrative for the situation in Canal Emilio Mitre as actually all these fractions are present as can be concluded from the sieve curves. The chosen fraction with a settling velocity of 0.5 mm/s is chosen as this shows a right balance between the two types of behaviour.

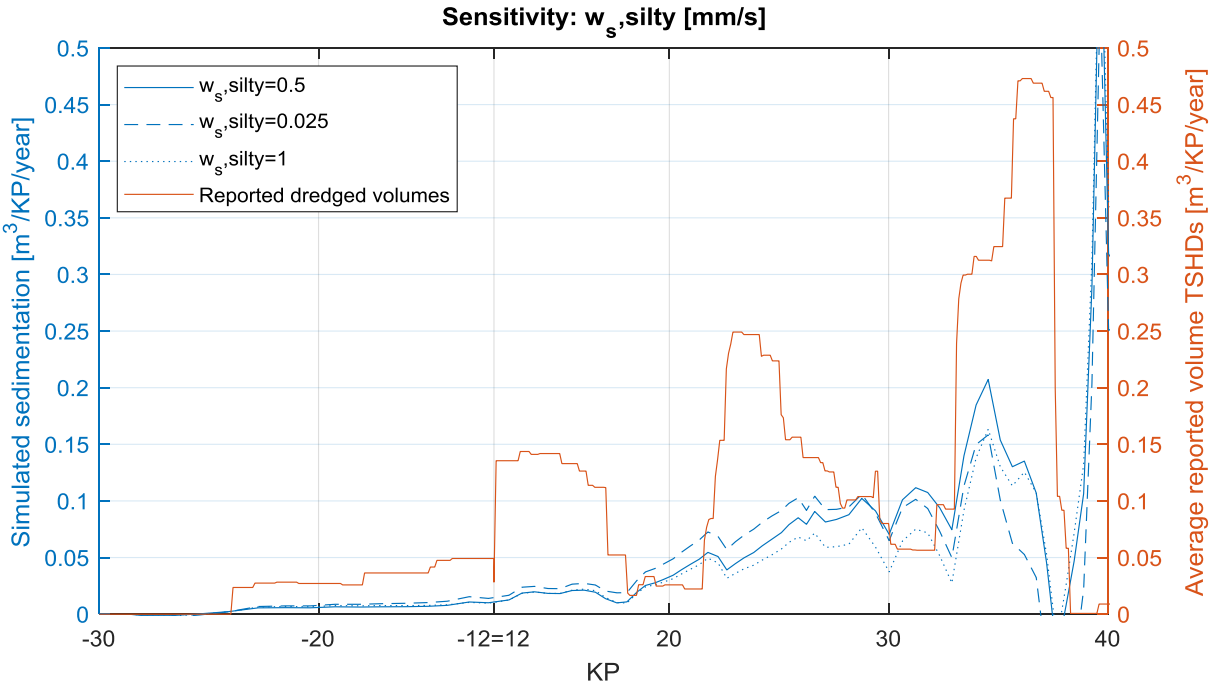

Figure 102 Calibration: settling velocity, silty

Figure 103 shows that the calibration of the settling velocity of the clayey fraction results in the same conclusion, if a lower settling velocity is chosen the material that did not settle in the upstream pit is deposited further downstream. The opposite is true for the higher settling velocity.

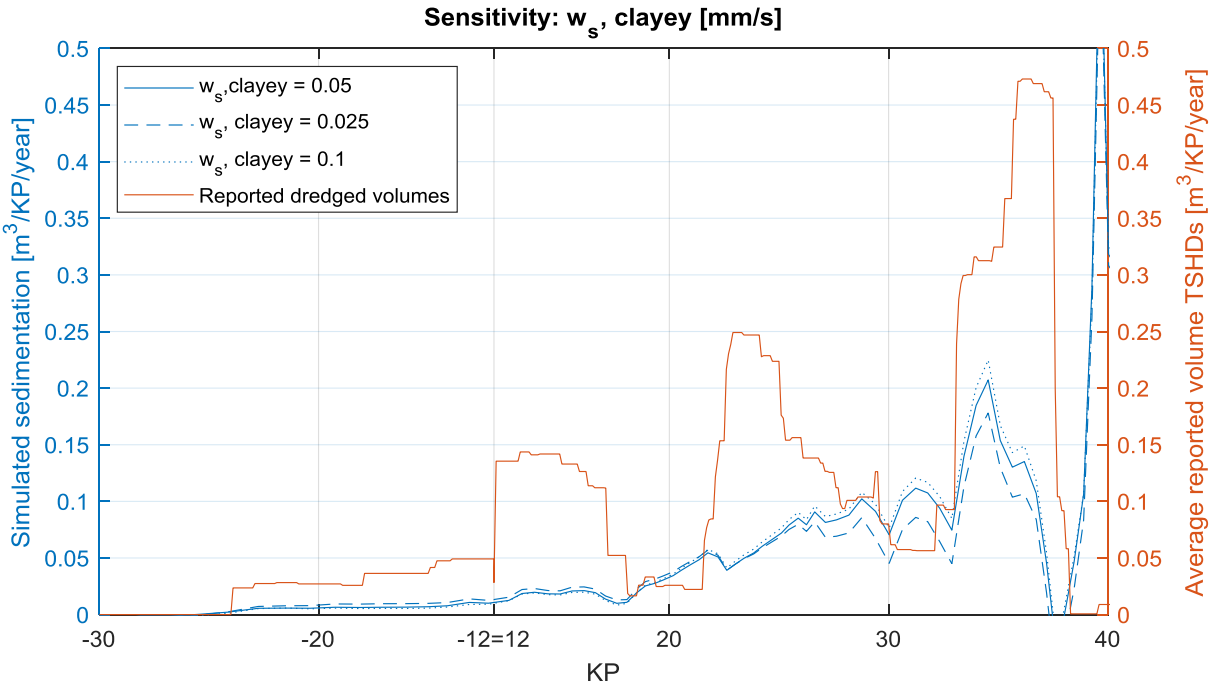

Figure 103 Calibration: settling velocity, clayey

The diameter of the sand does not affect the sedimentation pattern on the estuary too much (Figure 104), the sediment which is supplied from upstream already settles around the transition from the river to the estuary which also as expected from literature. There it is shown that the diameter does have a significant influence on the absolute value of the peak. It reveals that with a higher diameter the model shows a better match with the reported dredging volumes. This is point of improvement of the model.

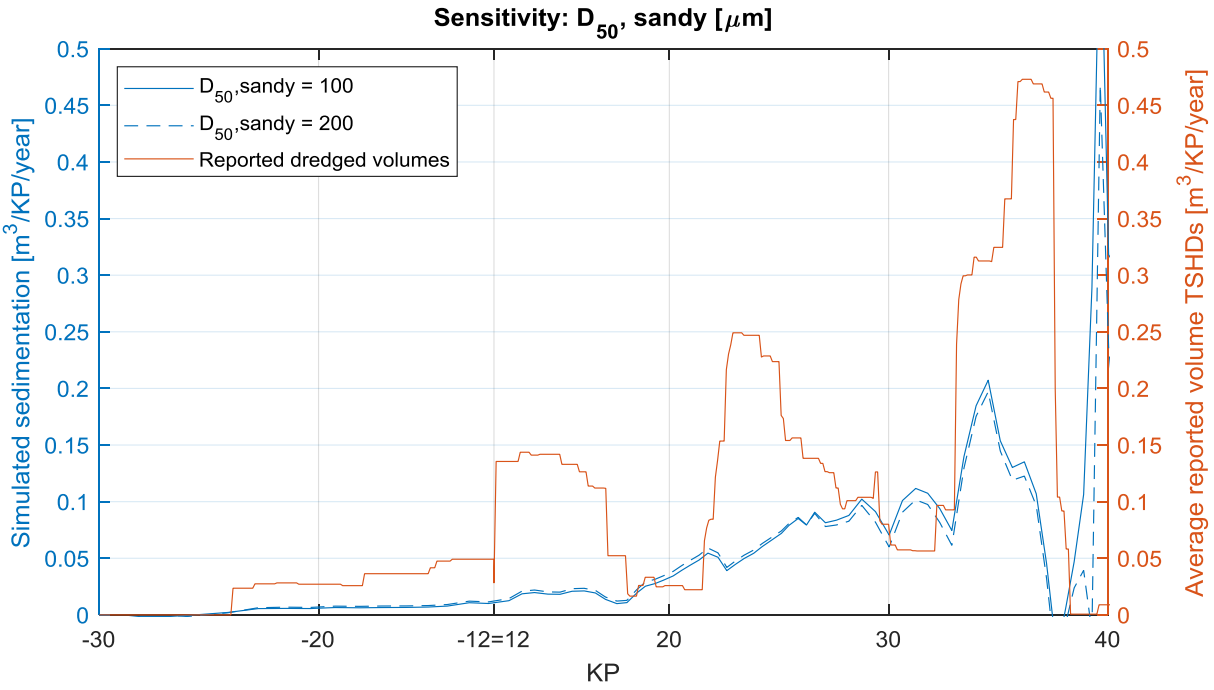

Figure 104 Calibration: D50, sandy

The influence of the horizontal eddy viscosity is as expected (Figure 105). Areas with high horizontal gradients in velocity experience more sedimentation when the value is higher, this can be explained

by the fact that it enhances the mixing. Lower values lead to less mixing of momentum, and thus less mixing of sediment, this reduces the sedimentation. Also, the effect is clearly visible around the downstream pit, after the pit the concentration of sediment in the water column went down, but with the maximum value of the eddy viscosity the mixing leads to a higher sedimentation rate than with the lower values. Therefore especially the behavior around the pits is affected to a large extent by this parameter. The choice for an horizontal eddy viscosity of 10 m^2/s shows reasonable results in the calibration and is also within the range of values for these type of models. Although a higher value leads to a lower RMSE and a higher normalizing factor (Table 10) it is not considered physically sound, as described in paragraph 5.2.5.

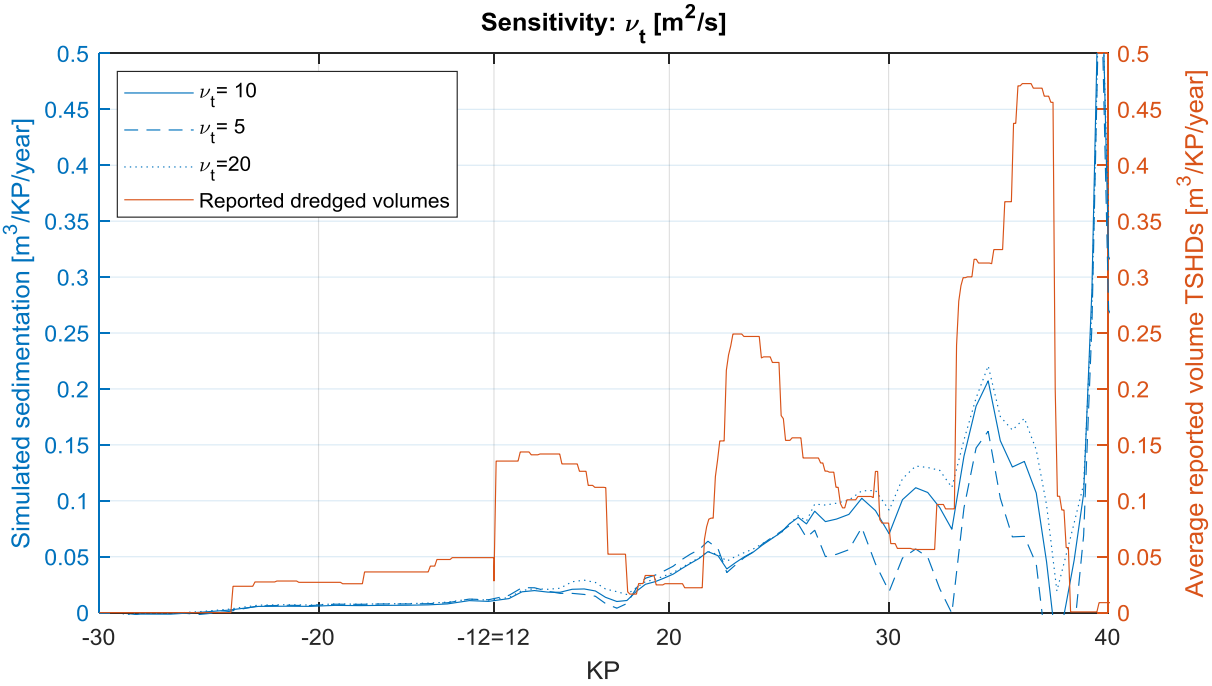

Figure 105 Calibration: horizontal eddy viscosity

The results are particularly sensitive to the critical shear stress for the silty fraction (Figure 106), this behavior can be explained very well by looking at the different physical processes. A low shear stress leads to higher suspended sediment concentrations, which move over the channel by the tide. This leads to higher sedimentation volumes over the whole canal. At the upstream pit is visible that with a critical shear stress for erosion even erosion occurs. This is not realistic and therefore the value should be at least 0.15 N/m^2 around that area. When looking at the maximum value, this does not lead to erosion around the upstream pit. When looking at the physical background of the system this can be explained very well. At the upstream part of the system the bed consists mainly of sand, for which a critical shear stress of 0.2 N/m^2 is even on the low side.

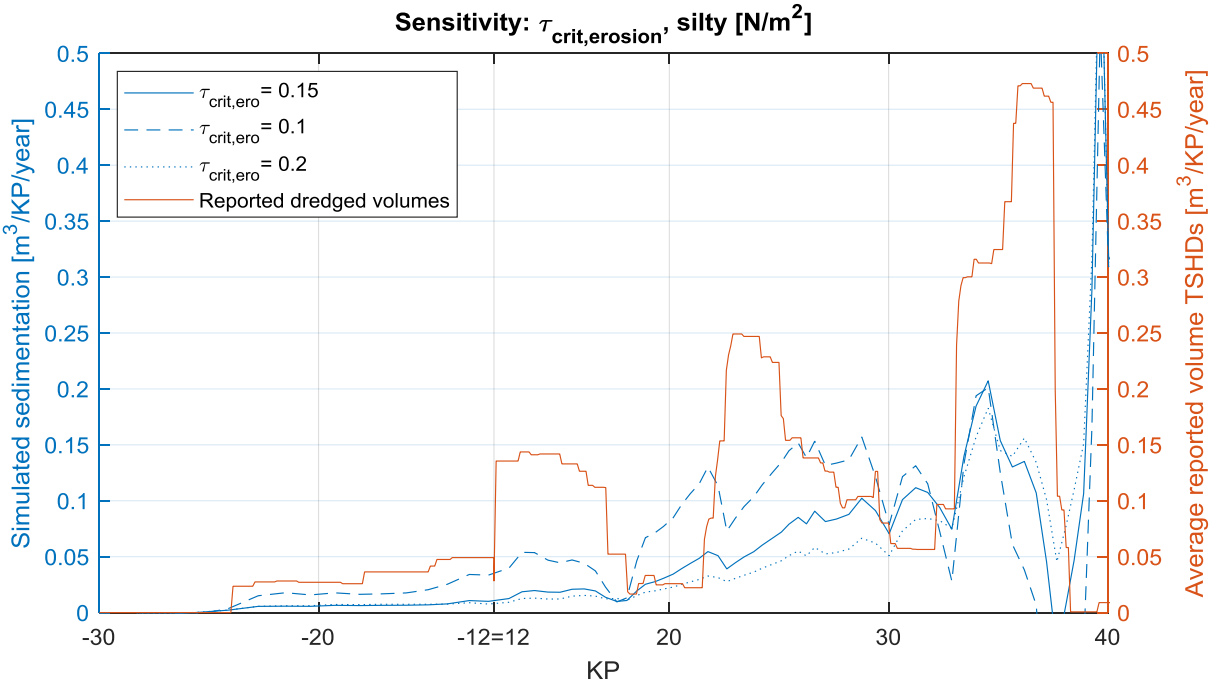

Figure 106 Calibration: critical bed shear stress for erosion, silty

The behavior for the clayey fraction shows the same behavior and trends (Figure 107), this is also what is expected since the two fractions interact. Also, here a higher value for the critical shear stress upstream seems reasonable, and lower values show a good match downstream.

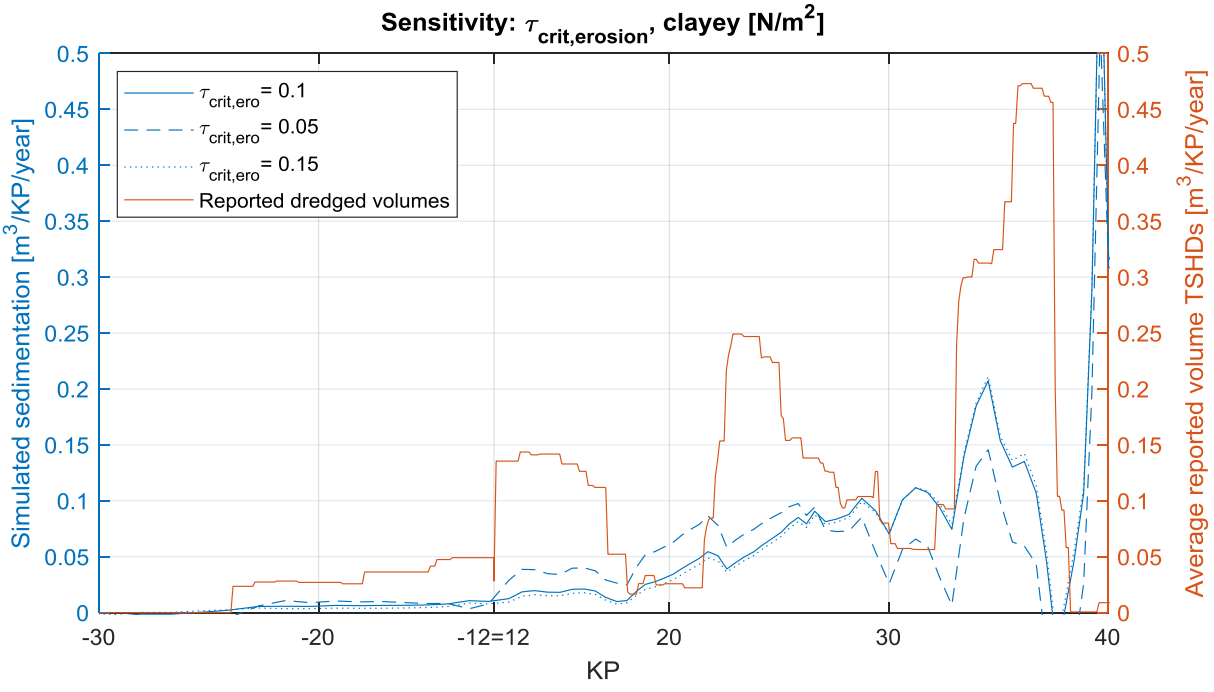

Figure 107 Calibration: critical bed shear stress for erosion, clayey

The erosion parameter of silt has major influence on the middle part of the channel (Figure 108), this matches the expectation since this is the area where most silt is present. Around the upstream pit a high erosion parameter leads to erosion just upstream of the pit, this is not realistic. A low erosion parameter however leads to serious sedimentation around that area which is also not realistic. Scaling the erosion parameter actually implies scaling the suspended sediment concentration of that fraction

in the system. The run with M=8e-5, showed the most realistic values for the suspended sediment concentration and is therefore considered a good choice. The same conclusions are true for the erosion parameter for the clayey fraction (Figure 109), however the effect of this parameter is way smaller. This is also as expected since the is fraction is mainly in suspension.

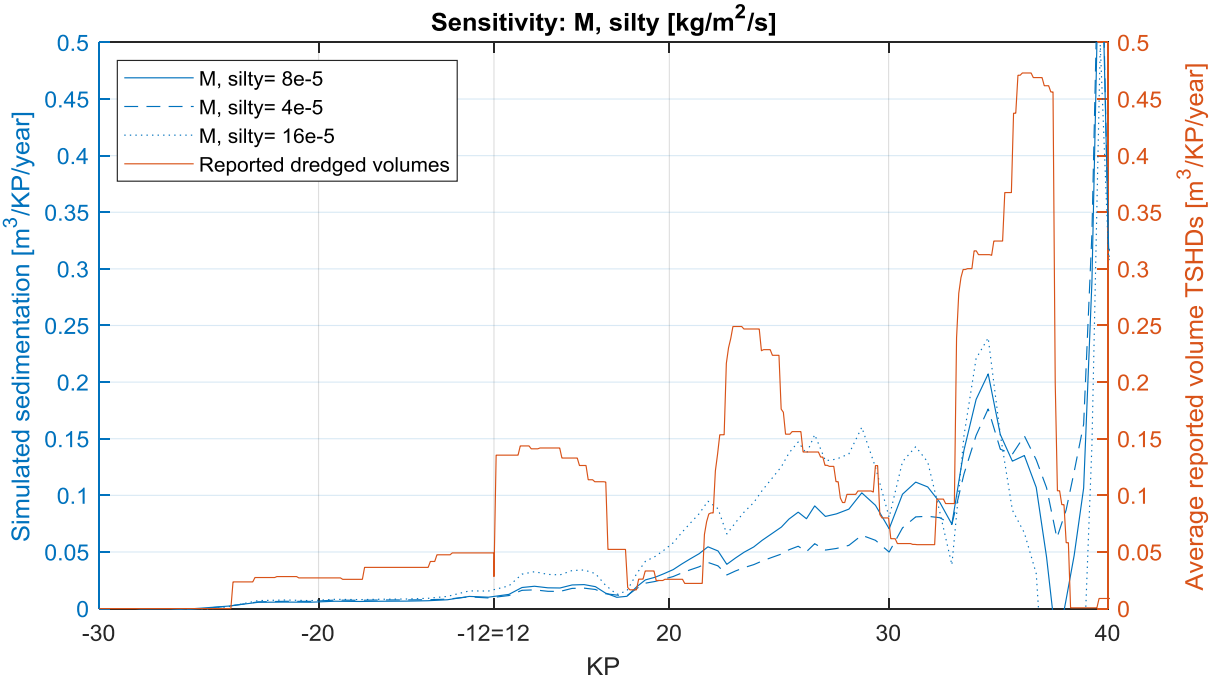

Figure 108 Calibration: erosion parameter, silty

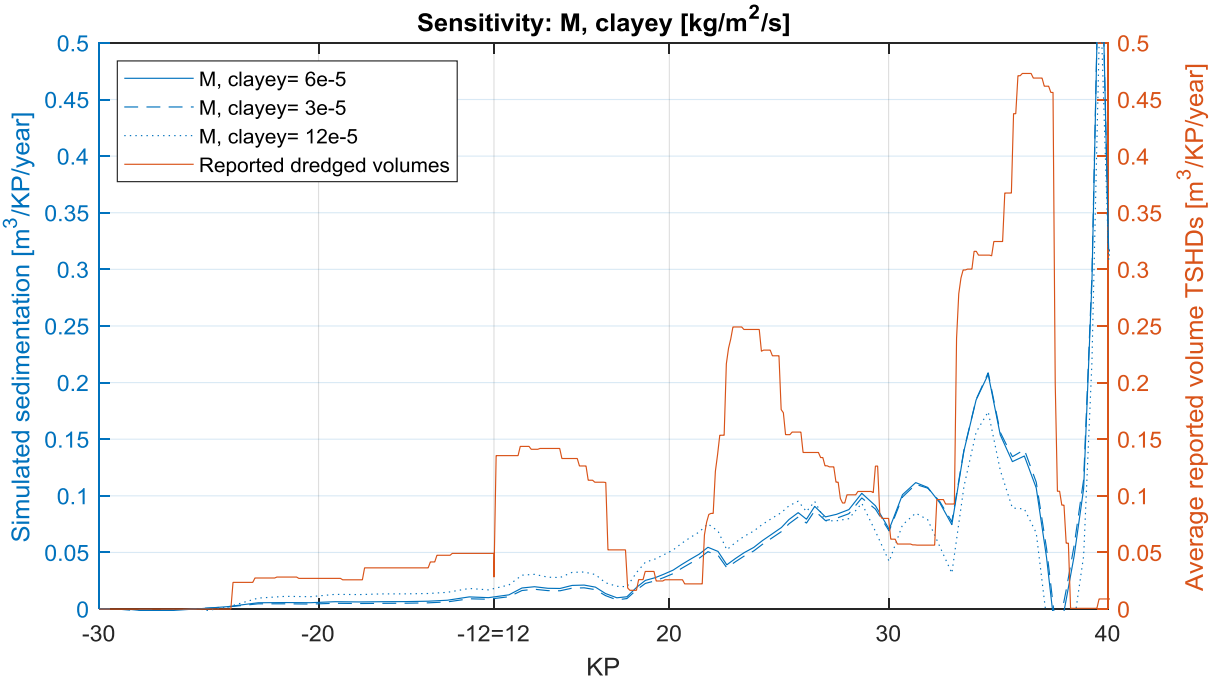

Figure 109 Calibration: erosion parameter, clayey

10.9 Appendix 9: Effect of wind on calibration water levels and sedimentation

This appendix presents the effect of the addition of temporally varying wind on the simulated water levels, in paragraph 5.3.2 it is concluded that this is expected to enhance the correct representation of the currents and therefore affect the sedimentation.

A RMSE analysis was done on the water levels for the Braga station without wind, with the wind of Pilote Norden (station on the estuary, indicated in Figure 88) and with reanalysis wind. The simulated water levels are presented in Figure 110. It shows that excluding the local wind provides the worst fit (purple line) missing out on the major effects due to local wind such as around half way October.

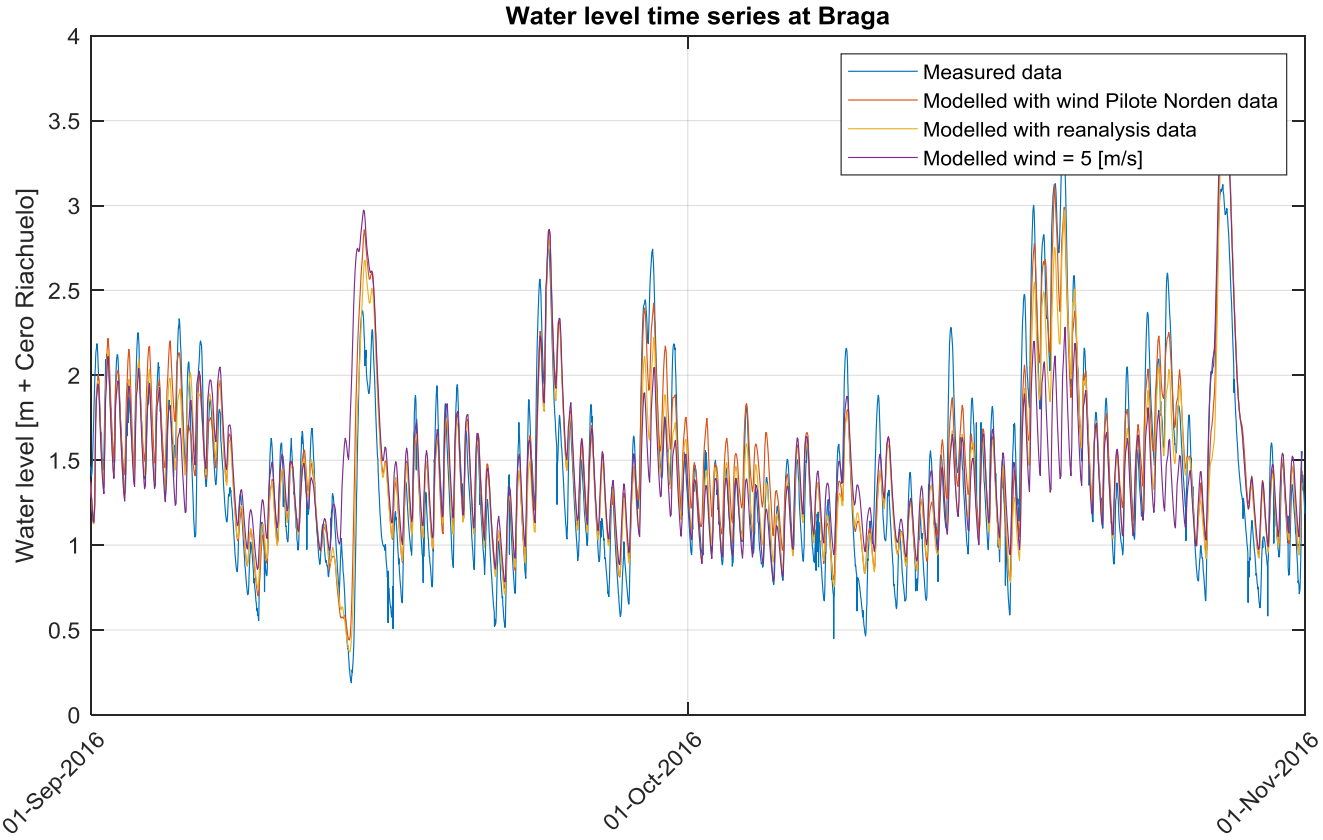

Figure 110 Water level time series: measured, simulated with PN data, simulated with reanalysis data, simulated without wind

Figure 111 shows that indeed excluding the temporally varying wind signal leads to a poor fit and that the reanalysis wind provides the best fit. Although the Pilote Norden data was available per minute and the reanalysis data was available every 3 hours, it still provides a better fit. From this it is concluded that adding the reanalysis wind over the FLOW and WAVE module leads to better representation of the water levels and thus of the currents. Moreover the extremes in wind speed are expected to significantly increase the expected sedimentation, this is addressed in paragraph 6.4.

The effect of time-varying wind signal on the sedimentation pattern is huge, mainly in absolute value, but also on the spatial pattern (Figure 113) . When time-varying wind is added to the model this leads to simulated sedimentation also downstream of KP -25 where no dredging is performed (although also the channel is also natural at depth here).

To conclude, the wind has a major effect on the sedimentation speed and spatial trend in Canal Emilio Mitre (Figure 112). With the previously calibrated sediment characteristics adding the wind to the numerical model leads to serious overestimation of the total sedimentation volume. Therefore it is

concluded that if the wind is added to the numerical model the calibration of the sediment dynamics has to be reconsidered.

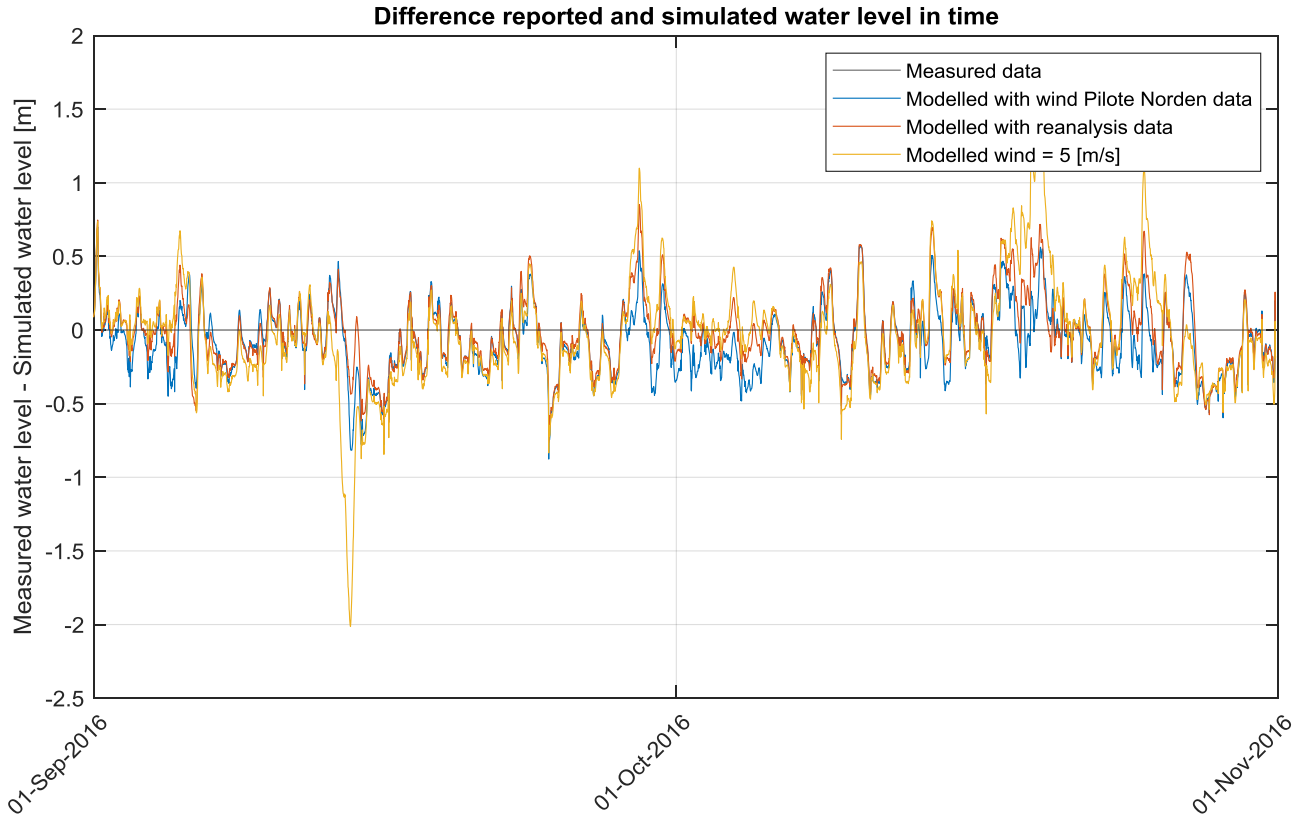

Figure 111 Difference reported and simulated water level in time for diffrent wind signals

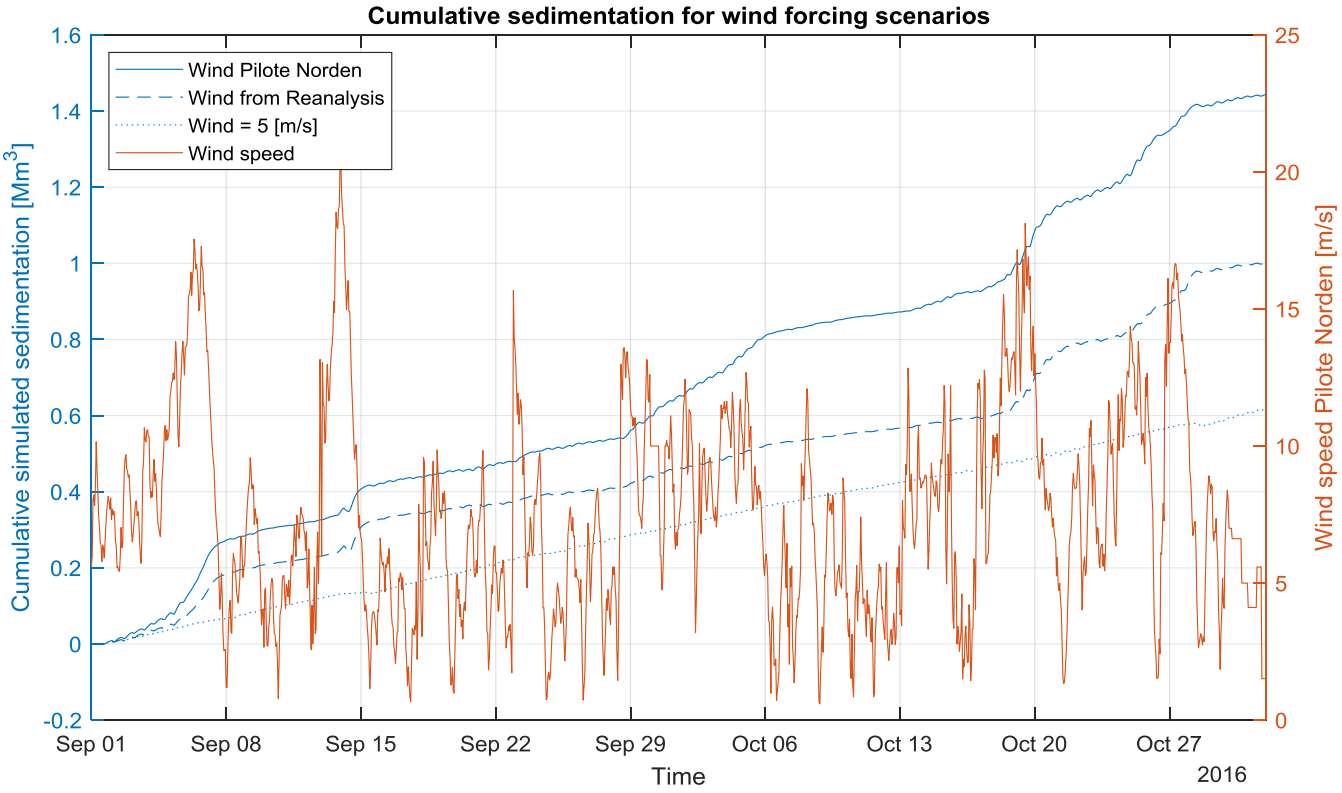

Figure 112 Cumulative sedimentation for wind forcing scenarios

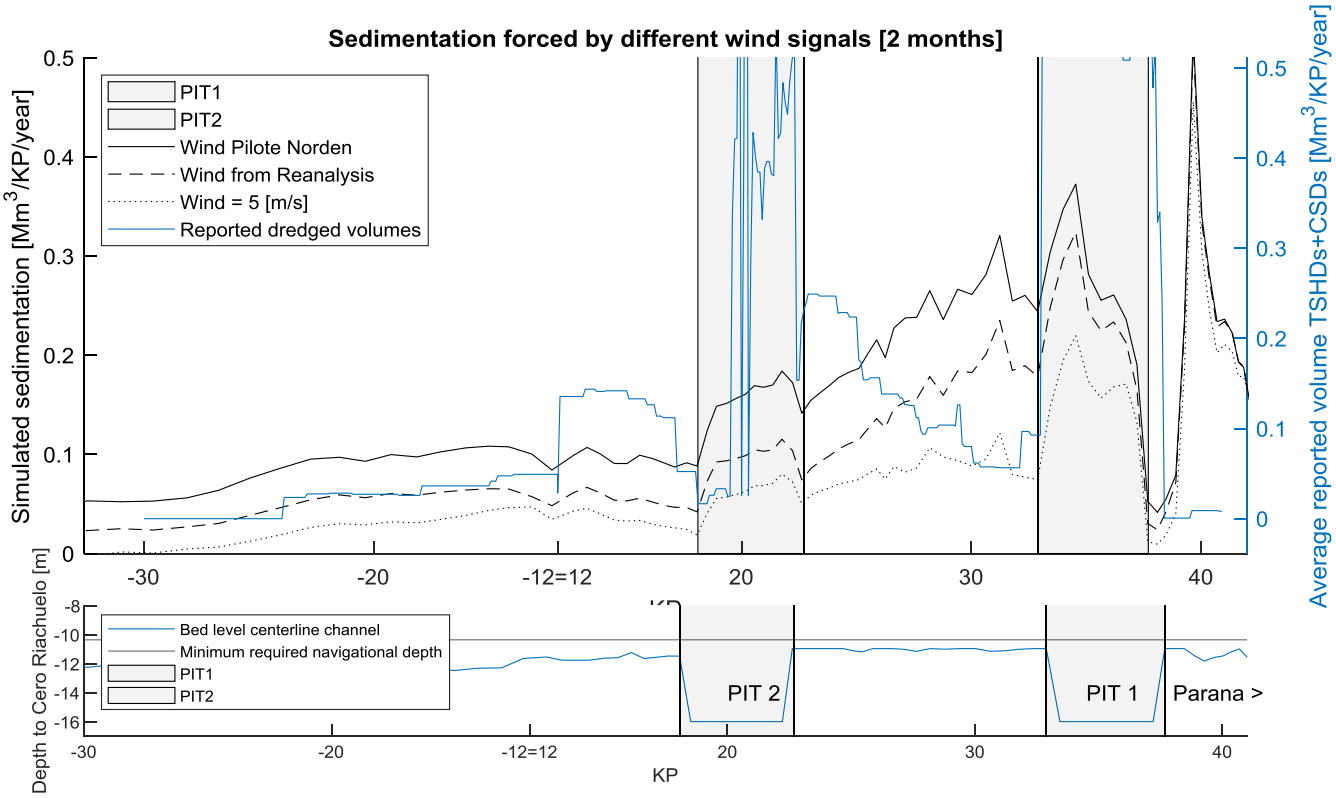

Figure 113 Sedimentation forced by different wind sceanrios

10.10 Appendix 10: Bathymetry Canal Emilio Mitre in time

Figure 114 shows the along-channel bathymetry of Canal Emilio Mitre between 2008 and 2018. It shows that the capacity and depth has varied a lot. Furthermore, the location of the downstream pit has been constant in space (although it varied in size). The upstream pit has been shifted in time towards the transition from the river to the estuary (upstream). Possible reasons for this shift are the fact that the trapping efficiency is the most upstream configuration is highest or the lack of capacity on the flats to dispose more sediment. Between 2008 and 2016 a cutter deepened the pits in 2010, 2014 and 2016.

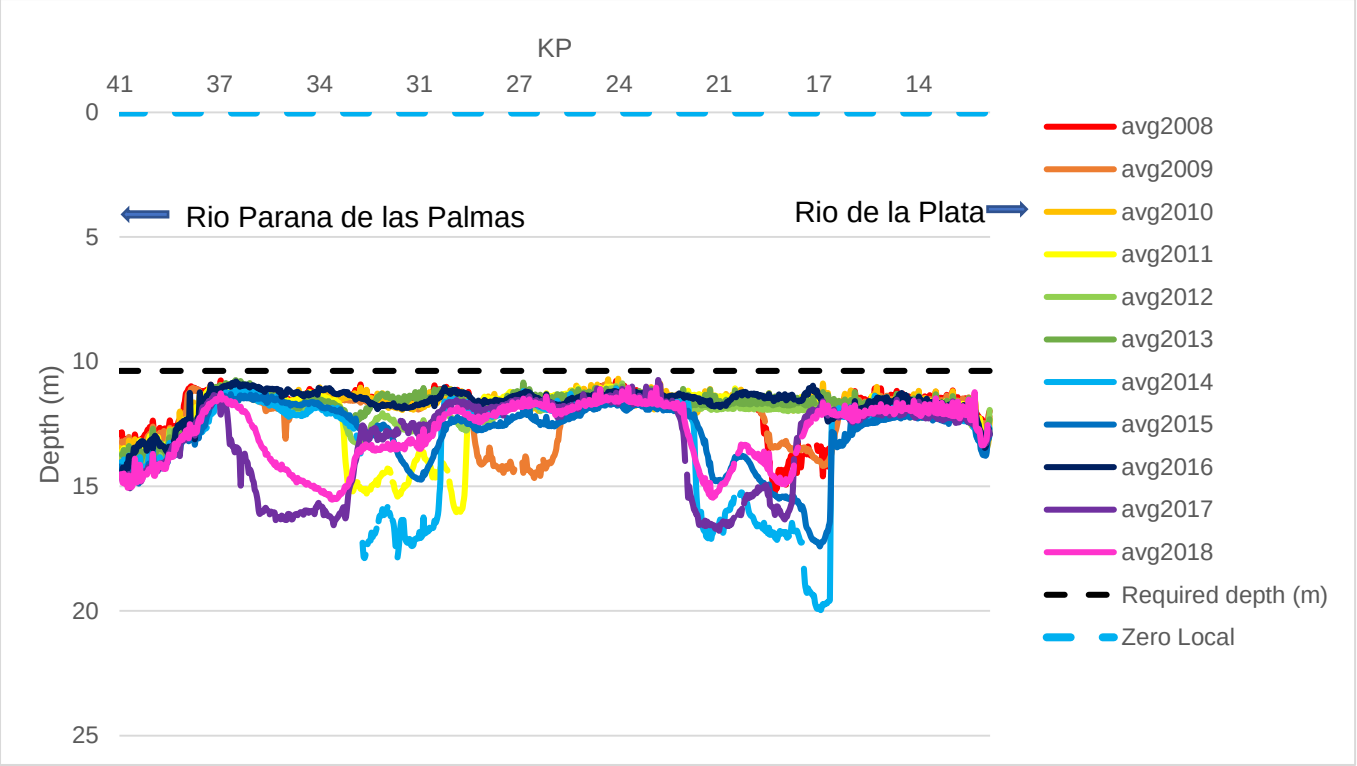

Figure 114 Longitudinal profile Canal Emilio Mitre through the years (KP 12-41)

10.11 Appendix 11: Overview local institutes and knowledge

This is study contributes to the knowledge about the sediment dynamics of the Rio de la Plata estuary. In this appendix an overview is provided, for future researchers, of the institutes and people which have done modelling studies on this region before.

The numerical modelling of the system until now was mostly done by three institutes. The first institute is the IMFIA (Instituto de Mecanica de los fluidos e Ingenieria Ambiental), situated in Montevideo and related to the Universidad de la Republica Uruguay. The main region of interest of the papers by this institute is located around the harbour of Montevideo, Uruguay. However they also did research on the estuary over all, mainly on the topic of fine sediments. The main authors from this institute are Pablo Santoro, Monica Fossati, Ismael Piedracueva, Luis Teixeira and Franciso Pedocchi.

The second institute is the INA (Instituto Nacional del Agua) situated in Buenos Aires, Argentina. This institute has most knowledge about the delta and the Rio Parana (knowledge on the estuary is limited). They performed modelling studie on the discharge of the different branches of the river and moreover provided all the data on the discharges and sediment load. The main authors from this institute are Mariano Re, Martin Sabarots-Gerbec, Angel Menendez and A Sarubbi.

The third institute that performed modelling studies on this topic is the Department of Science of the Atosphere and Ocean of the University of Buenos Aires. This institute works in close corporation with CIMA (Centre de Inverstigaciones del Mar y la Atmosfera). The main authors related to these institutes are Virna Loana Meccia, Claudia Simionato, Raul Guerrero and Vincente Barros. Their research mostly considers the whole estuary as spatial scale.